Universiteit
Leiden
The Netherlands

Targeted therapy for triple-negative breast cancer

McLaughlin, R.P.

Citation
McLaughlin, R. P. (2018, December 13). *Targeted therapy for triple-negative breast cancer*. Retrieved from https://hdl.handle.net/1887/68194

Version:	Not Applicable (or Unknown)
License:	Licence agreement concerning inclusion of doctoral thesis in the Institutional Repository of the University of Leiden
Downloaded from:	https://hdl.handle.net/1887/68194

Note: To cite this publication please use the final published version (if applicable).

Cover Page

Universiteit Leiden

The handle http://hdl.handle.net/1887/68194 holds various files of this Leiden University dissertation.

Author: McLaughlin, R.P.
Title: Targeted therapy for triple-negative breast cancer
Issue Date: 2018-12-13

TARGETED THERAPY FOR TRIPLE-NEGATIVE BREAST CANCER

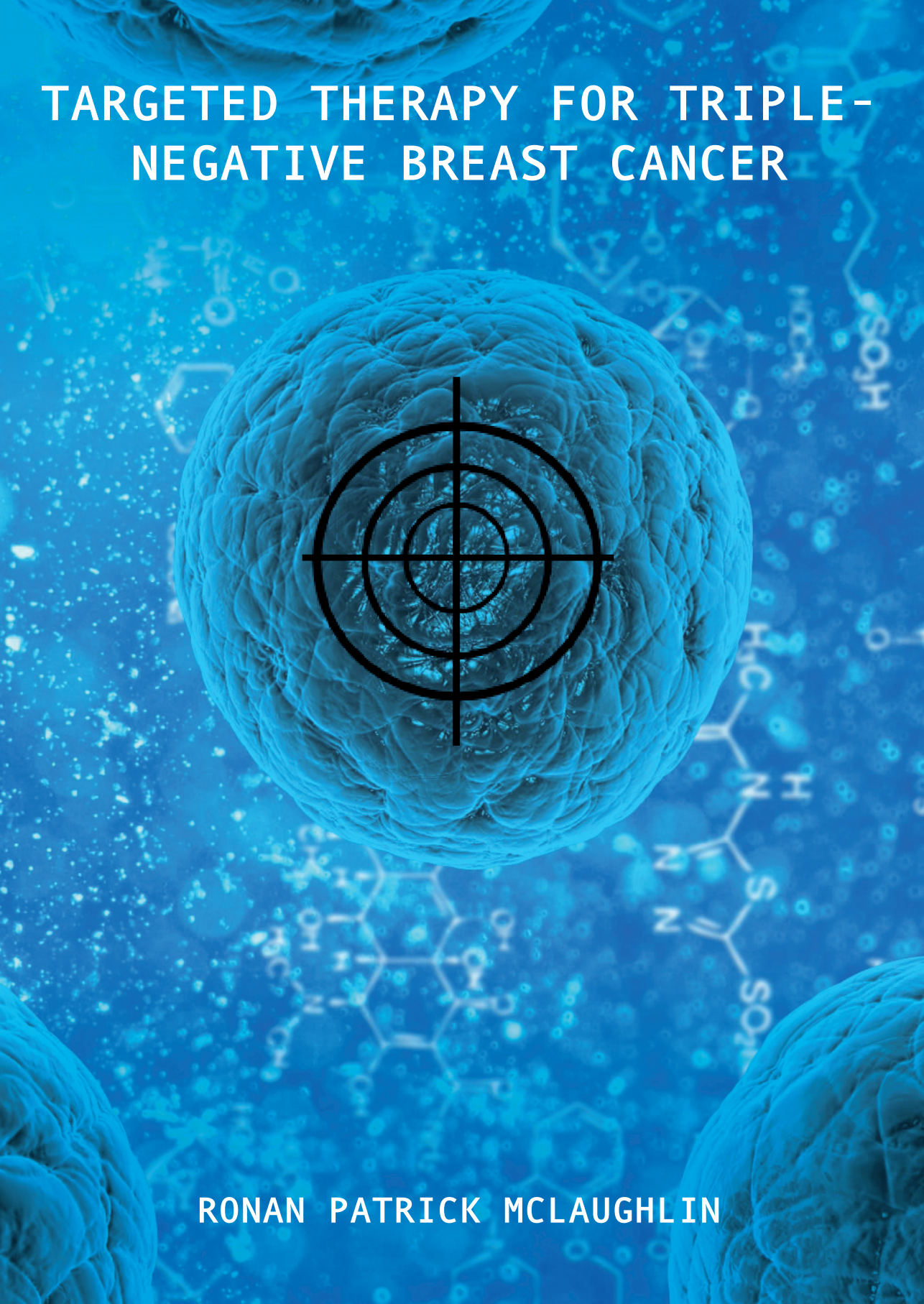

RONAN PATRICK MCLAUGHLIN

Targeted Therapy for Triple-Negative Breast Cancer

Ronan Patrick McLaughlin

Targeted Therapy for Triple-Negative Breast Cancer

PROEFSCHRIFT

ter verkrijging van de graad van Doctor aan de Universiteit Leiden,

op gezag van Rector Magnificus, Prof. mr. C.J.J.M. Stolker

volgens besluit van het College voor Promoties

te verdedigen op 13-12-2018

klokke 12:30 uur

door

Ronan Patrick McLaughlin

geboren op 11 juli 1990 te Edinburgh, Schotland (Verenigd Koninkrijk)

Promotor

Prof. Dr. Bob Van de Water (Drug Discovery & Safety, LACDR, Universiteit Leiden)

Co-Promotor

Dr. Yinghui Zhang (Drug Discovery & Safety, LACDR, Universiteit Leiden)

Promotion committee

Prof. Dr. Hubertus Irth (Scientific Director, LACDR, Universiteit Leiden, Voorzitter)

Prof. Dr. Joke Bouwstra (Biotherapeutics, LACDR, Universiteit Leiden, Secretaris)

Prof. Dr. Ad. IJzerman (Drug Discovery & Safety, LACDR, Universiteit Leiden)

Prof. Dr. John Martens (Medical Oncology, Erasmus MC Rotterdam)

Prof. Dr. Peter Devilee (Human Genetics, LUMC)

© 2018 Ronan Patrick McLaughlin. All rights reserved.

Cover By: Adapted from www.publicdomainpictures.net/en/view-image.php?image=42719&picture=cell (under CC0 license) by Ronan Patrick McLaughlin. 2018.

ISBN: 978-94-6361-205-0

An electronic version of this thesis can be found at https://openaccess.leidenuniv.nl

Printed by: Optima Grafische Communicatie B.V. Rotterdam

This research was conducted at the Division of Drug Discovery and Safety of the Leiden Academic Centre for Drug Research, Leiden University, Leiden, The Netherlands.

Table of Contents

Chapter 1 1

Introduction, Aim and Outline of this Thesis

Chapter 2 55

A cell cycle gene signature is associated with resistance to MEK and Akt inhibitors in triple-negative breast cancer

Chapter 3 100

Blockage of cdc7/CDK9 signalling sensitises triple-negative breast cancer to EGFR-targeted therapy

Chapter 4 139

Targeting the P-TEFb complex through CDK9 inhibition to combat triple-negative breast cancer

Chapter 5 183

The synergistic effect of combined P-TEFb and EGFR inhibition on triple-negative breast cancer

Chapter 6 216

Discussion & Future Perspectives

Appendix 238

Summary (English) 239

Resumen (Español) 244

Nederlandse samenvatting 249

List of Publications 254

Curriculum Vitae 255

Acknowledgements 256

Chapter 1

Introduction, Aim and Outline of this Thesis

Ronan P. McLaughlin[1], Yinghui Zhang[1], Bob van de Water[1]

[1] Department of Drug Discovery and Safety, Leiden Academic Centre for Drug Research, Leiden University, 2300 RA Leiden, The Netherlands.

This chapter is based on a manuscript in preparation

1. Triple-negative breast cancer

Triple-negative breast cancer continues to represent a significant problem for modern oncology practice, the disease being associated with a particularly poor prognosis in comparison to other subtypes of breast cancer. This review attempts to comprehensively summarise potential molecular targets for this intractable illness, paying particular attention to the plethora of drug resistance mechanisms employed by breast cancer cells to evade eradication and how these may be overcome. Additionally, the molecular classification of breast cancer and its relation to the triple-negative subtype is explained in detail. Particular emphasis is also placed on the utility of targeting the basal transcriptional apparatus as a means of combating triple-negative breast cancers as well as a method for subverting their resistance to other targeted therapies.

1. Aetiology, Pathophysiology & Cancer Stem Cells

Breast cancer is both the most commonly diagnosed cancer and the leading cause of cancer-related death amongst women worldwide[1]. Breast cancer has a diverse aetiology: exposure to tobacco or ionising radiation, consumption of alcohol, high BMI, nulliparity or Cowden syndrome, all increase the risk of breast cancer development[2–6]. Approximately 5-10% of breast tumours arise due to autosomal-dominant mutations in BRCA1 and BRCA2 genes, genes which play a crucial role in DNA repair by promoting checkpoint activation and homologous recombination, respectively[7]. Histologically, breast tumours arise from the glandular, terminal duct lobular units which contain branched, tubuloaveolar milk-producing glands centred around a lumen. Tumours arise from either the basal, structurally-supportive, contractile myoepithelial cells or the luminal epithelial cells responsible for milk production, both of which are believed to be derived from a breast stem cell

population[8]. This breast stem cell population is thought to have the potential to differentiate into either luminal-restricted progenitors, myoepithelial-restricted progenitors or bipotent progenitor cells, the latter retaining developmental plasticity, being capable of producing both luminal-restricted and myoepethelial-restricted progenitor populations responsible for the generation of fully differentiated luminal and myoepethelial cells, respectively[9,10]. Moreover, evidence suggests that this intricate hierarchy is also prone to oncogenic disruption at various levels, with transformation of the breast stem and progenitor populations increasingly thought to be responsible for the generation of breast cancer stem cells (BCSCs): self-renewing cancer cells capable of maintaining tumours via differentiation into tumour bulk, from which all tumour cells are, in theory, derived[11]. This cancer-driving subpopulation of cells is believed to be responsible for disease recurrence in later life and is notoriously refractory to therapy in various tumour types[12–19]. Various markers specific for BCSCs have been identified, including a CD44+/CD24- phenotype and a high ALDH1 activity[20,21]. However, the precise hierarchical origins of the CSC population in breast cancer and other tumours remain somewhat elusive, due to inconsistencies in marker expression and utility, discrepancies between mouse and human tissue and the lack of validated *in vivo* assays to accurately determine their abundance in human tumours[22]. Furthermore, given the striking inter-and intratumoural heterogeneity of breast cancers it is likely that the BCSC model may be too simplistic to fully explain the pathophysiology of the disease. This intracellular genetic variation may instead be explained by a “clonal evolution” model in which all tumour cells retain a certain degree of developmental plasticity, with clonal differences being attributed to epigenetic and genetic aberrations acquired during tumourigenesis[11]. In essence, understanding the factors governing this plasticity, be

they epigenetic or microenvironmental, will be crucial in unravelling the complexities of breast cancer tumourigenesis and heterogeneity. Typically, the most aggressive forms of breast cancer are enriched in these CSC populations, with standard cytotoxic chemotherapy against tumour bulk known to enhance this enrichment via the induction of hypoxia, highlighting the therapeutic utility of specifically targeting these tumourigenic cell populations and the influence of microenvironmental factors on CSC behaviour[27,28].

1.2 Histological Classification

The high degree of cellular heterogeneity in breast cancer translates to an equally varied histological presentation. Two broad histological classifications exist for terminal duct lobe-derived breast cancers: *in situ* breast carcinoma and invasive breast carcinoma[30–32]. *In situ* breast carcinoma can be classified as either Ductal Carcinoma In Situ (DCIS) or Lobular Carcinoma In Situ (LCIS), depending on its anatomical origins[30–32]. DCIS can be further sub-divided, based on morphological features, into Comedo, Cribiform, Micropapillary, Papillary and Solid forms[30–32]. Invasive breast carcinomas on the other hand comprise a more heterogeneous group of tumours similarly classified on the basis of histology. These include Invasive Ductal Carcinoma (IDC), Invasive Lobular Carcinoma (ILC), Tubular Carcinoma, Mucinous Carcinoma and Medullary Carcinoma, with IDC being the most common form of breast cancer, comprising around 80% of all cases[32]. IDC and ILC are tumours which have invaded the surrounding ductal or lobular tissue and have subsequently penetrated the ductal or lobular walls, permitting further invasion and destruction of stromal breast tissue and paving the way for metastasis to distant organs[33].

1.3 Molecular Classification

Besides being categorised based on histological characteristics, breast cancer has traditionally been broadly classified as either hormone receptor positive (HR+) or hormone receptor negative (HR-), referring to the expression of oestrogen receptor-α (ERα), progesterone receptor (PR) and human epidermal growth factor receptor 2 (HER2; ERBB2), with this classification influencing breast cancer management[34]. Influential studies which profiled the gene expression patterns of multiple breast tumours using DNA microarrays unveiled a greater degree of complexity to this complicated disease[35,36]. Based on these gene expression profiles, five main transcriptional subtypes of breast cancer were identified: claudin-low, basal-like, luminal A, luminal B and HER2-enriched (***Figure 1***)[35,36]. Luminal-derived breast tumours are more frequently HR+ than those derived from the basal myoepithelial cells[35]. HR+ breast cancers are often dependent upon deranged hormone-mediated signalling for their proliferation and progression, rendering these tumours amenable to treatment with oestrogen antagonists such as tamoxifen[34]. Moreover, HR+ tumours frequently display gene amplification of HER2, resulting in these cancers being dependent upon aberrant pro-proliferative signalling through constitutive activation of the HER2 pathway. ATP-competitive inhibitors of HER2-tyrosine kinase activity (e.g. lapatinib) and anti-HER2 monoclonal antibodies (e.g. trastuzumab) are therefore appropriate for the treatment of these tumours[37,38]. In contrast to HR+ breast cancers, triple-negative breast cancer (TNBC) is characterised as lacking gene expression or amplification of ERα, PR and HER2, respectively[34]. Consequently, TNBC is not responsive to treatment with anti-hormonal therapeutics nor to anti-HER2 agents. Compared to HR+ breast cancer, TNBC has a far poorer prognosis, characterised by a lower 5-year survival rate post-diagnosis and although

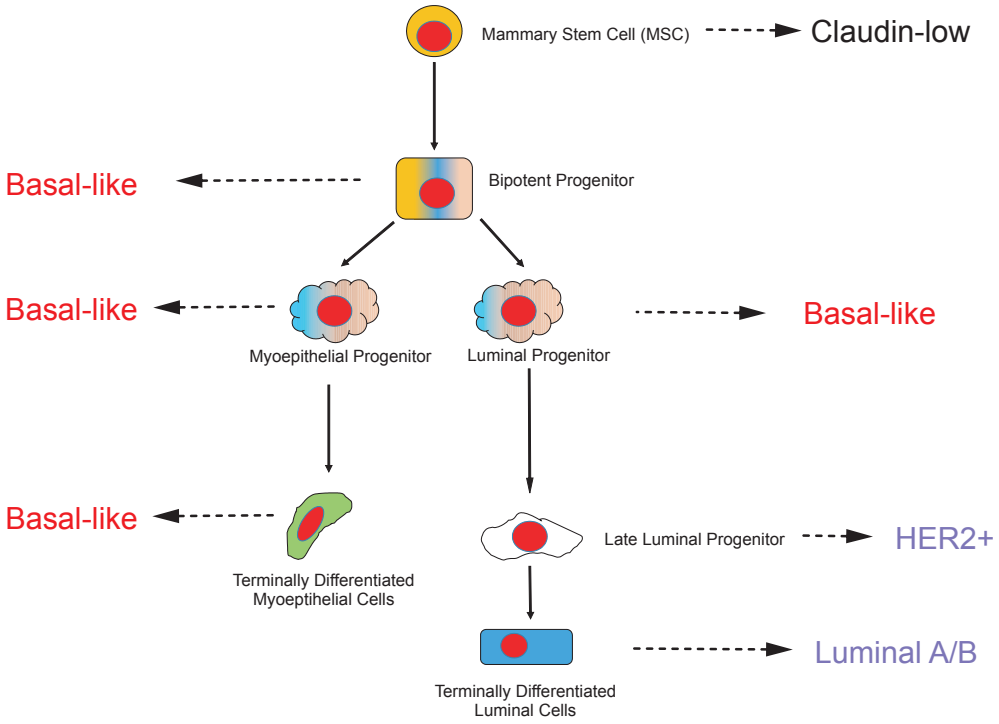

Figure 1. Molecular Classification of Breast Cancers. Diagram illustrating the association between the intrinsic subtypes of breast cancer and their putative cells-of-origin. The intrinsic subtypes of breast cancer are as follows: Claudin-low, basal-like, HER2-enriched, Luminal B and Luminal A. Each of these intrinsic subtypes is believed to originate from different cell populations during normal mammary gland development. Claudin-low tumours arise from mammary stem cells (MSCs) whilst basal-like tumours may arise from bipotent progenitor cells, myoepithelial progenitor cells, or terminally differentiated myoepithelial cells. As such, claudin-low tumours are frequently triple-negative, expressing high-levels of EMT markers and stem cell-related genes, whilst basal-like tumours exhibit high expression of basal cytokeratins (CK5, CK14, CK17) and EGFR, a minority of which may also show HER2 amplification[35,53–55]. HER2-enriched tumours may be derived from late luminal progenitor cells which acquire HER2 gene amplification. These tumours express high levels of HER2 and associated genes such as GRB7[36]. Luminal A and Luminal B tumour types may be a result of oncogenic transformation of differentiated myoepithelial or luminal cells. Luminal A tumours are frequently ER+ PR+ and HER2-, whilst Luminal B tumours are frequently "triple-positive", though these definitions are not mutually exclusive[56,57]. Luminal B tumours are often more highly enriched for pro-proliferative and cell cycle-related genes, compared with Luminal A tumours[58]. Adapted from *Prat & Perou (2009)*[59].

it accounts for approximately 15-20% of total breast cancer cases, it is disproportionately responsible for breast cancer-associated deaths[35,39–41]. Epidemiologically speaking, TNBC is more prevalent in pre-menopausal African-

American women younger than 40 years of age[42,43]. At diagnosis, TNBC often presents as a poorly differentiated, highly proliferative, high grade IDC with a necrotic core and varying levels of lymphocytic infiltration[42,44,45]. The pattern of metastasis is also markedly different for triple-negative tumours, with TNBC more likely to spread to the lungs and brain than HR+ tumours, which instead show greater propensity to spread to the bones[46,47]. *Lehmann et al* further sub-classified TNBC into six molecular subtypes (TNBCType) using k-means and consensus clustering: Basal-like 1 (BL1), Basal-like 2 (BL2), Mesenchymal (M), Mesenchymal stem-like (MSL), Immunomodulatory (IM) and Luminal Androgen Receptor (LAR)[48]. These subtypes displayed unique gene expression profiles with BL1 and BL2 subtypes enriched for expression of genes involved in cell cycle and growth factor signalling (specifically EGFR, IGF1R, Wnt/β-catenin and MET), respectively. Contrastingly, genes involved in regulation of cell motility and differentiation (e.g. Rho and TGF-β signalling pathways) are prevalent in the M subtype. Whilst the MSL subtype shares this enrichment, it is unique in also being enriched for genes linked to growth factor signalling pathways. Unsurprisingly, the IM subtype shows enrichment in genes linked to immune system regulation and cytokine signalling (e.g. IL-12, IL-7 and TH1/TH2 pathways). Interestingly, the LAR subtype is strongly enriched in pathways governing androgen/oestrogen metabolism and steroid synthesis. Moreover, the LAR subtype expresses greater levels of androgen receptor (AR) than the other subtypes, accompanied by up-regulation of signalling components or direct downstream targets of AR. These profiles have also been borne out in clinical practice, being highly relevant regarding drug sensitivity. *Masuda et al* analysed the response of 130 TNBC patients, classified into Lehmann et al's subtypes using gene expression microarrays, to neoadjuvant chemotherapy[51]. Basal-like TNBC is often the most sensitive to

standard chemotherapy, consistent with its enrichment in DNA-repair-related pathways, however, BL2-type tumours are considerably less sensitive to chemotherapeutic agents compared with BL1-type tumours, with pCR rates of 0% versus 52%, respectively, indicating that *Lehmann et al's* classifications have important implications for the clinical management of TNBC[51]. Nonetheless, this study was confounded by small sample sizes for certain tumour groups (particularly for BL2), and the lack of perfect overlap between gene expression profiles obtained from microarrays and those identified by *Lehmann et al*, precluding absolute translation of clinical relevance. Further research conducted by *Lehmann et al* reduced the original six subtypes to four (BL1, BL2, M, LAR), after refinement which took the low cellularity of IM and MSL tumours into account[52]. A retrospective analysis of 306 TNBC patients treated with neoadjuvant chemotherapy revealed substantial differences between these four classifications with BL2-type and LAR-type tumours again showing the lowest pCR rates, 18% and 23% respectively[52], signifying the need for targeted therapeutics in these instances, most likely receptor tyrosine kinase (RTK) inhibitors or androgen antagonists to counteract dependence on growth factor signalling and hormonally-regulated pathways[51].

2. Current Therapeutic Strategies and Mechanisms of Resistance in TNBC

2.1. Current management of TNBC

First-line treatment for TNBC is usually tumour-reductive surgery which consists of either simple or radical mastectomy or, if possible, breast-conserving surgery (BCS) in the form of lumpectomy or quadrenectomy[60,61]. Post-operative administration of radiotherapy is invariably given to patients receiving BCS and evidence suggests it is also beneficial to those who have undergone mastectomy by reducing 15-year breast

cancer mortality rates[61]. Given that TNBC is refractory to hormone antagonists such as tamoxifen, the primary systemic treatment is adjuvant or neoadjuvant chemotherapy. This typically consists of a combination of anthracyclines (e.g. doxorubicin), taxanes (e.g. paclitaxel) and platinum-based agents (e.g. carboplatin)[51,62]. Paradoxically, TNBC patients usually display higher rates of pCR in response to treatment with neoadjuvant chemotherapy compared to other BC subtypes[63–66]. However, only 30-45% of patients achieve pCR, with those who do not respond often relapsing far more rapidly with metastatic disease[41,67–70]. Upon progression into Stage III or IV TNBC, survival drops substantially, with a median survival of 2-3 years depending on location of the metastatic lesions[63,71]. The development of metastatic disease is therefore frequently met with fatal consequences and treatment is often palliative rather than curative[63,72]. Patients who present with inoperable metastatic disease are treated with neoadjuvant chemotherapy to render tumours amenable to resection[61]. Radiotherapy is used as a last resort for tumours which remain inoperable post-systemic chemotherapy[61]. The primary issue underlying the lack of response to therapeutic intervention, eventually leading to metastatic dissemination, is that of intrinsic or acquired drug resistance.

2.2. Mechanisms of drug resistance

Given the extensive molecular heterogeneity of TNBC, it is unsurprising that many of these tumours are often recalcitrant to standard chemotherapeutic regimens[69,73,74]. Drug resistance is pandemic amongst TNBC patients and proceeds via two broadly defined mechanisms: intrinsic or acquired resistance[75,76]. Intrinsic resistance denotes the outright insensitivity of tumour cells to anti-cancer agents, this being mediated by

pre-existing factors which render the tumour bulk impervious to treatment with chemotherapy or targeted agents[75–77]. Overexpression of transmembrane ATP-binding cassette (ABC) transporters, particularly BCRP and MDR1, promotes the efflux of anti-cancer drugs, and has been described as a mechanism of intrinsic resistance in breast cancer[78]. Moreover, CSCs often express higher levels of these drug pumps, including BCRP, thereby contributing to the insensitivity of this aggressive tumour cell population to therapy[79–81]. The quiescent state of CSCs also renders these cells refractory to treatment with DNA-damaging chemotherapeutics, since these agents preferentially target actively cycling cells[82,83]. Additionally, the elevated level of DNA repair systems in CSC populations confers resistance to DNA-damaging radiotherapy[84,85]. As such, the quality and efficiency of DNA damage repair in target cells is pivotal in determining the efficacy of DNA damaging agents[76,86]. Acquired resistance refers to an adaptive response to previously effective chemotherapeutics or targeted agents, which results in tumour cell survival in the presence of these drugs and develops over the course of treatment[76]. One such mechanism of acquired resistance comprises alterations in drug targets, which occurs in both solid and haematological malignancies alike[76]. BRCA1/2-mutant, homologous recombination-deficient breast cancers are sensitive to treatment with poly (ADP-ribose) polymerase (PARP) inhibitors[87,88]. The success of this synthetic lethal interaction is due to the inability of BRCA1/2-mutant cells to repair double-stranded DNA breaks (DSBs) in the absence of PARP, since intact HR pathways can overcome PARP inhibition[89–91]. However, in-frame deletions of BRCA2 can render cells insensitive to PARP inhibition by partially restoring BRCA2's HR capability[92,93]. Various cancers frequently become addicted to particular oncogenic kinases, as is the case in EGFR-mutant lung cancer, HER2+ BC and chronic myeloid leukaemia

(CML) driven by the BCR-ABL chromosomal translocation, in so-called “oncogene addiction[94–97]”. EGFR-mutant lung cancer cells are therefore sensitive to EGFR-tyrosine kinase inhibitors (EGFR-TKI) such as lapatinib, erlotinib or gefitinib, by virtue of a constitutively active EGFR pathway[98,99]. Initially, patients respond to EGFR-TKI therapy but resistance to such agents is almost invariably acquired, with additional mutations in EGFR often being responsible for the development of resistance[100,101]. Similar responses are seen in CML in response to BCR-ABL inhibitor imatinib as well as in HER2+ BC in response to anti-HER2 therapies such as trastuzumab or lapatinib[102,103]. Besides alterations in the drug targets themselves, mutations acquired in pathway components downstream of receptor tyrosine kinases (RTKs) such as EGFR also contribute to acquisition of resistant phenotypes in multiple cancers, as is the case in BRAF-mutant melanoma where mutations in KRAS or MEK confer resistance to BRAF inhibitors[104,105]. In response to targeted agents which inhibit the activation of oncogenic RTKs or other kinases, an adaptive transcriptional response can be initiated which results in the up-regulation of other RTKs capable of funnelling growth-factor mediated signal transduction through commonly regulated downstream pathways. This aberrant reprogramming of cellular circuitry which exploits pathway redundancy is known as “oncogenic bypass” since the drug target remains inhibited whilst treatment promotes activation of alternative pathways through which signalling may still occur, thereby circumventing the effects of inhibiting the original oncogenic kinase or RTK (see ***Figure 2***)[75,76]. For example, in HER2+ BC, up-regulation of HER3 (ERBB3) is seen in response to HER2-targeted therapy cetuximab[106–108]. In TNBC, inhibition of MEK1/2 leads to a rapid kinome rewiring, resulting in the increased expression of platelet-derived growth factor receptors (PDGFRs) and other RTKs, the crux of which involved the proteolytic

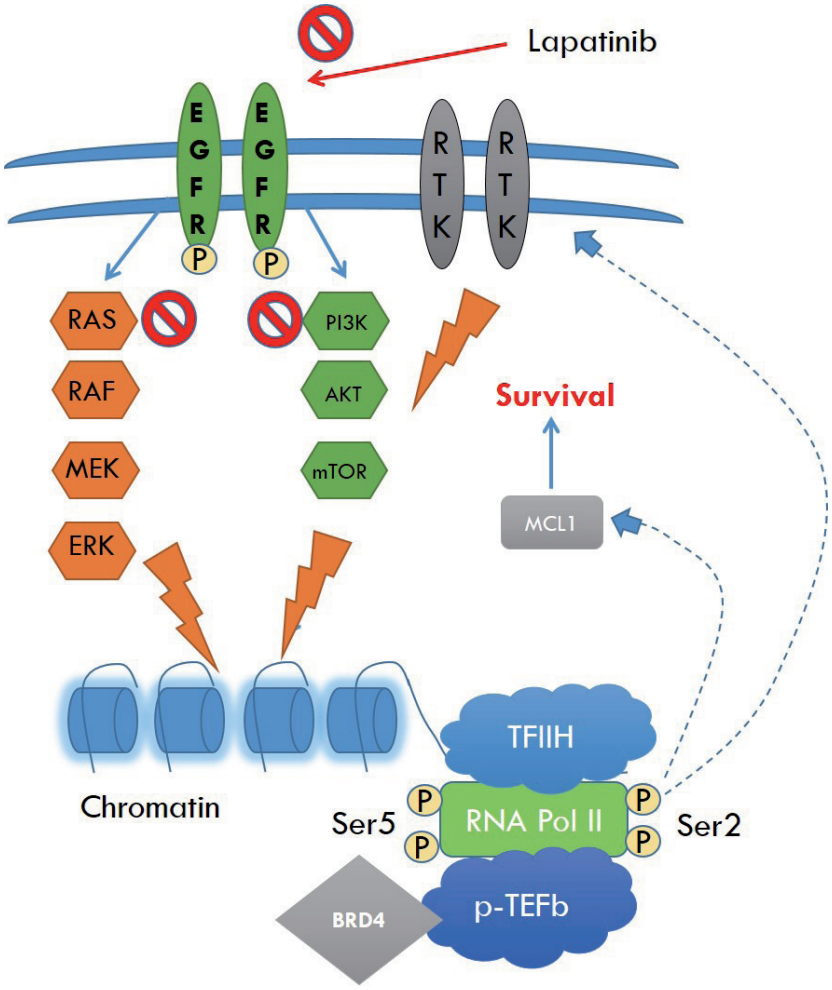

Figure 2. Oncogenic Bypass. Diagram illustrating oncogenic bypass-mediated mechanisms of resistance to RTK-targeted tyrosine kinase inhibitors in cancer. Inhibition of phosphorylation of the intracellular domains of RTKs by tyrosine kinase inhibitors such as lapatinib, prevents the downstream activation of signal transduction cascades responsible for controlling cell proliferation and survival. Amongst the most prominent of these pathways are the RAS-RAF-MEK-ERK and PI3K-AKT-mTOR pathways, which are frequently dysfunctional in multiple cancers. In cells with *de novo* or acquired resistance to such targeted therapies, an adaptive transcriptional response elicited by target kinase inhibition can promote the up-regulation of alternative RTKs which are capable of activating similar pro-proliferative downstream signal transduction cascades in the presence of inhibitor, despite complete inhibition of the originally targeted RTK, ultimately resulting in evasion of cell death. Mutations in downstream components of the MAPK or PI3K pathways which render certain kinases constitutively active, such as KRAS, BRAF or PIK3CA mutations as well as deletions in AKT's negative regulator PTEN can also contribute to oncogenic bypass since their presence renders the inhibition of upstream RTKs futile. Adapted from *Arteaga & Engelman*[140].

degradation of c-MYC, allowing de-repression of PDGFR, AXL and VEGFR expression, ultimately rescuing TNBC cells from MEK1/2 inhibitor-induced death[109]. Up-regulation of MET is also known to promote resistance to EGFR-TKIs in a subset

of EGFR-mutant lung cancer patients[110]. Downstream of RTK-controlled signal transduction pathways, acquired resistance to targeted therapies can also be attributed to dysfunctional regulation of the equilibrium between pro- and anti-apoptotic factors. The resistance of tumour cells to apoptosis has previously been described as one of the hallmarks of cancer, the interplay between BCL-2 family proteins controlling whether a tumour cell undergoes apoptosis or not[111–114]. This family can be roughly sub-divided into two groups: anti-apoptotic members (e.g. BCL-2, BCL-XL and MCL-1) and pro-apoptotic members (e.g. BAX, BAK, BIM, BAD, BID and NOXA). Pro-survival BCL-2 family members such as MCL-1, BCL-2 and BCL-xL bind to and antagonise the oligomerisation of pro-apoptotic BH3-only proteins, thereby preventing loss of mitochondrial membrane integrity, leakage of cytochrome c and subsequent cell death[112,114–116]. Inhibitor of apoptosis proteins (IAPs) (e.g. XIAP and Survivin) act in tandem with anti-apoptotic BCL-2 family members by preventing the cleavage of caspases 3, 7, 8 and 9, hindering the caspase-mediated induction of apoptosis[117–119]. Dependency upon multiple pro-survival BCL-2 family member proteins, including MCL-1, BCL-2 and BCL-xL is frequent in haematological malignancies where the equilibrium between pro- and anti-apoptotic factors is skewed in favour of cell survival[120,121]. Expression of pro-apoptotic BIM is also essential in regulating EGFR-TKI-induced apoptosis in NSCLC patients, with deletions of this gene conferring resistance to such inhibitors[122–124]. Consequently, multiple BH3-mimetics which interfere with the function of pro-survival, BCL-2 family member proteins have been developed as potential cancer therapies which have proven valuable as combination therapies. High levels of BCL-2 expression are also seen across breast cancer subtypes, with the highest levels seen primarily in ER+ breast cancer, though a proportion of TNBCs also exhibit similar

BCL-2 levels[125,126]. Additionally, MCL-1 is a key survival factor in TNBC cells, MCL-1 silencing proving more lethal than sole knockdown of BCL-xL alone with dual silencing of MCL-1 and BCL-xL incompatible with TNBC cell survival[127]. In TNBC tumour xenografts, treatment with BH3-mimetic ABT-737 sensitised tumours expressing high levels of BCL-2 to docetaxel, suggesting BCL-2 proteins contribute to docetaxel insensitivity illustrating the utility of manipulating BCL-2 and other similar proteins in overcoming resistance to chemotherapy[128]. Interestingly, MCL-1 and oncogene MYC have also been shown to cooperate in maintaining a BCSC population in chemotherapy-resistant TNBC by promoting mitochondrial oxidative phosphorylation-induced HIF-1α expression, a process upon which BCSCs are dependent[129]. Combining HIF-1α inhibition with chemotherapy dramatically reduced expansion of the BCSC population, indicating that the oncogenic interaction between BCL-2 family members, transcription factors and altered metabolism is amenable to therapeutic intervention[130]. Evidence increasingly suggests that the tumour microenvironment is also critically involved in conferring resistance to anticancer therapies in both solid and haematological tumours[131,132]. Tumours interact with their surroundings via integrin-mediated adhesion; integrins are large, cell surface proteins which interact with tumour extracellular matrix (ECM) components and in turn control a multitude of pro-proliferative pathways (e.g. PI3K-AKT and NF-κB) as well as intrinsic and extrinsic apoptosis[131]. This is strictly controlled by integrin ligation status and cooperation with RTKs. For example, αvβ3 integrin interacts with fibroblast growth factor receptor (FGFR) to promote signal transduction via RAS-RAF pathway, thereby exerting adhesion-dependent control over tumour cell proliferation[133,134]. In HER2+ breast cancer, enhanced β1-integrin-mediated adhesion to extracellular matrix (ECM) components causes resistance to anti-HER2 monoclonal antibody

trastuzumab[135]. The tumour stroma itself is composed of cancer-associated fibroblasts (CAFs; fibroblasts which have been activated by tumour-derived growth factors) which can communicate with tumour cells via paracrine signalling and the secretion of cytokines and/or growth factors such as EGF, HGF or FGF[136]. Stromal-derived cytokines and growth factors have clear roles in anticancer drug resistance across a vast number of tumour types; CAF-regulated secretion of HGF confers resistance to vemurafenib in melanoma, to lapatinib in HER2+ breast cancer and to EGFR-TKIs in non-small cell lung cancer (NSCLC)[137]. Immune evasion is another property conferred to tumours by the microenvironment; CAFs recruit macrophages and monocytes which can shift the immune microenvironment of the tumour towards tolerance and immune suppression, thus concealing the tumour from cytotoxic T-cell responses[138,139].

3. Possible therapeutic targets in TNBC

Despite the heterogeneous nature of TNBC tumours and the plethora of resistance mechanisms they adopt in response to treatment, promising drug targets amenable to pharmacological manipulation in TNBC do exist. Here, a number of these are described, particular emphasis being placed on RTK inhibitors and cyclin-dependent kinase (CDK) inhibitors as prospective therapies.

3.1. Epidermal Growth Factor Receptor (EGFR)

Epidermal Growth Factor Receptor (EGFR; also known as ERBB1/HER1) is a transmembrane receptor tyrosine kinase (RTK) consisting of an extracellular ligand-binding domain and an intracellular tyrosine kinase domain[141]. Epidermal growth factor (EGF) binds to the extracellular domain, triggering homodimerisation of the

receptor, followed by auto-phosphorylation of the intracellular tyrosine kinase domain, resulting in the activation of many signalling cascades, most notably the PI3K-AKT and RAS-RAF-MEK-ERK axes, which promote cell proliferation, migration, differentiation and survival[142–146]. EGFR expression varies considerably amongst TNBC tumours, though it is frequently overexpressed in basal-like tumours where high rates of EGFR gene amplification have also been reported[147–150]. This overexpression is also linked to a significantly poorer overall survival compared to TNBC patients lacking EGFR overexpression[147,148]. Contrastingly, EGFR is rarely expressed in luminal, ER+ tumours[151]. Constitutive activation of pathways downstream of EGFR is also common in TNBC tumours, particularly constitutive activation of BRAF, suggesting some TNBC tumours depend upon EGFR-mediated signalling pathways for their growth[120,152,153]. Furthermore, *Lehmann et al*[48] also demonstrated that EGF signalling is highly enriched in the BL2 and mesenchymal TNBC subtypes identified in their expression analyses. However, the use of EGFR-TKIs or anti-EGFR monoclonal antibodies in a monotherapeutic context has yet to deliver satisfactory results against TNBC in clinical trials. A Phase II clinical trial for gefitinib monotherapy demonstrated that disease progression occurred in 61.3% of metastatic breast cancer patients with no complete or partial tumour responses detected[154]. Despite clear inhibition of EGFR and downstream MAPK phosphorylation, AKT phosphorylation was unaffected by treatment and no impact on tumour proliferation markers (Ki67) was noted. Other Phase II trials have demonstrated similarly disappointing results, with *Dickler et al*[155] reporting a disease progression rate of 87% amongst patients after Erlotinib treatment, with only two confirmed partial responses identified. These trials did not, however, select for tumours displaying EGFR overexpression or gene amplification, or which were

dependent upon active EGFR signalling. Nor did they assess potential genetic aberrations present in the tumours which may allow constituent cells to bypass inhibition of EGFR-related signalling, such as oncogenic RAS mutations or PTEN deletions[156,157]. Nuclear translocation of EGFR is also associated with resistance to radiotherapy, chemotherapy and EGFR-targeted agents, since this protects the receptor from tyrosine kinase inhibition occurring at the cell membrane[158,159]. Nuclear EGFR acts as a transcription factor which can up-regulate the expression of cell cycle-related genes such as Cyclin D1, thereby promoting proliferation and cell cycle progression even in the presence of EGFR-TKIs or anti-EGFR monoclonal antibodies[160–162]. Moreover, these trials were not stratified according to breast cancer subtype, with both HR+ and HR- breast cancer patients included. However, Phase II trials of second generation EGFR-TKI afatinib have proven equally unsuccessful in patients stratified as TN or HER2-HR+ or in inflammatory breast cancer (IBC) treated with EGFR-TKI lapatinib[163,164]. Despite these disappointing results, combination therapies including EGFR inhibitors have been moderately more successful. A Phase II trial evaluating neoadjuvant chemotherapy combined with panitumumab (EGFR-mAb) showed pCR rates of 47% in cases of operable TNBC, whilst combining cetuximab and docetaxel in another cohort of operable TNBC tumours resulted in pCR rates of 24%[165,166]. Overall response rates (ORR) after co-treatment of metastatic TNBC tumours with irinotecan and cetuximab were approximately 11%, indicating modest benefit of combining EGFR-targeted therapies with standard chemotherapeutic regimens[167]. The use of EGFR-targeted radioimmunotherapy in the form of a radiolabelled anti-EGFR monoclonal antibody in combination with PARP inhibitors and chemotherapy (docetaxel and doxorubicin) has also shown pre-clinical benefit; this triple combination eliminated established metastases in xenograft

models, induced tumour apoptosis *in vivo* and significantly reduced the amount of CD44+ CD24- BCSCs present[168]. Evidently, the future of EGFR-targeted therapies in TNBC is dependent upon their efficacy when combined with other well-tolerated agents.

3.2. Fibroblast growth factor receptors (FGFRs)

Fibroblast growth factor receptors (FGFRs), upon binding FGFs 1-10, transduce pro-proliferative and pro-survival signals via downstream activation of PI3K-AKT and MAPK pathways[169]. Overexpression of FGFR1 and FGFR2 is less frequent than EGFR amplification, with FGFR2 amplification occurring in approximately 4% of TNBC cases[170]. The expression of FGFR ligand FGF2 is significantly higher in basal-like breast tumours, whilst RNAi-mediated silencing of FGF2 impedes the growth of multiple TNBC cell lines, which are incidentally also sensitive to selective FGFR1 inhibitor PD173074[171]. Inhibition of FGFR-controlled signal transduction prevents phosphorylation of both ERK1/2 and AKT, induces G1 cell cycle arrest and induces apoptosis whilst also leading to a significant reduction in the growth of FGFR1-expressing TNBC xenografts[171]. Furthermore, analysis of 782 TNBC tumours revealed high-level FGFR1 expression is more frequent in basal-like tumours and is associated with a significantly poorer overall survival (OS)[172]. Dovitinib, an FGFR-TKI with activity against FGFR1-3, has shown moderate efficacy against FGFR-amplified, metastatic breast tumours in a Phase II clinical trial, resulting in stable disease in a subset of HR+ patients, though no complete responses (CRs) and few pCRs were seen[173]. It therefore remains to be seen whether anti-FGFR therapies are of benefit to TNBC patients.

3.3. Platelet-derived growth factor receptors (PDGFRs)

Platelet-derived growth factors (PDGFs) PDGF-A, PDGF-B, PDGF-C, PDGF-D bind to two either PDGFR-α or PDGFR-β as hetero- or homodimers[174]. Dimerisation of PDGFR-α and/or PDGFR-β subsequently promotes autophosphorylation of their intracellular tyrosine kinase domains, thereby triggering downstream signal cascades[174]. PDGFR-α is expressed at higher levels in TNBC compared with HR+ breast cancer[175]. Activation of PDGFR-α in inflammatory breast cancer (IBC) patients is linked to a significantly poorer metastasis-free survival, suggesting PFGFR-α activity is linked to metastasis formation and disease progression[176]. The recruitment of bone marrow-derived mesenchymal stem cells (BM-MSCs) to the TNBC tumour microenvironment is a pivotal step in the metastatic cascade. Secretion of inflammatory cytokines (e.g. CCL5) by BM-MSCs activates AKT via binding to CCR5, thereby promoting tumour cell proliferation, subsequent extravasation into the vasculature and distant organ colonisation[177]. Additionally, BM-MSCs exhibit remarkable plasticity and can reversibly differentiate into CAFs which secrete pro-tumourigenic factors capable of inducing epithelial-to-mesenchymal transitions (EMTs), facilitating a pro-metastatic environment[178]. Tumour-secreted factors also enhance the BM-MSC/CAF-mediated secretion of these factors, indicating the presence of a signalling loop between the constituent cells of the primary tumour and its microenvironment[178]. PDGFR-β plays a fundamental role in regulating BM-MSC recruitment to primary and metastatic tumour sites[179]. PDGFR-β inhibition prevents intravasation of BM-MSCs into primary TNBC xenografted tumours, and reduces the number of lung metastases[179]. However, clinical trial data for PDGFR-specific inhibitors is scarce. Unfortunately, non-specific inhibitors of PDGFRs such as sunitinib and sorafenib, which also inhibit vascular endothelial growth factor

receptors, performed poorly in clinical trials either as single agents or in combination with chemotherapy[180,181]. In summary, targeting PDGFRs in TNBC may therefore be of use in preventing metastasis of TNBC cells, though the utility of PDGFR-specific inhibitors in a clinical context remains unknown.

3.4. PI3K-AKT-mTOR and MAPK Pathways

Downstream of most RTK-mediated signal transduction pathways, both the PI3K-AKT-mTOR and mitogen-activated protein kinase (MAPK) axes constitute vital pro-proliferative, pro-survival cascades for tumour cells. Heterodimeric phosphoinositide-3 kinases (PI3K) consist of regulatory (p85) and catalytic (p110) subunits; activation of a multitude of RTKs (including EGFR) and downstream adaptors induces recruitment of the regulatory p85 subunit, resulting in a conformational change permitting p110-mediated phosphorylation of PIP2 to PIP3, which subsequently activates AKT[182–184]. Negative feedback in the form of PTEN counteracts activation of the pathway by dephosphorylating PIP3[185]. PI3K-AKT-mediated regulation of mTOR activity controls cellular metabolism and protein translation[186,187]. mTOR forms complexes with RAPTOR and RICTOR proteins to form mTORC1 and mTORC2, respectively[182]. mTORC1 phosphorylates 4E-BP1 and S6K to enhance ribosomal biogenesis and protein translation whereas mTORC2 re-inforces AKT-mediated signalling[187–190]. Enhanced activation of the PI3K-AKT-mTOR axis is frequent in TNBC, as are oncogenic PIK3CA (p110) mutations and PTEN deletions which lead to constitutive activation of AKT[191–194]. PI3K inhibitors and mTOR inhibitors have been extensively tested both pre-clinically and clinically in TNBC with varying degrees of success[70,182]. As single agents, mimimal efficacy has been observed, whilst combination therapies appear to be of particular benefit. The PI3K pathway is critical in maintaining stability of the HR complex during DNA

repair[195,196]. Silencing PIK3CA in TNBC cells reduces BRCA1 levels which can be exploited by combining PI3K (p110)-selective inhibitor BKM120 with PARP inhibitor olaparib[197]. This combination sensitised BRCA1/2-proficient TNBC cells to olaparib *in vitro* and in TNBC patient-derived xenograft models[197]. Enhanced PFS has been observed in TNBC patients with PI3K-AKT-mTOR pathway alterations treated with combinations of PI3K-AKT-mTOR inhibitors and chemotherapy[198]. Nonetheless, adaptive resistance mechanisms due to the extensive functional overlap and cross-inhibition observed between the PI3K-AKT-mTOR and MAPK axes, invariably arise. MAPK signalling itself proceeds via activation of the RAS-RAF-MEK-ERK cascade; growth factor-induced activation of RAS GTPase phosphorylates effector kinase RAF which subsequently phosphorylates effector kinase MEK and finally ERK1/2, which promotes the function of terminal transcription factors (e.g. c-MYC and c-FOS) eventually leading to increased expression of pro-survival transcripts[199–201]. High expression of ERK1/2 correlates with poorer survival in TNBC whilst increased copy number of RAS or RAF leads to pathway overactivation, with mutations in RAS or RAF uncommon events in TNBC[69,152]. MEK inhibitors induce up-regulation of the PI3K-AKT-mTOR axis in TNBC xenografts and cell lines due to de-repression of MEK-induced inhibition of this pathway, likely via prevention of ERK-mediated GAB1 phosphorylation[202–204]. The apoptosis-inducing effect of PI3K inhibitors has also been attributed to their transient effects on the adjacent RAS-RAF-MEK-ERK pathway[202]. Intriguingly, pulsatile PI3K inhibition or combined MEK or AKT inhibition led to enhanced apoptosis in multiple cancer cell lines, highlighting important implications for the dosage of such targeted therapies[202].

3.5. DNA-Damaging Agents & Checkpoint Inhibitors

By their very nature, cancers display inherently high levels of genomic instability, a known hallmark of cancer which underlies their proclivity for the accumulation of DNA damage[205]. Oncogene activation causes replication-linked DNA lesions as a result of disproportionate replication origin firing due to excessive pro-proliferative signals, the implication of this being that malignant cells possess more endogenous replication errors than non-malignant cells[206–208]. Moreover, proteins involved in the DNA damage response (DDR) and associated cell cycle arrest are often mutated or dysfunctional in multiple cancers; tumour suppressor p53 being a prominent example[209,210]. Radiotherapy and chemotherapy take advantage of these properties by inducing exogenous DNA damage such that tumour cells can no longer repair the damage, leading to cell cycle arrest and ultimately apoptosis[208]. DNA-damaging agents induce this irreparable damage by various mechanisms: topoisomerase poisons (e.g. etoposide and doxorubicin) act by preventing topoisomerase II-mediated cutting of DNA double-helices and release of torsional strain, thereby trapping obstructing DNA replication resulting in double-stranded breaks (DSBs)[211–213]. Alkylating agents (e.g. cisplatin) bind to guanine residues in DNA, forming damaging adducts and intra-strand crosslinks[214]. Antimetabolites (e.g. 5-fluorouracil and gemcitabine) interfere with nucleotide metabolism by competing with other nucleotides during DNA synthesis, thus preventing incorporation of the correct nucleotides and inducing termination of chain elongation[215]. However, DNA-damaging agents are associated with considerable dose-limiting, off-target toxicity given their effects on non-malignant, rapidly dividing cells in the gastrointestinal system and bone marrow[216–218]. The redundancy between various DNA repair pathways is amenable to targeted therapy since cancer cells deficient for a particular

form of repair often become addicted to another, as is the case with the use of PARP inhibitors against BRCA1/2-deficient breast cancer and ovarian cancer[87,88]. Interfering with DNA damage checkpoints in the cell cycle is another strategy whereby aberrant cell cycle progression can lead to apoptosis due to accumulation of DNA lesions. These checkpoints are strictly controlled by ataxia telangiectasia mutated (ATM) and ataxia telangiectasia Rad3-related (ATR) proteins which are activated by DSBs and single-stranded breaks (SSBs), respectively[219,220]. In response to DSB detection, ATM phosphorylates histone H2AX which induces a change in chromatin architecture permitting the recruitment of other repair factors and ubiquitin ligases (e.g. MDC1, MRN and RNF8), ultimately leading to localisation of BRCA1, p53 and other vital repair factors to the site of damage. ATM-mediated phosphorylation of SMC1, MRN or KAP1 induces lesion repair, dissemination of damage signals or chromatin relaxation, respectively[221–223]. Checkpoint kinases 1 and 2 (CHK1 and CHK2) are serine-threonine kinases downstream of ATM and ATR, which act to halt cell cycle progression in the presence of DNA damage[224]. Phosphorylation of CHK2 (Thr68) and CHK1 (Ser345/Ser317) by ATM and ATR, respectively, halts cell cycle progression via CHK2- or CHK1-mediated phosphorylation of cdc25A or cdc25C, priming them for ubiquitination and proteasome-mediated degradation[225,226]. Degradation of cdc25A inhibits cyclin-dependent kinase 2 (CDK2) activity, thus arresting cell cycle progression in G1/S-phase. Whilst cdc25C degradation obstructs CDK1-CyclinB function, leading to G2/M arrest[225,226]. Activated CHK2 also phosphorylates substrates which amplify the DDR, including BRCA1, BRCA2 and XRCC1[227–229]. BRCA1 and BRCA2 are also substrates of ATM, indicating that CHK2 may also act to augment ATM function in DNA repair[227,228]. With respect to targeting CHK1 and CHK2 function in TNBC,

CHK1 inhibitor MK-8776 improves the radiosensitivity of multiple TNBC cell lines and xenografts by preventing CHK1-mediated activation of DNA repair and abrogating damage-induced G2/M arrest[230]. P53-deficient TNBC cell lines and xenografts are exquisitely sensitive to CHK1 inhibition, while p53 inhibition sensitises p53-proficient TNBC cells to CHK1 inhibitors UCN-01 and AZD7762, suggesting that stratifying patients based on p53 status may identify patients eligible for anti-CHK1/2 therapy[231]. Extensive pre-clinical evaluation of combining CHK1/2 inhibitors with chemotherapeutics has not necessarily been translated into successful clinical application, however[232]. Co-treatment of metastatic TNBC tumours with UCN-01 and irinotecan in a Phase I clinical trial was not associated with significant clinical benefit due to pharmacodynamic issues with UCN-01 and tumour heterogeneity. Induction of apoptosis markers in patients' tumours was minimal, alluding to the existence of possible bypass mechanisms[233]. The results of an ongoing clinical trial investigating the effect of LY2606368, a relatively specific CHK1 inhibitor with weaker effects on CHK2, in BRCA1/2-associated BC and TNBC on induction of complete and partial responses are yet to be published but will be made available in 2019 (NCT02203513). Considering that repair of DNA damage requires the function of multiple, often parallel, signalling pathways, the identification of novel synthetic lethal combinations using DNA damage checkpoint inhibitors is likely to be invaluable in designing efficacious, multi-faceted therapies which prevent tumour cell escape facilitated by pathway redundancy in TNBC and other malignancies.

3.6. Cyclin-dependent kinases

3.6.1. The role of cyclin-dependent kinases in controlling cell cycle progression

Cyclin-dependent kinases (CDKs) are serine/threonine protein kinases involved in control of cell proliferation and transcription, the expression of which is strictly controlled throughout the cell cycle and whose activity is dependent upon their binding to specific cyclin molecules[236–240]. Progression through the various phases of the cell cycle is governed by multiple CDKs and their corresponding cyclins with specific CDK-Cyclin complexes regulating the passage of the cell from one specific cell cycle phase to another[241]. During G1 phase, the transcriptional repressor Rb binds chromatin-modifying enzymes (HDAC1) and transcription factors (E2F1) which normally promote expression of genes necessary for transition into S phase[242–244]. The CDK4/6-Cyclin D1 complex phosphorylates Rb, leading to dissociation of both HDAC1 and E2F1 from Rb, thereby de-repressing E2F1's transcriptional activity and promoting S phase entry[242–244]. Rising levels of Cyclin E1/E2 expression as a result of enhanced E2F1-mediated transcription result in the formation of the CDK2-Cyclin E complex which subsequently hyperphosphorylates Rb, leading to increased expression of genes critical for DNA synthesis during S-phase[245–247]. The binding of Cyclin A, the transcription of which is dependent upon E2F1 activity, to CDK2 then terminates S phase by phosphorylating E2F1, thus abrogating its DNA-binding ability and forming a negative feedback loop[248–250]. During late S phase, Cyclin A forms a complex with CDK1 and is subsequently degraded upon entry into G2/M, resulting in formation of CDK1-Cyclin B complexes which bind to, phosphorylate and enhance the activity of FOXM1 transcription factors, thereby upregulating the expression of genes indispensable for mitosis[251,252]. Phosphorylation of the cytoplasmic-retention sequence on Cyclin B during late prophase is a critical step in mitotic progression,

resulting in rapid nuclear translocation[253]. The CDK1-Cyclin B complex subsequently phosphorylates multiple nuclear-localised substrates resulting in reorganisation of the nuclear architecture and eventual degradation of the nuclear membrane in preparation for mitosis[253–257]. CDK1-Cyclin B1-mediated activation of APC eventually promotes its own destruction, allowing chromosomal separation and cytokinesis[252]. Protein phosphatase 1 (PP1) then dephosphorylates Rb, allowing it to once more repress and bind E2F1 and HDAC1, thus preventing repetition of the cell cycle until appropriate mitogenic stimulation is received[258,259].

3.6.2. The role of CDKs in regulating transcriptional fidelity

Whilst CDKs are a vital mechanistic component in cell cycle regulation, they are equally as important for the correct transcription of protein-coding genes by RNA Polymerase II (RNA II). The C-terminal domain (CTD) of RNA II serves as a scaffold for the recruitment of key transcriptional regulators, including various CDKs, and the phosphorylation of numerous amino acid residues on this domain directly influences the fidelity of transcriptional initiation, elongation and termination[260,261]. For transcription to be initiated, RNA II must be recruited to the promoter of the gene in question and it must eventually vacate this position to permit transcriptional elongation[261]. The first step in transcriptional initiation involves the formation of the pre-initiation complex at the gene promoter. This process begins with the binding of the TATA-box binding protein (TBP) domain of general transcription factor TFIID to the core promoter and the subsequent association of RNA II with the Mediator complex by virtue of the affinity of its unmodified CTD for hydrophobic residues in the latter[262–264]. The Mediator complex is a crucial transcriptional co-activator which serves to recruit pro-elongation factors such as P-TEFb and to transduce signals from transcription factors bound at gene enhancer regions to the pre-initiation

complex machinery at gene promoters[265–268]. Mediator function is also governed by CDK8, which transiently associates with the Mediator complex and is therefore able to directly phosphorylate and thus modify the function of transcription factors, an event believed to be mutually exclusive with RNA II-Mediator binding and a putative transcriptional checkpoint[269,270]. The transition from initiation to elongation involves the recruitment of TFIIH to the pre-initiation complex, its helicase component inducing a conformational change in the DNA which facilitates the interaction of single-stranded DNA with the active site of RNA II[271,272]. CDK7 is a catalytic component of TFIIH and phosphorylates the CTD of RNA II at Ser5 and Ser7, thereby disrupting the interaction of RNA II with the pre-initiation complex and promoting the detachment of RNA II from the gene promoter[273,274]. CDK7 also possesses myriad functions other than transcriptional regulation, since it controls the functions of cell cycle-regulatory CDKs by phosphorylating CDK1 and CDK2, thus acting as a CDK-activating kinase (CAK) and linking transcription with cell cycle progression[275]. Elegant work conducted by Larochelle et al (2007) demonstrated that CDK7 inhibition during G1 phase impeded CDK2 activation and consequently hindered progression into S phase, whilst CDK7 inhibition during G2 phase and/or S phase prevented the onset of mitosis and activation of CDK1, with co-immunoprecipitation revealing disruption of the formation of CDK1-Cyclin B complexes[276]. Moreover, CDK7 has also been shown to regulate CDK4/6 function and is therefore essential for G1/S phase transition; CDK7 inhibition lead to the abrogation of Rb-kinase activity of both CDK4 and CDK6, due to impaired CDK4/6 activation and not due to inhibition of CDK4/6-Rb complex formation[277]. Furthermore, CDK7-mediated phosphorylation of the T-loops of CDK4 and CDK6 was required for maintenance of their activity, not just their activation, reinforcing the idea of CDK7 as

a master regulator of CDK function[277]. Intriguingly, apart from controlling transcriptional elongation and the activation of cell cycle-regulatory CDKs, CDK7 may also serve as a link between the transcriptional machinery and activation of the DNA damage response by p53. In response to DNA damage, CDK7 has been shown to phosphorylate and thereby activate p53, enhancing its binding with p53-responsive DNA elements[278,279]. In return, p53 binding reduces the activity of CDK7 at both the CTD of RNA II and CDK2, potentially leading to inhibition of transcription and subsequent cell cycle arrest[280]. CDK7-mediated CTD phosphorylation on Ser5 and Ser7 leads to “proximal promoter pausing” in which RNA II pauses approximately 20-100bps downstream of the transcriptional start site, thereby allowing mRNA modification and the binding of negative elongation factor (NELF) and DRB sensitivity-inducing factor (DSIF) to RNA II, preventing productive elongation of mRNA transcripts[281,282]. For productive elongation to occur, positive transcription elongation factor B (P-TEFb) which is composed of CDK9 and Cyclin T1, must be recruited to promoters and the associated transcriptional machinery[283,284]. Bromodomain-containing protein 4 (BRD4) is a chromatin reader needed for the transmission of epigenetic signatures during cell division. BRD4 binds to acetylated histones in all cell cycle phases to promote the maintenance of acetylated chromatin and its high-order architecture[285–289]. Crucially, BRD4 is required for both the formation of P-TEFb and its recruitment to promoters; via its P-TEFb-interacting domain (PID), BRD4 associates with P-TEFb and facilitates the dissociation of negative regulators (e.g. 7SKsnRNA) from P-TEFb, thereby activating the complex. CDK9 then phosphorylates both NELF and DSIF, resulting in NELF dissociation and conversion of DSIF into a positive elongation factor[290–292]. Concurrently, CDK9 phosphorylates the CTD of RNA II at Ser2, allowing the recruitment of more

elongation factors and the initiation of productive mRNA elongation. Additionally, BRD4 has been shown to potentiate the kinase activity of P-TEFb at promoters located in regions of highly acetylated chromatin, and render it less susceptible to inhibition, despite lacking CTD kinase activity itself[293–295]. Notably, the recruitment of P-TEFb, and thus CDK9-mediated Ser2 phosphorylation, is dependent upon the presence of phosphorylated Ser5 and Ser7 residues in the CTD, also indicating cross-talk between CDK7 and CDK9[276,296]. The presence of phosphorylated Ser2 on the CTD of RNA II also recruits factors required for termination of transcription and polyadenylation of mRNA transcripts[297,298]; once a termination signal is recognised by RNA Pol II, the phosphatases CTDP1 and SSU72 remove CTD phosphorylation marks at Ser2 and Ser5, restoring CTD phosphorylation to pre-initiation levels, whilst SSU72 also promotes cleavage of pre-mRNA transcripts to complete the process, allowing detachment of RNA II from the promoter and termination of transcription[299,300].

3.6.3. Targeting transcriptional CDKs in oncology

Given their critical roles in the regulation of transcriptional elongation as well as the regulation of cell cycle components in the case of CDK7, the pharmacological inhibition of both CDK7 and CDK9 has been the subject of multiple investigations into their potential utility as anticancer drug targets. Various studies have shown that multiple cancers are indeed exquisitely sensitive to CDK7 inhibitors (e.g. THZ1) and/or CDK9-specific inhibitors, including ovarian carcinoma, neuroblastoma, glioma, non-small cell lung cancer (NSCLC) and T-cell lymphomas[302–309]. Common to the majority of these cases, CDK7/9 inhibition led to downregulation of MYC resulting in decreased levels of short-lived, pro-survival, anti-apoptotic proteins such as MCL-1, leading to reduced cell proliferation and apoptosis[302,303,306,307,310]. As a

consequence, cells were also rendered more sensitive to BH3-mimetics such as ABT-199, with strong synergy observed in both T-cell lymphomas and acute myeloid leukaemia[302,311]. Moreover, in MYC-addicted hepatocellular carcinoma, CDK9-mediated transcription of MYC-regulated genes was found to be indispensable for MYC-driven tumourigenesis[312]. Inhibition of transcriptional elongation, regulated by CDK9 via phosphorylation of RNA-Polymerase II (Ser2/5), using a pharmacological cdc7/CDK9 inhibitor resulted in tumour regressions, abolition of tumour growth and decreased proliferative markers[312]. Regarding TNBC specifically, Horiuchi et al demonstrated that TNBC cells with elevated levels of MYC were particularly sensitive to pan-CDK inhibitors such as Dinaciclib[313]. Taken together, the evidence suggests that targeting currently non-druggable, master transcriptional regulators such as MYC, which act as a downstream convergence point for signals transduced via RTK-mediated signalling, through CDK7 or p-TEFb inhibition may represent a potent new strategy to identify novel therapies for TNBC as well as other cancers, whilst also identifying novel synergistic combinations with enhanced efficacy. Elaborate studies conducted by *Wang et al* illustrated that TNBC cells are uniquely dependent on transcriptional regulation, particularly by CDK7 and CDK9[314]. Their research demonstrated that a cluster of genes (including EGFR) whose transcription is regulated by CDK7 and which are associated with super-enhancers (clusters of enhancers with high transcriptional activity and which are characterised by exceptionally high levels of master transcription factor and Mediator complex binding[315]) was critical for the growth of TNBC cells[314]. Using multiple EGFR-TKIs, it was shown that despite clear inhibition of phosphorylation of EGFR and of its downstream components, cell proliferation was unaffected. However, CRISPR/Cas9-mediated editing of EGFR was detrimental to cell proliferation, with similar results

obtained using the CDK7 inhibitor THZ1, suggesting that eliminating EGFR transcriptional activity represents a more effective approach[314]. Zawitowski et al have recently demonstrated that TNBC tumours treated with Trametinib, a MEK inhibitor, rapidly rewire their signalling circuitry in order to bypass the effects of drug treatment, upregulating the levels of various RTKs such as PDGFR-B and FGFR2[109,316]. Disrupting p-TEFb activation through BRD4 inhibition potently reversed this adaptive transcriptional response, precluding RTK-upregulation and leading to durable responses in xenograft models of TNBC[316]. Interestingly, combining lapatinib treatment with BRD4 inhibitor JQ1 in HER2+ BC similarly led to abolition of an

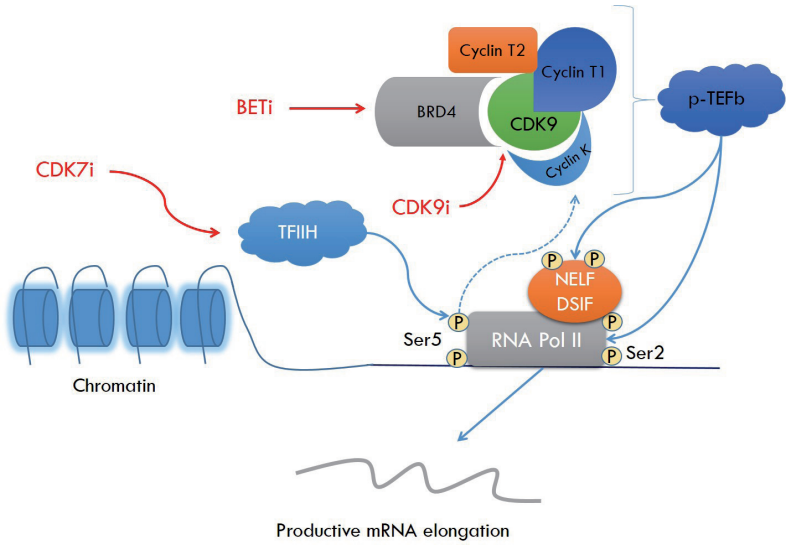

Figure 3: Drugging the transcriptional machinery in cancer. Possible ways of targeting the transcriptional machinery in malignant cells are represented here. Interfering with TFIIH function by inhibiting CDK7 would prevent phosphorylation of RNA Polymerase II's C-terminal domain (CTD) at Ser5, thereby precluding the initiation of transcription since TFIIH facilitates interaction of RNA Polymerase II with DNA. The TFIIH-dependent recruitment of the P-TEFb complex, a member of the super elongation complex (SEC) whose CDK9-mediated phosphorylation of RNA Polymerase II's CTD at Ser2 is vital for productive elongation of mRNA transcripts, would therefore also be averted. P-TEFb itself and its various components are also amenable to pharmacological manipulation. Kinase inhibitors which block the activity of CDK9 would obstruct CDK9-mediated phosphorylation of RNA Polymerase II's CTD at Ser2, as well as the dissociation of negative elongation factors NELF and DSIF, which induce proximal promoter pausing after CDK7-mediated phosphorylation of CTD residue Ser5, ultimately preventing resumption of productive mRNA transcription. Impeding BRD4 function by means of bromodomain inhibitors could also disrupt activation of the kinase component of P-TEFb, as well as its subsequent recruitment to the transcriptional machinery.

adaptive kinome response and reversal of resistance to lapatinib[317]. This evidence reiterates the utility of targeting the transcriptional program of cancer cells addicted to growth factor receptor signalling pathways by halting enhancer remodelling and transcriptional adaptation (see ***Figure 3***). However, there is a paucity of information regarding the possible use of EGFR-TKIs in combination inhibitors which interfere with P-TEFb function in TNBCs resistant to EGFR-TKI monotherapy. Since EGFR-TKIs are notoriously ineffective as monotherapies against TNBC, despite the dependence of these tumours on EGFR-mediated signalling, there is a clear rationale to inhibit both RTK-mediated signalling at the source and the P-TEFb complex which regulates the transcription of genes up-regulated via activation of these growth factor-mediated pathways. This two-pronged approach would seek to reverse the intrinsic resistance of TNBC cells to RTK-targeted therapies by eliminating their propensity for transcriptional plasticity in response to therapy, thereby sensitising them to EGFR-TKIs.

4. Conclusion

In summary, TNBC employs a vast arsenal of resistance mechanisms in order to evade elimination. This arsenal primarily consists of subversion of cellular signalling networks in response to kinase-targeted therapy, a testament to the plasticity of this disease. Evidently, given the critical role of transcription in the conduction and regulation of these adaptive responses, inhibition of such transcriptional machinery therefore represents an attractive strategy for the reversal of resistance to targeted therapies such as EGFR-tyrosine kinase inhibitors or PI3K-AKT-mTOR inhibitors. Notwithstanding the promising pre-clinical studies of transcriptional CDK inhibitors described here, the development of highly efficacious, selective agents remains an elusive prospect. This lack of specificity often results in undesirable or even life-

threatening side-effects, thereby limiting the anti-cancer potential of such agents. Future drug design programmes must therefore identify methods to circumvent the structural similarity between the various CDKs in order to address these issues. Moreover, whilst combining multiple kinase inhibitors as a means of depleting cancer cells of options to rewire their survival signalling appears sensible, the importance of practical considerations regarding dosage, toxicity and contraindications cannot be understated. Altogether, multiple options exist regarding the use of molecular targeted therapy against TNBC, including, but not limited to, DNA-damaging agents, EGFR-tyrosine kinase inhibitors, PI3K-Akt-mTOR inhibitors, FGFR inhibitors and CDK inhibitors. However, given the intricate and innumerable mechanisms of resistance, thinking one step ahead in order to predict and subsequently target possible pathways implicated in the development of resistance to such agents is essential if progress is to be made in improving the clinical management of TNBC.

5. Aims and Outline of this Thesis

The primary objective of the research described in this thesis was to identify novel therapeutic targets and synergistic combination treatments for TNBC. Primarily, this research focused on profiling the response of TNBC to multiple kinase inhibitors (e.g. MEK, AKT and EGFR inhibitors) and ascertaining which targeted agents were capable of subverting the refractory response of TNBC thereto, by means of high-throughput, compound library-based screening. Consequently, the potential of prospective, novel targeted agents, specifically CDK inhibitors, either as monotherapies or in combination with other kinase inhibitors was thoroughly evaluated. **Chapter 2** explores the differential sensitivity of TNBC cells to MEK and AKT inhibitors, illustrating the heterogeneity in response to such targeted agents. Here, the link between resistance to MEK/AKT inhibitors and cell cycle regulation is

emphasised, as well as how this cell cycle dependency can be exploited therapeutically in drug-resistant subtypes using potent CDK inhibitors. **Chapter 3** delineates the potential of combined cdc7/CDK9 inhibition as a means to overcome resistance to multiple EGFR-TKIs in TNBC. **Chapter 4** elaborates on these findings by describing the evaluation of a panel of novel CDK inhibitors as potential therapeutic agents in TNBC both *in vitro* and *in vivo*. Here, compound-based screening coupled with proliferation and apoptosis assays demonstrates that a selection of these novel CDK inhibitors are highly effective as anti-TNBC therapies. The effect of these drugs on relevant signal transduction pathways such as CDK-mediated transcription and the equilibrium between pro- and anti-apoptotic BCL-2 family members is extensively examined here. RNA Seq-based transcriptomic analysis was employed to further clarify the mechanisms of action of these compounds and define a set of transcription factors essential for TNBC proliferation, and which are exquisitely sensitive to CDK inhibition. The utility of combining EGFR-TKIs and BET inhibitor JQ1 with one of these novel CDK inhibitors is described in **Chapter 5**, in which it is shown that combining these agents is synergistic in inhibiting the proliferation of TNBC cells and augments the inhibitory effect of the CDK inhibitor on transcription and CDK-mediated signal transduction. Finally, **Chapter 6** provides a discussion and summary of the aforementioned results, focusing on the key conclusions derived from this research and possible avenues for future research.

References

1. Jemal, A., Bray, F. & Ferlay, J. Global Cancer Statistics. *CA Cancer J Clin*. **61,** 69–90 (2011).
2. Johnson, K. C. *et al.* Active smoking and secondhand smoke increase breast cancer risk: the report of the Canadian Expert Panel on Tobacco Smoke and Breast Cancer Risk (2009). *Tob. Control* **20,** e2 (2011).
3. Ronckers, C. M., Erdmann, C. a & Land, C. E. Radiation and breast cancer: a review of current evidence. *Breast Cancer Res.* **7,** 21–32 (2005).
4. Colditz, A. & Willett, W. C. NIH Public Access. *JAMA*. **306 (17),** 1884–1890 (2012).
5. Schedin, P. Pregnancy-associated breast cancer and metastasis. *Nat. Rev. Cancer* **6,** 281–91 (2006).
6. Hall, M. J. *et al.* Genetic testing for hereditary cancer predisposition: BRCA1/2, Lynch syndrome, and beyond. *Gynecol. Oncol.* **140,** 565–74 (2016).
7. Roy, R., Chun, J. & Powell, S. N. BRCA1 and BRCA2 : different roles in a common pathway of genome protection. *Nat Rev Cancer* **12 (1)**: 68-78 (2012).
8. Petersen, O. W. & Polyak, K. Stem Cells in the Human Breast. *Cold Spring Harb Prospect Biol.* **2 (5),** (2016).
9. Stingl, J., Eaves, C. J., Zandieh, I. & Emerman, J. T. Characterization of bipotent mammary epithelial progenitor cells in normal adult human breast tissue. *Breast Cancer Res. Treat.* **67,** 93–109 (2001).
10. Villadsen, R. *et al.* Evidence for a stem cell hierarchy in the adult human breast. *J. Cell Biol.* **177,** 87–101 (2007).
11. Polyak, K. Science in medicine Breast cancer : origins and evolution. *J Clin Invest*. **117 (11):** 3155-63 (2007).
12. Ishikawa, F. *et al.* Chemotherapy-resistant human AML stem cells home to and engraft within the bone-marrow endosteal region. *Nat. Biotechnol.* **25,** 1315–21 (2007).
13. Hu, X. *et al.* Genetic alterations and oncogenic pathways associated with breast cancer subtypes. *Mol. Cancer Res.* **7,** 511–22 (2009).
14. van Rhenen, A. *et al.* High stem cell frequency in acute myeloid leukemia at diagnosis predicts high minimal residual disease and poor survival. *Clin. Cancer Res.* **11,** 6520–7 (2005).
15. Singh, S. K. *et al.* Identification of human brain tumour initiating cells. *Nature* **432,** 396–401 (2004).
16. Pistollato, F. *et al.* Intratumoral hypoxic gradient drives stem cells distribution and MGMT expression in glioblastoma. *Stem Cells* **28,** 851–62 (2010).
17. Liu, G. *et al.* Analysis of gene expression and chemoresistance of CD133+ cancer stem cells in glioblastoma. *Mol. Cancer* **5**: 67 (2006).

18. Yu, F. *et al.* Let-7 Regulates Self Renewal and Tumorigenicity of Breast Cancer Cells. *Cell* **131,** 1109–23 (2007).

19. Creighton, C. J. *et al.* Residual breast cancers after conventional therapy display mesenchymal as well as tumor-initiating features. *Proc. Natl. Acad. Sci. U. S. A.* **106,** 13820–5 (2009).

20. Al-Hajj, M., Wicha, M. S., Benito-Hernandez, a., Morrison, S. J. & Clarke, M. F. Prospective identification of tumorigenic breast cancer cells. *Proc. Natl. Acad. Sci.* **100,** 3983–3988 (2003).

21. Ginestier, C. *et al.* ALDH1 is a marker of normal and malignant human mammary stem cells and a predictor of poor clinical outcome. *Cell Stem Cell* **1,** 555–67 (2007).

22. Brooks, M. D., Burness, M. L. & Wicha, M. S. Therapeutic Implications of Cellular Heterogeneity and Plasticity in Breast Cancer. *Cell Stem Cell* **17,** 260–71 (2015).

23. Shipitsin, M. *et al.* Molecular definition of breast tumor heterogeneity. *Cancer Cell* **11,** 259–73 (2007).

24. Anderson, K. *et al.* Genetic variegation of clonal architecture and propagating cells in leukaemia. *Nature* **469,** 356–61 (2011).

25. Piccirillo, S. G. M. *et al.* Distinct pools of cancer stem-like cells coexist within human glioblastomas and display different tumorigenicity and independent genomic evolution. *Oncogene* **28,** 1807–11 (2009).

26. Liu, S. *et al.* Breast cancer stem cells transition between epithelial and mesenchymal states reflective of their normal counterparts. *Stem cell reports* **2,** 78–91 (2014).

27. Idowu, M. O. *et al.* CD44(+)/CD24(-/low) cancer stem/progenitor cells are more abundant in triple-negative invasive breast carcinoma phenotype and are associated with poor outcome. *Hum. Pathol.* **43,** 364–73 (2012).

28. Samanta, D., Gilkes, D. M., Chaturvedi, P., Xiang, L. & Semenza, G. L. Hypoxia-inducible factors are required for chemotherapy resistance of breast cancer stem cells. *Proc. Natl. Acad. Sci. U. S. A.* **111,** E5429-38 (2014).

29. Jesinger, R. A. Breast anatomy for the interventionalist. *Techniques in Vascular and Interventional Radiology* **17,** 3–9 (2014).

30. Malhotra, G. K., Zhao, X., Band, H. & Band, V. Histological, molecular and functional subtypes of breast cancers. *Cancer Biol. Ther.* **10,** 955–960 (2014).

31. Association of Directors of Anatomic and Surgical Pathology, Recommendations for the Reporting of Breast Carcinoma. *American Journal of Clinical Pathology* **104**: 614–619 (1995).

32. Li, C. I., Uribe, D. J. & Daling, J. R. Clinical characteristics of different histologic types of breast cancer. *Br. J. Cancer* **93,** 1046–52 (2005).

33. Makki, J. Diversity of Breast Carcinoma : Histological Subtypes and Clinical Relevance. *Clin Med Insights Pathol,* **8**: 23–31 (2015).

34. Foulkes, W.D. *et al,* Triple-Negative Breast Cancer. *N Engl J Med*, **363**:1938-48

(2010).

35. Perou, C. M. *et al.* Molecular portraits of human breast tumours. *Nature,* **17**;406 (6797): 747-52 (2000).

36. Sørlie, T. *et al.* Gene expression patterns of breast carcinomas distinguish tumor subclasses with clinical implications. *PNAS*, **98 (19)**: 10869-10874 (2001).

37. Gomez, H. L. *et al.* Efficacy and safety of lapatinib as first-line therapy for ErbB2-amplified locally advanced or metastatic breast cancer. *J. Clin. Oncol.* **26,** 2999–3005 (2008).

38. Vogel, CL. *et al.* Efficacy and Safety of Trastuzumab as a Single Agent in first-line treatment of HER2-overexpressing metastatic breast cancer. *J Clin Oncol*. **20,** 719–726 (2016).

39. Dent, R. *et al.* Pattern of metastatic spread in triple-negative breast cancer. *Breast Cancer Res. Treat.* **115,** 423–8 (2009).

40. Cheang, M. C. U. *et al.* Basal-like breast cancer defined by five biomarkers has superior prognostic value than triple-negative phenotype. *Clin. Cancer Res.* **14,** 1368–76 (2008).

41. Boyle, P. Triple-negative breast cancer: epidemiological considerations and recommendations. *Ann. Oncol.* **23 Suppl 6,** vi7-12 (2012).

42. Carey, L. a *et al.* Race, breast cancer subtypes, and survival in the Carolina Breast Cancer Study. *Jama* **295,** 2492–502 (2006).

43. Morris, G. J. *et al.* Differences in breast carcinoma characteristics in newly diagnosed African-American and Caucasian patients: a single-institution compilation compared with the National Cancer Institute's Surveillance, Epidemiology, and End Results database. *Cancer* **110,** 876–84 (2007).

44. Thike, A. A. *et al.* Triple-negative breast cancer: clinicopathological characteristics and relationship with basal-like breast cancer. *Mod. Pathol.* **23,** 123–33 (2010).

45. Rakha, E. a *et al.* Prognostic markers in triple-negative breast cancer. *Cancer* **109,** 25–32 (2007).

46. Nam, B.-H. *et al.* Breast cancer subtypes and survival in patients with brain metastases. *Breast Cancer Res.* **10 (1)**: R20 (2008).

47. Kennecke, H. *et al.* Metastatic behavior of breast cancer subtypes. *J. Clin. Oncol.* **28,** 3271–7 (2010).

48. Lehmann, B. D. *et al.* Identification of human triple-negative breast cancer subtypes and preclinical models for selection of targeted therapies. *J. Clin. Invest.* **121 (7)**: 2750-67 (2011).

49. Abramson, V. G., Lehmann, B. D., Ballinger, T. J. & Pietenpol, J. A. Subtyping of triple-negative breast cancer: Implications for therapy. *Cancer* **121,** 8–16 (2015).

50. Lehmann, B. D. *et al.* PIK3CA mutations in androgen receptor-positive triple negative breast cancer confer sensitivity to the combination of PI3K and

androgen receptor inhibitors. *Breast Cancer Res.* **16 (4)**: 406 (2014).

51. Masuda, H. *et al.* Differential response to neoadjuvant chemotherapy among 7 triple-negative breast cancer molecular subtypes. *Clin. Cancer Res.* **19,** 5533–40 (2013).

52. Lehmann, B. D. *et al.* Refinement of Triple-Negative Breast Cancer Molecular Subtypes: Implications for Neoadjuvant Chemotherapy Selection. *PLoS One* **11,** e0157368 (2016).

53. Prat, A. *et al.* Phenotypic and molecular characterization of the claudin-low intrinsic subtype of breast cancer. *Breast Cancer Res.* **12 (5)**: R68 (2010).

54. Hennessy, B. T. *et al.* Characterization of a Naturally Occurring Breast Cancer Subset Enriched in Epithelial-to-Mesenchymal Transition and Stem Cell Characteristics. *Cancer Res.* **69,** 4116–4124 (2009).

55. Sotiriou, C. *et al.* Breast cancer classification and prognosis based on gene expression profiles from a population-based study. *Proc. Natl. Acad. Sci. U. S. A.* **100,** 10393–10398 (2003).

56. Vallejos, C. *et al.* Breast cancer classification according to immunohistochemistry markers: Subtypes and association with clinicopathologic variables in a peruvian hospital database. *Clin. Breast Cancer* **10,** 294–300 (2010).

57. Cheang, M. C. U. *et al.* Ki67 index, HER2 status, and prognosis of patients with luminal B breast cancer. *J. Natl. Cancer Inst.* **101,** 736–750 (2009).

58. Prat, A. *et al.* Clinical implications of the intrinsic molecular subtypes of breast cancer. *Breast* **24,** S26–S35 (2015).

59. Prat, A. & Perou, C. M. Mammary development meets cancer genomics. *Nat. Publ. Gr.* **15 (8)**: 842-4 (2009).

60. Eiermann, W. & Vallis, K. A. Locoregional treatments for triple-negative breast cancer. *Ann. Oncol.* **23,** Suppl 6: vi30-4 (2012).

61. Senkus, E. *et al.* Primary breast cancer: ESMO Clinical Practice Guidelines for diagnosis, treatment and follow-up. *Ann. Oncol.* **26,** v8–v30 (2015).

62. Rodler, E., Korde, L. & Gralow, J. Current treatment options in triple negative breast cancer. *Breast Dis.* **32,** 99–122 (2010).

63. Agarwal, G. *et al.* Outcomes of Triple-Negative Breast Cancers (TNBC) Compared with Non-TNBC: Does the Survival Vary for All Stages? *World J. Surg.* **40,** 1362–1372 (2016).

64. Pennisi, A., Kieber-Emmons, T., Makhoul, I. & Hutchins, L. Relevance of pathological complete response after neoadjuvant therapy for breast cancer. *Breast Cancer Basic Clin. Res.* **10,** 103–106 (2016).

65. Wahba, H. A. & El-Hadaad, H. A. Current approaches in treatment of triple-negative breast cancer. *Cancer Biol. Med.* **12,** 106–16 (2015).

66. Cleator, S., Heller, W. & Coombes, R. C. Triple-negative breast cancer: therapeutic options. *Lancet Oncol.* **8,** 235–244 (2007).

67. Masuda, H. *et al.* Predictive factors for the effectiveness of neoadjuvant chemotherapy and prognosis in triple-negative breast cancer patients. *Cancer Chemother. Pharmacol.* **67,** 911–917 (2011).

68. Liedtke, C. *et al.* Response to neoadjuvant therapy and long-term survival in patients with triple-negative breast cancer. *J. Clin. Oncol.* **26,** 1275–81 (2008).

69. Balko, J. M. *et al.* Molecular profiling of the residual disease of triple-negative breast cancers after neoadjuvant chemotherapy identifies actionable therapeutic targets. *Cancer Discov.* **4,** 232–245 (2014).

70. Kalimutho, M. *et al.* Targeted Therapies for Triple-Negative Breast Cancer: Combating a Stubborn Disease. *Trends Pharmacol. Sci.* **36,** 822–46 (2015).

71. Cardoso, F. *et al.* 1st International consensus guidelines for advanced breast cancer (ABC 1). *Breast* **21,** 242–252 (2012).

72. Kassam, F. *et al.* Survival outcomes for patients with metastatic triple-negative breast cancer: Implications for clinical practice and trial design. *Clin. Breast Cancer* **9,** 29–33 (2009).

73. Gómez-Miragaya, J. *et al.* Resistance to Taxanes in Triple-Negative Breast Cancer Associates with the Dynamics of a CD49f+ Tumor-Initiating Population. *Stem Cell Reports* **8,** 1392–1407 (2017).

74. Wein, L. & Loi, S. Mechanisms of resistance of chemotherapy in early-stage triple negative breast cancer (TNBC). *Breast* **34**, Suppl 1:S27-S30, (2017).

75. Groenendijk, F. H. & Bernards, R. Drug resistance to targeted therapies: déjà vu all over again. *Mol. Oncol.* **8,** 1067–83 (2014).

76. Holohan, C., Van Schaeybroeck, S., Longley, D. B. & Johnston, P. G. Cancer drug resistance: an evolving paradigm. *Nat. Rev. Cancer* **13,** 714–26 (2013).

77. Ramos, P. & Bentires-Alj, M. Mechanism-based cancer therapy: resistance to therapy, therapy for resistance. *Oncogene* **34 (28)**: 3617-26 (2015)

78. Doyle, L. A. *et al.* A multidrug resistance transporter from human MCF-7 breast cancer cells. *Proc. Natl. Acad. Sci. U. S. A.* **95,** 15665–70 (1998).

79. Balaji, S. A., Udupa, N., Chamallamudi, M. R., Gupta, V. & Rangarajan, A. Role of the drug transporter ABCC3 in breast cancer chemoresistance. *PLoS One* **11 (5)**: e0155013 (2016).

80. Lou, H. & Dean, M. Targeted therapy for cancer stem cells: The patched pathway and ABC transporters. *Oncogene* **26,** 1357–1360 (2007).

81. Shervington, A. & Lu, C. Expression of multidrug resistance genes in normal and cancer stem cells. *Cancer Invest.* **26,** 535–542 (2008).

82. Reya, T., Morrison, S. J., Clarke, M. F. & Weissman, I. L. Stem cells, cancer, and cancer stem cells. *Nature* **414,** 105–11 (2001).

83. McDermott, S. P. & Wicha, M. S. Targeting breast cancer stem cells. *Mol. Oncol.* **4,** 404–19 (2010).

84. Desai, A., Webb, B. & Gerson, S. L. CD133+ cells contribute to radioresistance via altered regulation of DNA repair genes in human lung cancer cells.

Radiother. Oncol. **110,** 538–545 (2014).

85. Bao, S. *et al.* Glioma stem cells promote radioresistance by preferential activation of the DNA damage response. *Nature* **444,** 756–760 (2006).

86. Salehan, M. R. & Morse, H. R. DNA damage repair and tolerance: A role in chemotherapeutic drug resistance. *British Journal of Biomedical Science* **70,** 31–40 (2013).

87. Bryant, H. E. *et al.* Specific killing of BRCA2-deficient tumours with inhibitors of poly(ADP-ribose) polymerase. *Nature* **434,** 913–917 (2005).

88. Farmer, H. *et al.* Targeting the DNA repair defect in BRCA mutant cells as a therapeutic strategy. *Nature* **434,** 917–921 (2005).

89. Helleday, T. The underlying mechanism for the PARP and BRCA synthetic lethality: clearing up the misunderstandings. *Mol. Oncol.* **5,** 387–93 (2011).

90. Dedes, K. J. *et al.* Synthetic lethality of PARP inhibition in cancers lacking BRCA1 and BRCA2 mutations. *Cell Cycle* **10,** 1192–1199 (2011).

91. Lord, C. J. & Ashworth, A. PARP inhibitors: Synthetic lethality in the clinic. *Science* **355,** 1152–1158 (2017).

92. Edwards, S. L. *et al.* Resistance to therapy caused by intragenic deletion in BRCA2. *Nature* **451,** 1111–1115 (2008).

93. Alli, E. *et al.* Enhanced sensitivity to cisplatin and gemcitabine in Brca1-deficient murine mammary epithelial cells. *BMC Pharmacol.* **11,** 7 (2011).

94. Sequist, L. V. *et al.* First-line gefitinib in patients with advanced non-small-cell lung cancer harboring somatic EGFR mutations. *J. Clin. Oncol.* **26,** 2442–2449 (2008).

95. Bose, R. *et al.* Activating HER2 mutations in HER2 gene amplification negative breast cancer. *Cancer Discov.* **3,** 224–237 (2013).

96. Druker, B. J. *et al.* Effects of a selective inhibitor of the Abl tyrosine kinase on the growth of Bcr–Abl positive cells. *Nat. Med.* **2,** 561–566 (1996).

97. Weinstein, I. B. & Joe, A. K. Mechanisms of Disease: oncogene addiction—a rationale for molecular targeting in cancer therapy. *Nat. Clin. Pract. Oncol.* **3,** 448–457 (2006).

98. Lynch, T. J. *et al.* Activating mutations in the epidermal growth factor receptor underlying responsiveness of non-small-cell lung cancer to gefitinib. *N Engl J Med* **350,** 2129–2139 (2004).

99. Pao, W. *et al.* EGF receptor gene mutations are common in lung cancers from never smokers'' and are associated with sensitivity of tumors to gefitinib and erlotinib. *Proc Natl Acad Sci USA.* **101 (36)***:* 13306-11 (2004).

100. Bell, D. W. *et al.* Inherited susceptibility to lung cancer may be associated with the T790M drug resistance mutation in EGFR. *Nat. Genet.* **37,** 1315–1316 (2005).

101. Kobayashi, S. *et al. EGFR* Mutation and Resistance of Non–Small-Cell Lung Cancer to Gefitinib. *N. Engl. J. Med.* **352,** 786–792 (2005).

102. Shah, N. P. *et al.* Multiple BCR-ABL kinase domain mutations confer polyclonal resistance to the tyrosine kinase inhibitor imatinib (STI571) in chronic phase and blast crisis chronic myeloid leukemia. *Cancer Cell* **2,** 117–125 (2002).

103. Zuo, W. J. *et al.* Dual characteristics of novel HER2 kinase domain mutations in response to HER2-targeted therapies in human breast cancer. *Clin. Cancer Res.* **22,** 4859–4869 (2016).

104. Wagle, N. *et al.* Dissecting therapeutic resistance to RAF inhibition in melanoma by tumor genomic profiling. *J. Clin. Oncol.* **29,** 3085–3096 (2011).

105. Johannessen, C. M. *et al.* COT drives resistance to RAF inhibition through MAP kinase pathway reactivation. *Nature* **468,** 968–972 (2010).

106. Wheeler, D. L. *et al.* Mechanisms of acquired resistance to cetuximab: Role of HER (ErbB) family members. *Oncogene* **27,** 3944–3956 (2008).

107. Huang, S. *et al.* Dual targeting of EGFR and HER3 with MEHD7945A overcomes acquired resistance to EGFR inhibitors and radiation. *Cancer Res.* **73,** 824–833 (2013).

108. Iida, M. *et al.* Overcoming acquired resistance to cetuximab by dual targeting HER family receptors with antibody-based therapy. *Mol. Cancer* **13,** 242 (2014).

109. Duncan, J. S. *et al.* Dynamic reprogramming of the kinome in response to targeted MEK inhibition in triple-negative breast cancer. *Cell* **149,** 307–21 (2012).

110. Bean, J. *et al.* MET amplification occurs with or without T790M mutations in EGFR mutant lung tumors with acquired resistance to gefitinib or erlotinib. *Proc. Natl. Acad. Sci.* **104,** 20932–20937 (2007).

111. Hanahan, D. & Weinberg, R. A. The hallmarks of cancer. *Cell* **100,** 57–70 (2000).

112. Han, J., Goldstein, L. A., Gastman, B. R. & Rabinowich, H. Interrelated roles for Mcl-1 and BIM in regulation of TRAIL-mediated mitochondrial apoptosis. *J. Biol. Chem.* **281,** 10153–10163 (2006).

113. Delbridge, A. R. D. & Strasser, A. The BCL-2 protein family , BH3-mimetics and cancer therapy. *Cell Death Differ.* **22,** 1071–1080 (2015).

114. Yang, J. *et al.* Prevention of apoptosis by Bcl-2: Release of cytochrome c from mitochondria blocked. *Science,* **275,** 1129–1132 (1997).

115. Perciavalle, R. M. *et al.* Anti-apoptotic MCL-1 localizes to the mitochondrial matrix and couples mitochondrial fusion to respiration. *Nat. Cell Biol.* **14,** 575–583 (2012).

116. Simonian, P. L., Grillot, D. a & Nuñez, G. Bcl-2 and Bcl-XL can differentially block chemotherapy-induced cell death. *Blood* **90,** 1208–16 (1997).

117. Deveraux, Q. L., Takahashi, R., Salvesen, G. S. & Reed, J. C. X-linked IAP is a direct inhibitor of cell-death proteases. *Nature* **388,** 300–304 (1997).

118. Tamm, I. *et al.* IAP-family protein Survivin inhibits caspase activity and apoptosis induced by Fas (CD95), bax, caspases, and anticancer drugs.

Cancer Res. **58,** 5315–5320 (1998).

119. Li, F. *et al.* Control of apoptosis and mitotic spindle checkpoint by survivin. *Nature* **396,** 580–584 (1998).

120. Beroukhim, R. *et al.* The landscape of somatic copy-number alteration across human cancers. *Nature* **463,** 899–905 (2010).

121. Majid, A. *et al.* BCL2 expression in chronic lymphocytic leukemia: lack of association with the BCL2 Ɣ938AĆC promoter single nucleotide polymorphism. *Blood.* **111 (2):** 874–877 (2008).

122. Costa, D. B. *et al.* BIM mediates EGFR tyrosine kinase inhibitor-induced apoptosis in lung cancers with oncogenic EGFR mutations. *PLoS Med.* **4,** 1669–1680 (2007).

123. Gong, Y. *et al.* Induction of BIM is essential for apoptosis triggered by EGFR kinase inhibitors in mutant EGFR-dependent lung adenocarcinomas. *PLoS Med.* **4,** 1655–1668 (2007).

124. Nakagawa, T. *et al.* Egfr-tki resistance due to BIM polymorphism can be circumvented in combination with HDAC inhibition. *Cancer Res.* **73,** 2428–2434 (2013).

125. Merino, D., Lok, S. W., Visvader, J. E. & Lindeman, G. J. Targeting BCL-2 to enhance vulnerability to therapy in estrogen receptor-positive breast cancer. *Oncogene* **35,** 1877–1887 (2016).

126. Dawson, S. J. *et al.* BCL2 in breast cancer: A favourable prognostic marker across molecular subtypes and independent of adjuvant therapy received. *Br. J. Cancer* **103,** 668–675 (2010).

127. Goodwin, C. M., Rossanese, O. W., Olejniczak, E. T. & Fesik, S. W. Myeloid cell leukemia-1 is an important apoptotic survival factor in triple-negative breast cancer. *Cell Death Differ.* **22 (12):** 2098–2106 (2015).

128. Oakes, S. R. *et al.* Sensitization of BCL-2-expressing breast tumors to chemotherapy by the BH3 mimetic ABT-737. *Proc. Natl. Acad. Sci.* **109,** 2766–2771 (2012).

129. Lee, K. *et al.* MYC and MCL1 Cooperatively Promote Chemotherapy-Resistant Breast Cancer Stem Cells via Regulation of Mitochondrial Oxidative Phosphorylation. *Cell Metab.* **26,** 633–647.e7 (2017).

130. Lee, K. *et al.* MYC and MCL1 Cooperatively Promote Chemotherapy-Resistant Breast Cancer Stem Cells via Regulation of Mitochondrial Oxidative Phosphorylation. *Cell Metab.* **26,** 633–647.e7 (2017).

131. Desgrosellier, J. S. & Cheresh, D. Integrins in cancer: biological implications and therapeutic opportunities. *Nat. Rev. Cancer* **10,** 9–22 (2010).

132. Seguin, L., Desgrosellier, J. S., Weis, S. M. & Cheresh, D. A. Integrins and cancer: Regulators of cancer stemness, metastasis, and drug resistance. *Trends in Cell Biology* **25,** 234–240 (2015).

133. Hood, J. D., Frausto, R., Kiosses, W. B., Schwartz, M. A. & Cheresh, D. A. Differential αv integrin-mediated Ras-ERK signaling during two pathways of

angiogenesis. *J. Cell Biol.* **162,** 933–943 (2003).

134. Bao, W. & Strömblad, S. Integrin αv-mediated inactivation of p53 controls a MEK1-dependent melanoma cell survival pathway in three-dimensional collagen. *J. Cell Biol.* **167,** 745–756 (2004).

135. Lesniak, D. *et al.* β1-integrin circumvents the antiproliferative effects of trastuzumab in human epidermal growth factor receptor-2-positive breast cancer. *Cancer Res.* **69,** 8620–8628 (2009).

136. Cirri, P. & Chiarugi, P. Cancer associated fibroblasts: the dark side of the coin. *Am. J. Cancer Res.* **1,** 482–97 (2011).

137. Wilson, T. R. *et al.* Widespread potential for growth-factor-driven resistance to anticancer kinase inhibitors. *Nature* **487,** 505–509 (2012).

138. Barnas, J. L., Simpson-Abelson, M. R., Yokota, S. J., Kelleher, R. J. & Bankert, R. B. T cells and stromal fibroblasts in human tumor microenvironments represent potential therapeutic targets. *Cancer Microenvironment* **3,** 29–47 (2010).

139. Raz, Y. & Erez, N. An inflammatory vicious cycle: Fibroblasts and immune cell recruitment in cancer. *Experimental Cell Research* **319,** 1596–1603 (2013).

140. Arteaga, C. L. & Engelman, J. a. ERBB receptors: from oncogene discovery to basic science to mechanism-based cancer therapeutics. *Cancer Cell* **25,** 282–303 (2014).

141. Yarden, Y. & Schlessinger, J. Epidermal growth factor induces rapid, reversible aggregation of the purified epidermal growth factor receptor. *Biochemistry* **26,** 1443–1451 (1987).

142. Lowenstein, E. J. *et al.* The SH2 and SH3 domain-containing protein GRB2 links receptor tyrosine kinases to ras signaling. *Cell* **70,** 431–442 (1992).

143. McGlade, C. J. *et al.* SH2 domains of the p85 alpha subunit of phosphatidylinositol 3-kinase regulate binding to growth factor receptors. *Mol. Cell. Biol.* **12,** 991–997 (1992).

144. Sakaguchi, K. *et al.* Shc phosphotyrosine-binding domain dominantly interacts with epidermal growth factor receptors and mediates Ras activation in intact cells. *Mol. Endocrinol. (Baltimore, Md)* **12,** 536–543 (1998).

145. Chattopadhyay, A., Vecchi, M., Ji, Q. S., Mernaugh, R. & Carpenter, G. The role of individual SH2 domains in mediating association of phospholipase C-γ1 with the activated EGF receptor. *J. Biol. Chem.* **274,** 26091–26097 (1999).

146. Walker, F. *et al.* Activation of the Ras/mitogen-activated protein kinase pathway by kinase-defective epidermal growth factor receptors results in cell survival but not proliferation. *Mol. Cell. Biol.* **18,** 7192–204 (1998).

147. Park, H. S. *et al.* High EGFR gene copy number predicts poor outcome in triple-negative breast cancer. *Mod. Pathol.* **27,** 1212–22 (2014).

148. Secq, V. *et al.* Triple negative breast carcinoma EGFR amplification is not associated with EGFR, Kras or ALK mutations. *Br. J. Cancer* **110,** 1045–52 (2014).

149. Reis-Filho, J. S. *et al.* EGFR amplification and lack of activating mutations in metaplastic breast carcinomas. *J. Pathol.* **209,** 445–53 (2006).

150. Gumuskaya, B. *et al.* EGFR expression and gene copy number in triple-negative breast carcinoma. *Cancer Genet. Cytogenet.* **203,** 222–9 (2010).

151. Changavi, Arathi A; Shashikala, Arundhathi; Ramji, A. Epidermal Growth Factor Receptor Expression in Triple Negative and Nontriple Negative Breast Carcinomas. *J Lab Physicians* **7,** 79–83 (2015).

152. Network, T. C. G. A. Comprehensive molecular portraits of human breast tumors. *Nature* **490,** 61–70 (2012).

153. Stephens, P. J. *et al.* The landscape of cancer genes and mutational processes in breast cancer. *Nature* **486,** 400–404 (2012).

154. Baselga, J. *et al.* Phase II and tumor pharmacodynamic study of gefitinib in patients with advanced breast cancer. *J. Clin. Oncol.* **23,** 5323–33 (2005).

155. Dickler, M. N., Cobleigh, M. a, Miller, K. D., Klein, P. M. & Winer, E. P. Efficacy and safety of erlotinib in patients with locally advanced or metastatic breast cancer. *Breast Cancer Res. Treat.* **115,** 115–21 (2009).

156. Linardou, H. *et al.* Assessment of somatic k-RAS mutations as a mechanism associated with resistance to EGFR-targeted agents: a systematic review and meta-analysis of studies in advanced non-small-cell lung cancer and metastatic colorectal cancer. *Lancet. Oncol.* **9,** 962–72 (2008).

157. Kurtze, I., Sonnemann, J. & Beck, J. F. KRAS-mutated non-small cell lung cancer cells are responsive to either co-treatment with erlotinib or gefitinib and histone deacetylase inhibitors or single treatment with lapatinib. *Oncol. Rep.* **25,** 1021–9 (2011).

158. Brand, T. M. *et al.* Nuclear epidermal growth factor receptor is a functional molecular target in triple-negative breast cancer. *Mol. Cancer Ther.* **13,** 1356–68 (2014).

159. Brand, T. M. *et al.* Nuclear EGFR as a molecular target in cancer. *Radiother. Oncol.* **108,** 370–7 (2013).

160. Lin, S. Y. *et al.* Nuclear localization of EGF receptor and its potential new role as a transcription factor. *Nat. Cell Biol.* **3,** 802–808 (2001).

161. Hadzisejdić, I., Mustać, E., Jonjić, N., Petković, M. & Grahovac, B. Nuclear EGFR in ductal invasive breast cancer: correlation with cyclin-D1 and prognosis. *Mod. Pathol.* **23,** 392–403 (2010).

162. Huo, L. *et al.* RNA helicase A is a DNA-binding partner for EGFR-mediated transcriptional activation in the nucleus. *Proc. Natl. Acad. Sci. U. S. A.* **107,** 16125–30 (2010).

163. Schuler, M. *et al.* A phase II trial to assess efficacy and safety of afatinib in extensively pretreated patients with HER2-negative metastatic breast cancer. *Breast Cancer Res. Treat.* **134,** 1149–1159 (2012).

164. Johnston, S. *et al.* Phase II study of predictive biomarker profiles for response targeting human epidermal growth factor receptor 2 (HER-2) in advanced

inflammatory breast cancer with lapatinib monotherapy. *J. Clin. Oncol.* **26,** 1066–72 (2008).

165. Nabholtz, J. M. *et al.* Multicentric neoadjuvant phase II study of panitumumab combined with an anthracycline/taxane based chemotherapy in operable triple negative breast cancer: Identification of biologically-defined signatures predicting treatment impact. *Ann. Oncol.* **25,** 1570–1577 (2014).

166. Nabholtz, J. M. *et al.* Multicentric neoadjuvant pilot Phase II study of cetuximab combined with docetaxel in operable triple negative breast cancer. *Int. J. Cancer* **138,** 2274–2280 (2016).

167. Crozier, J. A. *et al.* N0436 (Alliance): A Phase II Trial of Irinotecan with Cetuximab in Patients with Metastatic Breast Cancer Previously Exposed to Anthracycline and/or Taxane-Containing Therapy. *Clin. Breast Cancer* **16,** 23–30 (2016).

168. Al-Ejeh, F. *et al.* Treatment of Triple-Negative Breast Cancer Using Anti-EGFR–Directed Radioimmunotherapy Combined with Radiosensitizing Chemotherapy and PARP Inhibitor. *J Nucl Med.* **54 (6):** 913-21 (2013)

169. Brady, N., Chuntova, P., Bade, L. K. & Schwertfeger, K. L. The FGF/FGFR axis as a therapeutic target in breast cancer. *Expert Rev. Endocrinol. Metab.* **8,** 391–402 (2013).

170. Turner, N. *et al.* Integrative molecular profiling of triple negative breast cancers identifies amplicon drivers and potential therapeutic targets. *Oncogene* **29,** 2013–2023 (2010).

171. Sharpe, R. *et al.* FGFR signaling promotes the growth of triple-negative and basal-like breast cancer cell lines both in vitro and in vivo. *Clin. Cancer Res.* **17,** 5275–86 (2011).

172. Cheng, C. L. *et al.* Expression of FGFR1 is an independent prognostic factor in triple-negative breast cancer. *Breast Cancer Res. Treat.* **151 (1):** 99-111 (2015).

173. Andr E, F. *et al.* Targeting FGFR with Dovitinib (TKI258): Preclinical and Clinical Data in Breast Cancer. *Clin Cancer Res.* **19 (13):** 3693–702 (2013).

174. Heldin, C.-H. Targeting the PDGF signaling pathway in tumor treatment. *Cell Commun. Signal.* **11,** 97 (2013).

175. Jansson, S. *et al.* The three receptor tyrosine kinases c-KIT, VEGFR2 and PDGFRα, closely spaced at 4q12, show increased protein expression in triple-negative breast cancer. *PLoS One* **9 (7):** e102176 (2014).

176. Joglekar-Javadekar, M. *et al.* Characterization and Targeting of Platelet-Derived Growth Factor Receptor alpha (PDGFRA) in Inflammatory Breast Cancer (IBC). *Neoplasia* **19 (7)**: 564-573 (2017).

177. Karnoub, A. E. *et al.* Mesenchymal stem cells within tumour stroma promote breast cancer metastasis. *Nature* **449 (7162)**: 557-63 (2007).

178. Ihn Koh, B. & Kang, Y. The pro-metastatic role of bone marrow-derived cells: a focus on MSCs and regulatory T cells. *Nat. Publ. Gr.* **13,** 412–422 (2012).

179. Camorani, S. *et al.* Inhibition of Bone Marrow-Derived Mesenchymal Stem Cells Homing Towards Triple-Negative Breast Cancer Microenvironment Using an Anti-PDGFRβ Aptamer. *Theranostics* **7,** 3595–3607 (2017).

180. Bergh, J. *et al.* First-line treatment of advanced breast cancer with sunitinib in combination with docetaxel versus docetaxel alone: results of a prospective, randomized phase III study. *J. Clin. Oncol.* **30,** 921–9 (2012).

181. Bianchi, G. *et al.* Phase II multicenter, uncontrolled trial of sorafenib in patients with metastatic breast cancer. *Anticancer. Drugs* **20,** 616–624 (2009).

182. Gordon, V. & Banerji, S. Molecular pathways: PI3K pathway targets in triple-negative breast cancers. *Clin. Cancer Res.* **19,** 3738–3744 (2013).

183. Fruman, D. A., Meyers, R. E. & Cantley, L. C. Phosphoinositide kinases. *Annu. Rev. Biochem* **67,** 481–507 (1998).

184. Luo, J. & Cantley, L. C. The negative regulation of phosphoinositide 3-kinase signaling by p85 and it's implication in cancer. *Cell Cycle* **4,** 1309–1312 (2005).

185. Stambolic, V. *et al.* Negative regulation of PKB/Akt-dependent cell survival by the tumor suppressor PTEN. *Cell* **95,** 29–39 (1998).

186. Haar, E. Vander, Lee, S. il, Bandhakavi, S., Griffin, T. J. & Kim, D. H. Insulin signalling to mTOR mediated by the Akt/PKB substrate PRAS40. *Nat. Cell Biol.* **9,** 316–323 (2007).

187. Morita, M. *et al.* MTORC1 controls mitochondrial activity and biogenesis through 4E-BP-dependent translational regulation. *Cell Metab.* **18,** 698–711 (2013).

188. Oh, W. J. *et al.* MTORC2 can associate with ribosomes to promote cotranslational phosphorylation and stability of nascent Akt polypeptide. *EMBO J.* **29,** 3939–3951 (2010).

189. Sarbassov, D. D., Guertin, D. A., Ali, S. M. & Sabatini, D. M. Phosphorylation and regulation of Akt/PKB by the rictor-mTOR complex. *Science* **307,** 1098–1101 (2005).

190. Yun, Y. S. *et al.* mTORC1 Coordinates Protein Synthesis and Immunoproteasome Formation via PRAS40 to Prevent Accumulation of Protein Stress. *Mol. Cell* **61,** 625–639 (2016).

191. Hollestelle, A., Elstrodt, F., Nagel, J. H. a, Kallemeijn, W. W. & Schutte, M. Phosphatidylinositol-3-OH kinase or RAS pathway mutations in human breast cancer cell lines. *Mol. Cancer Res.* **5,** 195–201 (2007).

192. Shah, S. P. *et al.* The clonal and mutational evolution spectrum of primary triple-negative breast cancers. *Nature.* **486,** 395–399 (2012).

193. Wee, S. *et al.* PTEN-deficient cancers depend on PIK3CB. *Proc. Natl. Acad. Sci. U. S. A.* **105,** 13057–62 (2008).

194. Saal, L. H. *et al.* PIK3CA mutations correlate with hormone receptors, node metastasis, and ERBB2, and are mutually exclusive with PTEN loss in human breast carcinoma. *Cancer Res.* **65,** 2554–2559 (2005).

195. Kao, G. D., Jiang, Z., Fernandes, A. M., Gupta, A. K. & Maity, A. Inhibition of

phosphatidylinositol-3-OH kinase/Akt signaling impairs DNA repair in glioblastoma cells following ionizing radiation. *J. Biol. Chem.* **282,** 21206–21212 (2007).

196. Kumar, A., Fernandez-Capetillo, O., Fernadez-Capetillo, O. & Carrera, A. C. Nuclear phosphoinositide 3-kinase beta controls double-strand break DNA repair. *Proc. Natl. Acad. Sci. U. S. A.* **107,** 7491–6 (2010).

197. Ibrahim, Y. H. *et al.* PI3K inhibition impairs BRCA1/2 expression and sensitizes BRCA-proficient triple-negative breast cancer to PARP inhibition. *Cancer Discov.* **2,** 1036–1047 (2012).

198. Ganesan, P. *et al.* Triple-negative breast cancer patients treated at MD Anderson Cancer Center in phase I trials: improved outcomes with combination chemotherapy and targeted agents. *Mol. Cancer Ther.* **13,** 3175–84 (2014).

199. Sears, R. *et al.* Multiple Ras-dependent phosphorylation pathways regulate Myc protein stability. *Genes Dev.* **14,** 2501–2514 (2000).

200. Monje, P., Hernández-Losa, J., Lyons, R. J., Castellone, M. D. & Gutkind, J. S. Regulation of the transcriptional activity of c-Fos by ERK: A novel role for the prolyl isomerase Pin1. *J. Biol. Chem.* **280,** 35081–35084 (2005).

201. Pouysségur, J., Volmat, V. & Lenormand, P. Fidelity and spatio-temporal control in MAP kinase (ERKs) signalling. *Biochem. Pharmacol.* **64,** 755–763 (2002).

202. Will, M. *et al.* Rapid induction of apoptosis by PI3K inhibitors is dependent upon their transient inhibition of RAS-ERK signaling. *Cancer Discov.* **4,** 334–47 (2014).

203. Turke, A. B. *et al.* MEK inhibition leads to PI3K/AKT activation by relieving a negative feedback on ERBB receptors. *Cancer Res.* **72,** 3228–37 (2012).

204. Hoeflich, K. P. *et al.* In vivo Antitumor Activity of MEK and Phosphatidylinositol 3-Kinase Inhibitors in Basal-Like Breast Cancer Models. *Clin Cancer Res.* **15 (14):** 4649-64 (2009).

205. Negrini, S., Gorgoulis, V. G. & Halazonetis, T. D. Genomic instability an evolving hallmark of cancer. *Nature Reviews Molecular Cell Biology* **11,** 220–228 (2010).

206. Bartkova, J. *et al.* Oncogene-induced senescence is part of the tumorigenesis barrier imposed by DNA damage checkpoints. *Nature* **444,** 633–637 (2006).

207. Di Micco, R. *et al.* Oncogene-induced senescence is a DNA damage response triggered by DNA hyper-replication. *Nature* **444,** 638–642 (2006).

208. Helleday, T., Petermann, E., Lundin, C., Hodgson, B. & Sharma, R. A. DNA repair pathways as targets for cancer therapy. *Nature Reviews Cancer* **8,** 193–204 (2008).

209. Muller, P. A. J. & Vousden, K. H. p53 mutations in cancer. *Nat. Cell Biol.* **15,** 2–8 (2013).

210. Xue, W. *et al.* Senescence and tumour clearance is triggered by p53 restoration in murine liver carcinomas. *Nature* **445,** 656–660 (2007).

211. Chen, G. L. *et al.* Nonintercalative antitumor drugs interfere with the breakage-

reunion reaction of mammalian DNA topoisomerase II. *J. Biol. Chem.* **259,** 13560–13566 (1984).

212. Cheung-Ong, K., Giaever, G. & Nislow, C. Chemistry & Biology Perspective DNA-Damaging Agents in Cancer Chemotherapy: Serendipity and Chemical Biology. *Chem. Biol.* **20,** 648–659 (2013).

213. O'Connor, M. J. Targeting the DNA Damage Response in Cancer. *Mol. Cell* **60,** 547–560 (2015).

214. Kelland, L. The resurgence of platinum-based cancer chemotherapy. *Nature Reviews Cancer* **7,** 573–584 (2007).

215. Parker, W. & Cheng, Y. Metabolism and mechanism of action of 5-fluorouracil. *Pharmacol. Ther.* **48,** 381–395 (1990).

216. Hofland, K. F., Thougaard, A. V., Sehested, M. & Jensen, P. B. Dexrazoxane protects against myelosuppression from the DNA cleavage-enhancing drugs etoposide and daunorubicin but not doxorubicin. *Clin. Cancer Res.* **11,** 3915–3924 (2005).

217. Maxwell, M. B. & Maher, K. E. Chemotherapy-induced myelosuppression. *Semin. Oncol. Nurs.* **8,** 113–123 (1992).

218. Astolfi, L. *et al.* Correlation of adverse effects of cisplatin administration in patients affected by solid tumours: A retrospective evaluation. *Oncol. Rep.* **29,** 1285–1292 (2013).

219. Shiloh, Y. ATM and related protein kinases: Safeguarding genome integrity. *Nature Reviews Cancer* **3,** 155–168 (2003).

220. Branzei, D. & Foiani, M. Regulation of DNA repair throughout the cell cycle. *Nature Reviews Molecular Cell Biology* **9,** 297–308 (2008).

221. Bauerschmidt, C. *et al.* Cohesin phosphorylation and mobility of SMC1 at ionizing radiation-induced DNA double-strand breaks in human cells. *Exp. Cell Res.* **317,** 330–337 (2011).

222. Lavin, M. F., Kozlov, S., Gatei, M. & Kijas, A. W. ATM-dependent phosphorylation of all three members of the MRN complex: From sensor to adaptor. *Biomolecules* **5,** 2877–2902 (2015).

223. Ziv, Y. *et al.* Chromatin relaxation in response to DNA double-strand breaks is modulated by a novel ATM- and KAP-1 dependent pathway. *Nat. Cell Biol.* **8,** 870–876 (2006).

224. Bartek, J. & Lukas, J. Chk1 and Chk2 kinases in checkpoint control and cancer. *Cancer Cell* **3,** 421–429 (2003).

225. Mailand, N. *et al.* Rapid destruction of human Cdc25A in response to DNA damage. *Science* **288 (5470):**1425–1429 (2000).

226. Peng, C. Mitotic and G2 Checkpoint Control: Regulation of 14-3-3 Protein Binding by Phosphorylation of Cdc25C on Serine-216. *Science* **277 (5331):** 1501–1505 (1997).

227. Gatei, M. *et al.* Role for ATM in DNA damage-induced phosphorylation of BRCA1. *Cancer Res.* **60,** 3299–3304 (2000).

228. Matsuoka, S. *et al.* ATM and ATR substrate analysis reveals extensive protein networks responsive to DNA damage. *Science* **316,** 1160–1166 (2007).

229. Chou, W. C. *et al.* Chk2-dependent phosphorylation of XRCC1 in the DNA damage response promotes base excision repair. *EMBO J.* **27,** 3140–3150 (2008).

230. Zhou, Z. *et al.* The Chk1 inhibitor MK-8776 increases the radiosensitivity of human triple-negative breast cancer by inhibiting autophagy. *Nat. Publ. Gr.* **38,** 513–523 (2017).

231. Ma, C. X. *et al.* Targeting Chk1 in p53-deficient triple-negative breast cancer is therapeutically beneficial in human-in-mouse tumor models. *J. Clin. Invest.* **122,** 1541–1552 (2012).

232. Manic, G., Obrist, F., Sistigu, A. & Vitale, I. Trial Watch: Targeting ATM–CHK2 and ATR–CHK1 pathways for anticancer therapy. *Mol Cell Oncol.* **2 (4):** e1012976 (2015).

233. Ma, C. X. *et al.* A phase II study of UCN-01 in combination with irinotecan in patients with metastatic triple negative breast cancer. *Breast Cancer Res Treat.* **137 (2):** 483-92 (2013).

234. Barton, V. N. *et al.* Multiple Molecular Subtypes of Triple-Negative Breast Cancer Critically Rely on Androgen Receptor and Respond to Enzalutamide In Vivo. *Mol. Cancer Ther.* **14,** 769–778 (2015).

235. Mayer, I. A., Abramson, V. G., Lehmann, B. D. & Pietenpol, J. A. New strategies for triple-negative breast cancer-deciphering the heterogeneity. *Clin. Cancer Res.* **20,** 782–790 (2014).

236. Malumbres, M. & Barbacid, M. Cell cycle, CDKs and cancer: a changing paradigm. *Nat. Rev. Cancer* **9,** 153–166 (2009).

237. Malumbres, M. *et al.* Cyclin-dependent kinases: a family portrait. *Nat. Cell Biol.* **11,** 1275–1276 (2009).

238. Nurse, P. M. Cyclin dependent kinases and cell cycle control. in *Bioscience Reports* **22,** 487–499 (2002).

239. Ekholm, S. V. & Reed, S. I. Regulation of G1 cyclin-dependent kinases in the mammalian cell cycle. *Current Opinion in Cell Biology* **12,** 676–684 (2000).

240. Choi, Y. J. & Anders, L. Signaling through cyclin D-dependent kinases. *Oncogene* **33,** 1890–1903 (2014).

241. Malumbres, M. & Barbacid, M. Mammalian cyclin-dependent kinases. *Trends in Biochemical Sciences* **30,** 630–641 (2005).

242. Harbour, J. W., Luo, R. X., Dei Santi, A., Postigo, A. A. & Dean, D. C. Cdk phosphorylation triggers sequential intramolecular interactions that progressively block Rb functions as cells move through G1. *Cell* **98,** 859–869 (1999).

243. Zhang, H. S. & Dean, D. C. Rb-mediated chromatin structure regulation and transcriptional repression. *Oncogene* **20,** 3134–8 (2001).

244. Brehm, A. *et al.* Retinoblastoma protein recruits histone deacetylase to repress

transcription. *Nature* **391,** 597–601 (1998).

245. De Luca, A. *et al.* A unique domain of pRb2/p130 acts as an inhibitor of Cdk2 kinase activity. *J. Biol. Chem.* **272,** 20971–20974 (1997).

246. Okuda, M. *et al.* Nucleophosmin/B23 Is a Target of CDK2/Cyclin E in Centrosome Duplication. *Cell* **103,** 127–140 (2000).

247. Ma, T. *et al.* Cell cycle-regulated phosphorylation of p220(NPAT) by cyclin E/Cdk2 in Cajal bodies promotes histone gene transcription. *Genes Dev.* **14,** 2298–2313 (2000).

248. Krek, W., Xu, G. & Livingston, D. M. Cyclin A-kinase regulation of E2F-1 DNA binding function underlies suppression of an S phase checkpoint. *Cell* **83,** 1149–1158 (1995).

249. Krek, W. *et al.* Negative regulation of the growth-promoting transcription factor E2F-1 by a stably bound cyclin A-dependent protein kinase. *Cell* **78,** 161–172 (1994).

250. Dynlacht, B. D., Flores, O., Lees, J. A. & Harlow, E. Differential regulation of E2F transactivation by cyclin/cdk2 complexes. *Genes Dev.* **8,** 1772–1786 (1994).

251. Fu, Z. *et al.* Plk1-dependent phosphorylation of FoxM1 regulates a transcriptional programme required for mitotic progression. *Nat. Cell Biol.* **10,** 1076–1082 (2008).

252. Gavet, O. & Pines, J. Progressive Activation of CyclinB1-Cdk1 Coordinates Entry to Mitosis. *Dev. Cell* **18,** 533–543 (2010).

253. Santos, S. D. M., Wollman, R., Meyer, T. & Ferrell, J. E. Spatial positive feedback at the onset of mitosis. *Cell* **149,** 1500–1513 (2012).

254. Gavet, O. & Pines, J. Activation of cyclin B1-Cdk1 synchronizes events in the nucleus and the cytoplasm at mitosis. *J. Cell Biol.* **189,** 247–259 (2010).

255. Yamaguchi, T. *et al.* Phosphorylation by Cdk1 induces Plk1-mediated vimentin phosphorylation during mitosis. *J. Cell Biol.* **171,** 431–436 (2005).

256. Sirri, V., Hernandez-Verdun, D. & Roussel, P. Cyclin-dependent kinases govern formation and maintenance of the nucleolus. *J. Cell Biol.* **156,** 969–981 (2002).

257. Onischenko, E. A. Cdk1 and Okadaic Acid-sensitive Phosphatases Control Assembly of Nuclear Pore Complexes in Drosophila Embryos. *Mol. Biol. Cell* **16,** 5152–5162 (2005).

258. Egger, J. V., Lane, M. V., Antonucci, L. A., Dedi, B. & Krucher, N. A. Dephosphorylation of the Retinoblastoma protein (Rb) inhibits cancer cell EMT via Zeb. *Cancer Biol. Ther.* **17,** 1197–1205 (2016).

259. Nelson, D. A., Krucher, N. A. & Ludlow, J. W. High molecular weight protein phosphatase type 1 dephosphorylates the retinoblastoma protein. *J Biol Chem.* **272,** 4528–4535 (1997).

260. Hsin, J.-P. & Manley, J. L. The RNA polymerase II CTD coordinates transcription and RNA processing. *Genes Dev.* **26,** 2119–37 (2012).

261. Harlen, K. M. & Churchman, L. S. The code and beyond: transcription regulation by the RNA polymerase II carboxy-terminal domain. *Nat. Rev. Mol. Cell Biol.* **18,** 263–273 (2017).

262. Lu, H., Flores, O., Weinmann, R. & Reinberg, D. The nonphosphorylated form of RNA polymerase II preferentially associates with the preinitiation complex. *Proc. Natl. Acad. Sci. U. S. A.* **88,** 10004–10008 (1991).

263. Robinson, P. J. *et al.* Structure of a Complete Mediator-RNA Polymerase II Pre-Initiation Complex. *Cell* **166 (6):** 1411–1422.e16 (2016).

264. Robinson, P. J. J., Bushnell, D. A., Trnka, M. J., Burlingame, A. L. & Kornberg, R. D. Structure of the mediator head module bound to the carboxy-terminal domain of RNA polymerase II. *Proc. Natl. Acad. Sci. U. S. A.* **109,** 17931–5 (2012).

265. Allen, B. L. & Taatjes, D. J. The Mediator complex: a central integrator of transcription. *Nat. Rev. Mol. Cell Biol.* **16,** 155–166 (2015).

266. Conaway, R. C. & Conaway, J. W. Function and regulation of the Mediator complex. *Current Opinion in Genetics and Development* **21,** 225–230 (2011).

267. Conaway, R. C. & Conaway, J. W. The Mediator complex and transcription elongation. *Biochimica et Biophysica Acta - Gene Regulatory Mechanisms* **1829,** 69–75 (2013).

268. Yin, J. & Wang, G. The Mediator complex: a master coordinator of transcription and cell lineage development. *Development* **141,** 977–87 (2014).

269. Tsai, K.-L. *et al.* A conserved Mediator-CDK8 kinase module association regulates Mediator-RNA polymerase II interaction. *Nat. Struct. Mol. Biol.* **20, (5):** 611–619 (2013).

270. Knuesel, M. T., Meyer, K. D., Bernecky, C. & Taatjes, D. J. The human CDK8 subcomplex is a molecular switch that controls Mediator coactivator function. *Genes Dev.* **23,** 439–451 (2009).

271. Holstege, F. C., van der Vliet, P. C. & Timmers, H. T. Opening of an RNA polymerase II promoter occurs in two distinct steps and requires the basal transcription factors IIE and IIH. *EMBO J.* **15,** 1666–1677 (1996).

272. Moreland, R. J. *et al.* A role for the TFIIH XPB DNA helicase in promoter escape by RNA polymerase II. *J. Biol. Chem.* **274,** 22127–22130 (1999).

273. Akoulitchev, S., Makela, T. P., Weinberg, R. A. & Reinberg, D. Requirement for TFIIH kinase activity in transcription by RNA polymerase II. *Nature* **377,** 557–560 (1995).

274. Wong, K. H., Jin, Y. & Struhl, K. TFIIH Phosphorylation of the Pol II CTD Stimulates Mediator Dissociation from the Preinitiation Complex and Promoter Escape. *Mol. Cell* **54,** 601–612 (2014).

275. Larochelle S. *et al*. Requirements for Cdk7 in the Assembly of Cdk1 / Cyclin B and Activation of Cdk2 Revealed by Chemical Genetics in Human Cells. *Mol Cell.* **25 (6):** 839–850 (2007).

276. Larochelle, S. *et al.* Cyclin-dependent kinase control of the initiation-to-elongation switch of RNA polymerase II. *Nat. Struct. Mol. Biol.* **19,** 1108–1115 (2012).

277. Schachter M.M. *et al.* A Cdk7-Cdk4 T-Loop Phosphorylation Cascade Promotes G1 Progression. *Mol Cell.* **50 (2):** 250-60 (2013).

278. Lu, H. U. A. *et al.* The CDK 7 -cycH-p36 Complex of Transcription Factor IIH Phosphorylates p53 , Enhancing Its Sequence-Specific DNA Binding Activity In Vitro. *Mol Cell Biol.* **17 (10):** 5923–5934 (1997).

279. Ko, L. J. *et al.* p53 Is Phosphorylated by CDK7-Cyclin H in a p36 MAT1 - Dependent Manner. *Mol Cell Biol.* **17 (12):** 7220–7229 (1997).

280. Schneider, E., Montenarh, M. & Wagner, P. Regulation of CAK kinase activity by p53. *Oncogene* **17,** 2733–2741 (1998).

281. Wu, C. H. *et al.* NELF and DSIF cause promoter proximal pausing on the hsp70 promoter in Drosophila. *Genes Dev.* **17,** 1402–1414 (2003).

282. Jonkers, I., Kwak, H. & Lis, J. T. Promoter-proximal pausing of RNA polymerase II: emerging roles in metazoans. *Elife* **3,** 1–25 (2014).

283. Peterlin, B. M. & Price, D. H. Controlling the Elongation Phase of Transcription with P-TEFb. *Molecular Cell* **23,** 297–305 (2006).

284. Ni, Z. *et al.* P-TEFb is critical for the maturation of RNA polymerase II into productive elongation in vivo. *Mol. Cell. Biol.* **28,** 1161–1170 (2008).

285. Devaiah, B. N. *et al.* BRD4 is a histone acetyltransferase that evicts nucleosomes from chromatin. *Nat. Struct. Mol. Biol.* **23,** 540–8 (2016).

286. Devaiah, B. N. *et al.* BRD4 is an atypical kinase that phosphorylates Serine2 of the RNA Polymerase II carboxy-terminal domain. *Proc. Natl. Acad. Sci.* **109,** 6927–6932 (2012).

287. Chiang, C.-M. Brd4 engagement from chromatin targeting to transcriptional regulation: selective contact with acetylated histone H3 and H4. *F1000 Biol. Rep.* **1,** 98 (2009).

288. Wu, S. Y., Lee, A. Y., Lai, H. T., Zhang, H. & Chiang, C. M. Phospho switch triggers brd4 chromatin binding and activator recruitment for gene-specific targeting. *Mol. Cell* **49,** 843–857 (2013).

289. Dey, A., Chitsaz, F., Abbasi, A., Misteli, T. & Ozato, K. The double bromodomain protein Brd4 binds to acetylated chromatin during interphase and mitosis. *Proc. Natl. Acad. Sci. U. S. A.* **100,** 8758–8763 (2003).

290. Itzen, F., Greifenberg, A. K., Christian, A. B. & Geyer, M. Brd4 activates P-TEFb for RNA polymerase II CTD phosphorylation. **42,** 7577–7590 (2014).

291. Yang, Z. *et al.* Recruitment of P-TEFb for stimulation of transcriptional elongation by the bromodomain protein Brd4. *Mol. Cell* **19,** 535–545 (2005).

292. Moon, K. J. *et al.* The bromodomain protein Brd4 is a positive regulatory component of P-TEFb and stimulates RNA polymerase II-dependent transcription. *Mol. Cell* **19,** 523–534 (2005).

293. Lu, H. *et al.* Compensatory induction of MYC expression by sustained CDK9 inhibition via a BRD4-dependent mechanism. *Elife* **4:** e06535 (2015).

294. Lovén, J. *et al.* Selective inhibition of tumor oncogenes by disruption of super-enhancers. *Cell* **153,** 320–334 (2013).

295. Patel, M. C. *et al.* BRD4 Coordinates Recruitment of Pause Release Factor P-TEFb and the Pausing Complex NELF/DSIF To Regulate Transcription Elongation of Interferon-Stimulated Genes. *Mol. Cell. Biol.* **33,** 2497–2507 (2013).

296. Viladevall, L. *et al.* TFIIH and P-TEFb Coordinate Transcription with Capping Enzyme Recruitment at Specific Genes in Fission Yeast. *Mol. Cell* **33,** 738–751 (2009).

297. Lunde, B. M. *et al.* Cooperative interaction of transcription termination factors with the RNA polymerase II C-terminal domain. *Nat. Struct. Mol. Biol.* **17,** 1195–201 (2010).

298. Ahn, S. H., Kim, M. & Buratowski, S. Phosphorylation of serine 2 within the RNA polymerase II C-terminal domain couples transcription and 3' end processing. *Mol Cell* **13,** 67–76 (2004).

299. Krishnamurthy, S., He, X., Reyes-Reyes, M., Moore, C. & Hampsey, M. Ssu72 is an RNA polymerase II CTD phosphatase. *Mol. Cell* **14,** 387–394 (2004).

300. Cho, E. J., Kobor, M. S., Kim, M., Greenblatt, J. & Buratowski, S. Opposing effects of Ctk1 kinase and Fcp1 phosphatase at Ser 2 of the RNA polymerase II C-terminal domain. *Genes Dev.* **15,** 3319–3329 (2001).

301. Malumbres, M. Cyclin-dependent kinases. *Genome Biol.* **15 (6):** 122 (2014).

302. Cayrol, F. *et al.* THZ1 targeting CDK7 suppresses STAT transcriptional activity and sensitizes T-cell lymphomas to BCL2 inhibitors. *Nat. Commun.* **8,** 14290 (2017).

303. Christensen, C. L. *et al.* Targeting transcriptional addictions in small cell lung cancer with a covalent CDK7 inhibitor. *Cancer Cell* **26,** 909–22 (2014).

304. Greenall, S. A. *et al.* Cyclin-dependent kinase 7 is a therapeutic target in high-grade glioma. *Oncogenesis* **6,** e336 (2017).

305. Augert, A. & MacPherson, D. Treating Transcriptional Addiction in Small Cell Lung Cancer. *Cancer Cell* **26,** 783–784 (2014).

306. Francavilla, C. *et al.* Phosphoproteomics of Primary Cells Reveals Druggable Kinase Signatures in Ovarian Cancer. *Cell Rep.* **18,** 3242–3256 (2017).

307. Gao, Y., Liang, Y., Zhang, T., Gray, N. S. & George, R. E. Optimizing selective CDK7 inhibition in MYCN-driven neuroblastoma. *Mol. Cancer Ther.* **14,** (2015).

308. Xie, S. *et al.* Antitumor action of CDK inhibitor LS-007 as a single agent and in combination with ABT-199 against human acute leukemia cells. *Acta Pharmacol Sin.* **37 (11):** 1481–1489 (2016).

309. Lam, F. *et al.* Targeting RNA transcription and translation in ovarian cancer cells with pharmacological inhibitor CDKI-73. *Oncotarget* **5,** 7691–704 (2014).

310. Chipumuro, E. *et al.* CDK7 inhibition suppresses super-enhancer-linked oncogenic transcription in MYCN-driven cancer. *Cell* **159,** 1126–39 (2014).

311. Xie, S. *et al.* Antitumor action of CDK inhibitor LS-007 as a single agent and in combination with ABT-199 against human acute leukemia cells. *Acta Pharmacol. Sin.* **37 (11):** 1481-1489 (2016).

312. Huang, C.-H. *et al.* CDK9-mediated transcription elongation is required for MYC addiction in hepatocellular carcinoma. *Genes Dev.* **28,** 1800–14 (2014).

313. Horiuchi, D. *et al.* MYC pathway activation in triple-negative breast cancer is synthetic lethal with CDK inhibition. *J. Exp. Med.* **209,** 679–96 (2012).

314. Wang, Y. *et al.* CDK7-dependent transcriptional addiction in triple-negative breast cancer. *Cell* **163,** 174–86 (2015).

315. Pott, S. & Lieb, J. D. What are super-enhancers? *Nat. Genet.* **47,** 8–12 (2014).

316. Zawistowski, J. S. *et al.* Enhancer remodeling during adaptive bypass to MEK inhibition is attenuated by pharmacologic targeting of the P-TEFb complex. *Cancer Discov.* **7,** 302–321 (2017).

317. Stuhlmiller, T. J. *et al.* Inhibition of lapatinib-induced kinome reprogramming in ERBB2-positive breast cancer by targeting BET family bromodomains. *Cell Rep.* **11,** 390–404 (2015).

318. Bywater, M. J., Pearson, R. B., McArthur, G. A. & Hannan, R. D. Dysregulation of the basal RNA polymerase transcription apparatus in cancer. *Nat Rev Cancer* **13 (5):** 299-314 (2013).

Chapter 2

A cell cycle gene signature is associated with resistance to MEK and Akt inhibitors in triple-negative breast cancer

Vera E. van der Noord[1,3], Ronan P. McLaughlin[1,3], Marcel Smid[2], John A. Foekens[2], John W.M. Martens[2], Yinghui Zhang[1], Bob van de Water[1,4]

[1]Division of Drug Discovery and Safety, Leiden Academic Centre for Drug Research, Leiden University, The Netherlands

[2]Department of Medical Oncology, Erasmus MC Cancer Institute, Erasmus University Medical Center, Rotterdam, The Netherlands

[3]These authors contributed equally to the work.

This chapter is based on a manuscript submitted for publication

ABSTRACT

Background

Triple-negative breast cancer (TNBC) is a heterogeneous subtype of breast cancer, defined by the absence of the estrogen, progesterone and human epidermal growth factor 2 receptors. TNBC patients have a poor clinical prognosis due to the lack of effective targeted therapies. Although TNBC tumours often display elevated MAPK and PI3K pathway activity, the clinical benefit from inhibitors of these pathways is limited.

Methods

In this study, we investigated the heterogeneity in cellular responses to MEK and Akt inhibitors in TNBC cell lines. Mutations, phosphorylated proteins within the MAPK/PI3K pathway and large-scale transcriptomics and proteomics data were utilised to understand these differential responses. Gene set enrichment analysis was performed to provide biological insight into differential genes or proteins. Furthermore, clinical relevance of the discovered differential gene expression profile was established in breast cancer patient gene expression data.

Results

Akt and MEK inhibitor treatment led to three different responses in TNBC cell lines: Akt or MEK inhibitor resistance alone or Akt and MEK inhibitor double resistance. We found that MEK inhibitor-resistant cell lines had PIK3CA/PIK3R1/PTEN mutations, high p-Akt and low p-MEK levels and could thereby be discriminated from Akt inhibitor-resistant ones. Moreover, we identified a group of cell cycle genes associated with the Akt and MEK inhibitor double-resistant TNBC cells. A prominent

group of these genes was also differentially expressed in primary breast cancer in general as well as in TNBC patients. As an alternative to MEK or Akt inhibitors, we found that cyclin-dependent kinase inhibitors targeting this signature are especially effective in the Akt and MEK inhibitor double-resistant cells.

Conclusion

Together, these results unravel novel features of Akt and MEK independency in TNBC that can be exploited for predicting resistance to Akt and MEK inhibitors and provide possible alternative treatment options for this resistant group.

KEY WORDS

Triple-negative breast cancer, MEK inhibitors, Akt inhibitors, drug resistance, cell cycle

BACKGROUND

Triple-negative breast cancer (TNBC) is an aggressive subtype of breast cancer that is defined by the absence of the estrogen receptor (ER), progesterone receptor (PR) and the lack of overexpression or gene amplification of the human epidermal growth factor receptor 2 (HER2) [1]. TNBC comprises a clinically and molecularly heterogeneous group of breast cancers and accounts for approximately 15% of all breast cancer cases [2]. A subset of TNBC patients shows pathological complete response after neo-adjuvant chemotherapy and surgery. Yet, >60% of patients do not achieve complete remission and have poor event-free and overall survival rates [3]. As a result, TNBC accounts for a disproportionately high number of deaths compared with other breast cancer subtypes [4]. Developing effective targeted therapies for TNBC patients is thus crucial for reducing the mortality rate of this aggressive subtype.

TNBC tumours commonly have either activating mutations or amplifications of PIK3CA, BRAF, KRAS and/or EGFR and/or PTEN loss, causing abnormal activity of the Raf/MAPK/ERK or PI3K/Akt/mTOR pathway [5, 6]. Inhibiting these pathways using MEK and/or Akt inhibitors is thus an attractive strategy for treating TNBC [7]. However, resistance to these inhibitors is often observed in pre-clinical studies [8-11]. Efforts to overcome this resistance include reversing possible drug-induced loss of negative feedback, by combining MEK and Akt or PI3K inhibitors, or one of these with epidermal growth factor receptor (EGFR) inhibitors [8-14]. These strategies have now reached clinical trials, but their benefits remain elusive [14, 15]. Another challenge is the prediction of response to provide patients with optimal, personalised, treatment strategies. Various studies demonstrate that mutations in RAS and BRAF are associated with MEK inhibitor sensitivity and mutations in RAS, PIK3CA or PTEN

are associated with Akt inhibitor sensitivity [8-10]. Yet, these features do not completely correlate with sensitivity in (pre-)clinical studies in TNBC and other malignancies [14]. Novel insights in predicting the response and providing alternatives to drug-resistant tumours are thus essential in facilitating the clinical development of such inhibitors in TNBC.

Here, by assessing TNBC cell line groups that were differentially sensitive to Akt and MEK inhibitors, we have shown that Akt or MEK inhibitor sensitivity can be distinguished by the presence of mutations in the PI3K pathway and activity of the PI3K and MAPK pathway. By performing a large-scale gene set enrichment analysis, we found that Akt and MEK inhibitor double resistance is associated with elevated expression of cell cycle genes. On the other hand, MEK and Akt inhibitor double-resistant cell lines were more, but not exclusively, sensitive to inhibitors of this signature, such as dinaciclib and flavopiridol, which may constitute more appropriate treatment options for this TNBC subgroup. Our results thus shed light on a novel mechanism of resistance to MEK and Akt inhibitors and provide potential markers of response as well as alternative treatments.

MATERIALS AND METHODS

Cell culture

Twenty human TNBC cell lines were used including BT20, BT549, HCC1143, HCC1806, HCC1937, HCC38, HCC70, Hs578T, MDA-MB-231, MDA-MB-435s, MDA-MB-436, MDA-MB-453, MDA-MB-468, SKBR7, SUM1315M02, SUM149PT, SUM159PT, SUM185PE, SUM229PE and SUM52PE. All cells were cultured in RPMI-1640 medium containing L-glutamine and 25 mM HEPES (Gibco Fisher Scientific, Landsmeer, The Netherlands) supplemented with 10% fetal bovine serum (FBS), 25 U/mL penicillin and 25 µg/mL streptomycin (Fisher Scientific) in a humidified incubator with 5% CO2 at 37°C.

Reagents and antibodies

For screening and primary validations with MEK and Akt inhibitors, a library of 378 kinase inhibitors was used (L1200 library; Selleckchem, Huissen, The Netherlands). For further validation and other experiments, selumetinib (S1008), AZD8330 (S2134), PD184352 (S1020), MK-2206 (S1078), AZD5363 (S8019) and ipatasertib (GDC-0068; S2808) were purchased from Selleckchem.

The mouse antibody against MEK1/2 (4694S) and rabbit antibodies against phospho-MEK1/2 (Ser217/221, 9120), phospho-Akt (Ser473, 9271), phospho-p44/42 MAPK (ERK1/2, Thr202/Tyr204, 9101), phospho-mTOR (Ser2448, 5536S), Akt (9272), p44/42 MAPK (Erk1/2, 4695) were purchased from Cell Signaling (Leiden, The Netherlands). The mouse antibody against α-tubulin (T-9026) was from Sigma-Aldrich. Secondary goat antibodies horseradish peroxidase (HRP)-linked anti-rabbit (111-035-003) and anti-mouse (115-035-003) and Alexa-647-linked anti-mouse

(115-605-146) were purchased from Jackson Immunoresearch (Bio-Connect, Huissen, The Netherlands).

Cell proliferation assays

Cell proliferation was determined using a sulforhodamine B (SRB) colorimetric assay as described previously [16]. TNBC cell lines were plated at optimal cell densities ranging from 4,000 to 18,000 cells in 96-well plates and allowed to attach overnight before treatment. Cells were treated with kinase inhibitors for 4 days and thereafter fixed by adding 30 µL 50% trichloroacetic acid (TCA; Sigma-Aldrich). Cellular proteins were stained with 0.4% SRB (Sigma-Aldrich) and unbound SRB was removed with 1% acetic acid (VWR, Amsterdam, The Netherlands). Protein-bound SRB was solubilised in 10 mM aqueous unbuffered Tris (Fischer Scientific) and SRB absorbance was measured at 540 nm on an Infinite M1000 microplate reader (Tecan, Giessen, The Netherlands). Dose response curves and IC50 values were generated in GraphPad Prism (version 7.01).

Protein extraction and western blotting

Protein extraction and western blotting were conducted as described before [17]. Cellular proteins (20 µg/lane) were loaded on 7.5% polyacrylamide gels for SDS-PAGE. After electrophoresis, proteins were transferred to polyvinylidene fluoride (PVDF) membranes (Milipore, Amsterdam, The Netherlands) overnight and blocked in 5% bovine serum albumin (BSA; Sigma Aldrich) in Tris-buffered saline with 0.05% Tween (TBS-$T_{0.05}$). Primary and secondary antibodies were dissolved in 1% BSA in TBS-$T_{0.05}$. Using an Amersham Imager 600 (GE Healthcare Life Sciences, Eindhoven, The Netherlands) Alexa Fluor 647-conjugated antibodies were visualised by Cy5 fluorescence and HRP-conjugated antibodies by chemiluminescence after

staining with ECL (Prime) Western Blotting Detection Reagent (GE Healthcare Life Sciences). Signal intensities were quantified using ImageJ.

Cell line annotation

TNBC cell lines were classified into TNBC subtypes as indicated by Lehmann et al [18]. Mutations were derived from the COSMIC database cell line project [19].

Gene set enrichment analysis (GSEA) of TNBC cell lines

TNBC cell line mRNA microarray data were previously established [20]. In short, raw data (.CEL files) were processed using the robust multi-array average (RMA) method and data are available in the Gene Expression Omnibus data repository (GEO) (Accession number: GSE41313). Protein abundance in the TNBC cell lines was previously analysed using high-end proteomics (Manuscript in preparation, data available upon request). Data were log-transformed (log_2) and gene set enrichment was evaluated using GSEA software [21, 22]. Enrichment of canonical pathways was tested using the curated c2cp gene sets from KEGG and Reactome (1,000 permutations per gene set). To visualise the significantly enriched gene sets ($P<0.005$, FDR Q-value<0.1) Cytoscape was used to organise these in enrichment maps (similarity cut-off>0.7) [23]. For all the enriched gene sets involved in cell cycle, the genes that were core enriched (signal-to-noise score>0.1) were collected and used for plotting heatmaps of their expression in TNBC cell lines (mRNA and protein expression) and breast cancer patients (mRNA). Overlapping networks of these genes from mRNA and protein expression were made by retrieving their network in STRING (v10.0) and providing colour annotation in Cytoscape. Pathway mapping of the core enriched genes was performed in Ingenuity Pathway Analysis (IPA) software (QIAGEN Bioinformatics).

Gene expression in breast cancer patients

RNA sequencing and clinical data of breast cancer patients were retrieved from the TCGA database in R using the TCGAbiolinks package from Bioconductor [24]. Normalised RNA sequencing data from Illumina HiSeq platforms from primary solid tumour samples of the TCGA-BRCA project were downloaded. Cell cycle genes that were established as described in the previous section were used for generating heatmaps for both all breast cancer (n=1093) and TNBC patients (n=120) specifically. TNBC patients were selected on the absence of HER2, ER and PR, as annotated in the TCGA data.

Statistical analysis

All heatmaps and hierarchical clusters were generated using the CRAN pheatmap package in R studio (version 3.3.1) [25]. Statistical analysis of grouped western blot outcomes with replicated measurements was performed using a two-way ANOVA in GraphPad Prism (Version 7). Significance was set at $P < 0.05$. IC50 values were also calculated in GraphPad Prism.

RESULTS

TNBC cell lines cluster into three groups based on responses to MEK and Akt inhibitors

To explore heterogeneity in targeted therapy responses, we evaluated the proliferative responses to 378 kinase inhibitors in 20 TNBC cell lines using unsupervised hierarchical clustering. The TNBC cell lines largely demonstrated resistance to these inhibitors, but some inhibitors differentially affected the proliferation of the cell lines (Figure 1A). In particular, the responses to inhibitors of MEK and Akt were heterogeneous (Figure 1A, black box), classifying the TNBC cell lines into three subgroups (Figure 1B): cell lines were either resistant to Akt inhibitors, but sensitive to MEK inhibitors (Group 1, Akt-i resistant); resistant to MEK inhibitors, but sensitive to Akt inhibitors (Group 2, MEK-i resistant); or resistant to both Akt and MEK inhibitors (Group 3, Akt-i/MEK-i double-resistant). To further validate these classifications, we treated the TNBC cell lines with a dose range of the various MEK and Akt inhibitors (Figure 1C and Additional file 1: Figure S1). MEK inhibition effectively reduced the growth of Akt-i-resistant Group 1 cells at low concentrations (IC50s~10 nM, Additional file 2: Table S1), but not of MEK-i-resistant Group 2 or Akt-i/MEK-i-resistant Group 3 cells. Whereas Akt inhibitors affected the cell proliferation of MEK-i-resistant Group 2 cell lines (IC50s~0.1-1 μM), Akt-i-resistant Group 1 and Akt-i/MEK-i double-resistant Group 3 cell lines did not respond to these inhibitors (IC50s>3.16 μM).

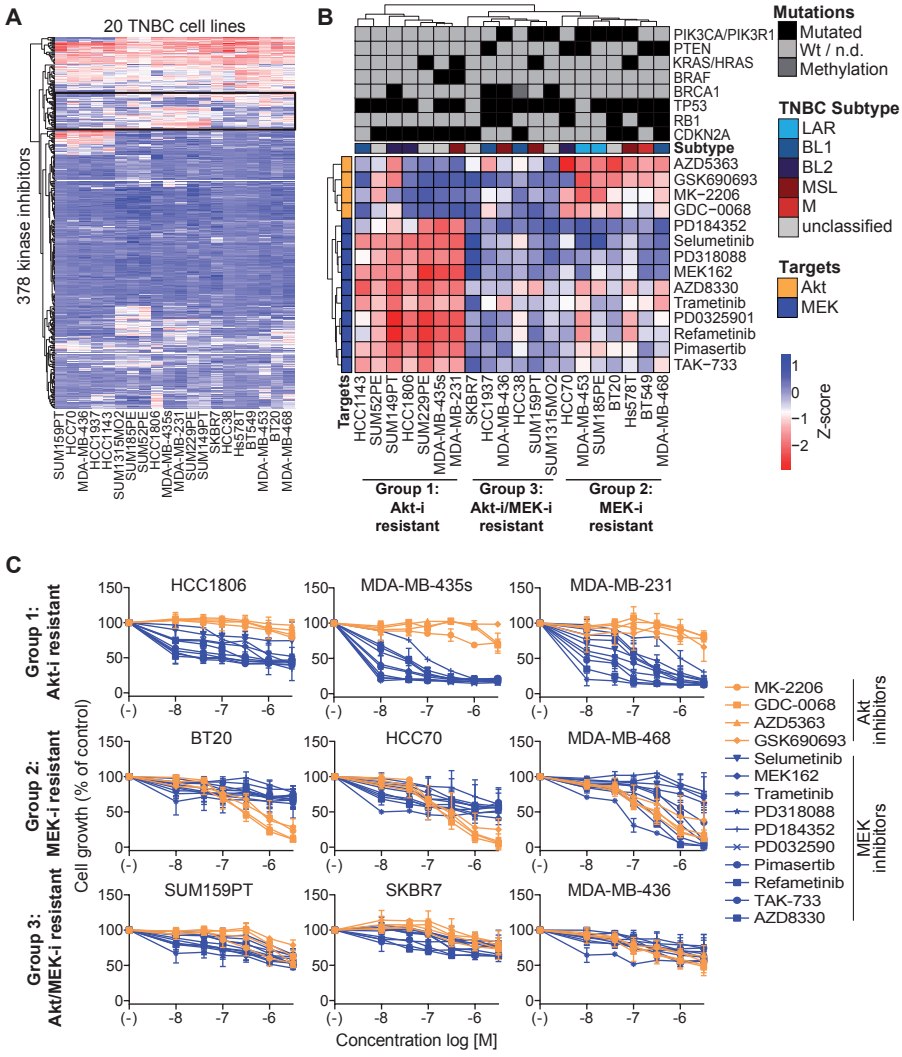

Figure 1. Proliferation of TNBC cell lines in response to MEK and Akt inhibitors. (A) A heatmap of proliferative responses of TNBC cell lines to kinase inhibitors (1 μM). Low Z-scores (red) indicate reduced cell growth, whereas high Z-scores indicate resistance (blue). The black box highlights multiple MEK and Akt inhibitors. (B) Clustering of responses to Akt and MEK inhibitors from this black box of TNBC cell lines among Group 1 (Akt-i resistant), Group 2 (MEK-i resistant) and Group 3 (Akt-i/MEK-i resistant) cell lines. (C) Dose responses of TNBC cell line groups to the Akt and MEK inhibitors (0.01–3.16 μM). Data are expressed as means ± SD from two independent experiments.

Activity and mutations of PI3K-MAPK pathway members distinguish between Akt-i-resistant and MEK-i-resistant cell lines

To understand the differential sensitivity to Akt and MEK inhibitors, we evaluated the basal phosphorylation levels of signalling components involved in the PI3K and MAPK pathways. Akt-i-resistant Group 1 cell lines expressed significantly higher levels of p-MEK compared with MEK-i-resistant Group 2 cell lines (P=0.0003, Figure 2A and B and Additional file 3: Figure S2). In contrast, Group 2 cell lines expressed higher levels of p-Akt compared with Group 1 cell lines (P=0.0072). Levels of p-Akt

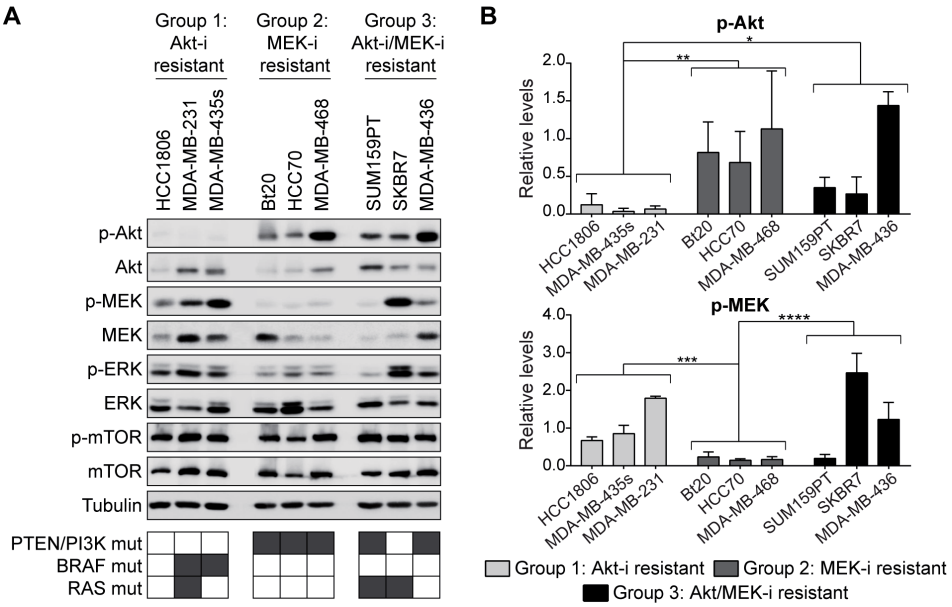

Figure 2. Basal levels of p-Akt and p-MEK in TNBC and drug resistance. (A) Western blot analysis and (B) quantification of p-Akt and p-MEK levels in the Akt-i resistant, MEK-i resistant and double-resistant cell lines. P-Akt and p-MEK levels were normalised to tubulin. Data are expressed as means ± SD of two independent experiments (two-way ANOVA, *P<0.05, **P<0.01, ***P<0.001, ****P<0.0001).

and p-MEK thus distinguish between Group 1 and 2 cell lines, suggesting that these groups exhibit a greater dependence on MAPK- or PI3K-mediated signalling, respectively, which may therefore account for the differential sensitivity of these groups to MEK and AKT inhibitors. Akt-i/MEK-i-resistant cell lines showed an average trend of increased p-Akt compared with Group 1 ($P=0.0315$) and increased p-MEK compared with Group 2 ($P<0.0001$) cell lines, respectively. However, Akt-i/MEK-i-resistant Group 3 cell line SUM159PT had low levels of p-MEK, indicating that this average trend is not completely discriminative. Therefore, p-Akt and p-MEK levels alone cannot discriminate between Akt-i/MEK-i-double-resistant and MEK- or AKT-i-sensitive cell lines.

Next, we evaluated the mutations present in the relevant genes in the three groups to further understand the differential phenotypes. All MEK-i-resistant Group 2 cell lines with high levels of p-Akt had mutations in PTEN, PIK3CA and/or PIK3R1 (6/6) (Additional file 4: Table S2). These mutations were completely absent in the Akt-i-resistant Group 1 cell lines (0/7). Akt-i/MEK-i-resistant Group 3 cell lines had a mixed mutational profile (5/7). In addition, Group 1 cell lines exhibited a higher frequency of BRAF mutations upstream of MEK (2/7), whereas these were absent in both Group 2 (0/6) and Group 3 (0/7) cell lines. Mutations in KRAS or HRAS did not differentiate between any of the groups (Group 1: 2/7, Group 2: 1/6 and Group 3: 2/7). Altogether, these features could distinguish between Akt-i and MEK-i resistance, but do not explain Akt-i/MEK-i double resistance.

Crosstalk between Akt and MEK is not essential for Akt-i/MEK-i resistance

To further explore this Akt-i/MEK-i double-resistant phenotype, we investigated the role of crosstalk between Akt and MEK pathways. Treatment with ATP non-competitive MEK inhibitors selumetinib and PD184352 resulted in accumulation of p-MEK accompanied by inhibition of ERK phosphorylation in all cell lines (Figure 3A). The extent of inhibition of ERK phosphorylation was similar across the cell line panel, indicating that MEK-i resistance is not related to lack of target inhibition. The allosteric Akt1/2/3 inhibitor MK-2206 fully prevented Akt phosphorylation in all cell lines, whilst ATP-competitive Akt1/2/3 inhibitor ipatasertib caused accumulation of p-Akt, as binding of this inhibitor to the active site protects Ser473 phosphorylation sites from phosphatases [26]. This implies that resistance to these agents is also not due to lack of target inhibition. The Akt inhibitors reduced p-mTOR levels in some, but not all cell lines, an event which was independent of Akt-i or MEK-i sensitivity status, suggesting mTOR activity is not critical in conferring resistance to such inhibitors. Akt inhibition slightly increased p-MEK levels in Akt-i-resistant Group 1 cell lines, but not in Akt-i/MEK-i-resistant Group 3 cell lines.

Next, we evaluated whether combining MEK inhibitors with Akt inhibitors enhances the growth-inhibitory effects of either drug. Cell lines were treated with a combination of selumetinib (MEK-i) and ipatasertib (Akt-i). The combined treatment of a dose range of selumetinib, together with a fixed concentration of ipatasertib (1 μM), and vice versa, did not overtly enhance the anti-proliferative effects of either agent in most cell lines (Figure 3B). The combination treatments moderately sensitised SUM159PT to either selumetinib or ipatasertib. For all of the Akt-i/MEK-i-resistant Group 3 cell lines, combination treatments were incapable of reducing cell proliferation to the same extent as in the Group 1 or Group 2 cell lines. Altogether,

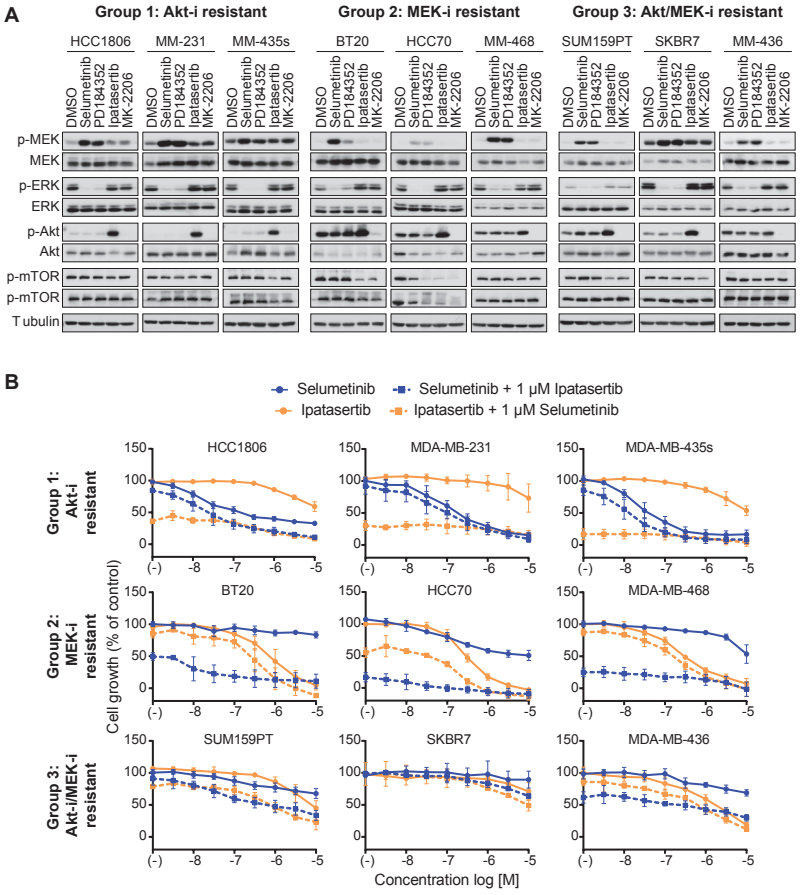

Figure 3. Cooperation of Akt and MEK signalling in TNBC proliferation. (A) Western blot analysis after inhibition by MEK inhibitors (selumetinib and PD184352) and Akt inhibitors (ipatasertib and MK-2206). Cells were treated with inhibitors (1 µM) for 24 hours. Data are representative of two independent experiments. (B) Combined inhibition by increasing concentrations of selumetinib or ipatasertib (0.00316–10 µM), together with a fixed concentration of ipatasertib or selumetinib (1 µM), respectively. Data are expressed as means ± SD from three independent experiments.

these results suggest that crosstalk or additive ERK and AKT proliferation signalling programs are not essential for the resistance observed in Akt-i/MEK-i-resistant Group 3 cell lines.

Akt-i/MEK-i-resistant cell lines can be distinguished by an elevated cell cycle gene expression signature

As a next step we explored the possible signalling pathways that contribute to the double-resistant phenotype of a subgroup of the TNBC cell lines. Therefore, we systematically compared the previously established transcriptomes and proteomes of the three different TNBC cell panel groups. Gene set enrichment analysis (GSEA) revealed enriched gene sets in Akt-i/MEK-i-resistant Group 3 cell lines compared with both Akt-i-resistant Group 1 and MEK-i-resistant Group 2 cell lines (Figure 4A, Additional file 5-7: Figure S3 and S4 and Table S3, respectively). The 37 and 62 significantly enriched gene sets ($p<0.005$, FDR q-value<0.1), based on mRNA and protein expression respectively, predominantly consisted of cell cycle-related gene sets. GSEA of protein expression data also revealed other enriched gene sets involved in translation, RNA and protein metabolism and the immune system. Genes related to this proteome-based analysis overlapped (in)directly with the cell cycle-related gene sets. Within these significantly enriched cell cycle-related gene sets, we selected and explored the genes that contributed to the enrichment result (signal-to-noise ratio>0.1) for both the transcriptomics (142 genes) and proteomics (102 genes) datasets (Figure 4B and 4C, Additional file 8: Table S4). These genes contribute to a variety of cell cycle processes, such as G1/S transition, G2/M transition, cell cycle regulation, ubiquitination and nuclear division, suggesting that the observed cell cycle enrichment is not due to a prolonged state of one specific cell cycle phase. The genes included, amongst others, cyclin-dependent kinases (CDK) 2, 4, 5, 6 and 9, cell-division cycle (CDC) 25A and polo-like kinases (PLK) 1, 2 and 4.

Next, to examine whether the elevated mRNA expression of these 142 selected cell cycle-related genes was reflected in patient tumours, we exploited expression data

from The Cancer Genome Atlas (TCGA). Hierarchical clustering uncovered a specific set of 54 genes that was consistently expressed at higher levels in a subgroup of the breast cancer patients (Figure 5A). This cluster mainly consisted of tumours from basal-like, HER2-enriched and luminal B PAM50 subtypes. Although most of the TNBC tumours had high expression of these genes, also within the TNBC subset, these genes were differentially expressed (Figure 5B). The hierarchical clustering revealed three clusters of TNBC tumours, with either high (42%), intermediate (42%) or low (16%) expression of the signature genes. The 54 genes selected from these differential cluster in patients still also subdivide TNBC cell lines in a similar manner as the original 142 genes (Additional File 9, Figure S5).

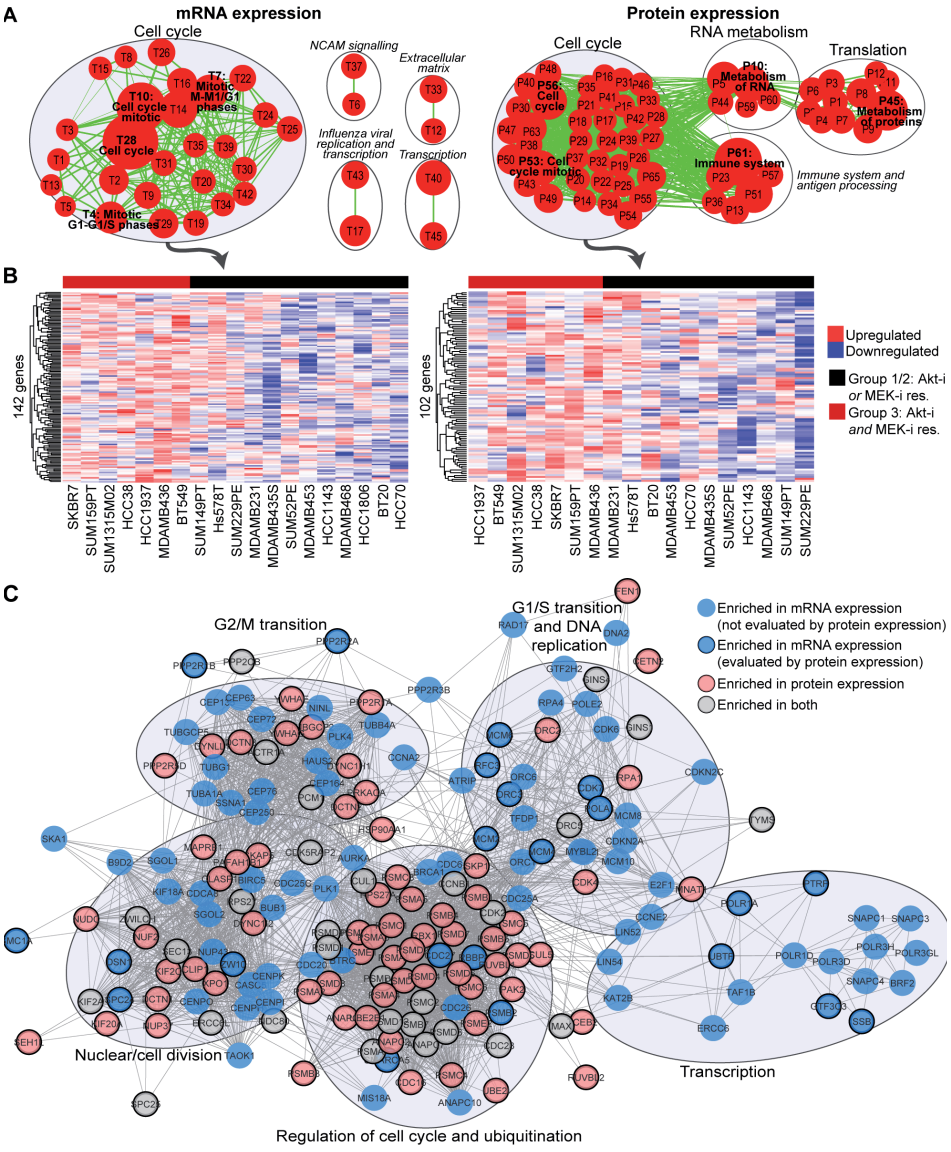

Figure 4. Gene set enrichment analysis (GSEA) in the Akt-i/MEK-i resistant cell lines. (A) mRNA (left) and protein (right) expression were compared between MEK and Akt inhibitor-resistant Group 3 versus MEK or Akt inhibitor-resistant Group 1 and 2 cell lines using GSEA. The enrichment maps visualise enriched gene sets (P<0.005, FDR Q-value<0.1, overlap>0.7), among which cell cycle gene sets were most abundant. Every node (red) represents a single overexpressed gene set and the size of the node indicates the size of the gene set. Every line (green) represents overlap between gene sets. Node numbers represent the corresponding gene set as listed in Additional file 7: Table S3. (B) Heatmaps of mRNA (left) and protein expression (right) of genes (log2 values and row-scaled) from the enriched genes from the cell cycle gene sets (signal-to-noise ratio > 0.1). (C) Overlapping networks of 102 protein (pink) and 142 mRNA (blue) expression enriched cell cycle genes indicate unique and shared (grey) genes. Some genes evaluated by mRNA expression were not included in the proteomics dataset and are indicated without border.

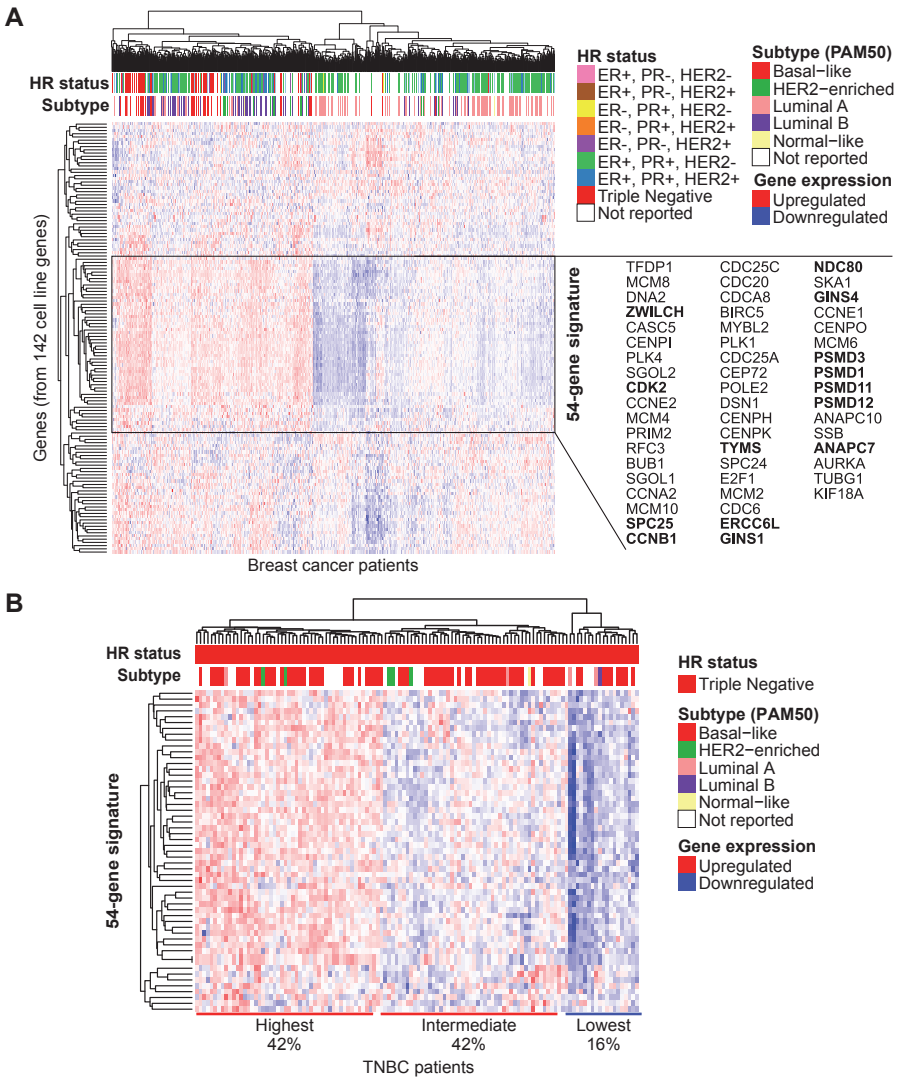

Figure 5. Expression of the Akt-i/MEK-i resistant cell cycle gene signature in breast cancer patients. (A) Clustering of all breast cancer patients (n=1093) from the TCGA database by gene expression levels of 134 expressed genes out of the 142 mRNA cell cycle genes found overexpressed in the Akt-i/MEK-i-resistant cell lines. The black box shows a cluster of 54 genes that was consistently expressed at a higher level in one of the two subsets of patients. Genes in bold indicate overexpressed genes that were shared in mRNA and protein expression GSEA of the Akt-i/MEK-i-resistant cell lines. (B) Clustering of TNBC patients (n=120) from the TCGA database based on expression of these 54 genes.

Elevated cell cycle gene expression signature provides novel targets for bypassing Akt-i/MEK-i resistance

Next, we investigated whether the aberrant cell cycle gene expression signature found in Akt-i/MEK-i-resistant Group 3 cell lines could be an alternative target for this subgroup. Pathway analysis of the overexpressed cell cycle genes visualised core components, including CDC25A, CDK2 and CDK4 (Figure 6A). Moreover, elevated E2F1 and DP1, together with low expression of RB1, were central in this pathway. Targeting the downstream CDKs affected by these transcription factors and CDC25A may therefore have detrimental direct and indirect effects on TNBC cell proliferation. From our kinase inhibitor screen, we selected dinaciclib (CDK1/2/5/9 inhibitor) and flavopiridol (CDK1/2/4/6 inhibitor) as CDK inhibitors that effectively reduced cell proliferation in all the TNBC cell lines at 1 μM (black box, Figure 6B). Subsequent validation showed that flavopiridol and dinaciclib strongly inhibited the growth of the Akt-i/MEK-i-resistant Group 3 cell lines (Figure 6C). Contrastingly, Group 1 cell lines HCC1806 and MDA-MB-435s showed a relatively reduced sensitivity to dinaciclib and flavopiridol, with an average 2-3-fold increase in IC50 for both CDK inhibitors (Figure 6C, Additional file 10: Table S5). Dinaciclib at 10 nM or 31.6 nM completely inhibited phosphorylation of RB1 at Ser780, an event specifically mediated by the CDK4/6-Cyclin D1 complex, in both HCC1806 and SUM159PT cells, indicative of cell cycle arrest (Figure 6D). Flavopiridol at 100 nM moderately reduced RB1-Ser780 levels in double-resistant Group 3 cell line SUM159PT but not in Akt-i-resistant Group 1 HCC1806 cells (Figure 6D). Similarly, CDK9/CDK7-mediated phosphorylation of RNA Polymerase II's C-terminal domain (POLR2A) at Ser2/5 was abolished by dinaciclib in both cell lines whereas flavopiridol exclusively reduced POLR2A phosphorylation in SUM159PT cells (Figure 6D). Dinaciclib induced cleavage of

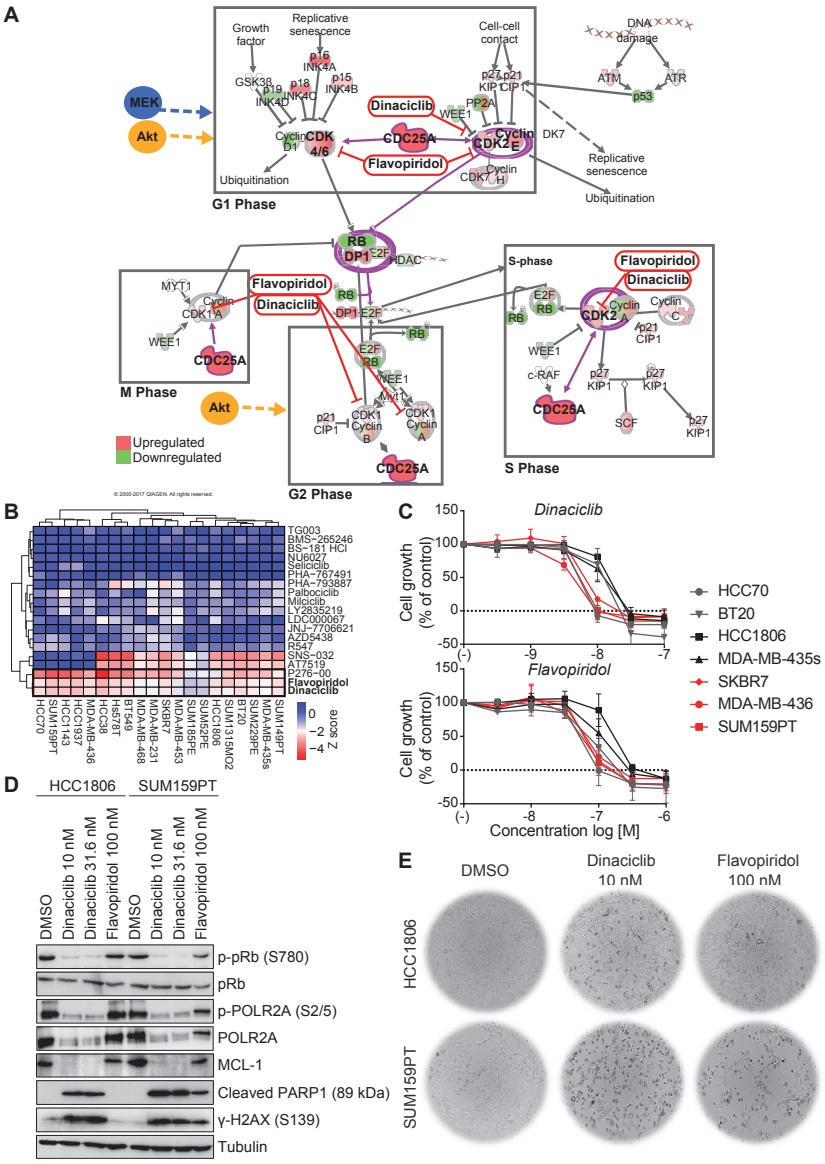

Figure 6. Enriched cell cycle gene expression signature provides alternative targets for Akt-i- and MEK-i-resistant TNBC cell lines. (A) Cell cycle pathway (IPA) and possible alternative drugs acting in this pathway. Green coloured targets indicate upregulation, whereas red coloured targets indicate downregulation in the Akt-i/MEK-i double-resistant cell lines. Purple circles indicate complexes with genes present in the 54-genes cluster from Figure 5A. (B) Heatmap of different CDK inhibitors (1 μM) on TNBC cell lines. Low Z-scores (red) indicate reduced cell growth, whereas high Z-scores indicate resistance (blue). (C) Concentration response effect of the cyclin-dependent kinase (CDK) inhibitors dinaciclib and flavopiridol in Akt-i/MEK-i resistant Group 3 cell lines (SKBR3, MDA-MB-436 and SUM159PT), Group 1 (HCC1806 and MDA-MB-435s) or Group 2 (HCC70 and BT20) TNBC cell lines. Data are expressed as mean ± SD and are representative of three independent experiments. (D) Western blot analysis of dinaciclib (10 or 31.6 nM) and flavopiridol (100 nM) on CDK function and apoptosis in HCC1806 and SUM159PT cells after 24 hours treatment. (E) Representative brightfield images of HCC1806 and SUM159PT cells treated with dinaciclib (10 nM) or flavopiridol (100 nM) taken 24 hours post-exposure.

PARP1 in both cell lines, whilst flavopiridol-induced PARP1 cleavage was solely visible in SUM159PT cells (Figure 6D). Concomitant depletion of BH3-only family member MCL-1 and induction of H2AX phosphorylation at Ser139 in double-resistant SUM159PT cells suggested induction of apoptosis and DNA damage response signalling. These effects were absent in HCC1806 cells after exposure to flavopiridol (Figure 6D). Cell death was clearly visible in SUM159PT cells 24 hours post-exposure to either inhibitor, but to a lesser extent in HCC1806 cells (Figure 6E). Notwithstanding this differential sensitivity, the Group 2 cell lines BT20 and HCC70 were equally as sensitive to the CDK inhibitors as Group 3 cell lines (Figure 6C). These data therefore suggest that CDK inhibitors which target the aberrant cell cycle profile are especially, but not exclusively, effective in Akt-i/MEK-i-resistant Group 3 cell lines.

DISCUSSION

Although various potential targets characterise TNBC tumours, no effective clinical targeted therapy is available for this aggressive disease. The ERK and Akt signalling programs are critical in various aspects of cancer biology, and MEK and Akt inhibitors have entered the clinic for various types of cancer [27, 28]. Given the genetic aberrations in upstream modulators of these pathways in TNBC, we addressed the heterogeneity in responses of a broad panel of TNBC cell lines to both MEK and Akt inhibitors. We here demonstrate that MEK and Akt double resistance is associated with the elevated expression of a cell cycle gene signature, while inhibition thereof effectively reduced cell proliferation in these MEK and Akt inhibitor double-resistant cell lines.

Previous studies have indicated that MEK or Akt inhibitor resistance in cancer can be caused by crosstalk between the PI3K/Akt/mTOR or RAF/MEK/ERK pathways [8, 9, 29]. Therefore, these studies suggest that combination therapy with MEK and Akt (or PI3K) inhibitors will reverse this resistance. In this study, we did not observe induction of the parallel pathways after Akt or MEK inhibition, with the exception of SUM159PT cells. Combination therapy also did not sufficiently sensitise the Akt- and MEK inhibitor-resistant cells to either therapy. These results suggest that crosstalk is not an essential mechanism of combined Akt-i and MEK-i resistance in TNBC. Indeed, even though various studies demonstrate synergistic effects of combination therapy, these did not disrupt cell viability completely [8, 9, 29]. Importantly, combination therapy with MEK and Akt inhibitors has also not shown promising results in clinical trials, as beneficial effects over single treatment are hardly obtained, instead causing more severe side effects [14, 15, 30]. For these reasons we sought to find another strategy to overcome the resistance in MEK-i- and Akt-i-resistant cells.

Our results demonstrate that Akt inhibitor-resistant cell lines can be distinguished from MEK inhibitor-resistant lines by increased levels of p-MEK and low levels of p-Akt. Additionally, mutations in PTEN, PI3KCA and/or PI3KR1 characterise MEK inhibitor-resistant but not Akt inhibitor-resistant cell lines. Similar observations were made in other cancer types by others [8-10]. However, these features do not entirely explain the observed resistance phenotypes in our panel of TNBC cell lines. Here, we further explored the underlying mechanisms responsible for double resistance to both Akt and MEK inhibitors. To this end, we took advantage of our unique transcriptome and proteome dataset of the entire TNBC cell line panel. Using large-scale gene set enrichment analysis, we revealed a 142-gene and 102-protein cell cycle-enriched signature associated with Akt and MEK inhibitor double resistance. Importantly, a signature of 54 of these genes subdivides all breast cancer patients, as well as TNBC patients, into separate groups based on their gene expression. The majority of TNBC patients had high expression of these genes, which is line with that so far, most TNBC patients are not responsive to MEK and Akt inhibitor treatments [8-11]. Yet, a minority of the TNBC patients may thus be sensitive to MEK or Akt inhibitors, depending on their p-MEK/p-Akt levels. Thus, stratification of patients in clinical trials of MEK or Akt inhibitors based on the features described in this study may reveal beneficial effects that would otherwise be neglected. Nevertheless, further studies are needed to translate the associations found here to patient treatment responses.

The overexpression of the cell cycle genes may render signals from Akt and MEK redundant. No studies have previously linked such a profile to Akt and MEK inhibitor resistance in TNBC. However, various studies in other cancer types have recently demonstrated the role of the cell cycle in this resistance by confirming synergy

between inhibitors of the PI3K/MAPK pathway and inhibitors of the cell cycle, such as CDK and PLK inhibitors [31-37]. These findings suggest that the enhanced expression and activity of cell cycle machinery components may have an important role in resistance to Akt and MEK inhibitors, not only in TNBC, but also in other cancer types.

Our data demonstrate that inhibition of CDKs that determine cell cycle progression and transcription can effectively kill TNBC cells that are otherwise resistant to Akt-i/MEK-i. For example, the pan-CDK inhibitors dinaciclib and flavopiridol inhibited proliferation of SUM159T cells that were resistant to both Akt-i and MEK-i. Interestingly, some, but not all, Akt or MEK inhibitor-sensitive cell lines were more resistant to these compounds compared to MEK-i/Akt-i double-resistant cell lines. Thus, these compounds are especially, but not exclusively, effective against this group and provide possible alternative treatments for overcoming Akt and MEK inhibitor double resistance. Notably, both lethal and sub-lethal concentrations of dinaciclib inhibited RB1 and POLR2A phosphorylation in HCC1806 cells, confirming that its relative insensitivity to this agent is not related to inefficient target inhibition, unlike flavopiridol. The superior activity of dinaciclib compared to flavopiridol was also evidenced by the complete abrogation of RB1 and POLR2A phosphorylation at concentrations ten times lower than those required for flavopiridol to elicit a moderately comparable effect, which was only visible in MEK-i/Akt-i double-resistant SUM159PT cells. Elucidating whether dependence on CDKs that regulate transcription (e.g. CDK7 and CDK9), or those that control cell cycle progression (e.g. CDK1, CDK2, CDK4 and CDK6), is responsible for the differential sensitivity of these groups to CDK inhibitors is essential for further mechanistic deconvolution. Additionally, considering that both dinaciclib and flavopiridol exhibit broad spectrum

activity against multiple CDKs and their association with severe side-effects in clinical trials, the development and subsequent evaluation of more specific CDK inhibitors in this subgroup would be prudent. Nonetheless, the relative sensitivity of MEK-i/Akt-i double-resistant TNBC cells to such agents could theoretically expand the therapeutic window to circumvent unwanted side-effects and thereby allow the combination of CDK inhibitors with other targeted therapies.

CONCLUSION

To conclude, we have been able to discriminate between Akt-i and MEK-i single agent-sensitive subsets of TNBC cells as well as double agent-resistant TNBC cells. For double-resistant cells we uncovered a high expression of a cell cycle gene signature. Accordingly, these double-resistant cells are relatively sensitive to inhibitors of CDKs. Importantly, a number of these genes are also differentially expressed in TNBC patients. Since our study describes clinically relevant features that can subdivide TNBC cells into their Akt and MEK inhibitor response profile, these features may also facilitate the prediction of response in patients. Future mechanistic studies may reveal the origin of the aberrant cell cycle signature, which could supplement this study by providing additional alternative targets and simplified biomarkers for clinical assessment. Altogether, this and future studies could therefore lead to a biomarker-based therapeutic strategy for treating TNBC patients with Akt, MEK and/or CDK inhibitors.

LIST OF ABBREVIATIONS

Akt-i: Akt inhibitor

BSA: bovine serum albumin

CDC: cell-division cycle

CDK: cyclin-dependent kinase

EGFR: epidermal growth factor receptor

ER: estrogen receptor

FBS: fetal bovine serum

GSEA: gene set enrichment analysis

HER2: human epidermal growth factor receptor 2

HRP: horseradish peroxidase

IPA: Ingenuity Pathway Analysis

MAPK: mitogen-activated protein kinase

MEK-i: MEK inhibitor

PBS: phosphate-buffered saline

PI3K: phosphoinositide 3-Kinase

PLK: polo-like kinases

POLR2A: RNA Polymerase II's C-terminal domain

PR: progesterone receptor

PVDF: polyvinylidene fluoride

RMA: robust multi-array average

SRB: sulforhodamine B

TBS-$T_{0.05}$: tris-buffered saline with 0.05% Tween 20

TCA: trichloroacetic acid

TCGA: The Cancer Genome Atlas

TNBC: triple negative breast cancer

FUNDING

This work was supported by the ERC Advanced grant Triple-BC (grant no. 322737) and the Dutch Cancer Society project (grant nr 2011-5124).

REFERENCES

1. Jun H, Zhong W: Descriptive analysis of estrogen receptor (ER)-negative, progesterone receptor (PR)-negative, and HER2-negative invasive breast cancer, the so-called triple-negative phenotype. Cancer Genetics and Epigenetics 2014, 2.
2. Bauer KR, Brown M, Cress RD, Parise CA, Caggiano V: Descriptive analysis of estrogen receptor (ER)-negative, progesterone receptor (PR)-negative, and HER2-negative invasive breast cancer, the so-called triple-negative phenotype: a population-based study from the California cancer Registry. Cancer 2007, 109(9):1721-1728.
3. Cortazar P, Zhang L, Untch M, Mehta K, Costantino JP, Wolmark N, Bonnefoi H, Cameron D, Gianni L, Valagussa P: Pathological complete response and long-term clinical benefit in breast cancer: the CTNeoBC pooled analysis. The Lancet 2014, 384(9938):164-172.
4. Dent R, Trudeau M, Pritchard KI, Hanna WM, Kahn HK, Sawka CA, Lickley LA, Rawlinson E, Sun P, Narod SA: Triple-negative breast cancer: clinical features and patterns of recurrence. Clinical cancer research 2007, 13(15):4429-4434.
5. Network CGA: Comprehensive molecular portraits of human breast tumors. Nature 2012, 490(7418):61.
6. Craig DW, Shaughnessy JA, Kiefer JA, Aldrich J, Sinari S, Moses TM, Wong S, Dinh J, Christoforides A, Blum JL et al: Genome and Transcriptome Sequencing in Prospective Metastatic Triple-Negative Breast Cancer Uncovers Therapeutic Vulnerabilities. Molecular Cancer Therapeutics 2013, 12(1):104.
7. Saini KS, Loi S, de Azambuja E, Metzger-Filho O, Saini ML, Ignatiadis M, Dancey JE, Piccart-Gebhart MJ: Targeting the PI3K/AKT/mTOR and Raf/MEK/ERK pathways in the treatment of breast cancer. Cancer treatment reviews 2013, 39(8):935-946.
8. Hoeflich KP, O'Brien C, Boyd Z, Cavet G, Guerrero S, Jung K, Januario T, Savage H, Punnoose E, Truong T: In vivo antitumor activity of MEK and phosphatidylinositol 3-kinase inhibitors in basal-like breast cancer models. Clinical Cancer Research 2009, 15(14):4649-4664.
9. Mirzoeva OK, Das D, Heiser LM, Bhattacharya S, Siwak D, Gendelman R, Bayani N, Wang NJ, Neve RM, Guan Y: Basal subtype and MAPK/ERK kinase

(MEK)-phosphoinositide 3-kinase feedback signaling determine susceptibility of breast cancer cells to MEK inhibition. Cancer research 2009, 69(2):565-572.
10. Sangai T, Akcakanat A, Chen H, Tarco E, Wu Y, Do K-A, Miller TW, Arteaga CL, Mills GB, Gonzalez-Angulo AM: Biomarkers of response to Akt inhibitor MK-2206 in breast cancer. Clinical Cancer Research 2012, 18(20):5816-5828.
11. Hirai H, Sootome H, Nakatsuru Y, Miyama K, Taguchi S, Tsujioka K, Ueno Y, Hatch H, Majumder PK, Pan B-S: MK-2206, an allosteric Akt inhibitor, enhances antitumor efficacy by standard chemotherapeutic agents or molecular targeted drugs in vitro and in vivo. Molecular cancer therapeutics 2010, 9(7):1956-1967.
12. Duncan JS, Whittle MC, Nakamura K, Abell AN, Midland AA, Zawistowski JS, Johnson NL, Granger DA, Jordan NV, Darr DB: Dynamic reprogramming of the kinome in response to targeted MEK inhibition in triple-negative breast cancer. Cell 2012, 149(2):307-321.
13. Maiello MR, D'Alessio A, Bevilacqua S, Gallo M, Normanno N, De Luca A: EGFR and MEK blockade in triple negative breast cancer cells. Journal of cellular biochemistry 2015, 116(12):2778-2785.
14. Shimizu T, Tolcher AW, Papadopoulos KP, Beeram M, Rasco DW, Smith LS, Gunn S, Smetzer L, Mays TA, Kaiser B: The clinical effect of the dual-targeting strategy involving PI3K/AKT/mTOR and RAS/MEK/ERK pathways in patients with advanced cancer. Clinical Cancer Research 2012, 18(8):2316-2325.
15. NCT01562275: A Study Evaluating the Safety, Tolerability, and Pharmacokinetics of GDC-0973 in Combination With GDC-0068 When Administered in Participants With Locally Advanced or Metastatic Solid Tumors. [http://clinicaltrials.gov/show/NCT01562275]
16. Zhang Y, Moerkens M, Ramaiahgari S, de Bont H, Price L, Meerman J, van de Water B: Elevated insulin-like growth factor 1 receptor signaling induces antiestrogen resistance through the MAPK/ERK and PI3K/Akt signaling routes. Breast cancer research 2011, 13(3):R52.
17. Qin Y, Stokman G, Yan K, Ramaiahgari S, Verbeek F, de Graauw M, van de Water B, Price LS: cAMP signalling protects proximal tubular epithelial cells from cisplatin–induced apoptosis via activation of Epac. British journal of pharmacology 2012, 165(4b):1137-1150.
18. Lehmann BD, Bauer JA, Chen X, Sanders ME, Chakravarthy AB, Shyr Y, Pietenpol JA: Identification of human triple-negative breast cancer subtypes and preclinical models for selection of targeted therapies. The Journal of clinical investigation 2011, 121(7):2750-2767.
19. Forbes SA, Beare D, Boutselakis H, Bamford S, Bindal N, Tate J, Cole CG, Ward S, Dawson E, Ponting L: COSMIC: somatic cancer genetics at high-resolution. Nucleic acids research 2016, 45(D1):D777-D783.

20. Riaz M, van Jaarsveld MT, Hollestelle A, Prager-van der Smissen WJ, Heine AA, Boersma AW, Liu J, Helmijr J, Ozturk B, Smid M: miRNA expression profiling of 51 human breast cancer cell lines reveals subtype and driver mutation-specific miRNAs. Breast cancer research 2013, 15(2):R33.
21. Subramanian A, Tamayo P, Mootha VK, Mukherjee S, Ebert BL, Gillette MA, Paulovich A, Pomeroy SL, Golub TR, Lander ES: Gene set enrichment analysis: a knowledge-based approach for interpreting genome-wide expression profiles. Proceedings of the National Academy of Sciences 2005, 102(43):15545-15550.
22. Mootha VK, Lindgren CM, Eriksson K-F, Subramanian A, Sihag S, Lehar J, Puigserver P, Carlsson E, Ridderstråle M, Laurila E: PGC-1α-responsive genes involved in oxidative phosphorylation are coordinately downregulated in human diabetes. Nature genetics 2003, 34(3):267-273.
23. Merico D, Isserlin R, Stueker O, Emili A, Bader GD: Enrichment map: a network-based method for gene-set enrichment visualization and interpretation. PloS one 2010, 5(11):e13984.
24. Colaprico A, Silva TC, Olsen C, Garofano L, Cava C, Garolini D, Sabedot TS, Malta TM, Pagnotta SM, Castiglioni I: TCGAbiolinks: an R/Bioconductor package for integrative analysis of TCGA data. Nucleic acids research 2015:gkv1507.
25. Kolde R: pheatmap: Pretty Heatmaps. R package version 1.0. 2. In.; 2015.
26. Lin J, Sampath D, Nannini MA, Lee BB, Degtyarev M, Oeh J, Savage H, Guan Z, Hong R, Kassees R: Targeting activated Akt with GDC-0068, a novel selective Akt inhibitor that is efficacious in multiple tumor models. Clinical Cancer Research 2013, 19(7):1760-1772.
27. LoRusso PM: Inhibition of the PI3K/AKT/mTOR pathway in solid tumors. Journal of Clinical Oncology 2016, 34(31):3803-3815.
28. Zhao Y, Adjei AA: The clinical development of MEK inhibitors. Nature reviews Clinical oncology 2014, 11(7):385.
29. Lee J, Galloway R, Grandjean G, Jacob J, Humphries J, Bartholomeusz C, Goodstal S, Lim B, Bartholomeusz G, Ueno NT: Comprehensive Two-and Three-Dimensional RNAi Screening Identifies PI3K Inhibition as a Complement to MEK Inhibitor AS703026 for Combination Treatment of Triple-Negative Breast Cancer. Journal of Cancer 2015, 6(12):1306.
30. NCT01658943: Selumetinib and Akt Inhibitor MK2206 or mFOLFOX Therapy Comprising Oxaliplatin and Fluorouracil in Treating Patients With Metastatic Pancreatic Cancer Previously Treated With Chemotherapy. [http://clinicaltrials.gov/show/NCT01658943]
31. Morgan-Lappe S, Woods KW, Li Q, Anderson MG, Schurdak ME, Luo Y, Giranda VL, Fesik SW, Leverson JD: RNAi-based screening of the human kinome identifies Akt-cooperating kinases: a new approach to designing efficacious multitargeted kinase inhibitors. Oncogene 2006, 25(9):1340-1348.

32. Vora SR, Juric D, Kim N, Mino-Kenudson M, Huynh T, Costa C, Lockerman EL, Pollack SF, Liu M, Li X: CDK 4/6 inhibitors sensitize PIK3CA mutant breast cancer to PI3K inhibitors. Cancer cell 2014, 26(1):136-149.
33. Lee MS, Helms TL, Feng N, Gay J, Chang QE, Tian F, Wu JY, Toniatti C, Heffernan TP, Powis G: Efficacy of the combination of MEK and CDK4/6 inhibitors in vitro and in vivo in KRAS mutant colorectal cancer models. Oncotarget 2016, 7(26):39595.
34. Eliades P, Miller DM, Miao B, Kumar R, Taylor M, Buch S, Srinivasa SP, Flaherty KT, Tsao H: A novel multi-CDK inhibitor P1446A-05 restricts melanoma growth and produces synergistic effects in combination with MAPK pathway inhibitors. Cancer biology & therapy 2016, 17(7):778-784.
35. Posch C, Cholewa BD, Vujic I, Sanlorenzo M, Ma J, Kim ST, Kleffel S, Schatton T, Rappersberger K, Gutteridge R: Combined inhibition of MEK and Plk1 has synergistic antitumor activity in NRAS mutant melanoma. Journal of Investigative Dermatology 2015, 135(10):2475-2483.
36. Beale G, Haagensen EJ, Thomas HD, Wang L-Z, Revill CH, Payne SL, Golding BT, Hardcastle IR, Newell DR, Griffin RJ: Combined PI3K and CDK2 inhibition induces cell death and enhances in vivo antitumour activity in colorectal cancer. British Journal of Cancer 2016.
37. Hu C, Dadon T, Chenna V, Yabuuchi S, Bannerji R, Booher R, Strack P, Azad N, Nelkin BD, Maitra A: Combined inhibition of cyclin-dependent kinases (dinaciclib) and AKT (MK-2206) blocks pancreatic tumor growth and metastases in patient-derived xenograft models. Molecular cancer therapeutics 2015, 14(7):1532-1539.

ADDITIONAL FILES

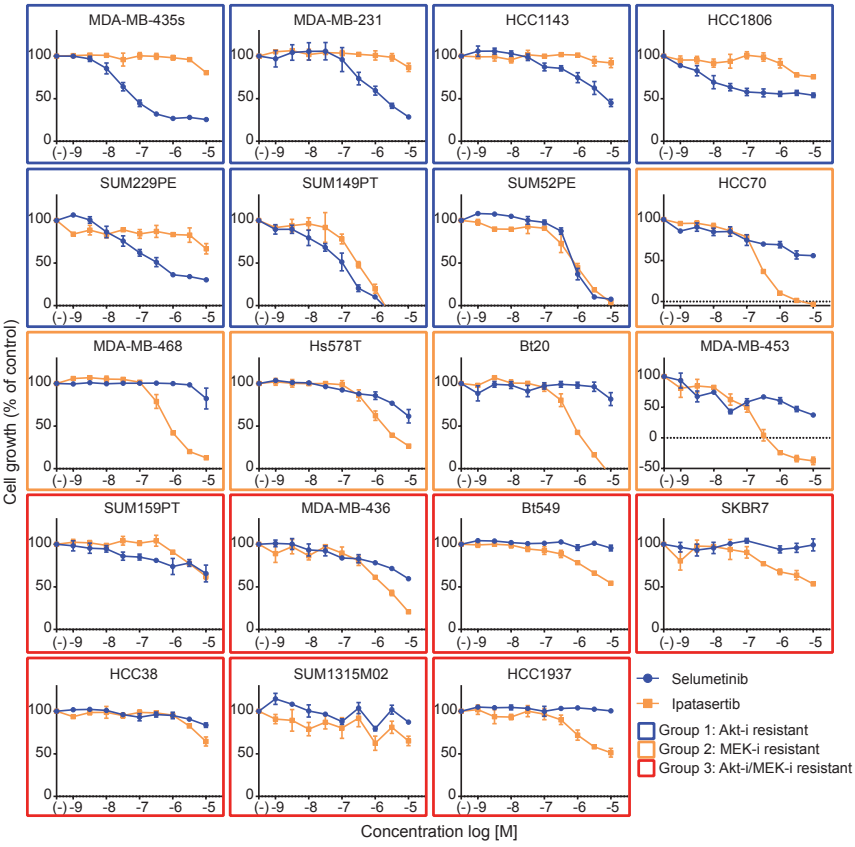

Additional file 1: Figure S1. Sensitivity profiling in TNBC cell lines. Validation of Akt-i/MEK-i sensitivity classifications from primary screening (Figure 1B). Proliferative responses of cell lines to increasing concentrations (0.001-10 µM) of selumetinib (MEK-i) and ipatasertib (Akt-i) are shown.

		Akt-i resistant			MEK-i resistant			Akt-i & MEK-i double resistant		
	IC50 (μM)	**MDA-MB-231**	**MDA-MB-435s**	**HCC1806**	**MDA-MB-468**	**BT20**	**HCC70**	**SKBR7**	**SUM159PT**	**MDA-MB-436**
Akt inhibitors	**MK-2206**	>3.16	>3.16	>3.16	0.30	>3.16	0.26	>3.16	1.35	>3.16
	GDC-0068	>3.16	>3.16	>3.16	0.16	0.38	0.21	>3.16	>3.16	>3.16
	AZD5363	>3.16	>3.16	>3.16	0.15	0.34	0.17	>3.16	~3.16	>3.16
	GSK690693	>3.16	>3.16	>3.16	>3.16	0.15	1.31	>3.16	>3.16	>3.16
MEK inhibitors	**Selumetinib**	0.05	0.03	>3.16	>3.16	>3.16	>3.16	>3.16	2.74	>3.16
	MEK-i162	<0.01	<0.01	7.617	>3.16	>3.16	>3.16	>3.16	~3.16	>3.16
	Trametinib	<0.01	<0.01	<0.01	0.03	>3.16	>3.16	>3.16	NA	NA
	PD318088	0.15	<0.01	<0.01	0.32	>3.16	>3.16	>3.16	>3.16	>3.16
	PD184352	0.79	0.12	<0.01	>3.16	>3.16	>3.16	>3.16	>3.16	>3.16
	PD032590	<0.01	<0.01	0.48	0.53	>3.16	>3.16	>3.16	>3.16	>3.16
	Pimasertib	<0.01	<0.01	2.27	2.39	>3.16	>3.16	>3.16	>3.16	>3.16
	Refametinib	<0.01	<0.01	<0.01	>3.16	>3.16	>3.16	>3.16	~3.16	>3.16
	TAK-733	<0.01	<0.01	<0.01	0.27	>3.16	>3.16	>3.16	~3.16	>3.16
	AZD8330	<0.01	<0.01	<0.01	>3.16	>3.16	>3.16	>3.16	>3.16	>3.16

Additional file 2: Table S1. IC50s for Akt and MEK inhibitors. In order to validate the resistance to Akt and/or MEK inhibitors, cells were treated with a dose range (0.01 – 3.16 μM) of inhibitors in three technical replicates. Proliferation was evaluated using an SRB assay and IC50's were calculated using GraphPad Prism. If 50% of proliferation was not reached, IC50's are noted as >3.16. For the case of more than 50% reduction of growth at the lowest concentration, IC50's were noted as <0.01.

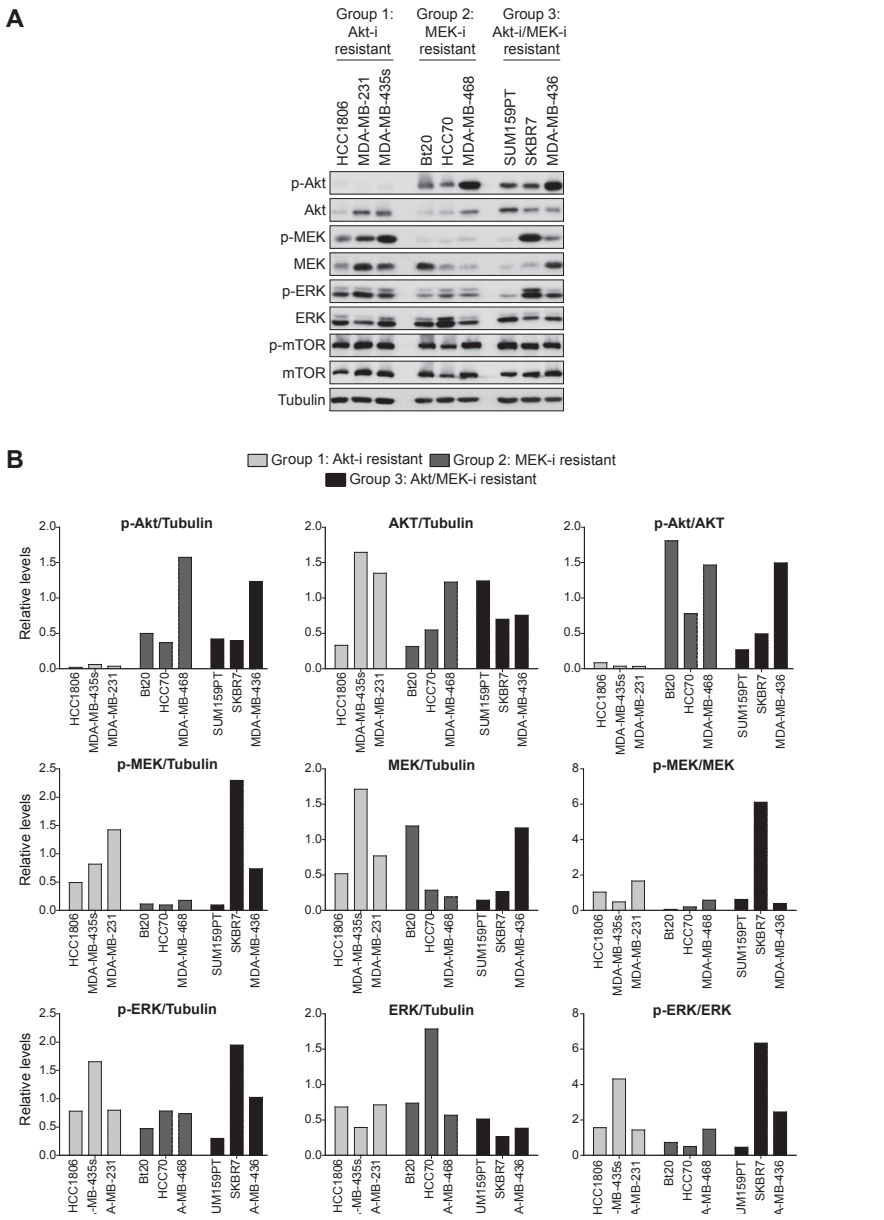

Additional file 3: Figure S2. Western blot quantifications of the Akt-i/MEK-i differentially resistant cell lines. Phosphorylation levels of Akt (p-Akt) and MEK (p-MEK) normalised to tubulin or total Akt and MEK respectively.

		PI3K	MAPK	PI3K/ MAPK	Cell cycle	DNA damage repair
1): Akt-i resistant	**HCC1143**			FGFR2	TP53	
	MDA-MB-435s		BRAF		TP53, CDKN2A, EP300	
	MDA-MB-231		BRAF,NF1	PDGFRA, KRAS	TP53, CDKN2A	
	HCC1806		NFATC2, ROS1	PDGFRB	TP53, CDKN2A	
	SUM229PE			KRAS	CDKN2A	
	SUM52PE				TP53, CDKN2A	
	SUM149PT				TP53, CDKN2A, EP300	BRCA1
2) MEK-i resistant	**HCC70**	PTEN			TP53, RB1	
	MDA-MB-453	PIK3CA, PTEN	ROS1		CREBBP, ATM, STAG2	CREBBP, ATM
	SUM185PE	PIK3CA			TP53	
	BT20	PIK3CA			ATM, CDKN2C, CDKN2A, RB1, TP53	MLH1
	Hs578T	PIK3R1	NF1	HRAS	TP53, CDKN2A, POLE	POLE
	MDA-MB-468	PTEN	CACNA1D, MAP3K13		TP53, CDKN2A, RB1	
3) Akt/MEK-i resistant	**BT549**	PTEN		FGFR1	TP53, RB1, BUB1B, (DCTN1), PCM1	MUTYH
	SKBR7			KRAS, NRAS	CDKN2A	
	HCC1937	PTEN	MAPK13		TP53, RB1	BRCA1
	MDA-MB-436	PIK3R1			TP53, RB1	BRCA1, POLE
	HCC38		IKBKB		TP53, CDKN2A	PMS2, BRCA1*
	SUM159PT	PIK3CA		HRAS	TP53	
	SUM1315MO2	PIK3CA			TP53	BRCA1

Additional file 4: Table S2. Common mutations in cell lines in components of the PI3K, MAPK, cell cycle and DNA damage repair pathways. Mutations in Cancer Gene Census genes were obtained from the COSMIC database (http://cancer.sanger.ac.uk/cosmic).

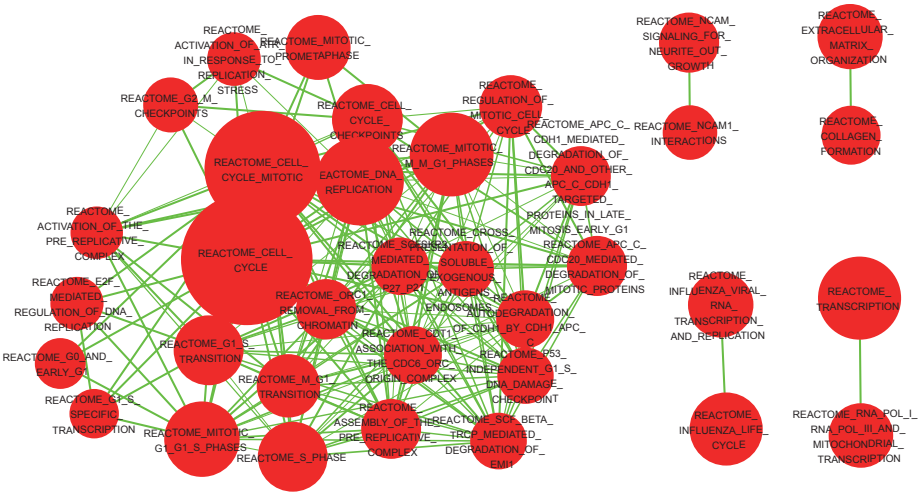

Additional file 5: Figure S3. Gene set enrichment map for sets enriched in mRNA expression for Akt-i/MEK-i resistant Group 3 cell lines. This figure represents an enlarged version and annotated version of Figure 4A (left part). mRNA expression was compared between MEK and Akt inhibitor-resistant Group 3 versus MEK or Akt inhibitor resistant Group 1 and 2 cell lines using gene set enrichment analysis (GSEA). The enrichment map visualizes enriched gene sets (P<0.005, FDR Q-value<0.1, overlap>0.7), among which cell cycle gene sets were most abundant. Every node (red) represents a single overexpressed gene set and the size of the node indicates the size of the gene set. Every line (green) represents overlap between gene sets.

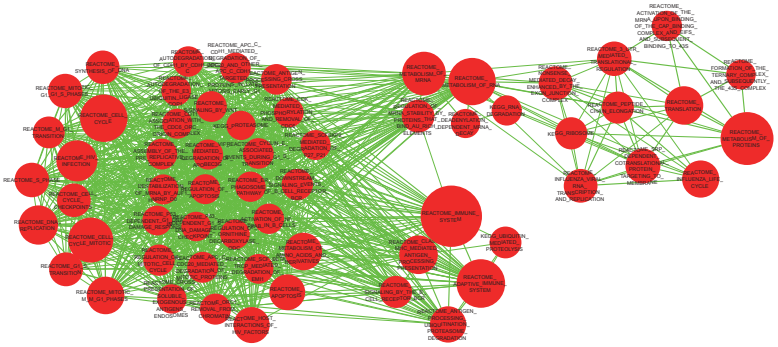

Additional file 6: Figure S4. Gene set enrichment map for sets enriched in protein expression for Akt-i/MEK-i resistant Group 3 cell lines. This figure represents an enlarged and annotated version of Figure 4A (right part). Protein expression was compared between MEK and Akt inhibitor-resistant Group 3 versus MEK or Akt inhibitor-resistant Group 1 and 2 cell lines using gene set enrichment analysis (GSEA). The enrichment map visualizes enriched gene sets (P<0.005, FDR Q-value<0.1, overlap>0.7), among which cell cycle gene sets were most abundant. Every node (red) represents a single overexpressed gene set and the size of the node indicates the size of the gene set. Every line (green) represents overlap between gene sets.

Gene set enrichment analysis for mRNA expression: Akt-i/MEK-i resistant Group 3 cell lines vs. Akt-i resistant Group 1 and MEK-i resistant Group 2 cell lines

NAME	Annotation Fig. 5C	SIZE	ES	NES	NOM p-	FDR q-val	FWER p-val	RANK AT MAX	LEADING EDGE
REACTOME_E2F_MEDIATED_REGULATION_OF_DNA_REPLICATION	T1	33	0.648059	2.000001	0	0.02188663	0.017		4199 tags=52%, list=21%, signal=65%
REACTOME_G1_S_TRANSITION	T2	105	0.517212	1.931039	0	0.03513823	0.054		4199 tags=36%, list=21%, signal=46%
REACTOME_ACTIVATION_OF_THE_PRE_REPLICATIVE_COMPLEX	T3	30	0.63881	1.919957	0	0.02569246	0.059		4199 tags=50%, list=21%, signal=63%
REACTOME_MITOTIC_G1_G1_S_PHASES	T4	129	0.490588	1.91859	0	0.01991754	0.061		6390 tags=54%, list=32%, signal=79%
REACTOME_G1_S_SPECIFIC_TRANSCRIPTION	T5	17	0.711817	1.873456	0	0.03074445	0.113		2071 tags=41%, list=10%, signal=46%
REACTOME_NCAM1_INTERACTIONS	T6	39	0.591172	1.870112	0	0.02800792	0.121		1305 tags=23%, list=7%, signal=25%
REACTOME_MITOTIC_M_M_G1_PHASES	T7	165	0.468203	1.856743	0	0.02984626	0.148		6392 tags=55%, list=32%, signal=80%
REACTOME_ACTIVATION_OF_ATR_IN_RESPONSE_TO_REPLICATION_STRI	T8	35	0.593487	1.839488	0.002212	0.03361766	0.187		4656 tags=49%, list=23%, signal=63%
REACTOME_M_G1_TRANSITION	T9	77	0.511562	1.828418	0	0.03464601	0.214		6390 tags=56%, list=32%, signal=82%
REACTOME_CELL_CYCLE_MITOTIC	T10	304	0.427041	1.828269	0	0.03118141	0.214		4788 tags=40%, list=24%, signal=52%
REACTOME_SMOOTH_MUSCLE_CONTRACTION	T11	21	0.673314	1.816516	0	0.03334333	0.246		1613 tags=43%, list=8%, signal=47%
REACTOME_COLLAGEN_FORMATION	T12	58	0.533975	1.815583	0	0.03077645	0.248		3325 tags=40%, list=17%, signal=47%
REACTOME_G0_AND_EARLY_G1	T13	23	0.652158	1.811426	0.002262	0.2979021	0.258		4349 tags=57%, list=22%, signal=72%
REACTOME_DNA_REPLICATION	T14	185	0.443186	1.806704	0	0.02988826	0.279		6392 tags=54%, list=32%, signal=78%
REACTOME_G2_M_CHECKPOINTS	T15	41	0.567241	1.793131	0	0.03425162	0.334		4656 tags=46%, list=23%, signal=60%
REACTOME_CELL_CYCLE_CHECKPOINTS	T16	109	0.468303	1.761241	0	0.04690277	0.431		6390 tags=55%, list=32%, signal=81%
REACTOME_INFLUENZA_LIFE_CYCLE	T17	119	0.460401	1.756614	0	0.04663166	0.446		5941 tags=34%, list=30%, signal=49%
KEGG_GLYCOSAMINOGLYCAN_BIOSYNTHESIS_CHONDROITIN_SULFATE	T18	22	0.641287	1.747796	0.002203	0.04383973	0.484		3826 tags=59%, list=19%, signal=73%
REACTOME_ASSEMBLY_OF_THE_PRE_REPLICATIVE_COMPLEX	T19	62	0.504069	1.744062	0	0.04819706	0.499		6390 tags=56%, list=32%, signal=83%
REACTOME_CDT1_ASSOCIATION_WITH_THE_CDC6_ORC_ORIGIN_COMPLI	T20	53	0.505585	1.72572	0	0.05613895	0.57		6576 tags=58%, list=33%, signal=87%
REACTOME_PROTEOLYTIC_CLEAVAGE_OF_SNARE_COMPLEX_PROTEINS	T21	16	0.674308	1.718836	0.008929	0.05921763	0.603		1914 tags=38%, list=10%, signal=41%
REACTOME_REGULATION_OF_MITOTIC_CELL_CYCLE	T22	75	0.484356	1.709248	0	0.06374024	0.653		6390 tags=59%, list=32%, signal=86%
REACTOME_BOTULINUM_NEUROTOXICITY	T23	18	0.667353	1.703353	0.006329	0.06511828	0.683		1914 tags=33%, list=10%, signal=37%
REACTOME_APC_C_CDH1_MEDIATED_DEGRADATION_OF_CDC20_AND_I	T24	62	0.491717	1.695015	0	0.06813725	0.71		6390 tags=60%, list=32%, signal=88%
REACTOME_APC_C_CDC20_MEDIATED_DEGRADATION_OF_MITOTIC_PRO	T25	63	0.486772	1.687013	0.002404	0.07142898	0.736		6390 tags=59%, list=32%, signal=86%
REACTOME_MITOTIC_PROMETAPHASE	T26	84	0.474831	1.684869	0	0.06878161	0.737		4562 tags=44%, list=23%, signal=57%
REACTOME_MUSCLE_CONTRACTION	T27	44	0.51859	1.673974	0.005155	0.07513121	0.779		2469 tags=32%, list=12%, signal=36%
REACTOME_CELL_CYCLE	T28	371	0.383318	1.654053	0	0.0871747	0.839		4788 tags=37%, list=24%, signal=48%
REACTOME_S_PHASE	T29	105	0.481455	1.651634	0	0.08605069	0.846		6390 tags=53%, list=32%, signal=78%
REACTOME_AUTODEGRADATION_OF_CDH1_BY_CDH1_APC_C	T30	54	0.489585	1.650928	0.00237	0.08369537	0.848		6390 tags=59%, list=32%, signal=87%
REACTOME_ORC1_REMOVAL_FROM_CHROMATIN	T31	64	0.477012	1.650509	0	0.08133798	0.851		6390 tags=55%, list=32%, signal=80%
REACTOME_INTERACTIONS_OF_VPR_WITH_HOST_CELLULAR_PROTEINS	T32	33	0.567535	1.645014	0.009009	0.08301806	0.866		5941 tags=50%, list=30%, signal=71%
REACTOME_EXTRACELLULAR_MATRIX_ORGANIZATION	T33	85	0.462485	1.64351	0	0.08152501	0.868		2863 tags=31%, list=14%, signal=36%
REACTOME_SCF_BETA_TRCP_MEDIATED_DEGRADATION_OF_EMI1	T34	48	0.494058	1.637799	0.004651	0.08363824	0.887		6390 tags=56%, list=32%, signal=83%
REACTOME_SCF(SKP2_MEDIATED_DEGRADATION_OF_P27_P21	T35	52	0.495648	1.636911	0.004963	0.08187833	0.892		6390 tags=56%, list=32%, signal=82%
REACTOME_TRANSPORT_OF_RIBONUCLEOPROTEINS_INTO_THE_HOST_NT	T36	27	0.569639	1.636694	0.006772	0.07978592	0.892		5941 tags=56%, list=30%, signal=79%
REACTOME_NCAM_SIGNALING_FOR_NEURITE_OUT_GROWTH	T37	63	0.464618	1.630578	0.002326	0.08278144	0.907		2834 tags=25%, list=14%, signal=30%
REACTOME_SYNTHESIS_OF_DNA	T38	89	0.443955	1.628377	0.007042	0.082221	0.909		6390 tags=53%, list=32%, signal=77%
REACTOME_CROSS_PRESENTATION_OF_SOLUBLE_EXOGENOUS_ANTIGEN	T39	45	0.49524	1.6227	0.002488	0.0845862	0.922		6390 tags=58%, list=32%, signal=85%
REACTOME_TRANSCRIPTION	T40	162	0.403929	1.614963	0	0.08899737	0.935		6750 tags=49%, list=34%, signal=73%
KEGG_RENIN_ANGIOTENSIN_SYSTEM	T41	17	0.623359	1.614658	0.010002	0.08717841	0.935		1309 tags=24%, list=7%, signal=25%
REACTOME_PS3_INDEPENDENT_G1_S_DNA_DAMAGE_CHECKPOINT	T42	47	0.489796	1.607394	0	0.09124204	0.945		6588 tags=57%, list=33%, signal=86%
REACTOME_INFLUENZA_VIRAL_RNA_TRANSCRIPTION_AND_REPLICATIO	T43	86	0.440785	1.605513	0.002392	0.09050808	0.945		7878 tags=50%, list=39%, signal=82%
REACTOME_CDK_MEDIATED_PHOSPHORYLATION_AND_REMOVAL_OF_CD	T44	45	0.489888	1.604504	0.009501	0.08934894	0.948		6390 tags=58%, list=32%, signal=85%
REACTOME_RNA_POL_I_RNA_POL_III_AND_MITOCHONDRIAL_TRANSCR	T45	82	0.444349	1.593924	0.002506	0.096904	0.967		5284 tags=37%, list=26%, signal=50%
REACTOME_FORMATION_OF_THE_TERNARY_COMPLEX_AND_SUBSEQUENT	T46	42	0.504504	1.583722	0.013793	0.10422498	0.977		4900 tags=31%, list=25%, signal=41%
REACTOME_MEF_M02_INTERACTS_WITH_THE_CELLULAR_EXPORT_MACHI	T47	27	0.543015	1.578537	0.013245	0.10654378	0.98		5941 tags=48%, list=30%, signal=68%
REACTOME_TRANSPORT_OF_MATURE_MRNA_DERIVED_FROM_AN_INTR	T48	31	0.531499	1.576246	0.018735	0.10636779	0.98		5941 tags=52%, list=30%, signal=73%
REACTOME_NONSENSE_MEDIATED_DECAY_ENHANCED_BY_THE_EXON_JU	T49	90	0.427204	1.565741	0.002463	0.11477371	0.986		5153 tags=26%, list=26%, signal=34%
REACTOME_FGFR_LIGAND_BINDING_AND_ACTIVATION	T50	22	0.565158	1.560974	0.018141	0.11706168	0.987		1455 tags=18%, list=7%, signal=20%
REACTOME_ACTIVATION_OF_NF_KAPPAB_IN_B_CELLS	T51	61	0.44663	1.560832	0.011765	0.11486716	0.987		6390 tags=56%, list=32%, signal=82%
REACTOME_CYCLIN_E_ASSOCIATED_EVENTS_DURING_G1_S_TRANSITION	T52	61	0.450873	1.55627	0.01139	0.11697339	0.987		6829 tags=57%, list=34%, signal=87%
REACTOME_RNA_POL_I_TRANSCRIPTION_INITIATION	T53	24	0.54619	1.549192	0.020833	0.12195884	0.989		3952 tags=38%, list=20%, signal=47%
REACTOME_MEIOTIC_RECOMBINATION	T54	46	0.469943	1.534439	0.024752	0.13586974	0.994		4688 tags=37%, list=23%, signal=48%
REACTOME_PREFOLDIN_MEDIATED_TRANSFER_OF_SUBSTRATE_TO_CCT_	T55	23	0.54353	1.532935	0.02603	0.13491896	0.994		5228 tags=70%, list=26%, signal=94%
KEGG_PYRIMIDINE_METABOLISM	T56	92	0.418559	1.532563	0.00489	0.13293453	0.994		5157 tags=40%, list=26%, signal=54%
REACTOME_NEGATIVE_REGULATION_OF_FGFR_SIGNALING	T57	36	0.49205	1.524753	0.009238	0.13898568	0.996		2152 tags=17%, list=11%, signal=19%
REACTOME_REGULATION_OF_GLUCOKINASE_BY_GLUCOKINASE_REGULAT	T58	27	0.532379	1.523443	0.021692	0.13822966	0.996		5941 tags=48%, list=30%, signal=68%
REACTOME_TCR_RECEPTOR_INTERACTION	T59	83	0.422086	1.523265	0.009524	0.13602167	0.996		2665 tags=29%, list=13%, signal=33%
REACTOME_MRNA_PROCESSING	T60	150	0.387745	1.521411	0.00266	0.13555897	0.996		6879 tags=51%, list=34%, signal=78%
REACTOME_RESPONSE_TO_ELEVATED_PLATELET_CYTOSOLIC_CA2_	T61	76	0.425666	1.518842	0.012376	0.1357997	0.997		1570 tags=24%, list=8%, signal=26%
REACTOME_3_UTR_MEDIATED_TRANSLATIONAL_REGULATION	T62	90	0.411892	1.518541	0.010499	0.133923	0.997		4900 tags=22%, list=25%, signal=29%
REACTOME_G_ALPHA_Z_SIGNALLING_EVENTS	T63	44	0.460424	1.515056	0.016432	0.13537064	0.997		4113 tags=48%, list=21%, signal=60%
REACTOME_RNA_POL_I_TRANSCRIPTION	T64	49	0.457567	1.515045	0.024155	0.13327673	0.997		3952 tags=27%, list=20%, signal=33%
REACTOME_DESTABILIZATION_OF_MRNA_BY_AUF1_HNRNP_D0	T65	47	0.459063	1.514599	0.022883	0.13187507	0.997		6390 tags=51%, list=32%, signal=75%
REACTOME_HDL_MEDIATED_LIPID_TRANSPORT	T66	15	0.589866	1.510133	0.048117	0.13398911	0.997		1607 tags=33%, list=8%, signal=36%
KEGG_RIBOSOME	T67	72	0.424792	1.509711	0.012438	0.13245842	0.997		4450 tags=19%, list=22%, signal=25%
REACTOME_METABOLISM_OF_RNA	T68	234	0.363513	1.508	0	0.13232476	0.997		5177 tags=32%, list=26%, signal=43%
REACTOME_ACTIVATED_POINT_MUTANTS_OF_FGFR2	T69	16	0.591351	1.501164	0.034632	0.13738668	0.999		1455 tags=19%, list=7%, signal=20%
REACTOME_RNA_POL_I_TRANSCRIPTION_TERMINATION	T70	21	0.550534	1.498635	0.048017	0.1384736	0.999		6829 tags=67%, list=34%, signal=101%
REACTOME_ACTIVATION_OF_THE_MRNA_UPON_BINDING_OF_THE_CAP_	T71	50	0.454135	1.498141	0.025172	0.13711037	0.999		4900 tags=28%, list=25%, signal=37%
KEGG_DNA_REPLICATION	T72	35	0.483945	1.494419	0.03125	0.13857788	0.999		5089 tags=46%, list=26%, signal=61%
KEGG_FOCAL_ADHESION	T73	195	0.364162	1.489596	0	0.14200616	0.999		2722 tags=28%, list=14%, signal=32%
REACTOME_TRANSCRIPTIONAL_ACTIVITY_OF_SMAD2_SMAD3_SMAD4_	T74	36	0.487264	1.487141	0.041575	0.14289495	0.999		3547 tags=33%, list=18%, signal=40%
KEGG_HYPERTROPHIC_CARDIOMYOPATHY_HCM	T75	82	0.409111	1.485718	0.01519	0.1425901	0.999		1342 tags=22%, list=7%, signal=23%
REACTOME_DOWNREGULATION_OF_SMAD2_3_SMAD4_TRANSCRIPTION	T76	19	0.547412	1.484456	0.040179	0.14208521	0.999		3547 tags=42%, list=18%, signal=51%
REACTOME_RNA_POL_II_PRE_TRANSCRIPTION_EVENTS	T77	56	0.433514	1.483658	0.023873	0.14117247	0.999		6829 tags=48%, list=34%, signal=73%
REACTOME_MRNA_CAPPING	T78	29	0.500418	1.48242	0.036075	0.14060088	0.999		7134 tags=59%, list=36%, signal=91%
REACTOME_PEPTIDE_CHAIN_ELONGATION	T79	70	0.424515	1.480256	0.014742	0.14092351	0.999		4450 tags=20%, list=22%, signal=26%
REACTOME_LATE_PHASE_OF_HIV_LIFE_CYCLE	T80	98	0.396686	1.479039	0.015464	0.14046529	0.999		5941 tags=38%, list=30%, signal=53%
KEGG_PRION_DISEASES	T81	34	0.49595	1.478952	0.032037	0.13879548	0.999		3840 tags=35%, list=19%, signal=44%
REACTOME_METABOLISM_OF_NON_CODING_RNA	T82	46	0.461348	1.478199	0.023697	0.13798027	0.999		6155 tags=52%, list=31%, signal=75%
REACTOME_SHC_MEDIATED_CASCADE	T83	28	0.501851	1.477855	0.04	0.13668393	0.999		1835 tags=18%, list=9%, signal=20%
REACTOME_SIGNALLING_TO_P38_VIA_RIT_AND_RIN	T84	15	0.591714	1.472287	0.0587	0.14045665	0.999		3533 tags=33%, list=18%, signal=40%
KEGG_PROTEASOME	T85	42	0.462873	1.4705	0.028436	0.14059675	0.999		6348 tags=55%, list=32%, signal=80%
REACTOME_ANTIGEN_PROCESSING_CROSS_PRESENTATION	T86	70	0.422172	1.470295	0.011574	0.13914405	0.999		6455 tags=51%, list=32%, signal=76%
KEGG_GLYOXYLATE_AND_DICARBOXYLATE_METABOLISM	T87	16	0.591183	1.467914	0.062241	0.13981594	0.999		4592 tags=50%, list=23%, signal=65%
REACTOME_METABOLISM_OF_MRNA	T88	191	0.355804	1.458679	0	0.14726261	1		5177 tags=31%, list=26%, signal=42%
REACTOME_PYRUVATE_METABOLISM	T89	18	0.550602	1.445359	0.072464	0.15994751	1		3772 tags=50%, list=19%, signal=62%
KEGG_CELL_CYCLE	T90	122	0.375778	1.445216	0.010417	0.15835667	1		4596 tags=41%, list=23%, signal=53%
REACTOME_LOSS_OF_NLP_FROM_MITOTIC_CENTROSOMES	T91	56	0.426316	1.443366	0.023697	0.1585718	1		5198 tags=46%, list=26%, signal=63%
REACTOME_P53_DEPENDENT_G1_DNA_DAMAGE_RESPONSE	T92	52	0.424226	1.440198	0.048165	0.16046782	1		6390 tags=54%, list=32%, signal=79%
REACTOME_FORMATION_OF_RNA_POL_II_ELONGATION_COMPLEX_	T93	41	0.461457	1.439894	0.042453	0.15900563	1		7249 tags=56%, list=36%, signal=88%
REACTOME_FRS2_MEDIATED_CASCADE	T94	36	0.472655	1.436715	0.048611	0.1608442	1		1959 tags=17%, list=10%, signal=18%
REACTOME_CLASS_I_MHC_MEDIATED_ANTIGEN_PROCESSING_PRESENTA	T95	230	0.345268	1.435638	0	0.16042122	1		5125 tags=36%, list=26%, signal=47%
REACTOME_PROSTACYCLIN_SIGNALLING_THROUGH_PROSTACYCLIN_REC	T96	19	0.528557	1.435359	0.076233	0.1589917	1		5064 tags=47%, list=25%, signal=63%
REACTOME_RNA_POL_II_TRANSCRIPTION_INITIATION_FROM_TYPE_3_	T97	26	0.500935	1.428223	0.063425	0.16563061	1		3935 tags=31%, list=20%, signal=38%
REACTOME_TRANSPORT_OF_MATURE_TRANSCRIPT_TO_CYTOPLASM	T98	50	0.427555	1.42259	0.034483	0.1705978	1		5941 tags=48%, list=30%, signal=68%
REACTOME_HIV_LIFE_CYCLE	T99	111	0.373193	1.41793	0.016173	0.17441289	1		5941 tags=38%, list=30%, signal=54%
REACTOME_FORMATION_OF_THE_HIV1_EARLY_ELONGATION_COMPLEX	T100	31	0.472332	1.413718	0.084233	0.17375754	1		7134 tags=55%, list=36%, signal=85%
REACTOME_RNA_POL_II_TRANSCRIPTION	T101	96	0.380368	1.414528	0.009639	0.17535326	1		6829 tags=50%, list=34%, signal=76%
REACTOME_PROCESSING_OF_CAPPED_INTRON_CONTAINING_PRE_MRNA	T102	130	0.366416	1.411436	0	0.1772638	1		6366 tags=45%, list=32%, signal=66%
REACTOME_SIGNAL_TRANSDUCTION_BY_L1	T103	33	0.466203	1.407837	0.061758	0.18031594	1		4555 tags=42%, list=23%, signal=54%
REACTOME_SMAD2_SMAD3_SMAD4_HETEROTRIMER_REGULATES_TRANS	T104	25	0.494013	1.406518	0.063043	0.17980595	1		5484 tags=48%, list=27%, signal=66%
KEGG_BASAL_TRANSCRIPTION_FACTORS	T105	33	0.460609	1.403523	0.053659	0.18200198	1		3877 tags=30%, list=19%, signal=38%
REACTOME_HIV_INFECTION	T106	189	0.341738	1.401486	0	0.18293051	1		6009 tags=40%, list=30%, signal=57%
REACTOME_DNA_REPAIR	T107	105	0.372818	1.400099	0.010076	0.18287727	1		5289 tags=37%, list=27%, signal=50%
KEGG_NUCLEOTIDE_EXCISION_REPAIR	T108	44	0.433853	1.398081	0.052995	0.18370856	1		4984 tags=43%, list=25%, signal=57%
REACTOME_PYRUVATE_METABOLISM_AND_CITRIC_ACID_TCA_CYCLE	T109	40	0.434457	1.396461	0.042411	0.1840345	1		4187 tags=35%, list=21%, signal=44%
REACTOME_HOST_INTERACTIONS_OF_HIV_FACTORS	T110	119	0.360205	1.39104	0.016	0.18885148	1		6390 tags=47%, list=32%, signal=69%
REACTOME_FANCONI_ANEMIA_PATHWAY	T111	21	0.507844	1.389159	0.106335	0.18967491	1		5093 tags=48%, list=26%, signal=64%
REACTOME_AUTODEGRADATION_OF_THE_E3_UBIQUITIN_LIGASE_COP1	T112	46	0.422033	1.388174	0.045675	0.18929283	1		6390 tags=54%, list=32%, signal=80%
KEGG_DILATED_CARDIOMYOPATHY	T113	89	0.383811	1.38627	0.030227	0.18992223	1		2528 tags=26%, list=13%, signal=29%
REACTOME_RNA_POL_II_TRANSCRIPTION_PRE_INITIATION_AND_PROMO	T114	39	0.441516	1.382238	0.071111	0.19334954	1		6829 tags=49%, list=34%, signal=74%
REACTOME_VIF_MEDIATED_DEGRADATION_OF_APOBEC3G	T115	48	0.412806	1.378232	0.059361	0.19665833	1		6390 tags=56%, list=32%, signal=83%
KEGG_RNA_DEGRADATION	T116	57	0.412827	1.37626	0.041379	0.19777042	1		4717 tags=42%, list=24%, signal=55%
REACTOME_MITOTIC_G2_G2_M_PHASES	T117	78	0.38632	1.373678	0.031863	0.19943047	1		5198 tags=46%, list=26%, signal=62%
REACTOME_TRANSLATION	T118	128	0.356748	1.372297	0.0180888	0.19968525	1		4900 tags=21%, list=25%, signal=28%
REACTOME_APC_C_CDC20_MEDIATED_DEGRADATION_OF_CYCLIN_B	T119	18	0.505936	1.366312	0.09205	0.20570807	1		4743 tags=50%, list=24%, signal=66%
REACTOME_TGF_BETA_RECEPTOR_SIGNALING_ACTIVATES_SMAD3	T120	24	0.487204	1.365968	0.083521	0.20428881	1		3547 tags=38%, list=18%, signal=46%
KEGG_CHONDROITIN_SULFATE_BIOSYNTHESIS	T121	19	0.503389	1.36513	0.101124	0.20376787	1		3826 tags=47%, list=19%, signal=59%
REACTOME_ELONGATION_ARREST_AND_RECOVERY	T122	29	0.465775	1.36083	0.118765	0.20791687	1		7249 tags=55%, list=36%, signal=87%
KEGG_HEMATOPOIETIC_CELL_LINEAGE	T123	83	0.376264	1.357019	0.023923	0.21142177	1		1309 tags=16%, list=7%, signal=17%
REACTOME_MRNA_SPLICING_MINOR_PATHWAY	T124	42	0.432808	1.355906	0.058667	0.21156281	1		6879 tags=52%, list=34%, signal=80%
REACTOME_INHIBITION_OF_INSULIN_SECRETION_BY_ADRENALINE_NORA	T125	25	0.465332	1.354809	0.088172	0.21140812	1		4113 tags=44%, list=21%, signal=55%
REACTOME_ANTIGEN_PROCESSING_UBIQUITINATION_PROTEASOME_DEG	T126	194	0.331493	1.352902	0.011429	0.212395	1		5125 tags=35%, list=26%, signal=47%
REACTOME_POST_CHAPERONIN_TUBULIN_FOLDING_PATHWAY	T127	16	0.521823	1.345578	0.115789	0.22053422	1		2748 tags=38%, list=14%, signal=43%
REACTOME_CYCLIN_A_B1_ASSOCIATED_EVENTS_DURING_G2_M_TRANSI	T128	15	0.533928	1.342824	0.107143	0.22253032	1		4257 tags=47%, list=21%, signal=59%
REACTOME_MITOCHONDRIAL_PROTEIN_IMPORT	T129	48	0.410805	1.34257	0.061758	0.2212598	1		3500 tags=27%, list=18%, signal=33%
REACTOME_IP_PHAGOSOME_PATHWAY	T130	57	0.398837	1.341142	0.079365	0.22123739	1		6390 tags=49%, list=32%, signal=72%
KEGG_RNA_POLYMERASE	T131	28	0.461994	1.339464	0.101655	0.2217246	1		6133 tags=46%, list=31%, signal=67%
REACTOME_FORMATION_OF_TUBULIN_FOLDING_INTERMEDIATES_BY_CT	T132	18	0.505339	1.33397	0.115044	0.22805455	1		5228 tags=61%, list=26%, signal=83%
REACTOME_SIGNALING_BY_FGFR1_MUTANTS	T133	28	0.445581	1.32964	0.104116	0.23223586	1		2944 tags=25%, list=15%, signal=29%
REACTOME_ANTIVIRAL_MECHANISM_BY_IFN_STIMULATED_GENES	T134	64	0.383898	1.327091	0.074813	0.2339016	1		3462 tags=30%, list=17%, signal=36%
REACTOME_INSULIN_RECEPTOR_SIGNALLING_CASCADE	T135	84	0.362596	1.32709	0.06068	0.23216899	1		3937 tags=27%, list=20%, signal=34%
REACTOME_APC_C0CD20_MEDIATED_DEGRADATION_OF_NEK2A	T136	20	0.484642	1.326972	0.120614	0.23063414	1		6223 tags=60%, list=31%, signal=87%
KEGG_HOMOLOGOUS_RECOMBINATION	T137	26	0.46517	1.321361	0.120455	0.23613864	1		5098 tags=50%, list=26%, signal=67%
REACTOME_DEADENYLATION_DEPENDENT_MRNA_DECAY	T138	44	0.412543	1.315331	0.082126	0.2433118	1		5177 tags=48%, list=26%, signal=64%
REACTOME_PHOSPHORYLATION_OF_THE_APC_C	T139	16	0.518451	1.312605	0.145161	0.24557786	1		5228 tags=88%, list=26%, signal=119%
REACTOME_INHIBITION_OF_THE_PROTEOLYTIC_ACTIVITY_OF_APC_C_RE	T140	17	0.518957	1.31201	0.127193	0.24473658	1		6223 tags=71%, list=31%, signal=102%
REACTOME_PROLONGED_ERK_ACTIVATION_EVENTS	T141	19	0.481932	1.309298	0.116424	0.24719223	1		2152 tags=32%, list=11%, signal=35%
REACTOME_DEFECTIVE_ELONGATION_OF_HIV1_TRANSCRIPT_IN_THE_ABS	T142	21	0.476509	1.308702	0.114407	0.24632841	1		7537 tags=57%, list=38%, signal=92%
REACTOME_G1_PHASE	T143	35	0.426149	1.3076	0.106695	0.24616238	1		4349 tags=34%, list=22%, signal=44%
REACTOME_STRIATED_MUSCLE_CONTRACTION	T144	27	0.448002	1.291222	0.112613	0.26896715	1		2463 tags=26%, list=12%, signal=30%
REACTOME_PKB_MEDIATED_EVENTS	T145	28	0.447949	1.289677	0.125	0.26955526	1		4149 tags=43%, list=21%, signal=54%
REACTOME_GLUCOSE_TRANSPORT	T146	38	0.414376	1.284561	0.113586	0.27543095	1		3222 tags=21%, list=16%, signal=25%
REACTOME_REGULATION_OF_ORNITHINE_DECARBOXYLASE_ODC	T147	47	0.389885	1.277152	0.110112	0.28575787	1		6390 tags=53%, list=32%, signal=78%
REACTOME_RECRUITMENT_OF_MITOTIC_CENTROSOME_PROTEINS_AND_	T148	63	0.363629	1.271434	0.088729	0.2930652	1		5198 tags=46%, list=26%, signal=62%
KEGG_UBIQUITIN_MEDIATED_PROTEOLYSIS	T149	132	0.328768	1.270505	0.041237	0.292693	1		3853 tags=30%, list=19%, signal=36%
REACTOME_DOWNREGULATION_OF_TGF_BETA_RECEPTOR_SIGNALING	T150	21	0.465955	1.266985	0.164733	0.29651362	1		3166 tags=33%, list=16%, signal=40%
KEGG_OOCYTE_MEIOSIS	T151	108	0.33485	1.264301	0.071247	0.29892904	1		4835 tags=39%, list=24%, signal=51%

Legend

Bold text: significantly enriched gene sets (P<0.005, FDR q-value <0.1)

Red text: Cell cycle associated gene sets

ES = Enrichment Score

NES = Normalized Enrichment Score

FDR = False-discovery rate

FWER = Family-wise error rate

REACTOME_DNA_STRAND_ELONGATION	T152	30	0.426106	1.256174	0.168591	0.3115897	1	4644	tags=40%, list=23%, signal=52%
REACTOME_SIGNALING_BY_BMP	T153	22	0.451501	1.253789	0.172113	0.3136895	1	3609	tags=41%, list=18%, signal=50%
REACTOME_CELL_SURFACE_INTERACTIONS_AT_THE_VASCULAR_WALL	T154	84	0.341284	1.244604	0.087629	0.3284132	1	2569	tags=25%, list=13%, signal=29%
REACTOME_PYRIMIDINE_METABOLISM	T155	23	0.441983	1.237013	0.162447	0.340179	1	3430	tags=30%, list=17%, signal=37%
REACTOME_RNA_POL_III_TRANSCRIPTION	T156	33	0.411975	1.236485	0.142534	0.3391626	1	5579	tags=39%, list=28%, signal=55%
REACTOME_INCRETIN_SYNTHESIS_SECRETION_AND_INACTIVATION	T157	20	0.458919	1.233509	0.184211	0.34283078	1	5342	tags=40%, list=27%, signal=55%
REACTOME_CHONDROITIN_SULFATE_DERMATAN_SULFATE_METABOLISM	T158	47	0.378456	1.228519	0.16532	0.35039797	1	3313	tags=36%, list=17%, signal=43%
REACTOME_AXON_GUIDANCE	T159	238	0.295116	1.224762	0.047319	0.3553026	1	2359	tags=21%, list=12%, signal=24%
REACTOME_BASIGIN_INTERACTIONS	T160	24	0.438367	1.221668	0.188341	0.35932344	1	3200	tags=33%, list=16%, signal=40%
REACTOME_ADP_SIGNALLING_THROUGH_P2RY12	T161	21	0.445885	1.219349	0.200357	0.36143684	1	3822	tags=38%, list=19%, signal=47%
REACTOME_DOUBLE_STRAND_BREAK_REPAIR	T162	22	0.434107	1.219146	0.177778	0.35957527	1	5181	tags=45%, list=26%, signal=61%
REACTOME_GLUCAGON_SIGNALING_IN_METABOLIC_REGULATION	T163	33	0.400259	1.21878	0.158986	0.35809395	1	4121	tags=33%, list=21%, signal=42%
REACTOME_THROMBOXANE_SIGNALLING_THROUGH_TP_RECEPTOR	T164	23	0.431685	1.216823	0.190583	0.35959515	1	3951	tags=35%, list=20%, signal=43%
REACTOME_DEPOSITION_OF_NEW_CENPA_CONTAINING_NUCLEOSOMES	T165	38	0.385845	1.215941	0.174497	0.35910583	1	6392	tags=53%, list=32%, signal=77%
REACTOME_METABOLISM_OF_POLYAMINES	T166	15	0.477989	1.212572	0.211921	0.36380264	1	3963	tags=40%, list=20%, signal=50%
REACTOME_SIGNALING_BY_FGFR_MUTANTS	T167	42	0.38074	1.212067	0.167901	0.36259085	1	2944	tags=21%, list=15%, signal=25%
KEGG_CYTOSOLIC_DNA_SENSING_PATHWAY	T168	53	0.360651	1.206303	0.125628	0.37193778	1	3935	tags=34%, list=20%, signal=42%
REACTOME_PI3K_CASCADE	T169	68	0.343035	1.201916	0.152074	0.3784682	1	3937	tags=25%, list=20%, signal=31%
REACTOME_MRNA_SPLICING	T170	101	0.319379	1.196825	0.114286	0.38668767	1	6750	tags=48%, list=34%, signal=71%
KEGG_REGULATION_OF_ACTIN_CYTOSKELETON	T171	209	0.294143	1.196619	0.091691	0.38490027	1	2528	tags=22%, list=13%, signal=25%
KEGG_NOD_LIKE_RECEPTOR_SIGNALING_PATHWAY	T172	62	0.345031	1.195266	0.153846	0.3854222	1	3533	tags=29%, list=18%, signal=35%
REACTOME_SHC1_EVENTS_IN_ERBB4_SIGNALING	T173	20	0.443661	1.194427	0.231579	0.38499512	1	1959	tags=30%, list=10%, signal=33%
REACTOME_GENERIC_TRANSCRIPTION_PATHWAY	T174	330	0.278026	1.193158	0.040816	0.38540095	1	3547	tags=24%, list=18%, signal=29%
REACTOME_RNA_POL_III_TRANSCRIPTION_TERMINATION	T175	19	0.446982	1.192601	0.23185	0.38439593	1	6133	tags=42%, list=31%, signal=61%
REACTOME_PTM_GAMMA_CARBOXYLATION_HYPUSINE_FORMATION_AN	T176	25	0.419142	1.190994	0.204348	0.3853311	1	164	tags=12%, list=1%, signal=12%
REACTOME_PROTEIN_FOLDING	T177	46	0.365539	1.18229	0.198529	0.40005004	1	5228	tags=48%, list=26%, signal=65%
KEGG_PROTEIN_EXPORT	T178	23	0.416777	1.18149	0.216981	0.39949024	1	3130	tags=22%, list=16%, signal=26%
REACTOME_ARMS_MEDIATED_ACTIVATION	T179	17	0.461449	1.180808	0.236364	0.3986647	1	2152	tags=29%, list=11%, signal=33%
REACTOME_NUCLEOTIDE_EXCISION_REPAIR	T180	49	0.355577	1.180788	0.173267	0.3965087	1	5289	tags=35%, list=27%, signal=47%
REACTOME_SYNTHESIS_AND_INTERCONVERSION_OF_NUCLEOTIDE_DI_AT	T181	16	0.463601	1.176492	0.243902	0.40308508	1	6621	tags=56%, list=33%, signal=84%
REACTOME_FORMATION_OF_TRANSCRIPTION_COUPLED_NER_NER_R	T182	29	0.401763	1.173049	0.217687	0.40795967	1	5057	tags=34%, list=25%, signal=46%
REACTOME_TAK1_ACTIVATES_NFKB_BY_PHOSPHORYLATION_AND_ACTIV	T183	22	0.430448	1.171562	0.22561	0.40877402	1	2138	tags=23%, list=11%, signal=25%
REACTOME_G_BETA_GAMMA_SIGNALLING_THROUGH_PLC_BETA	T184	20	0.43455	1.167697	0.238197	0.41455093	1	5064	tags=40%, list=25%, signal=54%
KEGG_MAPK_SIGNALING_PATHWAY	T185	257	0.276806	1.163076	0.090164	0.42231947	1	3533	tags=27%, list=18%, signal=32%
REACTOME_ANTIGEN_PRESENTATION_FOLDING_ASSEMBLY_AND_PEPTID	T186	20	0.427782	1.159431	0.244493	0.4278266	1	4146	tags=40%, list=21%, signal=50%
REACTOME_CONVERSION_FROM_APC_C_CDC20_TO_APC_C_CDH1_IN_LA	T187	15	0.463105	1.157203	0.269807	0.43035576	1	5529	tags=60%, list=28%, signal=83%
REACTOME_SIGNALING_BY_INSULIN_RECEPTOR	T188	104	0.305524	1.157063	0.152062	0.42844003	1	4196	tags=28%, list=21%, signal=35%
REACTOME_RNA_POL_III_CHAIN_ELONGATION	T189	17	0.442009	1.156894	0.257996	0.42662185	1	6133	tags=41%, list=31%, signal=59%
KEGG_MELANOMA	T190	71	0.329842	1.156316	0.173367	0.42557186	1	2152	tags=23%, list=11%, signal=25%
KEGG_ARRHYTHMOGENIC_RIGHT_VENTRICULAR_CARDIOMYOPATHY_ARV	T191	73	0.327267	1.154351	0.173594	0.42760262	1	2528	tags=26%, list=13%, signal=30%
KEGG_PROGESTERONE_MEDIATED_OOCYTE_MATURATION	T192	83	0.316725	1.153744	0.16792	0.42678824	1	4743	tags=45%, list=24%, signal=58%
REACTOME_GLYCOSAMINOGLYCAN_METABOLISM	T193	107	0.306113	1.153014	0.157025	0.42610925	1	3313	tags=27%, list=17%, signal=32%
REACTOME_SRP_DEPENDENT_COTRANSLATIONAL_PROTEIN_TARGETING_	T194	93	0.314304	1.151108	0.170483	0.4278336	1	4450	tags=16%, list=22%, signal=21%
KEGG_GLYCOSAMINOGLYCAN_DEGRADATION	T195	21	0.409963	1.148023	0.275229	0.4327191	1	4574	tags=33%, list=23%, signal=43%
KEGG_SMALL_CELL_LUNG_CANCER	T196	83	0.316637	1.145318	0.191142	0.43615726	1	3186	tags=25%, list=16%, signal=30%
REACTOME_INTEGRIN_CELL_SURFACE_INTERACTIONS	T197	77	0.321443	1.14434	0.199017	0.4360976	1	2657	tags=25%, list=13%, signal=28%
KEGG_COMPLEMENT_AND_COAGULATION_CASCADES	T198	67	0.325802	1.143163	0.218045	0.4365552	1	1570	tags=15%, list=8%, signal=16%
REACTOME_L1CAM_INTERACTIONS	T199	82	0.317209	1.142588	0.199495	0.43567815	1	4614	tags=40%, list=23%, signal=52%
REACTOME_PHOSPHOLIPASE_C_MEDIATED_CASCADE	T200	51	0.340628	1.140535	0.233173	0.4380549	1	2102	tags=16%, list=11%, signal=17%
REACTOME_SHC_MEDIATED_SIGNALLING	T201	15	0.45388	1.139291	0.285412	0.43882284	1	3683	tags=33%, list=18%, signal=41%
REACTOME_SIGNALING_BY_TGF_BETA_RECEPTOR_COMPLEX	T202	60	0.332345	1.137149	0.227723	0.4413425	1	3547	tags=27%, list=18%, signal=32%
REACTOME_DIABETES_PATHWAYS	T203	124	0.295438	1.136544	0.175573	0.4404595	1	3785	tags=24%, list=19%, signal=30%
KEGG_SNARE_INTERACTIONS_IN_VESICULAR_TRANSPORT	T204	37	0.368662	1.135997	0.275862	0.43958065	1	1914	tags=19%, list=10%, signal=21%
REACTOME_DOWNSTREAM_SIGNALING_EVENTS_OF_B_CELL_RECEPTOR_	T205	92	0.306022	1.134098	0.189258	0.44162133	1	6390	tags=49%, list=32%, signal=72%
KEGG_BETA_ALANINE_METABOLISM	T206	22	0.414284	1.13066	0.278146	0.44708169	1	3963	tags=36%, list=20%, signal=45%
REACTOME_NUCLEAR_SIGNALING_BY_ERBB4	T207	38	0.357066	1.125719	0.278146	0.45599124	1	2646	tags=29%, list=13%, signal=33%
KEGG_TASTE_TRANSDUCTION	T208	44	0.34595	1.124001	0.25537	0.45764118	1	2204	tags=16%, list=11%, signal=18%
REACTOME_REGULATION_OF_INSULIN_SECRETION	T209	88	0.310494	1.121062	0.221675	0.46213493	1	4220	tags=31%, list=21%, signal=39%
REACTOME_PRE_NOTCH_TRANSCRIPTION_AND_TRANSLATION	T210	27	0.385297	1.112283	0.293598	0.48050696	1	2530	tags=26%, list=13%, signal=30%
KEGG_PATHWAYS_IN_CANCER	T211	321	0.258137	1.109474	0.13099	0.484285	1	2630	tags=21%, list=13%, signal=24%
REACTOME_INTEGRATION_OF_ENERGY_METABOLISM	T212	115	0.293221	1.104255	0.262599	0.49403554	1	4298	tags=32%, list=22%, signal=41%
REACTOME_TELOMERE_MAINTENANCE	T213	51	0.339344	1.098225	0.27169	0.5062168	1	5083	tags=27%, list=25%, signal=37%
KEGG_BIOSYNTHESIS_OF_UNSATURATED_FATTY_ACIDS	T214	19	0.404489	1.096196	0.293362	0.5088595	1	2919	tags=26%, list=15%, signal=31%
REACTOME_EXTENSION_OF_TELOMERES	T215	26	0.381092	1.092191	0.306452	0.5164866	1	4644	tags=35%, list=23%, signal=45%
KEGG_APOPTOSIS	T216	87	0.300618	1.091627	0.255208	0.5153859	1	3454	tags=25%, list=17%, signal=30%
REACTOME_DEVELOPMENTAL_BIOLOGY	T217	378	0.249162	1.080371	0.163934	0.54654177	1	2729	tags=19%, list=14%, signal=22%
KEGG_SPHINGOLIPID_METABOLISM	T218	36	0.350045	1.079601	0.32634	0.54015803	1	2661	tags=28%, list=13%, signal=32%
REACTOME_FORMATION_OF_INCISION_COMPLEX_IN_GG_NER	T219	21	0.388272	1.078422	0.343348	0.5450556	1	5289	tags=43%, list=27%, signal=58%
REACTOME_PLATELET_ACTIVATION_SIGNALING_AND_AGGREGATION	T220	190	0.263006	1.076186	0.229412	0.54372483	1	3444	tags=25%, list=17%, signal=30%
REACTOME_LIPOPROTEIN_METABOLISM	T221	28	0.372366	1.076129	0.364055	0.5414142	1	1607	tags=18%, list=8%, signal=19%
REACTOME_GASTRIN_CREB_SIGNALLING_PATHWAY_VIA_PKC_AND_MAPK	T222	192	0.266654	1.074343	0.240356	0.54339296	1	2074	tags=17%, list=10%, signal=18%
REACTOME_INWARDLY_RECTIFYING_K_CHANNELS	T223	31	0.357818	1.073268	0.328467	0.5435736	1	5479	tags=39%, list=27%, signal=53%
REACTOME_METABOLISM_OF_PROTEINS	T224	395	0.244985	1.072495	0.197411	0.54325163	1	4225	tags=23%, list=21%, signal=29%
REACTOME_G_ALPHA_I_SIGNALLING_EVENTS	T225	184	0.26529	1.071468	0.259459	0.54333586	1	2721	tags=16%, list=14%, signal=18%
REACTOME_SIGNALING_BY_ILS	T226	105	0.285494	1.071087	0.289216	0.54198503	1	2695	tags=23%, list=14%, signal=26%
REACTOME_TRANSCRIPTION_COUPLED_NER_TC_NER	T227	44	0.325951	1.056156	0.368182	0.5779218	1	5057	tags=30%, list=25%, signal=39%
REACTOME_COMPLEMENT_CASCADE	T228	28	0.356335	1.050777	0.368545	0.5897792	1	100	tags=7%, list=1%, signal=7%
REACTOME_PERK_REGULATED_GENE_EXPRESSION	T229	27	0.364791	1.050725	0.378132	0.58738005	1	4616	tags=41%, list=23%, signal=53%

KEGG_NICOTINATE_AND_NICOTINAMIDE_METABOLISM	T230	23	0.371543	1.050436	0.371111	0.58563346	1	501	tags=17%, list=3%, signal=18%
KEGG_DORSO_VENTRAL_AXIS_FORMATION	T231	23	0.379939	1.049384	0.376596	0.58583415	1	1504	tags=13%, list=8%, signal=14%
REACTOME_OXYGEN_DEPENDENT_PROLINE_HYDROXYLATION_OF_HYPOX	T232	15	0.421197	1.048503	0.376682	0.5853292	1	3034	tags=13%, list=15%, signal=39%
KEGG_HEDGEHOG_SIGNALING_PATHWAY	T233	54	0.307442	1.046425	0.354988	0.5885344	1	2395	tags=22%, list=12%, signal=25%
REACTOME_METABOLISM_OF_CARBOHYDRATES	T234	225	0.252201	1.043636	0.308682	0.59303844	1	3313	tags=21%, list=17%, signal=25%
KEGG_MISMATCH_REPAIR	T235	22	0.378364	1.043631	0.399093	0.59052044	1	4972	tags=41%, list=25%, signal=54%
REACTOME_SIGNALING_BY_WNT	T236	62	0.305728	1.041047	0.359712	0.59467554	1	6390	tags=50%, list=32%, signal=73%
REACTOME_REGULATION_OF_MRNA_STABILITY_BY_PROTEINS_THAT_BIN	T237	78	0.285926	1.034104	0.356021	0.6111984	1	6390	tags=46%, list=32%, signal=68%
REACTOME_SIGNAL_AMPLIFICATION	T238	31	0.344947	1.03379	0.385681	0.6094037	1	3951	tags=32%, list=20%, signal=40%
REACTOME_GLUCAGON_TYPE_LIGAND_RECEPTORS	T239	33	0.335882	1.032336	0.378076	0.6108204	1	5064	tags=33%, list=25%, signal=45%
REACTOME_HEMOSTASIS	T240	429	0.237284	1.031303	0.307971	0.61102736	1	3200	tags=21%, list=16%, signal=25%
REACTOME_G_BETA_GAMMA_SIGNALLING_THROUGH_PI3KGAMMA	T241	25	0.361718	1.026386	0.438479	0.62160057	1	5064	tags=40%, list=25%, signal=54%
REACTOME_SHC_RELATED_EVENTS	T242	17	0.408699	1.025692	0.432314	0.6209794	1	3683	tags=29%, list=18%, signal=36%
REACTOME_TRAFFICKING_OF_GLUR2_CONTAINING_AMPA_RECEPTORS	T243	15	0.396084	1.023864	0.427083	0.62320954	1	4511	tags=27%, list=23%, signal=34%
REACTOME_G_ALPHA_Q_SIGNALLING_EVENTS	T244	171	0.253145	1.017219	0.409836	0.6387233	1	2074	tags=16%, list=10%, signal=17%
KEGG_GAP_JUNCTION	T245	86	0.281757	1.017072	0.420455	0.63646646	1	2748	tags=22%, list=14%, signal=26%
REACTOME_NETRIN1_SIGNALING	T246	37	0.324194	1.010373	0.441048	0.65244085	1	2310	tags=22%, list=12%, signal=24%
REACTOME_OPIOID_SIGNALLING	T247	75	0.280031	1.009297	0.425581	0.6528012	1	4365	tags=35%, list=22%, signal=44%
REACTOME_GABA_B_RECEPTOR_ACTIVATION	T248	38	0.317682	1.00661	0.428571	0.6580735	1	3434	tags=26%, list=17%, signal=32%
KEGG_LYSINE_DEGRADATION	T249	44	0.303889	1.002419	0.431111	0.6674801	1	5097	tags=41%, list=26%, signal=55%
KEGG_RENAL_CELL_CARCINOMA	T250	67	0.286329	1.000348	0.457547	0.6704222	1	3010	tags=27%, list=15%, signal=32%
REACTOME_ADAPTIVE_IMMUNE_SYSTEM	T251	495	0.22358	0.996562	0.465455	0.6785471	1	4021	tags=24%, list=20%, signal=29%
REACTOME_CITRIC_ACID_CYCLE_TCA_CYCLE	T252	19	0.374838	0.996071	0.463918	0.6772482	1	4187	tags=26%, list=21%, signal=33%
REACTOME_TRIGLYCERIDE_BIOSYNTHESIS	T253	38	0.326799	0.985675	0.477376	0.7043376	1	2139	tags=24%, list=11%, signal=26%
REACTOME_ACTIVATION_OF_BH3_ONLY_PROTEINS	T254	16	0.386607	0.984973	0.487356	0.7036195	1	2630	tags=31%, list=13%, signal=36%
REACTOME_HOMOLOGOUS_RECOMBINATION_REPAIR_OF_REPLICATION_	T255	16	0.388863	0.981667	0.493478	0.7105615	1	4760	tags=38%, list=24%, signal=49%
REACTOME_CHROMOSOME_MAINTENANCE	T256	93	0.262905	0.981193	0.505236	0.70912707	1	4835	tags=30%, list=24%, signal=40%
REACTOME_METABOLISM_OF_NUCLEOTIDES	T257	68	0.27447	0.974183	0.512019	0.72642976	1	3430	tags=26%, list=17%, signal=32%
REACTOME_PEPTIDE_LIGAND_BINDING_RECEPTORS	T258	173	0.24188	0.971053	0.524242	0.7323754	1	2419	tags=13%, list=12%, signal=15%
REACTOME_GLOBAL_GENOMIC_NER_GG_NER	T259	33	0.314011	0.970163	0.471655	0.73223233	1	5289	tags=36%, list=27%, signal=49%
REACTOME_REGULATION_OF_APOPTOSIS	T260	55	0.284861	0.968178	0.525701	0.73504525	1	6390	tags=51%, list=32%, signal=75%
REACTOME_REGULATORY_RNA_PATHWAYS	T261	24	0.344912	0.965794	0.489178	0.7388468	1	7582	tags=50%, list=38%, signal=81%
REACTOME_PI_3K_CASCADE	T262	54	0.292257	0.965604	0.527845	0.7365091	1	3010	tags=19%, list=15%, signal=22%
REACTOME_MEIOSIS	T263	74	0.269466	0.962359	0.5625	0.7429622	1	4835	tags=30%, list=24%, signal=39%
REACTOME_TCA_CYCLE_AND_RESPIRATORY_ELECTRON_TRANSPORT	T264	119	0.250022	0.954699	0.584615	0.76264733	1	4845	tags=23%, list=24%, signal=30%
REACTOME_SIGNALING_BY_FGFR	T265	106	0.253489	0.953686	0.584488	0.7625413	1	4121	tags=25%, list=21%, signal=32%
KEGG_REGULATION_OF_AUTOPHAGY	T266	33	0.306359	0.952675	0.525424	0.76263225	1	3904	tags=21%, list=20%, signal=26%
REACTOME_DARPP_32_EVENTS	T267	22	0.337638	0.952523	0.518605	0.760178	1	4365	tags=45%, list=22%, signal=58%
REACTOME_DESTABILIZATION_OF_MRNA_BY_TRISTETRAPROLIN_TTP	T268	17	0.375589	0.951133	0.509804	0.7612762	1	3480	tags=41%, list=17%, signal=50%
KEGG_GLYCOSPHINGOLIPID_BIOSYNTHESIS_GANGLIO_SERIES	T269	15	0.384385	0.950269	0.537445	0.760916	1	2363	tags=33%, list=12%, signal=38%
REACTOME_ENERGY_DEPENDENT_REGULATION_OF_MTOR_BY_LKB1_AM	T270	17	0.369056	0.949969	0.515824	0.75900245	1	6149	tags=47%, list=31%, signal=59%
REACTOME_RNA_POL_III_TRANSCRIPTION_INITIATION_FROM_TYPE_2_PR	T271	23	0.342377	0.948537	0.505855	0.7600805	1	6417	tags=43%, list=32%, signal=64%
REACTOME_G_PROTEIN_BETA_GAMMA_SIGNALLING	T272	28	0.318672	0.94751	0.524823	0.76036733	1	5064	tags=36%, list=25%, signal=48%
REACTOME_ACTIVATED_TAK1_MEDIATES_P38_MAPK_ACTIVATION	T273	17	0.354298	0.940458	0.56405	0.7786691	1	2695	tags=24%, list=14%, signal=27%
KEGG_EPITHELIAL_CELL_SIGNALING_IN_HELICOBACTER_PYLORI_INFECTIO	T274	67	0.268368	0.939922	0.571754	0.776187	1	2138	tags=18%, list=11%, signal=20%
REACTOME_LIPID_DIGESTION_MOBILIZATION_AND_TRANSPORT	T275	45	0.288126	0.93913	0.586047	0.77557284	1	1607	tags=13%, list=8%, signal=14%
REACTOME_SIGNALING_BY_FGFR_IN_DISEASE	T276	119	0.243756	0.938973	0.603675	0.773203	1	4121	tags=25%, list=21%, signal=32%
REACTOME_POST_NMDA_RECEPTOR_ACTIVATION_EVENTS	T277	31	0.311455	0.932913	0.535792	0.78736866	1	3533	tags=32%, list=18%, signal=39%
KEGG_SPLICEOSOME	T278	116	0.242668	0.932635	0.638728	0.78531456	1	6955	tags=48%, list=35%, signal=74%
REACTOME_NOD1_2_SIGNALING_PATHWAY	T279	29	0.317136	0.932384	0.555556	0.78317195	1	2138	tags=21%, list=11%, signal=23%
REACTOME_CLASS_A1_RHODOPSIN_LIKE_RECEPTORS	T280	279	0.220071	0.929572	0.740964	0.78806645	1	2432	tags=13%, list=12%, signal=14%
REACTOME_JNK_C_JUN_KINASES_PHOSPHORYLATION_AND_ACTIVATION	T281	16	0.369683	0.929551	0.57377	0.78534514	1	1595	tags=19%, list=8%, signal=20%
KEGG_LONG_TERM_POTENTIATION	T282	67	0.267984	0.92948	0.619403	0.78275543	1	2152	tags=18%, list=11%, signal=20%
REACTOME_G_PROTEIN_ACTIVATION	T283	27	0.319572	0.928993	0.559242	0.7813969	1	3822	tags=30%, list=19%, signal=37%
KEGG_CALCIUM_SIGNALING_PATHWAY	T284	173	0.231047	0.928971	0.673629	0.77871495	1	2102	tags=14%, list=11%, signal=15%
KEGG_PANCREATIC_CANCER	T285	69	0.264045	0.927486	0.641604	0.7799544	1	3032	tags=32%, list=15%, signal=37%
KEGG_PYRUVATE_METABOLISM	T286	39	0.296042	0.926758	0.588983	0.7792651	1	4187	tags=33%, list=21%, signal=42%
REACTOME_ACTIVATION_OF_NMDA_RECEPTOR_UPON_GLUTAMATE_BIN	T287	35	0.295535	0.925456	0.60274	0.7802403	1	3533	tags=29%, list=18%, signal=35%
REACTOME_GLUTAMATE_NEUROTRANSMITTER_RELEASE_CYCLE	T288	15	0.37106	0.924428	0.562241	0.7805037	1	3838	tags=40%, list=19%, signal=49%
REACTOME_PACKAGING_OF_TELOMERE_ENDS	T289	25	0.324914	0.917691	0.575688	0.795496	1	8011	tags=44%, list=40%, signal=73%
REACTOME_RNA_POL_I_PROMOTER_OPENING	T290	24	0.325658	0.915859	0.577878	0.79759103	1	5083	tags=25%, list=25%, signal=34%
REACTOME_DEADENYLATION_OF_MRNA	T291	19	0.344603	0.915404	0.562358	0.7962136	1	3831	tags=26%, list=19%, signal=33%
REACTOME_PLATELET_CALCIUM_HOMEOSTASIS	T292	16	0.362215	0.914645	0.566591	0.79542977	1	1774	tags=19%, list=9%, signal=21%
REACTOME_DOWNSTREAM_SIGNALING_OF_ACTIVATED_FGFR	T293	95	0.245247	0.912377	0.681265	0.7985592	1	4121	tags=25%, list=21%, signal=32%
REACTOME_THROMBIN_SIGNALLING_THROUGH_PROTEINASE_ACTIVATE	T294	32	0.304811	0.911692	0.594655	0.79790015	1	3951	tags=28%, list=20%, signal=35%
KEGG_GLYCOSAMINOGLYCAN_BIOSYNTHESIS_KERATAN_SULFATE	T295	15	0.364618	0.910275	0.612009	0.7984949	1	632	tags=13%, list=3%, signal=14%
KEGG_CHRONIC_MYELOID_LEUKEMIA	T296	73	0.257587	0.905687	0.71178	0.80788517	1	3878	tags=34%, list=19%, signal=42%
REACTOME_UNFOLDED_PROTEIN_RESPONSE	T297	75	0.257031	0.903986	0.673469	0.8093614	1	4884	tags=32%, list=24%, signal=42%
REACTOME_INSULIN_SYNTHESIS_AND_PROCESSING	T298	20	0.331771	0.901454	0.598214	0.8128552	1	1557	tags=10%, list=8%, signal=11%
REACTOME_SIGNALING_BY_PDGF	T299	116	0.233814	0.899005	0.771117	0.8373789	1	3042	tags=21%, list=15%, signal=24%
KEGG_CARDIAC_MUSCLE_CONTRACTION	T300	74	0.246875	0.884858	0.738849	0.8498589	1	2233	tags=12%, list=11%, signal=14%
REACTOME_IL1_SIGNALING	T301	38	0.286106	0.883778	0.676399	0.8500836	1	2695	tags=24%, list=14%, signal=27%
KEGG_GALACTOSE_METABOLISM	T302	26	0.306704	0.879047	0.660131	0.85867053	1	1410	tags=15%, list=7%, signal=17%
KEGG_PURINE_METABOLISM	T313	152	0.218264	0.858955	0.8602069	0.8740322	1	5157	tags=35%, list=26%, signal=47%
REACTOME_INTRINSIC_PATHWAY_FOR_APOPTOSIS	T314	29	0.294526	0.8571	0.75087	0.87523633	1	2630	tags=17%, list=13%, signal=20%
KEGG_INOSITOL_PHOSPHATE_METABOLISM	T315	54	0.256042	0.854723	0.759815	0.8775051	1	2102	tags=19%, list=11%, signal=21%
REACTOME_MEF_MEDIATES_DOWN_MODULATION_OF_CELL_SURFACE_R	T316	20	0.270389	0.852194	0.676991	0.88004893	1	496	tags=10%, list=2%, signal=10%
KEGG_ANTIGEN_PROCESSING_AND_PRESENTATION	T317	74	0.239959	0.851926	0.781638	0.8778946	1	4903	tags=28%, list=25%, signal=37%
REACTOME_NUCLEOTIDE_BINDING_DOMAIN_LEUCINE_RICH_REPEAT_CO	T318	44	0.26766	0.851303	0.735803	0.8765748	1	1595	tags=14%, list=8%, signal=15%
KEGG_AMINOACYL_TRNA_BIOSYNTHESIS	T319	40	0.270389	0.851046	0.746377	0.87437457	1	4065	tags=23%, list=20%, signal=28%
KEGG_SYSTEMIC_LUPUS_ERYTHEMATOSUS	T320	82	0.238708	0.850804	0.795062	0.87227273	1	5083	tags=24%, list=25%, signal=33%
REACTOME_MRNA_3_END_PROCESSING	T321	31	0.289246	0.849503	0.714286	0.8723618	1	5248	tags=42%, list=26%, signal=57%
REACTOME_TRANSCRIPTIONAL_REGULATION_OF_WHITE_ADIPOCYTE_DIF	T322	72	0.23883	0.849304	0.811083	0.8700321	1	1712	tags=13%, list=9%, signal=14%
REACTOME_INHIBITION_OF_VOLTAGE_GATED_CA2_CHANNELS_VIA_GBET	T323	25	0.300804	0.847607	0.715835	0.8710393	1	3199	tags=20%, list=16%, signal=24%
KEGG_COLORECTAL_CANCER	T324	62	0.244869	0.842198	0.812207	0.87961626	1	3547	tags=27%, list=18%, signal=33%
REACTOME_ADP_SIGNALLING_THROUGH_P2RY1	T325	25	0.294477	0.841531	0.697987	0.8783363	1	3951	tags=28%, list=20%, signal=35%
KEGG_PROPANOATE_METABOLISM	T326	32	0.280139	0.839147	0.724057	0.88051397	1	3700	tags=31%, list=19%, signal=38%
REACTOME_PROCESSING_OF_CAPPED_INTRONLESS_PRE_MRNA	T327	22	0.304819	0.83724	0.729546	0.8817384	1	6750	tags=50%, list=34%, signal=75%
KEGG_HUNTINGTONS_DISEASE	T328	168	0.209122	0.835578	0.92515	0.8828086	1	4845	tags=25%, list=24%, signal=30%
REACTOME_NEUROTRANSMITTER_RECEPTOR_BINDING_AND_DOWNSTRE	T329	131	0.214346	0.833164	0.88946	0.8844543	1	3628	tags=20%, list=18%, signal=24%
REACTOME_YAP1_AND_WWTR1_TAZ_STIMULATED_GENE_EXPRESSION	T330	24	0.296461	0.827419	0.734783	0.89270025	1	3423	tags=29%, list=17%, signal=35%
REACTOME_CREB_PHOSPHORYLATION_THROUGH_THE_ACTIVATION_OF	T331	25	0.288237	0.825212	0.770642	0.89413005	1	3533	tags=32%, list=18%, signal=39%
REACTOME_ASSOCIATION_OF_TRIC_CCT_WITH_TARGET_PROTEINS_DURI	T332	24	0.291864	0.82484	0.743764	0.8922203	1	2115	tags=21%, list=11%, signal=23%
REACTOME_GABA_SYNTHESIS_RELEASE_REUPTAKE_AND_DEGRADATION	T333	16	0.317637	0.821363	0.715556	0.8960188	1	3838	tags=31%, list=19%, signal=39%
REACTOME_SIGNALING_BY_ROBO_RECEPTOR	T334	29	0.277943	0.820748	0.734597	0.8945165	1	3542	tags=31%, list=18%, signal=38%
REACTOME_MICRORNA_MIRNA_BIOGENESIS	T335	21	0.302426	0.820277	0.736018	0.8927124	1	7582	tags=48%, list=38%, signal=77%
REACTOME_MYOGENESIS	T336	27	0.277136	0.815164	0.767281	0.8991027	1	3332	tags=26%, list=17%, signal=31%
REACTOME_FACTORS_INVOLVED_IN_MEGAKARYOCYTE_DEVELOPMENT_T	T337	113	0.216071	0.813381	0.915601	0.8996822	1	4121	tags=27%, list=21%, signal=34%
KEGG_BASE_EXCISION_REPAIR	T338	32	0.267591	0.813333	0.802273	0.89707017	1	5947	tags=38%, list=30%, signal=53%
REACTOME_PLATELET_AGGREGATION_PLUG_FORMATION	T339	33	0.273105	0.81133	0.769401	0.8978102	1	1269	tags=12%, list=6%, signal=13%
REACTOME_SIGNALING_BY_THE_B_CELL_RECEPTOR_BCR	T340	119	0.209158	0.801839	0.912596	0.9111219	1	4104	tags=26%, list=21%, signal=33%
REACTOME_ACTIVATION_OF_KAINATE_RECEPTORS_UPON_GLUTAMATE_	T341	29	0.274679	0.799033	0.809735	0.9129087	1	2074	tags=14%, list=10%, signal=15%
REACTOME_REGULATION_OF_INSULIN_SECRETION_BY_GLUCAGON_LIKE_	T342	41	0.25334	0.798444	0.834515	0.9111859	1	4121	tags=27%, list=21%, signal=34%
REACTOME_LAGGING_STRAND_SYNTHESIS	T343	19	0.306236	0.794331	0.773626	0.9145458	1	4644	tags=32%, list=24%, signal=41%
REACTOME_GABA_RECEPTOR_ACTIVATION	T344	52	0.234929	0.789938	0.855814	0.91853905	1	3434	tags=21%, list=17%, signal=25%
REACTOME_POTASSIUM_CHANNELS	T345	96	0.210733	0.789427	0.918317	0.91672	1	2195	tags=11%, list=11%, signal=13%
REACTOME_G_ALPHA_S_SIGNALLING_EVENTS	T346	115	0.206555	0.788055	0.9935	0.9161409	1	5064	tags=29%, list=25%, signal=38%
KEGG_PANTOTHENATE_AND_COA_BIOSYNTHESIS	T347	16	0.314165	0.786511	0.775862	0.915619	1	3430	tags=25%, list=17%, signal=30%
REACTOME_RECYCLING_PATHWAY_OF_L1	T348	26	0.273346	0.77535	0.822757	0.9288561	1	4614	tags=42%, list=23%, signal=55%
REACTOME_SYNTHESIS_OF_PA	T349	26	0.264738	0.76013	0.849188	0.9455162	1	2139	tags=15%, list=11%, signal=17%
REACTOME_SIGNALLING_TO_ERKS	T350	36	0.242727	0.754822	0.863436	0.9495944	1	2152	tags=19%, list=11%, signal=22%
KEGG_ONE_CARBON_POOL_BY_FOLATE	T351	16	0.293176	0.753488	0.809129	0.94838417	1	3722	tags=31%, list=19%, signal=38%
REACTOME_DEGRADATION_OF_THE_EXTRACELLULAR_MATRIX	T352	27	0.249028	0.74727	0.857143	0.95813507	1	2688	tags=19%, list=13%, signal=21%
REACTOME_BIOSYNTHESIS_OF_THE_N_GLYCAN_PRECURSOR_DOLICHOL_L	T353	26	0.25739	0.733413	0.861991	0.96545625	1	2652	tags=19%, list=13%, signal=22%
REACTOME_RESPIRATORY_ELECTRON_TRANSPORT	T354	66	0.21156	0.728369	0.962217	0.967572	1	4845	tags=18%, list=24%, signal=24%
REACTOME_SYNTHESIS_SECRETION_AND_INACTIVATION_OF_GLP1	T355	17	0.280888	0.726876	0.860636	0.96618477	1	5342	tags=29%, list=27%, signal=40%
REACTOME_VOLTAGE_GATED_POTASSIUM_CHANNELS	T356	43	0.225781	0.719964	0.928412	0.9695743	1	2195	tags=12%, list=11%, signal=13%
REACTOME_SYNTHESIS_OF_BILE_ACIDS_AND_BILE_SALTS_VIA_7ALPHA_H	T357	15	0.280916	0.71597	0.852941	0.9703184	1	2407	tags=20%, list=12%, signal=23%
REACTOME_INTEGRIN_ALPHAIIB_BETA3_SIGNALING	T358	25	0.241096	0.694753	0.929185	0.98447	1	1269	tags=12%, list=6%, signal=13%
KEGG_GRAFT_VERSUS_HOST_DISEASE	T359	33	0.226679	0.684979	0.947242	0.9883942	1	4583	tags=21%, list=23%, signal=27%
REACTOME_CTLA4_INHIBITORY_SIGNALING	T360	21	0.248923	0.684359	0.895197	0.98602594	1	5132	tags=38%, list=26%, signal=51%
REACTOME_SYNTHESIS_OF_GLYCOSYLPHOSPHATIDYLINOSITOL_GPI	T361	16	0.268203	0.676901	0.913319	0.9880582	1	4164	tags=38%, list=21%, signal=47%
REACTOME_GENERATION_OF_SECOND_MESSENGER_MOLECULES	T362	23	0.23362	0.667241	0.930283	0.99078804	1	5524	tags=39%, list=28%, signal=54%
REACTOME_TRAF6_MEDIATED_NFKB_ACTIVATION	T363	20	0.242538	0.650175	0.922374	0.99402634	1	3419	tags=25%, list=17%, signal=30%
KEGG_GLYCOSYLPHOSPHATIDYLINOSITOL_GPI_ANCHOR_BIOSYNTHESIS	T364	24	0.23112	0.643518	0.939189	0.9960422	1	5095	tags=38%, list=26%, signal=50%
REACTOME_NEPHRIN_INTERACTIONS	T365	19	0.241118	0.639141	0.940092	0.9950686	1	3364	tags=26%, list=17%, signal=32%
REACTOME_ACTIVATION_OF_CHAPERONE_GENES_BY_XBP1S	T366	43	0.197983	0.63494	0.979215	0.9939006	1	3683	tags=21%, list=18%, signal=26%
REACTOME_MITOCHONDRIAL_TRNA_AMINOACYLATION	T367	20	0.232357	0.627601	0.952278	0.99388915	1	5427	tags=30%, list=27%, signal=41%
REACTOME_AMYLOIDS	T368	42	0.196863	0.622905	1	0.99276006	1	5173	tags=21%, list=26%, signal=29%
KEGG_CYSTEINE_AND_METHIONINE_METABOLISM	T369	34	0.200437	0.616902	0.99117	0.99196076	1	5859	tags=32%, list=29%, signal=46%
REACTOME_PROCESSIVE_SYNTHESIS_ON_THE_LAGGING_STRAND	T370	15	0.239584	0.596241	0.954262	0.99483673	1	4644	tags=33%, list=23%, signal=43%
REACTOME_ENOS_ACTIVATION_AND_REGULATION	T371	17	0.214839	0.562547	0.977035	0.9985243	1	5566	tags=35%, list=28%, signal=49%
REACTOME_TRNA_AMINOACYLATION	T372	41	0.17267	0.544731	0.995204	0.9981765	1	4065	tags=17%, list=20%, signal=21%
REACTOME_OLFACTORY_SIGNALING_PATHWAY	T373	75	0.123331	0.436246	1	1	1	5684	tags=19%, list=28%, signal=26%
REACTOME_RESPIRATORY_ELECTRON_TRANSPORT_ATP_SYNTHESIS_BY_C	T374	83	0.111229	0.395134	1	0.9997916	1	4845	tags=16%, list=24%, signal=21%

Gene set enrichment analysis for protein expression: Akt-i/MEK-i resistant Group 3 cell lines vs. Akt-i resistant Group 1 and MEK-i resistant Group 2 cell line:									
NAME	Annotation Fig. 5C	SIZE	ES	NES	NOM p-val	FDR q-val	FWER p-val	RANK AT LEADING EDGE	
REACTOME_PEPTIDE_CHAIN_ELONGATION	P1	55	0.871731	3.501589	0	0	0	184	tags=89%, list=10%, signal=97%
KEGG_RIBOSOME	P2	56	0.85176	3.404396	0	0	0	184	tags=86%, list=10%, signal=94%
REACTOME_3_UTR_MEDIATED_TRANSLATIONAL_REGULATION	P3	74	0.805443	3.400304	0	0	0	184	tags=79%, list=10%, signal=75%
REACTOME_INFLUENZA_VIRAL_RNA_TRANSCRIPTION_AND_REPLICATION	P4	68	0.821496	3.388601	0	0	0	184	tags=78%, list=10%, signal=85%
REACTOME_METABOLISM_OF_MRNA	P5	146	0.689257	3.242836	0	0	0	497	tags=56%, list=13%, signal=62%
REACTOME_NONSENSE_MEDIATED_DECAY_ENHANCED_BY_THE_EXON_JUNCTION_COMPLEX	P6	69	0.789879	3.242701	0	0	0	184	tags=77%, list=10%, signal=77%
REACTOME_SRP_DEPENDENT_COTRANSLATIONAL_PROTEIN_TARGETING_TO_MEMBRANE	P7	77	0.753862	3.229672	0	0	0	184	tags=64%, list=10%, signal=69%
REACTOME_TRANSLATION	P8	195	0.658173	3.11766	0	0	0	470	tags=53%, list=12%, signal=61%
REACTOME_INFLUENZA_LIFE_CYCLE	P9	95	0.709428	3.106416	0	0	0	184	tags=57%, list=10%, signal=61%
REACTOME_METABOLISM_OF_RNA	P10	174	0.644268	3.09422	0	0	0	497	tags=49%, list=13%, signal=54%
REACTOME_FORMATION_OF_THE_TERNARY_COMPLEX_AND_SUBSEQUENTLY_THE_43S_COMPLEX	P11	35	0.779994	2.819188	0	0	0	565	tags=77%, list=14%, signal=89%
REACTOME_ACTIVATION_OF_THE_MRNA_UPON_BINDING_OF_THE_CAP_BINDING_COMPLEX_AND_EIFS_AND_SUBSE	P12	41	0.748855	2.7346162	0	0	0	565	tags=68%, list=14%, signal=79%
REACTOME_ANTIGEN_PROCESSING_UBIQUITINATION_PROTEASOME_DEGRADATION	P13	88	0.683475	2.703755	0	0	0	973	tags=70%, list=25%, signal=91%
REACTOME_CD4_PRESENTATION_OF_SOLUBLE_EXOGENOUS_ANTIGENS_ENDOSOMES	P14	34	0.741269	2.68291	0	0	0	497	tags=71%, list=13%, signal=80%
KEGG_PROTEASOME	P15	33	0.746669	2.662676	0	0	0	497	tags=76%, list=13%, signal=86%
REACTOME_AUTODEGRADATION_OF_CDH1_BY_CDH1_APC_C	P16	42	0.709238	2.660711	0	0	0	973	tags=88%, list=25%, signal=110%
REACTOME_VIF_MEDIATED_DEGRADATION_OF_APOBEC3G	P17	37	0.719209	2.659408	0	0	0	565	tags=81%, list=14%, signal=88%
REACTOME_ASSEMBLY_OF_THE_PRE_REPLICATIVE_COMPLEX	P18	45	0.69966	2.652361	0	0	0	565	tags=58%, list=14%, signal=67%
REACTOME_REGULATION_OF_ORNITHINE_DECARBOXYLASE_ODC	P19	35	0.728316	2.649344	0	0	0	697	tags=80%, list=13%, signal=91%
REACTOME_REGULATION_OF_MITOTIC_CELL_CYCLE	P20	49	0.694741	2.648507	0	0	0	973	tags=80%, list=25%, signal=106%
REACTOME_CDT1_ASSOCIATION_WITH_THE_CDC6_ORC_ORIGIN_COMPLEX	P21	39	0.721374	2.644993	0	0	0	565	tags=67%, list=14%, signal=77%
REACTOME_APC_C_CDC20_MEDIATED_DEGRADATION_OF_MITOTIC_PROTEINS	P22	46	0.693364	2.644584	0	0	0	565	tags=63%, list=14%, signal=73%
REACTOME_CLASS_I_MHC_MEDIATED_ANTIGEN_PROCESSING_PRESENTATION	P23	106	0.59924	2.637359	0	0	0	973	tags=64%, list=25%, signal=85%
REACTOME_AUTODEGRADATION_OF_THE_E3_UBIQUITIN_LIGASE_COP1	P24	38	0.720703	2.632081	0	0	0	565	tags=68%, list=14%, signal=79%
REACTOME_SCF_BETA_TRCP_MEDIATED_DEGRADATION_OF_EMI1	P25	37	0.731216	2.623196	0	0	0	570	tags=78%, list=14%, signal=91%
REACTOME_ACTIVATION_OF_NF_KAPPAB_IN_B_CELLS	P26	41	0.709885	2.62216	0	0	0	619	tags=71%, list=16%, signal=85%
REACTOME_DOWNSTREAM_SIGNALING_EVENTS_OF_B_CELL_RECEPTOR_BCR	P27	49	0.675971	2.619842	0	0	0	619	tags=61%, list=16%, signal=72%
REACTOME_SCF(SKP2_MEDIATED_DEGRADATION_OF_P27_P21	P28	38	0.72407	2.619032	0	0	0	565	tags=66%, list=14%, signal=77%
REACTOME_DESTABILIZATION_OF_MRNA_BY_AUF1_HNRNP_D0	P29	39	0.700107	2.605325	0	0	0	565	tags=66%, list=14%, signal=76%
REACTOME_M_G1_TRANSITION	P30	53	0.664866	2.598291	0	0	0	973	tags=64%, list=25%, signal=86%
REACTOME_APC_C_CDH1_MEDIATED_DEGRADATION_OF_CDC20_AND_OTHER_APC_C_CDH1_TARGETED_PROTEINS	P31	43	0.690844	2.596	0	0	0	595	tags=65%, list=15%, signal=76%
REACTOME_PS3_PROPENDENT_G1_S_DNA_DAMAGE_CHECKPOINT	P32	35	0.726974	2.576572	0	0	0	565	tags=72%, list=14%, signal=83%
REACTOME_CDK_MEDIATED_PHOSPHORYLATION_AND_REMOVAL_OF_CDC6	P33	36	0.715959	2.576479	0	0	0	973	tags=89%, list=25%, signal=117%
REACTOME_ORC1_REMOVAL_FROM_CHROMATIN	P34	47	0.663231	2.557409	0	0	0	565	tags=55%, list=14%, signal=64%
REACTOME_AUTODEGRADATION_OF_THE_E3_UBIQUITIN_LIGASE_COP1	P35	36	0.70178	2.552274	0	0	0	565	tags=69%, list=14%, signal=80%
REACTOME_SIGNALING_BY_THE_B_CELL_RECEPTOR_BCR	P36	55	0.654593	2.538132	0	0	0	619	tags=58%, list=16%, signal=68%
REACTOME_PS3_DEPENDENT_G1_DNA_DAMAGE_RESPONSE	P37	37	0.688353	2.511951	0	0	0	973	tags=86%, list=25%, signal=114%
REACTOME_CELL_CYCLE_CHECKPOINTS	P38	67	0.669216	2.506097	0	0	0	973	tags=58%, list=25%, signal=76%
REACTOME_ER_PHAGOSOME_PATHWAY	P39	41	0.672626	2.500307	0	0	0	565	tags=61%, list=14%, signal=70%
REACTOME_MITOTIC_G1_G1_S_PHASES	P40	73	0.588824	2.497768	0	0	0	570	tags=62%, list=14%, signal=73%
REACTOME_SIGNALING_BY_WNT	P41	45	0.664962	2.485457	0	0	0	570	tags=64%, list=14%, signal=74%
REACTOME_CYCLIN_E_ASSOCIATED_EVENTS_DURING_G1_S_TRANSITION_	P42	44	0.66315	2.472338	0	0	0	570	tags=62%, list=14%, signal=71%
REACTOME_G1_S_TRANSITION	P43	69	0.591684	2.468389	0	0	0	570	tags=54%, list=14%, signal=63%
REACTOME_REGULATION_OF_MRNA_STABILITY_BY_PROTEINS_THAT_BIND_AU_RICH_ELEMENTS	P44	60	0.608422	2.433617	0	0	0	973	tags=67%, list=25%, signal=87%
REACTOME_METABOLISM_OF_PROTEINS	P45	218	0.484309	2.417666	0	0	0	470	tags=30%, list=12%, signal=35%
REACTOME_ANTIGEN_PROCESSING_CROSS_PRESENTATION	P46	44	0.648364	2.390128	0	0	0	973	tags=84%, list=25%, signal=111%
REACTOME_S_PHASE	P47	74	0.570346	2.364854	0	0	0	570	tags=61%, list=14%, signal=71%
REACTOME_SYNTHESIS_OF_DNA	P48	60	0.576761	2.341357	0	0	0	497	tags=39%, list=13%, signal=44%
REACTOME_MITOTIC_M_M_G1_PHASES	P49	98	0.5506994	2.2386115	3	2.22E-05	3.001	973	tags=47%, list=25%, signal=61%
REACTOME_DNA_REPLICATION	P50	111	0.5441412	2.2057739	3	3.07E-04	3.019	1014	tags=49%, list=26%, signal=58%
REACTOME_ADAPTIVE_IMMUNE_SYSTEM	P51	184	0.4282649	2.0759156	3	3.89E-04	3.019	973	tags=46%, list=25%, signal=59%
REACTOME_CYTOSOLIC_TRNA_AMINOACYLATION	P52	22	0.6450904	2.0701127	3	4.03E-04	3.019	677	tags=73%, list=17%, signal=87%
REACTOME_CELL_CYCLE_MITOTIC	P53	156	3.4338	2.0295053	3	6.15E-04	3.03	1102	tags=46%, list=28%, signal=62%
REACTOME_HOST_INTERACTIONS_OF_HIV_FACTORS	P54	86	0.4551164	1.9461383	0	0.0001306306	3.066	973	tags=55%, list=25%, signal=66%
REACTOME_APOPTOSIS	P55	84	0.443281	1.9088842	0	0.0002776204	3.128	565	tags=38%, list=14%, signal=44%
REACTOME_CELL_CYCLE	P56	175	0.3389763	1.8419469	3	0.0037382099	3.174	1130	tags=45%, list=29%, signal=61%
KEGG_UBIQUITIN_MEDIATED_PROTEOLYSIS	P57	53	0.477715	1.8783616	0.001960784	0.0030203312	3.184	959	tags=38%, list=24%, signal=50%
REACTOME_PROTEIN_FOLDING	P58	25	0.553731	1.8377798	0.005628518	0.0057599429	3.265	715	tags=56%, list=18%, signal=68%
REACTOME_DEADENYLATION_DEPENDENT_MRNA_DECAY	P59	32	0.513624	1.8339134	0	0.0106515093	3.28	1376	tags=72%, list=35%, signal=111%
KEGG_RNA_DEGRADATION	P60	40	0.490943	1.8172398	0.001926782	0.0070595585	3.325	1251	tags=60%, list=32%, signal=87%
REACTOME_IMMUNE_SYSTEM	P61	284	0.349187	1.7651815	3	0.0130369	3.489	1042	tags=40%, list=26%, signal=53%
KEGG_GLYCOLYSIS_GLUCONEOGENESIS	P62	33	0.490644	1.7495933	0.011583012	0.013464889	3.546	993	tags=65%, list=25%, signal=86%
REACTOME_HIV_INFECTION	P63	125	0.381137	1.7488461	3	0.0133381117	3.547	1130	tags=49%, list=29%, signal=68%
REACTOME_GLYCOLYSIS	P64	17	0.558804	1.6814187	0.007952286	0.023610462	3.751	1530	tags=82%, list=39%, signal=134%
REACTOME_METABOLISM_OF_AMINO_ACIDS_AND_DERIVATIVES	P65	96	0.377053	1.6454511	0.010395472	0.013536454	3.853	154	tags=12%, list=4%, signal=12%
KEGG_RIG_I_LIKE_RECEPTOR_SIGNALING_PATHWAY	P66	16	0.542932	1.6116617	0.020484172	0.03940435	3.916	894	tags=50%, list=23%, signal=64%
REACTOME_IRON_UPTAKE_AND_TRANSPORT	P67	15	0.554588	1.5580799	0.022482212	0.05068827	3.965	1338	tags=87%, list=34%, signal=131%
REACTOME_TRNA_AMINOACYLATION	P68	36	0.431926	1.5664808	0.020637898	0.056029182	3.979	677	tags=58%, list=17%, signal=69%
REACTOME_LOSS_OF_NLP_FROM_MITOTIC_CENTROSOMES	P69	24	0.471252	1.5216468	0.029150296	0.07552633	3.989	713	tags=42%, list=18%, signal=51%
KEGG_PURINE_METABOLISM	P70	55	0.334051	1.5134551	0.032949151	0.07837875	3.992	389	tags=36%, list=25%, signal=48%
REACTOME_MITOTIC_G2_G2_M_PHASES	P71	34	0.427668	1.49001	0.025390425	0.08427122	3.994	713	tags=62%, list=18%, signal=76%
KEGG_RECRUITMENT_OF_MITOTIC_CENTROSOME_PROTEINS_AND_COMPLEXES	P72	20	0.442506	1.4972411	0.04681431	0.08309314	3.994	713	tags=60%, list=18%, signal=72%
REACTOME_CYTOKINE_SIGNALING_IN_IMMUNE_SYSTEM	P73	86	0.345859	1.495326	0.012987013	0.085907734	3.994	1193	tags=55%, list=35%, signal=83%
REACTOME_ENDOSOMAL_SORTING_COMPLEX_REQUIRED_FOR_TRANSPORT_ESCRT	P74	18	0.481165	1.4597	0.035905512	0.103736555	3.999	691	tags=44%, list=17%, signal=53%
REACTOME_SIGNALING_BY_ILS	P75	30	0.417343	1.4551055	0.039160307	0.112393156	1	721	tags=30%, list=18%, signal=36%
KEGG_ANDROGEN_AND_ESTROGEN_BIOSYNTHESIS	P76	32	0.410753	1.4422318	0.044082219	0.117436874	1	1079	tags=44%, list=27%, signal=61%
KEGG_NUCLEOTIDE_EXCISION_REPAIR	P77	31	0.398504	1.3757799	0.07141449	3.1735169	1	1069	tags=42%, list=27%, signal=57%
REACTOME_RIG_I_MDA5_MEDIATED_INDUCTION_OF_IFN_ALPHA_BETA_PATHWAYS	P78	23	0.440823	1.3543917	0.097232224	3.1935185	1	619	tags=35%, list=16%, signal=41%
REACTOME_ANTIVIRAL_MECHANISM_BY_IFN_STIMULATED_GENES	P79	65	0.330766	1.3347544	0.09048086	3.1991177	1	1295	tags=58%, list=33%, signal=85%
KEGG_PENTOSE_PHOSPHATE_PATHWAY	P80	18	0.43787	1.3337644	0.113616317	3.2070108	1	1286	tags=56%, list=33%, signal=82%
REACTOME_ACTIVATION_OF_THE_PRE_REPLICATIVE_COMPLEX	P81	18	0.435312	1.3312163	0.119674	3.2162786	1	1762	tags=67%, list=45%, signal=121%
REACTOME_METABOLISM_OF_NUCLEOTIDES	P82	39	0.353158	1.3113944	0.111984228	3.2344616	1	1008	tags=38%, list=26%, signal=51%
KEGG_CYSTEINE_AND_METHIONINE_METABOLISM	P83	15	0.453303	1.3360006	0.117165468	3.2703854	1	1172	tags=60%, list=30%, signal=85%
REACTOME_CELL_SURFACE_INTERACTIONS_AT_THE_VASCULAR_WALL	P84	26	0.39021	1.3003161	0.11132076	3.2442102	1	598	tags=35%, list=15%, signal=41%
REACTOME_SIGNALING_BY_INSULIN_RECEPTOR	P85	34	0.343156	1.286792	0.112121215	3.2595289	1	1338	tags=56%, list=34%, signal=86%
REACTOME_RNA_POL_I_RNA_POL_III_AND_MITOCHONDRIAL_TRANSCRIPTION	P86	31	0.341628	1.2587653	0.15104099	3.2977071	1	590	tags=29%, list=15%, signal=34%
REACTOME_G2_M_CHECKPOINTS	P87	21	0.395607	1.248877	0.18114683	3.3095235	1	1781	tags=67%, list=46%, signal=123%
REACTOME_PURINE_METABOLISM	P88	21	0.388354	1.216669	0.19889502	3.3597744	1	989	tags=38%, list=25%, signal=51%
REACTOME_INTERFERON_SIGNALING	P89	60	0.294874	1.188417	0.16307656	3.4078252	1	1349	tags=50%, list=34%, signal=82%
KEGG_FRUCTOSE_AND_MANNOSE_METABOLISM	P90	18	0.391207	1.1724354	0.24652868	3.4339475	1	854	tags=33%, list=22%, signal=42%
REACTOME_GLUCONEOGENESIS	P91	21	0.376289	1.167893	0.24023408	3.4381903	1	624	tags=43%, list=21%, signal=54%
REACTOME_GLUCOSE_METABOLISM	P92	39	0.317356	1.1198913	0.24124418	3.4492817	1	1338	tags=49%, list=34%, signal=74%
REACTOME_RNA_POL_I_TRANSCRIPTION	P93	18	0.378987	1.1567251	0.25343812	3.4503383	1	610	tags=22%, list=16%, signal=25%
REACTOME_E2F_MEDIATED_REGULATION_OF_DNA_REPLICATION	P94	16	0.386274	1.1564838	0.26568267	3.4644102	1	1568	tags=69%, list=40%, signal=114%
KEGG_NOD_LIKE_RECEPTOR_SIGNALING_PATHWAY	P95	15	0.39937	1.1462613	0.27142859	3.4624793	1	987	tags=47%, list=25%, signal=62%
REACTOME_ACTIVATION_OF_ATR_IN_RESPONSE_TO_REPLICATION_STRESS	P96	19	0.368153	1.1191251	0.26027896	3.4724743	1	1781	tags=89%, list=45%, signal=162%
REACTOME_DOWNSTREAM_SIGNAL_TRANSDUCTION	P97	30	0.331255	1.1384771	0.2653866	3.4693264	1	1348	tags=67%, list=34%, signal=102%
REACTOME_PI3K_CASCADE	P98	16	0.38396	1.1358008	0.29181546	3.4817968	1	1274	tags=56%, list=32%, signal=83%
KEGG_PORPHYRIN_AND_CHLOROPHYLL_METABOLISM	P99	17	0.382306	1.115923	0.30095237	3.5065029	1	514	tags=29%, list=13%, signal=34%
KEGG_PYRUVATE_METABOLISM	P100	24	0.32658	1.1002928	0.31427186	3.534624	1	1187	tags=42%, list=30%, signal=59%
KEGG_PYRIMIDINE_METABOLISM	P101	43	0.290847	1.08619	0.3314521	3.5603778	1	1008	tags=35%, list=26%, signal=46%
KEGG_REGULATION_OF_ACTIN_CYTOSKELETON	P102	66	0.267356	1.0848832	0.33265308	3.5577615	1	941	tags=33%, list=24%, signal=43%
KEGG_MTOR_SIGNALING_PATHWAY	P103	25	0.326245	1.0734145	0.36	3.5763896	1	549	tags=25%, list=14%, signal=29%
REACTOME_MITOTIC_PROMETAPHASE	P104	43	0.281715	1.072757	0.33206108	3.5744145	1	1199	tags=40%, list=30%, signal=56%
KEGG_CELL_CYCLE	P105	51	0.273407	1.0715	0.3825048	3.5728174	1	748	tags=24%, list=19%, signal=29%
REACTOME_INSULIN_RECEPTOR_SIGNALLING_CASCADE	P106	24	0.324467	1.0541402	0.375969	3.6066275	1	1274	tags=42%, list=32%, signal=61%
KEGG_EPITHELIAL_CELL_SIGNALING_IN_HELICOBACTER_PYLORI_INFECTION	P107	29	0.304463	1.0147803	0.37406145	3.6194566	1	1371	tags=59%, list=35%, signal=89%
REACTOME_EXTENSION_OF_TELOMERES	P108	20	0.33615	1.0457449	0.41505793	3.6149887	1	132	tags=10%, list=3%, signal=10%
KEGG_PI3K_SIGNALING_PATHWAY	P109	17	0.349124	1.04341	0.39085427	3.6144524	1	780	tags=24%, list=20%, signal=31%
REACTOME_SIGNALING_BY_ERBB2	P110	35	0.290419	1.0319329	0.39130414	3.6310767	1	1348	tags=46%, list=34%, signal=65%
REACTOME_METABOLISM_OF_NON_CODING_RNA	P111	31	0.294791	1.0329182	0.37277148	3.6276369	1	175	tags=13%, list=4%, signal=13%
REACTOME_TRANSCRIPTION	P112	81	0.238366	1.0100969	0.44337812	3.6772145	1	613	tags=22%, list=16%, signal=24%
REACTOME_SIGNALING_BY_ERBB4	P113	27	0.296084	0.9943452	0.44482717	3.7108523	1	570	tags=22%, list=14%, signal=26%
REACTOME_RNA_POL_II_TRANSCRIPTION_PRE_INITIATION_AND_PROMOTER_OPENING	P114	26	0.318361	0.9917567	0.4304762	3.7134072	1	613	tags=23%, list=16%, signal=28%
KEGG_ENDOCYTOSIS	P115	71	0.232202	0.9771183	0.50118868	3.7636967	1	691	tags=25%, list=17%, signal=32%
KEGG_LEUKOCYTE_TRANSENDOTHELIAL_MIGRATION	P116	24	0.298611	0.9674821	0.5331621	3.7587996	1	948	tags=29%, list=24%, signal=39%
REACTOME_SIGNALING_BY_PDGF	P117	32	0.273984	0.9665511	0.4952381	3.7545627	1	120	tags=19%, list=13%, signal=21%
REACTOME_ELONGATION_ARREST_AND_RECOVERY	P118	19	0.307473	0.9545864	0.4934383	3.7737383	1	381	tags=21%, list=10%, signal=23%
REACTOME_UNFOLDED_PROTEIN_RESPONSE	P119	40	0.254163	0.9482393	0.51005548	3.7874908	1	778	tags=28%, list=20%, signal=34%
KEGG_SMALL_CELL_LUNG_CANCER	P120	21	0.296973	0.9477519	0.53133149	3.7823465	1	686	tags=30%, list=17%, signal=37%
REACTOME_TRIF_MEDIATED_TLR3_SIGNALING	P121	24	0.288688	0.9343893	0.53178928	3.7853224	1	1616	tags=58%, list=41%, signal=98%
REACTOME_TELOMERE_MAINTENANCE	P122	22	0.301284	0.9430237	0.54780877	3.7897264	1	132	tags=9%, list=3%, signal=9%
REACTOME_NFKB_AND_MAP_KINASES_ACTIVATION_MEDIATED_BY_TLR4_SIGNALING_REPERTOIRE	P123	24	0.288688	0.9403324	0.5426744	3.7809963	1	1616	tags=58%, list=41%, signal=98%
KEGG_FOCAL_ADHESION	P124	53	0.234485	0.9193941	0.6019583	3.8258916	1	1196	tags=40%, list=30%, signal=57%
KEGG_PATHWAYS_IN_CANCER	P125	79	0.214741	0.9216332	0.6228872	3.8408745	1	721	tags=20%, list=18%, signal=24%
KEGG_COLORECTAL_CANCER	P126	17	0.306678	0.8961818	0.59309024	3.8692949	1	193	tags=12%, list=5%, signal=12%
REACTOME_DIABETES_PATHWAYS	P127	56	0.222504	0.8851556	0.6842745	3.8978024	1	778	tags=20%, list=20%, signal=31%
KEGG_VIBRIO_CHOLERAE_INFECTION	P128	22	0.272351	0.8866772	0.6450382	3.9212506	1	1236	tags=55%, list=31%, signal=79%
REACTOME_INTEGRIN_CELL_SURFACE_INTERACTIONS	P129	22	0.269451	0.8827888	0.6542969	3.9275486	1	834	tags=18%, list=8%, signal=20%
REACTOME_MHC_CLASS_II_ANTIGEN_PRESENTATION	P130	47	0.223543	0.8581776	0.75308057	3.9318878	1	741	tags=28%, list=19%, signal=34%
KEGG_ANTIGEN_PROCESSING_AND_PRESENTATION	P131	15	0.298506	0.8567709	0.65151	3.9282313	1	1593	tags=79%, list=41%, signal=131%
REACTOME_SEMAPHORIN_INTERACTIONS	P132	18	0.283804	0.845332	0.69818806	3.9667762	1	1506	tags=67%, list=38%, signal=107%
REACTOME_SIGNALING_BY_FGFR_IN_DISEASE	P133	15	0.23887	0.8345947	0.75396224	3.9693097	1	1529	tags=60%, list=39%, signal=74%
KEGG_INSULIN_SIGNALING_PATHWAY	P134	45	0.203809	0.8402339	3.75	3.9438819	1	1109	tags=29%, list=28%, signal=40%
KEGG_ERBB_SIGNALING_PATHWAY	P135	24	0.256649	0.8351101	3.7579148	3.948167	1	1616	tags=58%, list=41%, signal=98%
REACTOME_RNA_POL_II_PRE_TRANSCRIPTION_EVENTS	P136	32	0.239572	0.8321217	0.73954374	3.9470954	1	702	tags=22%, list=18%, signal=26%
KEGG_ACUTE_MYELOID_LEUKEMIA	P137	18	0.271543	0.8193466	3.74	3.9654525	1	1616	tags=56%, list=41%, signal=96%
KEGG_FC_GAMMA_R_MEDIATED_PHAGOCYTOSIS	P138	27	0.241516	0.8149856	3.7976167	3.9688162	1	940	tags=30%, list=24%, signal=39%
REACTOME_LATE_PHASE_OF_HIV_LIFE_CYCLE	P139	62	0.200135	0.8161366	0.81877023	3.9626363	1	1128	tags=34%, list=29%, signal=47%
REACTOME_GLOBAL_GENOMIC_NER_GG_NER	P140	26	0.246027	0.8131834	3.7956047	3.9958508	1	1569	tags=35%, list=40%, signal=57%
KEGG_OOCYTE_MEIOSIS	P141	43	0.211202	0.79451	0.82811555	3.9832269	1	749	tags=23%, list=19%, signal=28%
REACTOME_FORMATION_OF_RNA_POL_II_ELONGATION_COMPLEX_	P142	28	0.227011	0.7731873	3.7970205	1	1	393	tags=14%, list=10%, signal=16%
KEGG_NEUROTROPHIN_SIGNALING_PATHWAY	P143	39	0.209391	0.7695956	3.8545455	1	1	749	tags=21%, list=19%, signal=25%
REACTOME_SIGNALING_BY_FGFR	P144	28	0.227259	0.7679797	3.810757	1	1	1529	tags=36%, list=39%, signal=75%
REACTOME_SIGNALING_BY_SCF_KIT	P145	22	0.233049	0.7531385	3.8540146	1	1	520	tags=14%, list=13%, signal=16%
REACTOME_MITOSIS	P146	24	0.226472	0.74212	0.85915964	1	1	1130	tags=39%, list=29%, signal=52%
REACTOME_PYRUVATE_METABOLISM_AND_CITRIC_ACID_TCA_CYCLE	P147	32	0.212399	0.7335154	3.8769231	1	1	622	tags=16%, list=11%, signal=17%
KEGG_PROPANOATE_METABOLISM	P148	23	0.227013	0.7331206	3.8513514	1	1	992	tags=35%, list=25%, signal=46%
REACTOME_DOWNSTREAM_SIGNALING_OF_ACTIVATED_FGFR	P149	26	0.223906	0.7301115	3.8507463	1	1	377	tags=15%, list=10%, signal=16%
REACTOME_ACTIVATED_TLR4_SIGNALLING	P150	26	0.218301	0.7234547	0.86307023	1	1	1616	tags=54%, list=41%, signal=91%
REACTOME_MRNA_CAPPING	P151	21	0.233183	0.7327252	3.8536312	1	1	580	tags=19%, list=15%, signal=22%
KEGG_PATHOGENIC_ESCHERICHIA_COLI_INFECTION	P152	21	0.226391	0.7089777	3.8747623	1	1	900	tags=29%, list=23%, signal=37%
REACTOME_NUCLEOTIDE_EXCISION_REPAIR	P153	52	0.200099	0.7084137	0.91312385	1	1	1126	tags=39%, list=29%, signal=55%
REACTOME_RESPONSE_TO_ELEVATED_PLATELET_CYTOSOLIC_CA2_	P154	25	0.20874	0.6908869	3.9111111	1	1	1049	tags=36%, list=27%, signal=49%
KEGG_APOPTOSIS	P155	28	0.198418	0.6851552	3.9338192	1	1	607	tags=18%, list=16%, signal=21%
KEGG_TOLL_LIKE_RECEPTOR_SIGNALING_PATHWAY	P156	19	0.217877	0.6610369	0.92022264	1	1	1371	tags=47%, list=35%, signal=72%
KEGG_ARGININE_AND_PROLINE_METABOLISM	P157	26	0.191778	0.6458868	0.94176049	1	1	1488	tags=38%, list=38%, signal=61%
REACTOME_MYD88_MAL_CASCADE_INITIATED_ON_PLASMA_MEMBRANE	P158	25	0.194023	0.6540656	3.9558541	1	1	1616	tags=52%, list=41%, signal=88%
REACTOME_TRAF6_MEDIATED_INDUCTION_OF_NFKB_AND_MAP_KINASES_UPON_TLR7_8_OR_9_ACTIVATION	P159	25	0.194023	0.6439154	0.95982275	1	1	1616	tags=52%, list=41%, signal=88%
KEGG_FATTY_ACID_METABOLISM	P160	26	0.190389	0.6313909	3.9491525	1	1	1005	tags=31%, list=26%, signal=41%
KEGG_HYPERTROPHIC_CARDIOMYOPATHY_HCM_	P161	17	0.206484	0.61237	0.95589506	1	1	937	tags=29%, list=21%, signal=36%
KEGG_VASOPRESSIN_REGULATED_WATER_REABSORPTION	P162	18	0.19965	0.6039187	0.95714285	1	1	1173	tags=39%, list=30%, signal=55%
KEGG_GALACTOSE_METABOLISM	P163	15	0.211361	0.6045844	0.9383643	1	1	490	tags=13%, list=12%, signal=15%
KEGG_DILATED_CARDIOMYOPATHY	P164	17	0.203753	0.6022363	0.94160609	1	1	937	tags=29%, list=21%, signal=36%
REACTOME_MAP_KINASE_ACTIVATION_IN_TLR_CASCADE	P165	17	0.202571	0.6011036	0.95864646	1	1	1616	tags=52%, list=41%, signal=88%
KEGG_AMINO_SUGAR_AND_NUCLEOTIDE_SUGAR_METABOLISM	P166	21	0.176456	0.5985644	0.97180996	1	1	937	tags=19%, list=21%, signal=24%
REACTOME_METABOLISM_OF_CARBOHYDRATES	P167	86	0.136701	0.5917358	3.9981982	1	1	1295	tags=38%, list=33%, signal=56%
KEGG_AD

mRNA expression		Protein expression		Shared		
PROBE	Signal-to-noise	PROBE	Signal-to-noise	PROBE	Signal-to-noise (mRNA)	Signal-to-noise (protein)
1. SNAP25	0.710	1. SEC13	0.797	1. PSMD11	0.447	0.631
2. STX11	0.640	2. RUVBL1	0.765	2. PSMC2	0.379	0.632
3. KAT2B	0.530	3. PSMC4	0.737	3. SEC13	0.124	0.797
4. PPP2R3B	0.528	4. PSMD3	0.737	4. PSMD3	0.107	0.737
5. SGOL1	0.499	5. PSMA3	0.693	5. PSMD1	0.106	0.678
6. PTRF	0.489	6. PSMD1	0.678	6. PCM1	0.409	0.336
7. TUBB4A	0.448	7. PSMA4	0.670	7. PSMD12	0.103	0.611
8. PSMD11	0.447	8. CKAP5	0.666	8. PSMA7	0.139	0.574
9. CDC25A	0.425	9. YWHAG	0.647	9. PSMB7	0.117	0.571
10. STX2	0.423	10. PSMC2	0.632	10. ORC5	0.240	0.424
11. PCM1	0.409	11. PSMD11	0.631	11. RPS27	0.108	0.545
12. CENPI	0.393	12. PSMD12	0.611	12. PSMD9	0.375	0.239
13. PSMC2	0.379	13. RUVBL2	0.604	13. CCNB1	0.170	0.415
14. PSMD9	0.375	14. PSMD4	0.589	14. CDC23	0.267	0.308
15. NINL	0.360	15. PSMA7	0.574	15. GINS4	0.143	0.414
16. POLR3D	0.332	16. PSMB7	0.571	16. ACTR1A	0.150	0.375
17. RFC3	0.316	17. PSMA1	0.569	17. CUL1	0.164	0.338
18. HIST1H2AC	0.308	18. SKP1	0.557	18. ANAPC7	0.141	0.338
19. CENPO	0.298	19. RPS27	0.545	19. NDC80	0.104	0.360
20. PPP2R1B	0.293	20. CDK4	0.533	20. CDK2	0.138	0.316
21. RPA4	0.289	21. PSME2	0.526	21. CDK5RAP2	0.180	0.255
22. GTF3C3	0.284	22. PSMC5	0.514	22. TYMS	0.228	0.198
23. GTF2H2	0.283	23. PSMD8	0.504	23. SPC25	0.209	0.147
24. SNAPC1	0.277	24. RBX1	0.498	24. PPP2CB	0.107	0.223
25. TUBA1A	0.274	25. NUDC	0.487	25. ZWILCH	0.154	0.176
26. POLR1A	0.274	26. PSMC1	0.478	26. ERCC6L	0.175	0.127
27. CDK6	0.269	27. PSME1	0.478	27. KIF2A	0.117	0.143
28. CDC23	0.267	28. PSMB4	0.472	28. GINS1	0.115	0.141
29. LIN54	0.250	29. PSMD13	0.466	29. SYNE1	0.112	0.120
30. STX4	0.245	30. DCTN2	0.445	30. MAX	0.116	0.116
31. CEP250	0.244	31. RPS27A	0.443			
32. ORC5	0.240	32. CLASP1	0.442			
33. CDC6	0.235	33. UBE2E1	0.440			
34. TFDP1	0.232	34. MAGED1	0.438			
35. MCM6	0.232	35. DCTN3	0.435			

36. ATRIP	0.229	**36. ORC5**	0.424
37. TYMS	0.228	**37. UBE2I**	0.423
38. WRAP53	0.223	**38. CUL5**	0.422
39. NUP43	0.222	**39. CCNB1**	0.415
40. BUB1	0.220	**40. GINS4**	0.414
41. BRCA1	0.218	**41. PSMD7**	0.382
42. VAMP1	0.218	**42. ACTR1A**	0.375
43. E2F1	0.211	**43. PAFAH1B1**	0.365
44. STX1B	0.210	**44. PSMB1**	0.364
45. SPC25	0.209	**45. PSMC3**	0.361
46. TUBG1	0.205	**46. NDC80**	0.360
47. ERCC6	0.205	**47. PSMD6**	0.355
48. SKA1	0.201	**48. CLIP1**	0.352
49. CCNE1	0.199	**49. XPO1**	0.347
50. ORC1	0.199	**50. ANAPC2**	0.338
51. TAOK1	0.192	**51. CUL1**	0.338
52. CCNE2	0.190	**52. PCM1**	0.336
53. HIST1H4J	0.187	**53. ANAPC7**	0.333
54. GTF2H2B	0.187	**54. LMNA**	0.331
55. CCNA2	0.184	**55. KIF2C**	0.328
56. CDKN2C	0.181	**56. CDK2**	0.316
57. CDK5RAP 2	0.180	**57. TUBGCP2**	0.314
58. TUBGCP5	0.179	**58. TCEB2**	0.309
59. BTRC	0.178	**59. CDC23**	0.308
60. PSMB2	0.177	**60. PSMB5**	0.288
61. ERCC6L	0.175	**61. DYNLL1**	0.279
62. CENPK	0.172	**62. PSMB8**	0.277
63. CCNB1	0.170	**63. CDK5RAP2**	0.255
64. POLE2	0.169	**64. PSMD2**	0.251
65. CEP135	0.167	**65. NUF2**	0.248
66. CUL1	0.164	**66. PSMD9**	0.239
67. RBBP4	0.163	**67. CETN2**	0.233
68. DNA2	0.161	**68. PSMC6**	0.232
69. DIDO1	0.160	**69. DYNC1I2**	0.232
70. PPP2R2A	0.156	**70. KIF20A**	0.226

71. CEP72	0.156	**71. RPA1**	0.226
72. ZWILCH	0.154	**72. PPP2CB**	0.223
73. HAUS2	0.152	**73. HSPA2**	0.222
74. CENPH	0.151	**74. PSMD10**	0.217
75. CDC25C	0.150	**75. PPP2R1A**	0.206
76. ACTR1A	0.150	**76. FEN1**	0.200
77. TAF1B	0.147	**77. TYMS**	0.198
78. MCM10	0.147	**78. MNAT1**	0.178
79. UBTF	0.145	**79. PPP2R5D**	0.177
80. MCM4	0.144	**80. ZWILCH**	0.176
81. CDC27	0.144	**81. ANAPC5**	0.176
82. ANAPC10	0.143	**82. PRKACA**	0.166
83. LIN52	0.143	**83. ORC2**	0.166
84. GINS4	0.143	**84. SEH1L**	0.155
85. SNAPC3	0.142	**85. YWHAE**	0.153
86. SNAPC4	0.142	**86. DCTN1**	0.150
87. SGOL2	0.142	**87. PSMA2**	0.150
88. PLK4	0.141	**88. HSP90AA1**	0.149
89. ANAPC7	0.141	**89. NUP37**	0.148
90. MIS18A	0.139	**90. SPC25**	0.147
91. PSMA7	0.139	**91. KIF2A**	0.143
92. CDK2	0.138	**92. TERF2**	0.141
93. ZW10	0.138	**93. GINS1**	0.141
94. KIF18A	0.138	**94. PAK2**	0.132
95. CDCA8	0.136	**95. ERCC6L**	0.127
96. CCDC99	0.135	**96. SYNE1**	0.120
97. PRIM2	0.134	**97. MAX**	0.116
98. CEP41	0.134	**98. PSMD5**	0.112
99. TFAM	0.134	**99. CDC16**	0.106
100.CDC20	0.132	**100.PSMA5**	0.104
101.POLR3H	0.129	**101.DYNC1H1**	0.103
102.CEP76	0.126	**102.MAPRE1**	0.101
103.POLA1	0.126		
104.AURKA	0.125		
105.BIRC5	0.124		

106.SEC13	0.124
107.CEP63	0.123
108.SMC1A	0.123
109.POLR1D	0.122
110.BRF2	0.119
111.KIF2A	0.117
112.PSMB7	0.117
113.B9D2	0.117
114.SPC24	0.117
115.MAX	0.116
116.STX1A	0.116
117.CEP164	0.115
118.SMARCA5	0.115
119.CDKN2A	0.115
120.PLK1	0.115
121.ORC3	0.115
122.GINS1	0.115
123.CDC26	0.113
124.SYNE1	0.112
125.RAD17	0.112
126.DSN1	0.111
127.HIST1H2AJ	0.110
128.POLR3GL	0.110
129.CDK7	0.109
130.RPS27	0.108
131.PSMD3	0.107
132.PPP2CB	0.107
133.CASC5	0.107
134.PSMD1	0.106
135.MYBL2	0.106
136.ORC6	0.105
137.NDC80	0.104
138.SSNA1	0.104
139.PSMD12	0.103
140.SSB	0.101

141.MCM2	0.100
142.MCM8	0.100

Additional file 8: Table S4. Enriched cell cycle genes in Akt-i/MEK-i resistant group 3 cell lines. From the significantly enriched, cell cycle-associated gene sets, enriched genes (signal-to-noise < 0.1) were merged for further analysis.

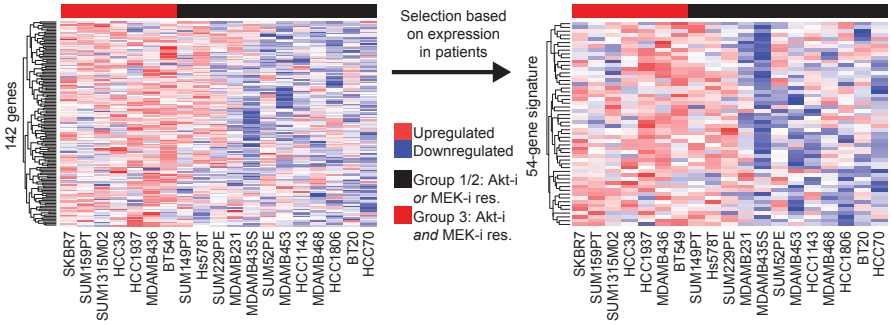

Additional file 9: Figure S5. Expression of 142 cell cycle genes and 52-gene signature derived from gene expression in patients in TNBC cell lines.

	Group 1 (Akt-i-resistant)		Group 2 (MEK-i-resistant)		Group 3 (Akt-i/MEK-i-resistant)		
IC50 (μM)	HCC1806	MDA-MB-435s	BT20	HCC70	SKBR7	MDA-MB-436	SUM159PT
Dinaciclib	0.2973	0.3121	0.2069	0.1371	0.1465	0.1095	0.1543
Flavopiridol	0.4887	0.2758	0.149	0.1246	0.09521	0.1775	0.1768

Additional file 10: Table S5. Differential sensitivity of group 3 cell lines to CDK inhibitors dinaciclib and flavopiridol**.** IC50 values for selected cell lines from Group 1 (Akt-i-resistant), Group 2 (MEK-i-resistant) and Group 3 (Akt-i/MEK-i double-resistant) for pan-CDK inhibitors dinaciclib and flavopiridol. IC50 values were calculated using non-linear regression fitting in GraphPad Prism (version 7.01).

Chapter 3

Blockage of cdc7/CDK9 signalling sensitises triple-negative breast cancer to EGFR-targeted therapy

Ronan P. McLaughlin[1], Jichao He[1], Vera van der Noord[1], Jevin Redel[1], Marcel Smid[2], John W.M. Martens[2], John A. Foekens[2], Yinghui Zhang[1], Bob van de Water[1]

[1]Department of Drug Discovery and Safety, Leiden Academic Centre for Drug Research, Leiden University, 2300 RA Leiden, The Netherlands.

[2]Department of Medical Oncology and Cancer Genomic Netherlands, Erasmus MC Cancer Institute, Erasmus Medical Center, 3000 CA Rotterdam, The Netherlands.

This chapter is based on a manuscript submitted for publication

ABSTRACT

Background

The effective treatment of triple-negative breast cancer (TNBC) remains a profound clinical challenge. Despite frequent EGFR overexpression and reliance on downstream signalling pathways in TNBC, resistance to EGFR-tyrosine kinase inhibitors (TKIs) remains endemic. Therefore, the identification of targeted agents, which synergise with current therapeutic options, is paramount.

Methods

Compound-based, high-throughput, proliferation screening was used to profile the response of TNBC cell lines to EGFR-TKIs; western blotting and siRNA transfection being used to examine the effect of inhibitors on EGFR-mediated signal transduction and cellular dependence on such pathways, respectively. A kinase inhibitor combination screen was used to identify compounds that synergised with EGFR-TKIs in TNBC, utilising sulphorhodamine B (SRB) assay as read-out for proliferation. The impact of drug combinations on cell cycle arrest, apoptosis and signal transduction was assessed using flow cytometry, automated live-cell imaging and western blotting, respectively. RNA-sequencing was employed to unravel transcriptomic changes elicited by this synergistic combination and to permit identification of the signalling networks most sensitive to co-inhibition.

Results

We demonstrate that dual Cdc7/CDK9 inhibitor PHA-767491 synergises with multiple EGFR-TKIs (lapatinib, erlotinib and gefitinib) to overcome resistance to EGFR-targeted therapy in various TNBC cell lines. Combined inhibition of EGFR and Cdc7/

CDK9 resulted in reduced cell proliferation, accompanied by induction of apoptosis, G2-M cell cycle-arrest, inhibition of DNA replication and abrogation of CDK9-mediated transcriptional elongation, in contrast to mono-inhibition. Moreover, high expression of cdc7 and RNA polymerase II Subunit A (POLR2A), the direct target of CDK9, is significantly correlated with poor metastasis-free survival in a cohort of breast cancer patients. RNA-sequencing revealed marked down-regulation of pathways governing proliferation, transcription and cell survival in TNBC cells treated with the combination of an EGFR-TKI and a dual Cdc7/CDK9 inhibitor. A number of genes enriched in these down-regulated pathways are associated with poor metastasis-free survival in TNBC.

Conclusions

Our results highlight that dual inhibition of Cdc7 and CDK9 is a potential strategy for targeting TNBC resistant to EGFR-TKIs.

Key words: CDK9/Cdc7 inhibition, EGFR-targeted therapy, drug resistance, triple-negative breast cancer

BACKGROUND

Triple-negative breast cancer (TNBC) is a notoriously aggressive, heterogeneous disease defined as lacking expression of oestrogen receptor (ER) and/or progesterone receptor (PR) as well as amplification of human epidermal growth factor receptor 2 (HER2), respectively[1]. Although TNBC only constitutes approximately 15-20% of breast cancer cases, it is disproportionately responsible for breast cancer-associated deaths and carries a dismal prognosis, compared with hormone receptor-positive (HR+) breast cancers[2–4]. For patients with HR+ breast cancer, endocrine therapy targeting ER is available in the form of aromatase inhibitors and selective oestrogen receptor modulators (e.g. tamoxifen) and other antagonists[1]. Contrastingly, no effective targeted therapy which exploits the molecular properties of tumour cells exists for TNBC patients; clinical trials of targeted agents in TNBC have been disappointing[5,6]. Consequently, aggressive chemotherapy, radiotherapy and surgery remain the mainstay treatments[7]. Furthermore, patients who develop resistance to treatment, or who do not respond to treatment whatsoever, follow an aggressive clinical course characterised by metastasis and a higher 5-year mortality post-diagnosis[8]. Further complicating the treatment of TNBC is the degree of genetic heterogeneity observed in this disease. By analysing the gene expression profiles of TNBC cases, *Lehmann et al* sub-classified TNBC into six different molecular subtypes: mesenchymal (M), mesenchymal stem-like (MSL), luminal androgen receptor-positive (LAR), immunomodulatory (IM), basal-like 1 (BL1) and basal-like 2 (BL2)[9]. Most importantly, these subtypes exhibit dissimilar drug-sensitivity profiles, resulting in varied clinical responses[9,10]. The nature of TNBC clearly necessitates a more tailored approach to treatment, one which exploits the unique oncogenic addictions present. For

chemotherapy-resistant TNBC patients, the development of targeted therapeutics which synergise with current treatment options to overcome resistance is therefore paramount.

Epidermal growth factor receptor (EGFR; also known as ERBB1/HER1) is often expressed at higher levels in triple-negative tumours than in HR+ tumours[11], though expression levels vary, with up to ~80% of TNBC cases reported as being EGFR+[12]. EGFR amplification has also been reported to occur in a substantial proportion of TNBC cases[13–15] with EGFR overexpression associated with a much poorer prognosis in general[8]. Furthermore, EGF signalling is highly enriched in the basal and mesenchymal TNBC subtypes[9]. EGFR therefore represents a *bona fide* drug target in triple-negative tumours. Various EGFR inhibitors have been developed, most notably anti-EGFR monoclonal antibodies (e.g. cetuximab) and EGFR-tyrosine kinase inhibitors (EGFR-TKIs) (e.g. erlotinib, gefitinib and lapatinib)[16]. Despite these efforts, EGFR-TKI single treatment has performed poorly in clinical trials for TNBC patients with advanced or metastatic breast cancer, despite clear inhibition of EGFR[17,18] suggesting bypass inhibition of EGFR-related signalling in TNBC tumors[19,20]. Nonetheless, EGFR-TKIs have shown more promising results as combination therapies in TNBC[21], perhaps indicating that monotherapeutic inhibition of EGFR is insufficient to shut down the myriad signalling pathways responsible for promoting aberrant proliferation and survival.

Here we demonstrate that multiple EGFR-TKIs synergise with the dual cdc7/CDK9 inhibitor PHA-767491 in a panel of TNBC cell lines resistant to EGFR-TKIs. This combination inhibited cell proliferation, induced apoptosis and G2-M arrest and down-regulated components critical to cell cycle progression, DNA-replication and transcription, thereby reversing resistance to EGFR-TKIs. Therefore, targeting

deficiencies in regulation of the cell cycle and DNA-replication in conjunction with transcriptional addiction downstream of growth factor pathways may constitute a powerful therapeutic opportunity for this difficult-to-treat breast cancer subtype.

MATERIALS & METHODS

Cell culture

All cell lines were maintained in RPMI-1640 medium (Gibco, ThermoFisher Scientific, Breda, The Netherlands) supplemented with 10% FBS (Thermo Fisher Scientific; 10270106) and 25 IU/ml Penicillin and 25 µg/ml Streptomycin (ThermoFisher Scientific; 15070-063). Cells were cultured in a humidified incubator at 37^{o}C, 5% CO_2.

Antibodies and kinase inhibitors

The primary antibodies against pEGFR (Y1173, #4407), pERK1/2 (T202/Y204, #9101), ERK1/2 (#4695), pAKT (S473, #9271), AKT (#9272), MCM2 (#3619), pRNA-II (S2/5; #4735), RNA-II (#2629), p-pRb (S780, # 9307) were commercially supplied from Cell Signaling TECHNOLOGY®, EGFR (sc-03), pRb (sc-102), CDK4 (sc-601), Cyclin D1 (sc-20044) from Santa Cruz BIOTECHNOLOGY®, Cdc7 (ab10535) and pMCM2 (S40/41; ab70371) from Abcam®, and Tubulin (T-9026) from Sigma®. Secondary antibodies included Cy5-conjugated anti-mouse and horseradish peroxidase (HRP) anti-mouse or anti-rabbit (Jackson ImmunoResearch). Individual kinase inhibitors lapatinib (S2111), gefitinib (S1025), erlotinib (S7786) and PHA-767491 (S2742), plus the 273 kinase inhibitor library (L1200) were purchased from Selleckchem® and dissolved in DMSO solution at 10mM.

Kinase inhibitor treatment and drug combination screen

Cells were seeded into 96-well plates at the appropriate densities. The following day, cells were treated with individual kinase inhibitors in dose range as indicated. Vehicle DMSO (1:1000) was used as control. For the kinase inhibitor library screen, cells were screened in duplicate against the kinase inhibitor library containing 273 kinase inhibitors at concentration of 1 μM alone, or the 1μM library inhibitors in combination with lapatinib at 3.16 μM, since this concentration effectively inhibited EGFR phosphorylation in all cell lines tested and since studies have shown that levels of lapatinib in patient tumours vary between 1-12 μM depending on dosing schedule[22]. After 4-day treatment, proliferation was evaluated by sulphorhodamine B (SRB) colorimetric assay[23], and analysed by % of control cell growth = (mean sample OD – mean 0-day OD) / (mean control OD – mean 0-day OD) × 100. To assess synergistic interaction of combined drugs, combination index (CI) analysis[24,25] was performed, using the formula 'CI = (D)1/(Dx)1 + (D)2/(Dx)2'. (D)1 and (D)2 are respective combination doses of two compounds that yield an effect of 50% of proliferation inhibition, with (Dx)1 and (Dx)2 being the corresponding single doses for either compound that results in the same effect, which is by definition the IC50 of each compound. CI values less than 1 (CI < 1), equal to 1 (CI = 1) or greater than 1 (CI > 1), indicate synergy, additivity or antagonism, respectively.

Western blotting

Cells were seeded in 6-well plates at the appropriate density. For stimulation/ starvation assays, medium was refreshed with serum-free medium (SFM) the following day and cells were starved overnight. Thereafter, cells were pre-treated with drug solutions for 4 hours, then stimulated with 100 ng/ml EGF (Sigma; E9644) for 5

minutes in SFM. For time-course exposures to drugs, cells were treated with drug solutions prepared in complete medium. Cell lysates were harvested at the indicated time points in RIPA lysis buffer with 1:100 Protease Inhibitor Cocktail (Sigma; P8340). Cellular proteins were denatured in sample buffer containing 10% β-mercaptoethanol, loaded with 30 µg/lane into 7.5% polyacrylamide gels, resolved using SDS-PAGE and subsequently transferred to PVDF membranes (Merck Chemicals; IPVH00010) overnight. PVDF membranes were then blocked with 5% BSA-TBST (Tris-buffered saline 0.05 % Tween-20) and subsequently incubated at 4^{o}C overnight with appropriate primary antibodies. The following day, membranes were incubated for 1 hour with HRP- or Cy5-conjugated secondary antibodies and chemiluminescence or fluorescence was detected using the Las4000 (GE Healthcare).

Annexin-V staining

Cells were seeded overnight in 96-well µCLEAR plates (Corning) at appropriate densities, then treated with drug solutions at indicated concentrations. At 24, 48 or 72 hours post-treatment, cells were stained with Hoechst 33258 (1:10,000) and Annexin-V (1:1000) for 45 minutes at 37^{o}C, 5% CO_2 before being imaged using BD Pathway 855 Microscope (BD Biosciences). Annexin-V staining was quantified using Cell Profiler software.

Cell cycle flow cytometry analysis

Cells were seeded in 6-well plates at the appropriate density. 24 or 48 hours post-treatment all cells were harvested, re-suspended in ice-cold 200 µl 1 mM EDTA-PBS and 800 µl 100% Ethanol, and stored at -20^{o}C before being centrifuged at 1000 rpm

at 4°C. Cells were then re-suspended in 1 ml PBS and rehydrated for 15 minutes. After being spun at 1000rpm for 5 minutes at room temperature, the pellet was re-suspended in 250µl 3mM DAPI (Sigma, 10236276001) staining buffer (100 µM Tris pH7.4, 150 mM NaCl, 1 mM $CaCl_2$, 0.5 mM $MgCl_2$), incubated for 15 minutes at room temperature in the dark, followed by filtration through 70µm EASYstrainer filters and analysed using FACS Conto II (*BD Biosciences).* Data were analysed using FlowJo V10.

siRNA transfection

Cells were seeded in 96-well plates at the appropriate density. For each siRNA transfection, 50 nM siGENOME siRNAs (Dharmacon) were transfected into cells per 96-well using INTERFERin transfection reagent (Polyplus; 409-50). The following day medium was refreshed. 48 hours post-transfection, cells were either lysed for western blot to confirm knockdown or treated with drugs for the appropriate duration as described, then fixed for SRB proliferation assay.

Clinical evaluation of candidate target genes

The clinical relevance of CDC7, POLR2A and CDK9 was evaluated using in-house gene expression and metastasis-free survival data of 123 lymph node-negative, non-neoadjuvantly treated, oestrogen receptor-negative (ER-neg) primary breast cancer patients. The clinical relevance of synergy-related candidate genes was evaluated using in-house as well as publicly available gene expression and MFS data of lymph node-negative, non-neoadjuvantly treated primary breast cancer patients, leading to a cohort of 142 triple-negative patients. Data were gathered from Gene Expression Omnibus (http://www.ncbi.nlm.nih,gov/geo/) entries GSE2034, GSE5327, GSE2990,

GE7390 and GSE11121, with all data available on Affymetrix U133A chip. Raw.cel files were processed using fRMA parameters (median polish)[26] after which batch effects were corrected using ComBat[27].

Transcriptome RNA-Sequencing and pathway integration analysis

Cells were seeded overnight in 6-well plates and treated in triplicate for 6 hours with individual or combined kinase inhibitors at indicated concentrations, or vehicle. RNA was isolated with RNeasy Plus Mini Kit as described by manufacturer (QIAGEN, Cat. 74136). Transcriptome RNA-Sequencing (RNA-Seq) was performed using Illumina high-throughput RNA sequencing. DNA libraries were prepared from the samples with the TruSeq Stranded mRNA Library Prep Kit. The DNA libraries were sequenced according to the Illumina TruSeq v3 protocol on an Illumina HiSeq2500 sequencer. Paired-end reads were generated of 100 base-pairs in length were generated. Alignment was performed against the human GRCh38 reference genome using the STAR aligner (version 2.4.2a). Marking duplicates, sorting and indexing were performed using Sambamba (version 0.6.6). Gene expression was quantified using the FeatureCounts software (version 1.4.6) based on the ENSEMBL gene annotation for GRCH38 (release 84). RNA-Seq data were normalised by TMM using EdgeR's normalisation-factor[28], followed by quantile normalisation and presented in Log2 fold change (Log2 FC) scales. Genes with significant down- or up-regulation (Log2 FC ≥ | 0.5|) under indicated conditions were analysed by web-based functional analysis tool Ingenuity Pathway Analysis (IPA, QIAGEN®) to visualise and annotate their biological functions and pathways.

Statistical Analyses

All statistical analyses, where appropriate, were performed in GraphPad Prism software version 7.0. One-way ANOVA multiple comparison test with Tukey's post-hoc test was applied with p-values less than 0.05 considered as statistically significant.

RESULTS

TNBC cells are resistant to EGFR-TKIs

EGFR is expressed at higher levels in TNBC tumours compared to ER-positive BC tumours (Figure 1a); also in human basal A and basal B TNBC cell lines there is higher EGFR expression than in human luminal cell lines (Figure 1b). Therefore, we sought to systematically elucidate the response of TNBC to a broad range of different EGFR kinase inhibitors. A panel of TNBC cell lines with varying EGFR expression (Figure 1c) was screened against 24 EGFR-TKIs (Figure 1d). 12 cell lines (> 57%) could be classified as refractory to almost all 24 EGFR-TKIs; only HCC1806 was highly sensitive to most EGFR-TKIs, the remainder having variable sensitivity to EGFR-TKIs (Figure 1d). Next, three TNBC cell lines highly resistant to EGFR-TKIs, Hs578T, BT549 and SKBR7, and one sensitive cell line, HCC1806, were selected for further evaluation. The proliferation of Hs578T, BT549 and SKBR7 cells was unaffected by dual EGFR-HER2 inhibitor lapatinib, up to the concentration of 10 μM (Figure 1e). Concordantly, lapatinib failed to significantly induce apoptosis in these cell lines at 3.16 μM (Figure S1a). In contrast, HCC1806 cells displayed enhanced growth inhibition in response to lapatinib (IC50 ~100 nM; Figure 1e) with significantly increased Annexin-V apoptotic signal (Figure S1a). Regardless of their response to lapatinib, all these cell lines maintained functional EGFR-mediated signal

transduction, with prominent phosphorylation of EGFR (Y1173) and downstream components AKT (S473) and ERK1/2 (T202/Y204) in response to EGF stimulation (Figure 1f), indicating that resistance was not due to absence of a functionally intact EGFR pathway. In response to lapatinib, EGFR phosphorylation was completely inhibited in all cell lines (Figure 1f). However, EGF-induced ERK activation persisted in all lapatinib-resistant cell lines, with AKT phosphorylation also unaffected in Hs578T and BT549 cells. These data suggest that these resistant cells are capable of bypassing EGFR-kinase inhibition through the activation of downstream pro-proliferative pathways. Despite the lack of impact of EGFR-TKIs on TNBC proliferation, siRNA-mediated silencing of EGFR and downstream components, including ERK2 and FRAP1 (mTOR), led to a significant reduction in cell proliferation, supporting the notion TNBC cells depend to a certain extent on EGFR-mediated signalling for their proliferation (Figure S1b).

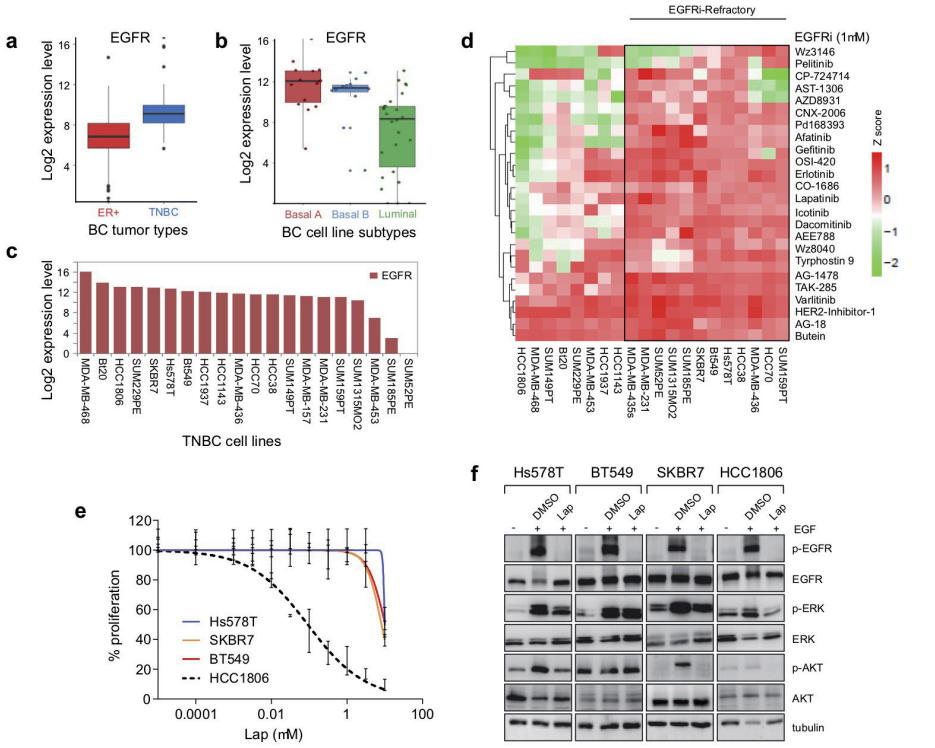

Figure 1. Resistance of TNBC cells to EGFR-TKIs. a. RNA-Seq-based log_2 EGFR expression levels in oestrogen receptor-positive (ER+) breast cancer (991 cases) and TNBC tumours (116 cases) derived from 1107 cases in The Cancer Genome Atlas (TCGA) database. Graphs show data distribution, the mean, and the lower and upper quartiles. Error bars represent standard deviation. **b.** RNA-Seq based log_2 EGFR expression in basal-like and luminal-like BC cell line subtypes (total 50 BC cell lines, in-house). Graphs show data distribution, the mean, and the lower and upper quartiles. Error bars represent standard deviation **c.** EGFR expression in 20 TNBC cell lines. **d.** Resistance of TNBC cells to EGFR inhibitors (EGFRi). Cells were treated with 1μM inhibitor for 4 days. Proliferation was assessed using sulphorhodamine B (SRB) assay. Z-score was represented by normalising raw values to those of DMSO control. **e.** Dose response of EGFRi-resistant TNBC cell lines (Hs578T, BT549 & SKBR7) and an EGFRi-sensitive cell line (HCC1806) to lapatinib. Percentage of proliferation was normalised to DMSO control. Data shown as mean +/- standard deviation for two independent experiments performed in triplicate. **f.** EGFR pathway functionality in TNBC cell lines Hs578T, BT549 & SKBR7 and HCC1806. Cells were starved for 24h in serum-free medium, treated with drug solutions prepared in serum-free medium for 4 hours, then stimulated with 100ng/ml EGF for 5 minutes.

Kinase inhibitor combination screening identifies a dual Cdc7/CDK9 inhibitor PHA-767491 which synergises with lapatinib in TNBC.

Next, we sought to identify compounds which synergise with lapatinib by performing a combinatorial kinase inhibitor screen in Hs578T cells treated with 273 kinase inhibitors at 1 μM with or without 3.16 μM lapatinib. Most notably, amongst a number of compounds which augmented the response of TNBC cells to EGFR inhibition, the dual Cdc7/CDK9 inhibitor PHA-767491 inhibited proliferation by >90% compared to control or either monotherapy (Figure 2a). Subsequent dose response experiments revealed that combinations of 1-3.16 μM PHA-767491 with 0.0316-3.16 μM lapatinib greatly enhanced inhibition of Hs578T growth compared to either monotherapy (Figure 2b), indicative of synergy. To confirm this interaction was not cell line-specific, 17 TNBC cell lines were screened with a dose range of lapatinib or PHA-767491 (0.0316-3.16 μM) or with a dose-range of lapatinib in combination with either 1 μM or 3.16μM PHA-767491. These TNBC cell lines were generally resistant to both monotherapies at doses equal to or less than 1 μM, but lapatinib and PHA-767491 co-treatment strongly inhibited proliferation (Figure 2c). Combining lapatinib (3.16 μM) with PHA-767491 at either 1 μM or 3.16 μM led to strong synergistic responses in the vast majority of TNBC cell lines (with some additive responses also evident), yielding CI values well below 1 (Figure 2d), thus confirming the synergistic nature of this interaction.

Dual pharmacological inhibition of EGFR and Cdc7/CDK9 suppresses components of the transcriptional machinery and DNA-replicative program

Having confirmed the synergistic effect of PHA-767491 and lapatinib on TNBC proliferation, we elucidated the impact of co-treatment on EGFR, cdc7 and CDK9-mediated signalling transduction. 48 hours post-exposure, lapatinib in combination with PHA-767491 at synergistic concentrations led to depletion of Cdc7, accompanied by decreased phosphorylation of its downstream target MCM2 (Ser40/41), a critical component of DNA helicase, suggesting an inhibitory effect on initiation of DNA-replication in Hs578T, BT549 and SKBR7 cells (Figure 2e). The combination therapy also decreased CDK9-mediated phosphorylation of Ser2/5 residues in the C-terminal domain of RNA Polymerase II (RNAII), implying impairment of CDK9 and/or CDK7-mediated productive transcriptional elongation (Figure 2e). These data indicate that co-treatment of TNBC cells with lapatinib and a dual Cdc7/CDK9 inhibitor blocks components essential for initiation of DNA replication and RNA polymerase II-mediated transcription.

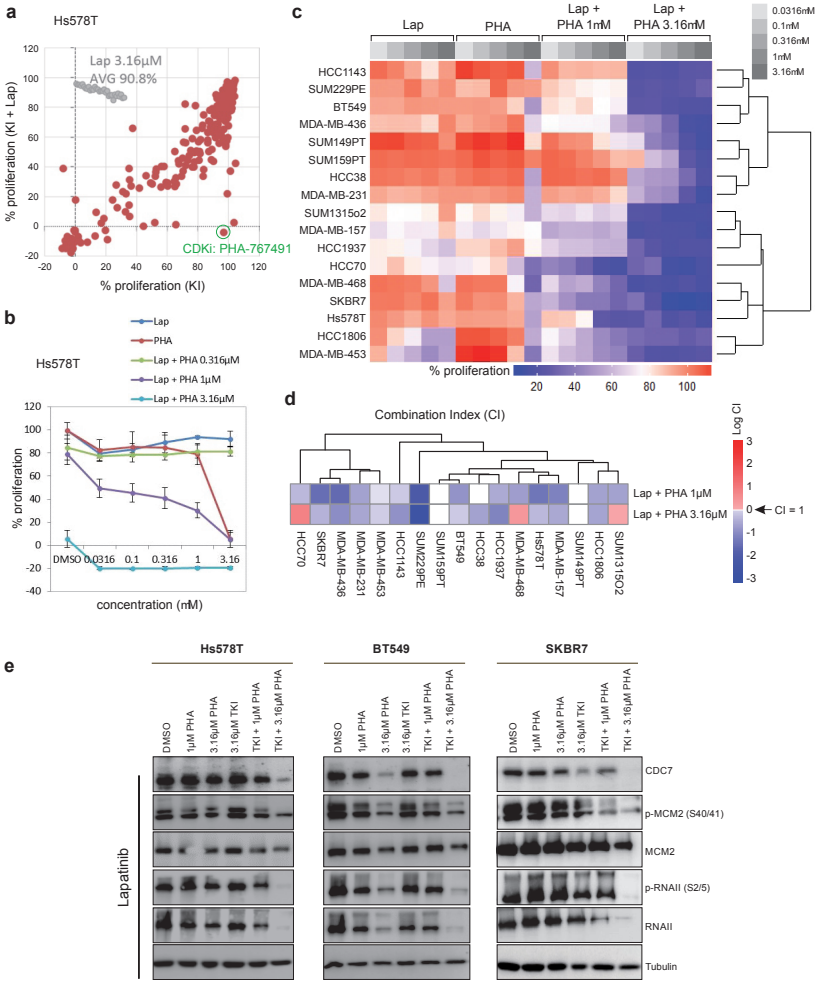

Figure 2: Kinase inhibitor combination screening identifies compounds which synergise with EGFR-TKIs in TNBC. a. EGFRi lapatinib (Lap) and kinase inhibitor (KI) combination screen in EGFRi-resistant Hs578T cells. Cells (8,000/well) were treated with 1 μM of 273 individual KIs alone, or in combination with lapatinib at 3.16 μM, for 4 days. The dual Cdc7/CDK9 inhibitor PHA-767491, one of the KIs which most strongly synergised with lapatinib is singled out, as indicated. **b.** Dose response curves for Hs578T cells. Cells were treated with a dose range of PHA-767491 or lapatinib (0.0316-3.16μM) or lapatinib combined with 0.316, 1 or 3.16 μM PHA-767491. Data shown as mean +/- standard deviation for two independent experiments. **c.** Validation screen of lapatinib/ PHA-767491 synergistic effect in a panel of 17 TNBC cell lines, under indicated combinations. Cells were treated with dose ranges of lapatinib or PHA-767491 (0.0316-3.16 μM) or the indicated combinations. **d.** Combination Indices (CI) for Lapatinib (3.16 μM) combined with either 1 μM or 3.16 μM PHA-767491. Log CI is shown. **e.** Initiation of DNA replication and productive transcriptional elongation in Hs578T, BT549 and SKBR7 cells treated with lapatinib and/or PHA-767491 as indicated, for 48h. TKI refers to lapatinib at 3.16 μM.

Selective EGFR-TKIs erlotinib and gefitinib also synergise with PHA-767491 in TNBC

To verify whether synergy between lapatinib and PHA-767491 represents a general EGFR-TKI-related phenomenon, TNBC cells were treated with other selective EGFR-TKIs, erlotinib and gefitinib[29], in combination with PHA-767491. At a concentration of 3.16 μM, erlotinib and gefitinib inhibited EGF-mediated activation of EGFR phosphorylation and downstream phosphorylation of ERK1/2 and AKT in Hs578T and SKBR7 cells (Figure 3a), perhaps reflective of their increased potency compared to lapatinib in eliciting EGFR inhibition. However, proliferation of all cell lines tested was refractory to erlotinib and gefitinib monotherapy up to 3.16 μM (Figure 3b). Strikingly, at concentrations of 0.1 μM or above, erlotinib and gefitinib strongly synergised with 1 μM and 3.16 μM PHA-767491, almost completely inhibiting the proliferation of Hs578T and SKBR7 cells (Figure 3b-c). The effect of combining erlotinib or gefitinib with PHA-767491 on DNA-replication and transcription-related signal transduction largely resembled that of lapatinib combined with PHA-767491 (Figure 3d). Only combinations of erlotinib or gefitinib and PHA-767491 were capable of decreasing Cdc7 levels and consequently phosphorylation of MCM2 (Ser40/41). Similarly, inhibition of CDK9-mediated RNA-II (S2/S5) phosphorylation was most prominent after co-treatment. To validate the hypothesis that EGFR inhibition is critical for the synergistic interaction between EGFR-TKIs and PHA-767491, an EGFR-negative triple-negative cell line, SUM185PE (Figure S2a), was treated with this combination. Neither AKT nor ERK1/2 was activated in response to stimulation with EGF, confirming EGF-mediated signalling is redundant in SUM185PE (Figure S2b). As expected, lapatinib and PHA-767491 did not synergise in EGFR-negative SUM185PE cells (Figure S2c).

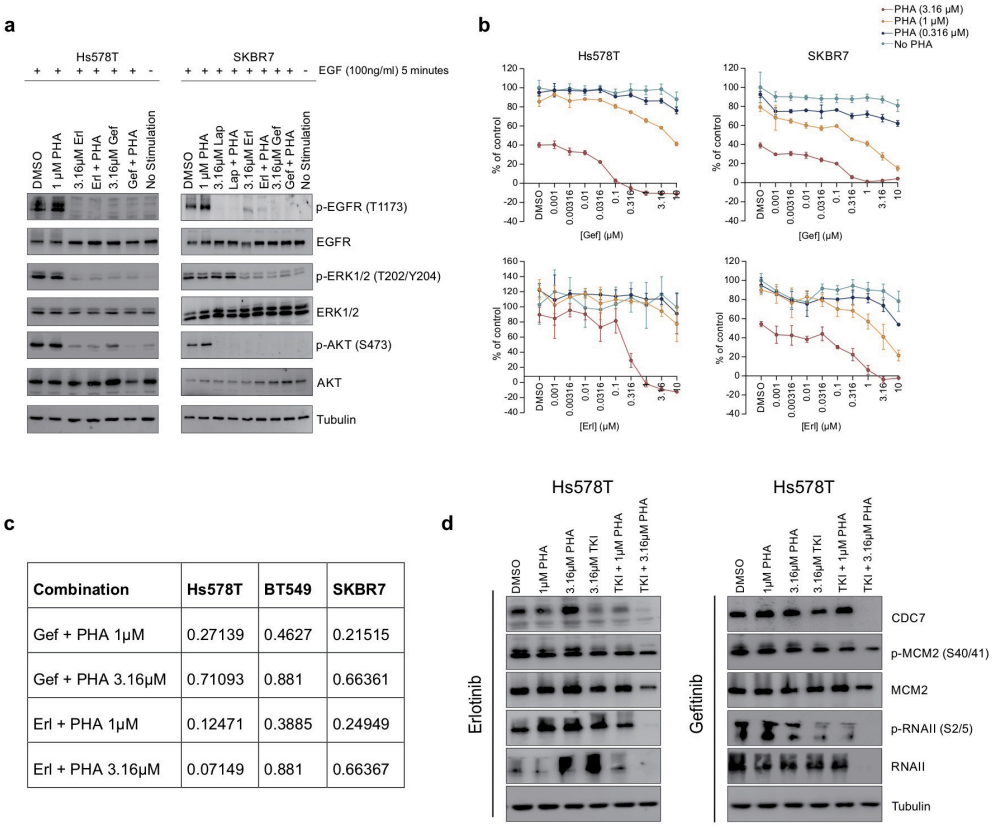

Combination	Hs578T	BT549	SKBR7
Gef + PHA 1µM	0.27139	0.4627	0.21515
Gef + PHA 3.16µM	0.71093	0.881	0.66361
Erl + PHA 1µM	0.12471	0.3885	0.24949
Erl + PHA 3.16µM	0.07149	0.881	0.66367

Figure 3: Selective EGFR-TKIs Erlotinib and Gefitinib also synergise with PHA-767491 in TNBC. a. Inhibitory impact of erlotinib and gefitinib on EGFR-mediated signal transduction in Hs578T and SKBR7 cells. **b.** Dose response of Hs578T and SKBR7 cells to gefitinib or erlotinib (0.0316-3.16 µM) combined with 0.316, 1 or 3.16 µM PHA-767491. Data shown as mean +/- standard deviation. Each graph shows one representative of two independent experiments performed in triplicate. Combination Indices (CI) of gefitinib (3.16 µM) or erlotinib (3.16 µM) with PHA-767491 (1 µM or 3.16 µM) in Hs578T, BT549 and SKBR7 cells. **d.** Initiation of DNA replication and productive transcriptional elongation in Hs578T cells treated with erlotinib or gefitinib and/or PHA-767491 as indicated, for 48h. TKI refers to either erlotinib or gefitinib at 3.16 µM.

Dual treatment of TNBC cells with EGFR-TKIs and PHA-767491 induces G2/M cell cycle arrest and apoptosis

Whilst PHA-767491 at 3.16 μM inhibits cdc7 and phosphorylation of MCM2 and RNA polymerase II, parallel inhibition of EGFR was necessary for eliciting a similar effect on cell cycle components. Decreased levels of CDK4, Cyclin D1 and phosphorylated-pRb were observed 48 hours post-exposure to co-treatment (Figure 4a), suggesting concomitant inhibition of EGFR, Cdc7 and CDK9 obstructs cell cycle progression in TNBC cells. Flow cytometric analysis confirmed that G2-M cell cycle arrest occurred only when lapatinib, erlotinib or gefitinib were combined with 3.16 μM PHA-767491 in Hs578T and SKBR7 cells (Figure 4b; Figure S3a). Accordingly, Annexin-V staining indicated that monotherapies failed to induce appreciable levels of apoptosis in lapatinib-resistant TNBC cells, whilst combination treatments enhanced apoptosis (Figure 4c; Figure S3b).

Expression of CDC7 and RNAII (POLR2A) is linked to poor prognosis in breast cancer

Next, in relation to an in-house cohort of lymph node-negative, non-neoadjuvantly treated 123 oestrogen receptor-negative (ER-neg) breast cancer patients, high expression of CDC7 was significantly associated with a poor metastasis-free survival (MFS) (Figure 5a). Interestingly, high expression of POLR2A (RNA-II), the essential downstream target of CDK9, was also significantly associated with a poor metastasis-free survival in this patient group (Figure 5b), though CDK9 expression level was not.

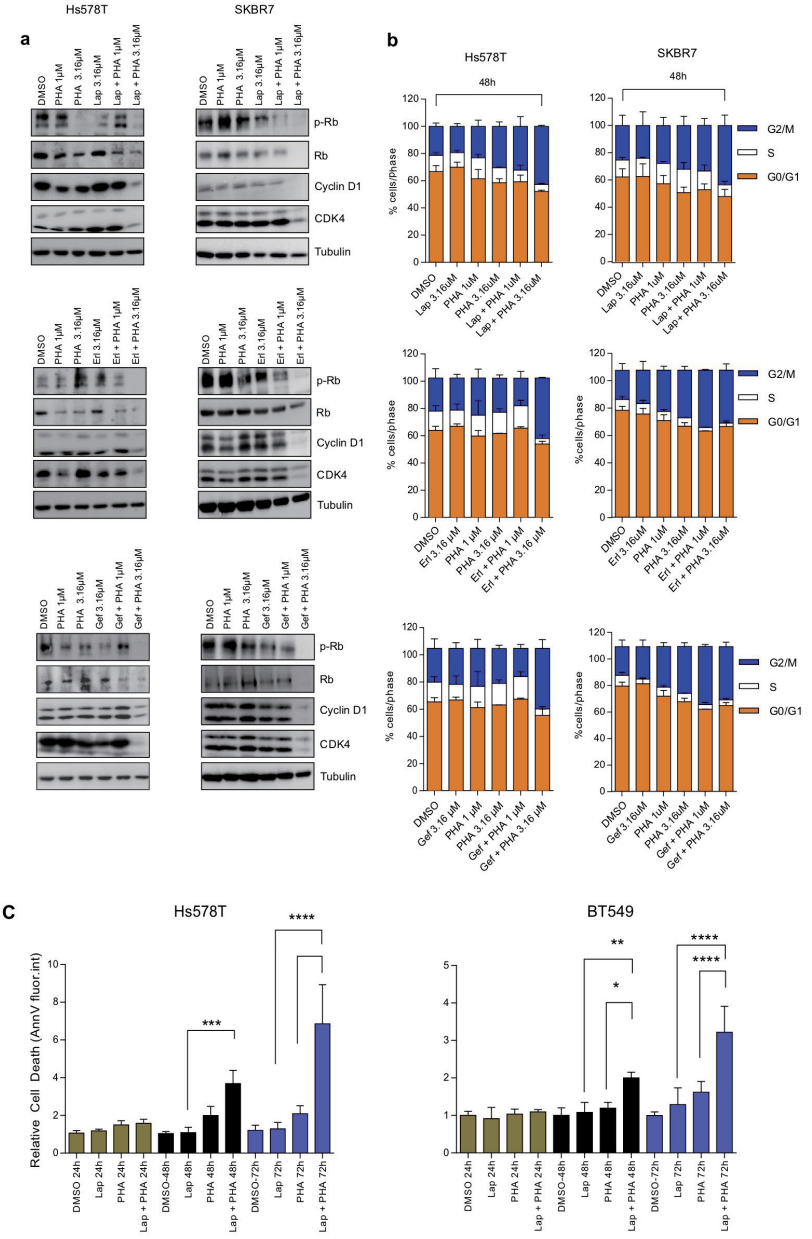

Figure 4: EGFR-TKIs and PHA-767491 synergise to induce G2/M cell cycle arrest and apoptosis. a. Inhibition of cell cycle components by co-treatment with EGFR-TKIs (lapatinib, erlotinib or gefitinib) and PHA-767491. Hs578T and SKBR7 cells were treated with EGFR-TKI alone (3.16 μM) or combined with PHA-767491 (1 μM or 3.16 μM) for 48 hours as indicated. **b.** Cell cycle distribution of Hs578T and SKBR7 cells after 48h treatment with EGFR-TKIs (3.16μM) alone or combined with PHA-767491 (1 μM or 3.16 μM), as indicated. Data shown as mean of two independent experiments +/- standard deviation. **c.** Induction of apoptosis by EGFR-TKI and PHA-767491 co-treatment. Hs578T and BT549 cells were treated with lapatinib (3.16 μM), PHA-767491 (3.16 μM), alone or combined, as indicated, for 24h, 48h or 72h, respectively, and then stained with Annexin-V and Hoechst, followed by imaging and image quantification. Data shown as mean +/- standard deviation of two independent experiments. Relative cell death was quantified by normalising the intensity of Annexin-V signal to that of DMSO control. One-way ANOVA **** $P \leq 0.0001$, *** $P \leq 0.001$, ** $P \leq 0.01$, * $P \leq 0.05$.

Co-treatment of TNBC cells with lapatinib and PHA-767491 inhibits crucial signalling networks and the expression of genes linked to poor survival in TNBC

To investigate how combined EGFR-TKI and PHA-767491 treatment distorts the global transcriptional signature of TNBC cells, we performed RNA sequencing in Hs578T and SKBR7 cells treated with monotherapies or combination therapy (Figure 6a). We identified 2614 genes up-regulated by co-treatment in Hs578T cells, with 243 genes being up-regulated in SKBR7 cells under the same conditions (Figure 6b). 1387 and 2747 genes were down-regulated in co-treated Hs578T and SKBR7 cells, respectively (Figure 6b). Amongst these genes, 141 up- and 704 down-regulated genes (845 transcripts) were commonly responsive to co-treatment in both Hs578T and SKBR7 cells (Figure 6c). Integrated pathway analysis of these 845 synergy-related genes revealed striking disturbance of pro-proliferative pathways mediated by growth factors such as TGF-β, EGF and insulin, as well as pathways governing angiogenesis, stem cell pluripotency and metastatic signalling (Figure 6d). More specifically, an enrichment of genes related to biological networks governing cell survival, viability, migration, RNA transcription, cytokinesis, mitosis, and cell cycle progression, was found amongst the genes commonly down-regulated by co-treatment (Figure 6e). 34 (2 up- and 32 down-regulated) genes out of the 845 lapatinib and PHA-767491 co-targeted genes were significantly correlated with metastasis-free survival (MFS) in 142 lymph node-negative, non-neoadjuvantly treated TNBC patients, including LMBR1L, APAF1, DDX3X and GCNT3, with hazard ratios >2 (Figure 7a and Supplementary Table 1). These 34 clinically relevant genes were present in the main biological networks of apoptosis, transcription and proliferation (Figure 7b), in which MITF, HOXC6 and ROCK2 were all involved. MITF

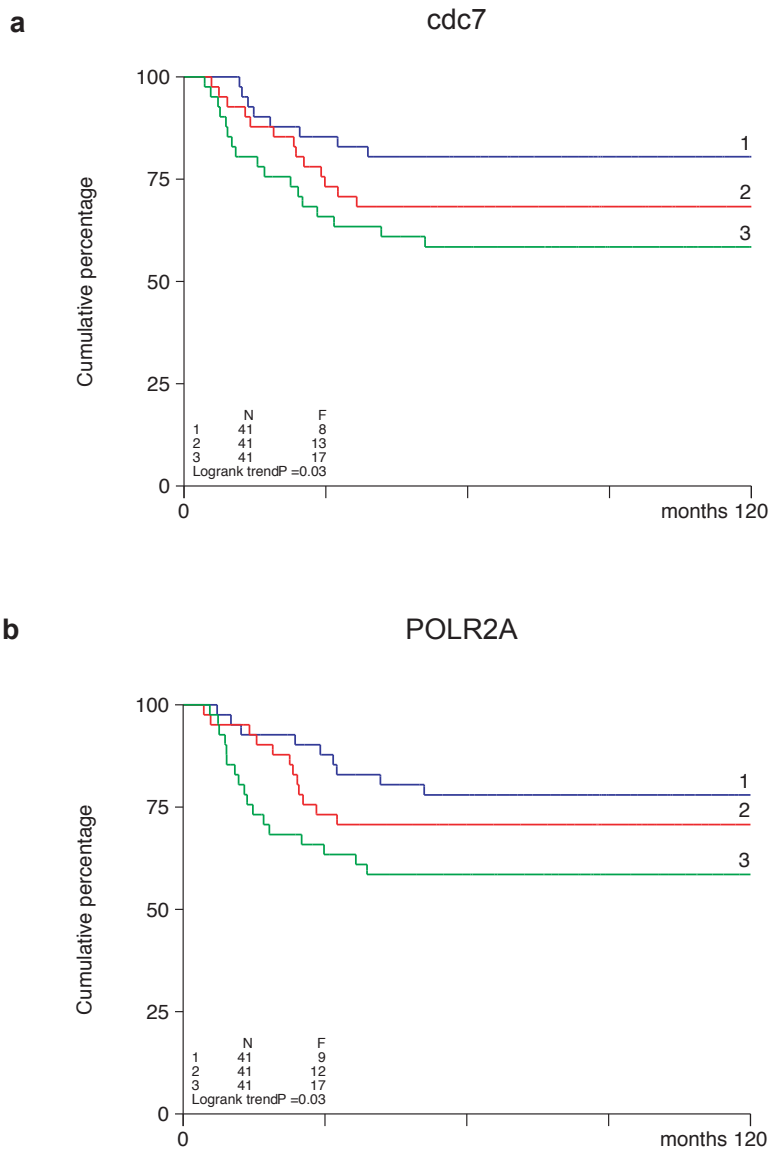

Figure 5. Expression of cdc7 and RNAII (POLR2A) is linked to poor prognosis in breast cancer patients. Metastasis-free survival curves illustrating the relationship between expression of cdc7 or RNAII (POLR2A) and prognosis in ER-negative breast cancer patients. Curves derived from gene expression and available survival data for 123 lymph node-negative, non-neoadjuvantly treated, ER-negative breast cancer patients at Erasmus MC Rotterdam.

was defined as a regulator known to influence the levels of anti-apoptotic protein BCL-2 as well as transcriptional regulators (ZNF114), G2/M regulators (CDC25B), mitotic regulators (DSN1) and DNA replication/repair proteins (TDG and PIF-1) these being down-regulated in response to MITF inhibition (Figure 7c).

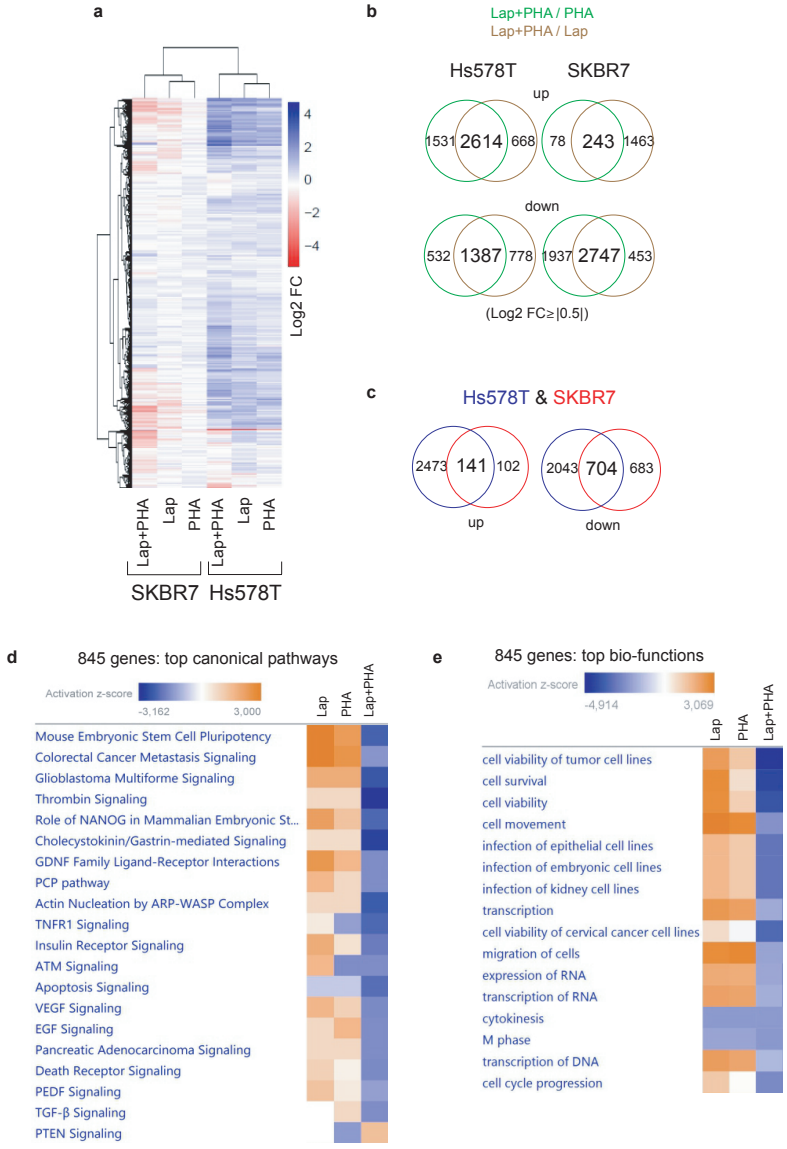

Figure 6: Co-treatment of TNBC cells with lapatinib and PHA-767491 inhibits crucial signalling networks in TNBC. **a.** Global transcriptomic signature in SKBR7 and Hs578T cells after 6h of treatment with lapatinib (3.16 µM), PHA-767491 (1 µM) or a combination of these two doses. Log_2 Fold Change (FC) normalised to DMSO control shown. **b.** Venn diagrams showing the number of genes significantly (Log_2 FC ≥0.5) up- or down-regulated after monotherapy and combination therapy in Hs578T and SKBR7 cells. **c.** Venn diagrams showing the number of genes commonly and significantly (Log_2 FC ≥0.5) up-or down-regulated after combination therapy in both Hs578T and SKBR7 cells. **d.** Top canonical pathways enriched in 845 significantly differentially expressed genes in combination therapy as predicted by IPA online analysis. Z-score indicates activation (orange) or inhibition (blue) of the pathway under indicated conditions, respectively. **e.** Top bio-functions enriched in 845 significantly differentially expressed genes in combination therapy conditions as predicted by IPA software.

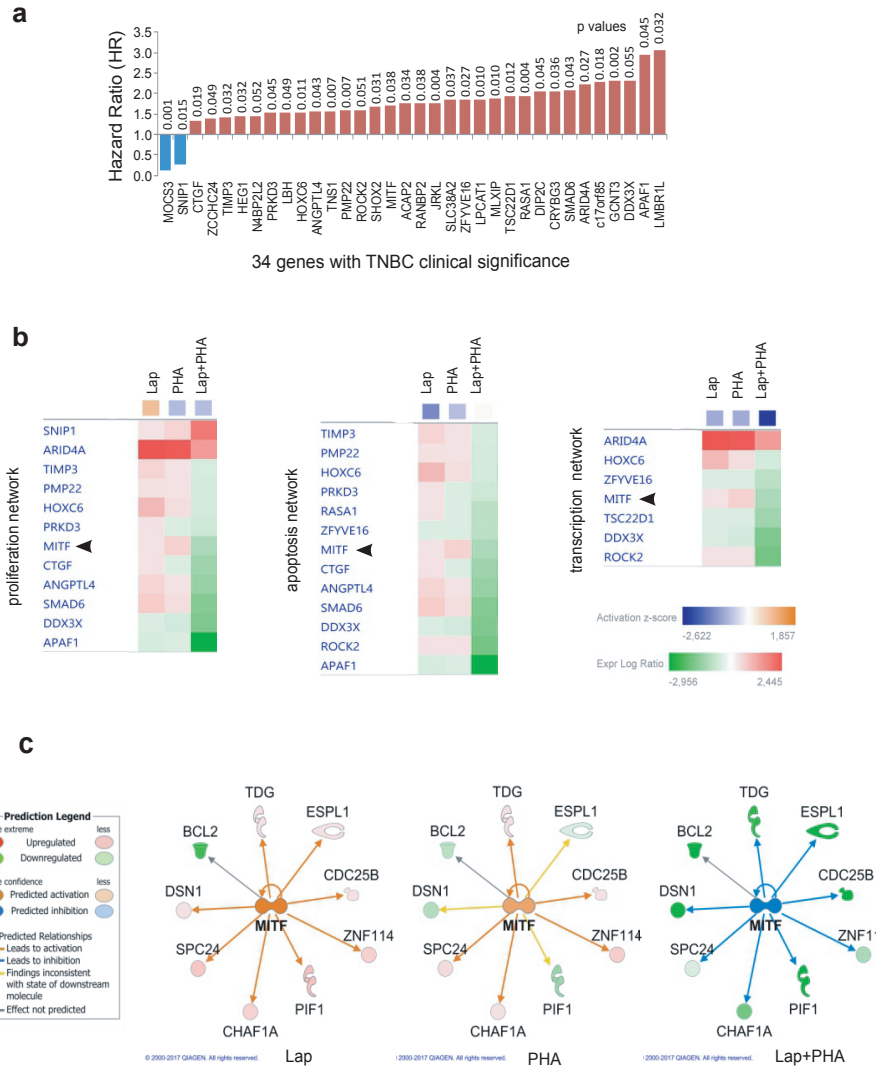

Figure 7: RNA-Seq reveals genes linked to poor survival in TNBC which are involved in regulation of transcription, apoptosis, and proliferation. **a.** 34 genes specifically down-regulated by combination therapy whose expression is significantly correlated with metastasis-free survival in 142 lymph node-negative, non-neoadjuvantly treated, TNBC patients (data derived from in-house cohort as well as from publicly available datasets). HR: Hazard Ratio. **b.** Presence of aforementioned clinically relevant, down-regulated genes in the top biological networks inhibited by combination therapy. **c.** MITF, an upstream regulator of genes which are down-regulated in response to inhibition of MITF under combination therapy.

DISCUSSION

EGFR is highly expressed in both TNBC tumours and cell lines, supporting a role for EGFR as an oncogenic driver in TNBC. However, clinical trials suggest single inhibition of EGFR signalling is incapable of eliminating TNBC cells[17,18,21,30]. Consistently, our results demonstrated that targeting EGFR kinase activity by EGFR-TKIs, including lapatinib, erlotinib and gefitinib, insufficiently inhibits TNBC cell proliferation, despite inhibition of EGFR phosphorylation. Our kinase inhibitor combination screen demonstrated that targeting Cdc7/CDK9 signalling pathways in tandem enables EGFR-TKIs to inhibit proliferation, induce G2-M cell cycle arrest and promote apoptosis in various TNBC cell lines expressing high levels of EGFR. This synergistic drug interaction down-regulates the activity of components of the transcription apparatus and the DNA replication programme, including Cdc7, CDK9, pMCM2 (S40/41), p-RNAII (S2/5), CDK4, cyclin D1 and Rb, making the combination of EGFR and Cdc7/CDK9 molecular-targeted therapies promising for this subgroup of breast cancer.

CDK9 is a member of positive elongation factor P-TEFb, and together with CDK7 is vital for gene transcription since CDK7 and CDK9 sequentially phosphorylate the C-terminal domain (CTD) of RNA Polymerase II (RNA II) at Ser5/Ser7 and Ser2, respectively, allowing dissociation of negative elongation factors and subsequent elongation of mRNA transcripts[31–33]. CDK9 is essential for growth of both HR+ and TNBC cell lines, whilst EGFR is one of many “Achilles’cluster” genes sensitive to CDK7 inhibition and vital for TNBC survival[34]. Consistently, we showed that despite being resistant to inhibition of EGFR kinase activity by various EGFR-TKIs, complete silencing of EGFR is detrimental to TNBC cell growth.. In addition, EGFR is capable of acting as a transcription factor[35,36]. The nuclear translocation of EGFR is

associated with resistance to chemotherapeutics in TNBC[35,37–39] and shields the RTK from the effects of TKIs limited to the cell membrane, permitting EGFR to enhance transcription of genes which govern cell cycle progression, such as Cyclin D1 and Aurora Kinase[36,40]. Cdc7 kinase is itself indispensable for correct regulation of cell cycle progression, exerting control over both initiation of DNA replication and the DNA damage response[41,42]. By phosphorylating mini-chromosome maintenance proteins (MCM2-7) present in pre-replicative complexes formed during G1 phase, Cdc7 activates the helicase activity of these proteins, leading to unwinding of DNA strands and thereby initiating DNA replication at the G1-S phase checkpoint[43,44]. It also has been reported that EGFR indirectly influences the initiation of DNA replication by eliciting phosphorylation of MCM7 in a Lyn kinase-dependent fashion, thereby delineating possible functional overlap between Cdc7 and EGFR[45]. TNBC cells often possess p53-inactivating mutations which abolish the DNA replication origin activation checkpoint, rendering them susceptible to the induction of replicative-stress[46]. Induction of G2-M arrest in our TNBC cell lines after combined inhibition of EGFR and Cdc7/CDK9 is consistent with data from other studies which demonstrated that a p53-dependent checkpoint is critical for mitigating aberrant cell cycle progression after cdc7 depletion[47,48].

The CDK4/Cyclin D1 complex phosphorylates Rb at Ser780/795 thereby inactivating Rb in G1/S checkpoint regulation[49,50]. Consistently, co-inhibition of Cdc7/CDK9 and EGFR signalling in our TNBC cell lines reduces CDK4 and Cyclin D1 levels accompanied by reduced phosphorylation of Rb, thereby resulting in G2-M arrest and ultimately apoptosis. Whether the down-regulation of Cyclin D1 and CDK4 by EGFR-TKIs and PHA-767491 represents a global decrease in the transcription of rapidly expressed, immediate response genes due to inhibition of CDK9-mediated

transcriptional elongation, a decrease in the transcriptional activity of EGFR, or a by-product of the cell cycle arrest induced by Cdc7 depletion, merits further investigation. Taken together, these results identify possible functional links between signalling downstream of EGFR and the function of both Cdc7 and CDK9, which may to some extent explain the observed synergy between EGFR-TKIs and PHA-767491. Additionally, silencing of cell cycle-regulatory or transcriptional CDKs in combination with a Cdc7-specific inhibitor (XL413) in breast cancer cells has been shown to mimic the cell cycle disruption caused by PHA-767491[51]. Silencing of CDK9 led to negligible impact on progression of MCF10A cells through S-phase, whilst CDK9-depleted cells treated with XL413 accumulated in late S-phase, suggesting that the profound cell cycle arrest in TNBC cells caused by PHA-767491 or cdc7 depletion may be somewhat dependent on CDK9 or can at least be augmented by inhibiting CDK9.

RNA-seq transcriptomics identified genes specifically down-regulated by co-treatment with EGFR-TKIs and PHA-767491, which were involved in pathways regulating survival, transcription and cell cycle progression. The decreased expression of these genes (a number of them associated with poorer MFS in TNBC) by co-inhibition of EGFR and Cdc7/CDK9 leads to apoptosis and down-regulation of transcription and proliferation. Interestingly, the transcription factor MITF (microphthalamia-associated transcription factor), a major upstream regulator of pathways governing apoptosis, proliferation and transcription, was decreased together with its downstream targets pro-survival BCL-2 and cell cycle-regulatory CDC25B as a result of combining lapatinib and PHA-767491. With regards to TNBC, little is known about MITF's contribution to EGFRi-resistant phenotypes. Further research is therefore required to validate whether targeting of MITF function

constitutes a logical therapeutic avenue in TNBC, or whether MITF inhibition is sufficient to reverse the resistance of TNBC cells to EGFR targeted therapies.

CONCLUSIONS

In summary, we show that multiple EGFR-TKIs synergise with the dual Cdc7/CDK9 inhibitor PHA-767491 in various EGFR-TKI-resistant TNBC cell lines resulting in decreased proliferation, induction of apoptosis and G2/M cell cycle arrest. Combination therapy leads to inhibition of proteins crucial for accurate DNA-replication and CDK9/RNAII-mediated gene transcription. This combination also leads to inhibition of crucial pro-oncogenic networks and reduces the expression of genes linked to ERK/mTOR signalling and poor progression-free survival in TNBC patients, perhaps identifying possible candidate genes for further research into the mechanism of this synergy and as therapeutic targets.

LIST OF ABBREVIATIONS

AKT: v-akt murine thymoma viral oncogene homologue

BL1: Basal-like 1 subtype

BL2: Basal-like 2 subtype

Cdc7: cell division cycle 7-related protein kinase

CDK4: Cyclin-dependent kinase 4

CDK7: Cyclin-dependent kinase 7

CDK9: Cyclin-dependent kinase 9

CI: Combination index

CTD: C-terminal domain

EGFR: Epidermal growth factor receptor

EGFR-TKI: Epdiermal growth factor receptor tyrosine kinase inhibitor

ERK1/2: Extracellular signal-regulated kinase 1/2

HER2: human epidermal growth factor receptor 2

HR+/-: Hormone receptor-positive/negative

IM: Immunomodulatory subtype

LAR: Luminal androgen receptor-positive subtype

M: Mesenchymal subtype

MCM2: Mini-chromosome maintenance protein 2

MEK: Mitogen-activated protein kinase kinase

MITF: Microphthalamia-associated transcription factor

MSL: Mesenchymal stem-like subtype

POLR2A: RNA Polymerase II subunit 2A

P-TEFb: Positive transcription elongation factor b

Rb: Retinoblastoma protein

RNA II: RNA Polymerase II

S2/5: Serine 2/5 of RNA polymerase II subunit 2A's C-terminal domain

SRB: Sulphorhodamine B

TNBC: triple-negative breast cancer

FUNDING

This work was supported by the ERC Advanced grant Triple-BC (grant no. 322737) and the Dutch Cancer Society project (grant nr 2011-5124).

REFERENCES

1. Foulkes, W.D. *et al,* Triple-Negative Breast Cancer. *N Engl J Med*, **363**:1938-48 (2010).
2. Cheang, M. C. U. *et al.* Basal-like breast cancer defined by five biomarkers has superior prognostic value than triple-negative phenotype. *Clin. Cancer Res.* **14,** 1368–76 (2008).

3. Perou, C. M. *et al.* Molecular portraits of human breast tumours. *Nature.* **406 (6797):** 747–752 (2000).

4. Boyle, P. Triple-negative breast cancer: epidemiological considerations and recommendations. *Ann. Oncol.* **23 Suppl 6,** vi7-12 (2012).

5. Finn, R. S. *et al.* Estrogen Receptor , Progesterone Receptor , Human Epidermal Growth Factor Receptor 2 (HER2), and Epidermal Growth Factor Receptor Expression and Benefit From Lapatinib in a Randomized Trial of Paclitaxel With Lapatinib or Placebo As First-Line Treatment. *J Clin Oncol.* **27 (24):** 3908-3915 (2009).

6. Schuler, M. *et al.* A phase II trial to assess efficacy and safety of afatinib in extensively pretreated patients with HER2-negative metastatic breast cancer. *Breast Cancer Res. Treat.* **134,** 1149–1159 (2012).

7. Mohamed, A., Krajewski, K., Cakar, B. & Ma, C. X. Targeted therapy for breast cancer. *Am. J. Pathol.* **183,** 1096–112 (2013).

8. Dent, R. *et al.* Pattern of metastatic spread in triple-negative breast cancer. *Breast Cancer Res. Treat.* **115,** 423–8 (2009).

9. Lehmann, B. D. *et al.* Identification of human triple-negative breast cancer subtypes and preclinical models for selection of targeted therapies. *J. Clin. Invest.* **121 (7)**: 2750-67 (2011).

10. Masuda, H. *et al.* Differential response to neoadjuvant chemotherapy among 7 triple-negative breast cancer molecular subtypes. *Clin. Cancer Res.* **19,** 5533–40 (2013).

11. Rakha, E. a *et al.* Prognostic markers in triple-negative breast cancer. *Cancer* **109,** 25–32 (2007).

12. Park, H. S. *et al.* High EGFR gene copy number predicts poor outcome in triple-negative breast cancer. *Mod. Pathol.* **27,** 1212–22 (2014).

13. Secq, V. *et al.* Triple negative breast carcinoma EGFR amplification is not associated with EGFR, Kras or ALK mutations. *Br. J. Cancer* **110,** 1045–52 (2014).

14. Reis-Filho, J. S. *et al.* EGFR amplification and lack of activating mutations in metaplastic breast carcinomas. *J. Pathol.* **209,** 445–53 (2006).

15. Gumuskaya, B. *et al.* EGFR expression and gene copy number in triple-negative breast carcinoma. *Cancer Genet. Cytogenet.* **203,** 222–9 (2010).

16. Ciardiello, F. & Tortora, G. EGFR Antagonists in Cancer Treatment. *N. Engl. J. Med.* **358,** 1160–1174 (2008).

17. Baselga, J. *et al.* Phase II and tumor pharmacodynamic study of gefitinib in patients with advanced breast cancer. *J. Clin. Oncol.* **23,** 5323–33 (2005).

18. Dickler, M. N., Cobleigh, M. a, Miller, K. D., Klein, P. M. & Winer, E. P. Efficacy and safety of erlotinib in patients with locally advanced or metastatic breast cancer. *Breast Cancer Res. Treat.* **115,** 115–21 (2009).

19. Linardou, H. *et al.* Assessment of somatic k-RAS mutations as a mechanism associated with resistance to EGFR-targeted agents: a systematic review and meta-analysis of studies in advanced non-small-cell lung cancer and metastatic colorectal cancer. *Lancet. Oncol.* **9,** 962–72 (2008).

20. Kurtze, I., Sonnemann, J. & Beck, J. F. KRAS-mutated non-small cell lung cancer cells are responsive to either co-treatment with erlotinib or gefitinib and histone deacetylase inhibitors or single treatment with lapatinib. *Oncol. Rep.* **25,** 1021–9 (2011).

21. Baselga, J. *et al.* Randomized phase II study of the anti-epidermal growth factor receptor monoclonal antibody cetuximab with cisplatin versus cisplatin alone in patients with metastatic triple-negative breast cancer. *J. Clin. Oncol.* **31,** 2586–92 (2013).

22. Spector, N. L. *et al.* Lapatinib Plasma and Tumor Concentrations and Effects on HER Receptor Phosphorylation in Tumor. *PLoS One* **10,** 142845 (2015).

23. Vichai, V. & Kirtikara, K. Sulforhodamine B colorimetric assay for cytotoxicity screening. *Nat. Protoc.* **1,** 1112–1116 (2006).

24. Huang, L., Jiang, Y. & Chen, Y. Predicting Drug Combination Index and Simulating the Network-Regulation Dynamics by Mathematical Modeling of Drug-Targeted EGFR-ERK Signaling Pathway. *Sci. Rep.* **7,** (2017).

25. Foucquier, J. & Guedj, M. Analysis of drug combinations: current methodological landscape. *Pharmacology Research and Perspectives* **3,** (2015).

26. McCall, M. N., Bolstad, B. M. & Irizarry, R. A. Frozen robust multiarray analysis (fRMA). *Biostatistics* **11,** 242–253 (2010).

27. Johnson, W. E., Li, C. & Rabinovic, A. Adjusting batch effects in microarray expression data using empirical Bayes methods. *Biostatistics* **8,** 118–127 (2007).

28. Robinson, M. D., McCarthy, D. J. & Smyth, G. K. edgeR: a Bioconductor package for differential expression analysis of digital gene expression data. *Bioinformatics* **26,** 139–40 (2010).

29. Schettino, C., Bareschino, M. A., Ricci, V. & Ciardiello, F. Erlotinib: an EGF receptor tyrosine kinase inhibitor in non-small-cell lung cancer treatment. *Expert Rev. Respir. Med.* **2,** 167–178 (2008).

30. Nakai, K., Hung, M. C. & Yamaguchi, H. A perspective on anti-EGFR therapies targeting triple-negative breast cancer. *American Journal of Cancer Research*

6, 1609–1623 (2016).

31. Viladevall, L. *et al.* TFIIH and P-TEFb Coordinate Transcription with Capping Enzyme Recruitment at Specific Genes in Fission Yeast. *Mol Cell* **33,** 738–751 (2009).

32. Yang, Z. *et al.* Recruitment of P-TEFb for stimulation of transcriptional elongation by the bromodomain protein Brd4. *Mol Cell* **19,** 535–545 (2005).

33. Ahn, S. H., Kim, M. & Buratowski, S. Phosphorylation of serine 2 within the RNA polymerase II C-terminal domain couples transcription and 3' end processing. *Mol Cell* **13,** 67–76 (2004).

34. Wang, Y. *et al.* CDK7-dependent transcriptional addiction in triple-negative breast cancer. *Cell* **163,** 174–86 (2015).

35. Lo, H.-W. & Hung, M.-C. Nuclear EGFR signalling network in cancers: linking EGFR pathway to cell cycle progression, nitric oxide pathway and patient survival. *Br. J. Cancer* **94,** 184–8 (2006).

36. Lin, S. Y. *et al.* Nuclear localization of EGF receptor and its potential new role as a transcription factor. *Nat. Cell Biol.* **3,** 802–808 (2001).

37. Lo, H.-W. *et al.* Nuclear interaction of EGFR and STAT3 in the activation of the iNOS/NO pathway. *Cancer Cell* **7,** 575–89 (2005).

38. Brand, T. M. *et al.* Nuclear epidermal growth factor receptor is a functional molecular target in triple-negative breast cancer. *Mol. Cancer Ther.* **13,** 1356–68 (2014).

39. Huang, W.-C. *et al.* Nuclear translocation of epidermal growth factor receptor by Akt-dependent phosphorylation enhances breast cancer-resistant protein expression in gefitinib-resistant cells. *J. Biol. Chem.* **286,** 20558–68 (2011).

40. Hung, L. Y. *et al.* Nuclear epidermal growth factor receptor (EGFR) interacts with signal transducer and activator of transcription 5 (STAT5) in activating Aurora-A gene expression. *Nucleic Acids Res.* **36,** 4337–4351 (2008).

41. Swords, R. *et al.* Cdc7 kinase - a new target for drug development. *Eur. J. Cancer* **46,** 33–40 (2010).

42. Yamada, M., Masai, H. & Bartek, J. Regulation and roles of Cdc7 kinase under replication stress. *Cell Cycle* **13,** 1859–66 (2014).

43. Tudzarova, S. *et al.* Molecular architecture of the DNA replication origin activation checkpoint. *EMBO J.* **29,** 3381–94 (2010).

44. Tudzarova, S. *et al.* p53 controls CDC7 levels to reinforce G1 cell cycle arrest upon genotoxic stress. *Cell Cycle* **15,** 2958–2972 (2016).

45. Huang, T.-H. *et al.* Epidermal growth factor receptor potentiates MCM7-mediated DNA replication through tyrosine phosphorylation of Lyn kinase in

human cancers. *Cancer Cell* **23,** 796–810 (2013).

46. Network, T. C. G. A. Comprehensive molecular portraits of human breast tumors. *Nature* **490,** 61–70 (2012).

47. Montagnoli, A. *et al.* A Cdc7 kinase inhibitor restricts initiation of DNA replication and has antitumor activity. *Nat. Chem. Biol.* **4,** 357–65 (2008).

48. Montagnoli, A. *et al.* Cdc7 Inhibition Reveals a p53-Dependent Replication Checkpoint That Is Defective in Cancer Cells. *Cancer Res.* **64 (19):** 7110–7116 (2004).

49. Connell-Crowley, L., Harper, J. W. & Goodrich, D. W. Cyclin D1/Cdk4 regulates retinoblastoma protein-mediated cell cycle arrest by site-specific phosphorylation. *Mol. Biol. Cell* **8,** 287–301 (1997).

50. Kato, J., Matsushime, H., Hiebert, S. W., Ewen, M. E. & Sherr, C. J. Direct binding of cyclin D to the retinoblastoma gene product (pRb) and pRb phosphorylation by the cyclin D-dependent kinase CDK4. *Genes Dev.* **7,** 331–342 (1993).

51. Rainey, M. D., Quachthithu, H., Gaboriau, D. & Santocanale, C. DNA Replication Dynamics and Cellular Responses to ATP Competitive CDC7 Kinase Inhibitors. *ACS Chem. Biol.* **12,** 1893–1902 (2017).

ADDITIONAL FILES

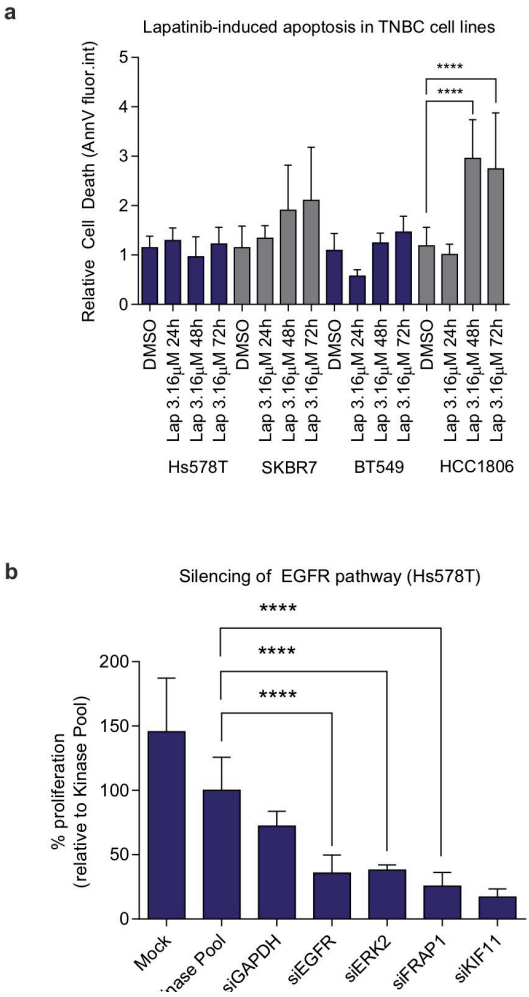

Additional File 1. Figure S1. Resistance of TNBC cells to EGFR-TKIs. a. Effect of Lapatinib on induction of apoptosis in selected lapatinib-resistant and sensitive TNBC cell lines. Hs578T, BT549, SKBR7 and HCC1806 cells were treated with lapatinib (3.16 μM) as indicated, for 24, 48 or 72 hrs, respectively, stained with Annexin-V and Hoechst, followed by imaging and image quantification. Relative cell death was quantified by normalising the intensity of Annexin-V signal to that of DMSO control. One-way ANOVA **** $P \leq 0.0001$, *** $P \leq 0.001$, ** $P \leq 0.01$, * $P \leq 0.05$. **b.** Impact of silencing EGFR and downstream components of EGFR signalling pathway on the proliferation of Hs578T cells. Hs578T cells were transfected with siRNAs targeting EGFR, ERK2 and FRAP1 as well as positive (siKIF11) and negative controls (siGAPDH and siKinase Pool) as described and grown for 4 days. Proliferation was then assessed using sulphorhodamine B assay. Results were normalised to Kinase Pool using the % control method as described in materials and methods.

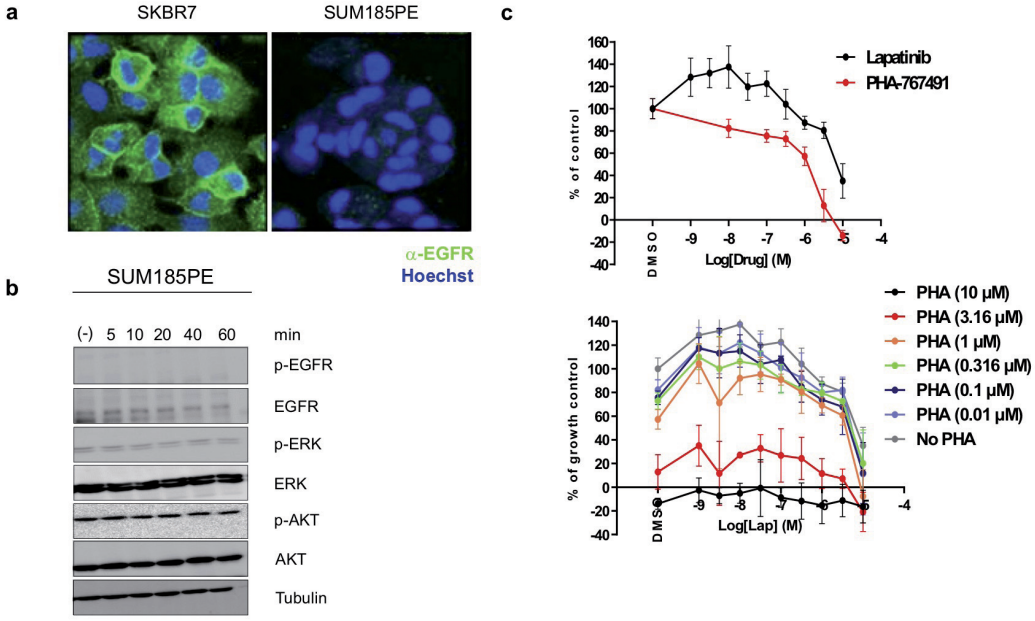

Additional File 2. Figure S2: EGFR-negative TNBC cell line SUM185PE is insensitive to co-treatment with lapatinib and PHA-767491. **a.** Immunofluorescence imaging of EGFR-positive (SKBR7) and EGFR-negative (SUM185PE) TNBC cell lines. Cells were fixed using 1% paraformaldehyde and 0.1% Triton-X for 15 minutes before being washed thrice with 1x PBS and blocked with 0.5% bovine serum albumin in PBS for 30 minutes. EGFR antibody (sc-03; Santa Cruz Biotechnology ®) was used to stain EGFR overnight at 4°C. Fixed cells were then incubated with anti-rabbit Alexa 488-conjugated secondary antibody (A11008; Molecular Probes ®) or Hoechst (nuclear stain; 1:10,000) for 1 hour at room temperature in the dark before being imaged at 20x magnification. **b.** Impact of EGF-stimulation on EGFR-mediated signal transduction in EGFR-negative cell line SUM185PE. Cells were starved overnight in serum-free medium before being treated with lapatinib (3.16 μM) for 4 hours and subsequently stimulated with EGF (100 ng/ml) for 5 minutes. Cells were then lysed and protein samples subjected to SDS-PAGE and immunoblotting with indicated antibodies. **c.** Dose-response experiment combining lapatinib and PHA-767491 in SUM185PE cells. Upper graph shows response of SUM185PE cells to lapatinib and PHA-767491 monotherapies. Lower graph displays proliferation of SUM185PE cells after combining lapatinib (3.16 μM) with dose range (0.01-10 μM) of PHA-767491. Proliferation was assessed using sulphorhodamine B assay and results were normalised to DMSO using the % control method as outlined in materials and methods.

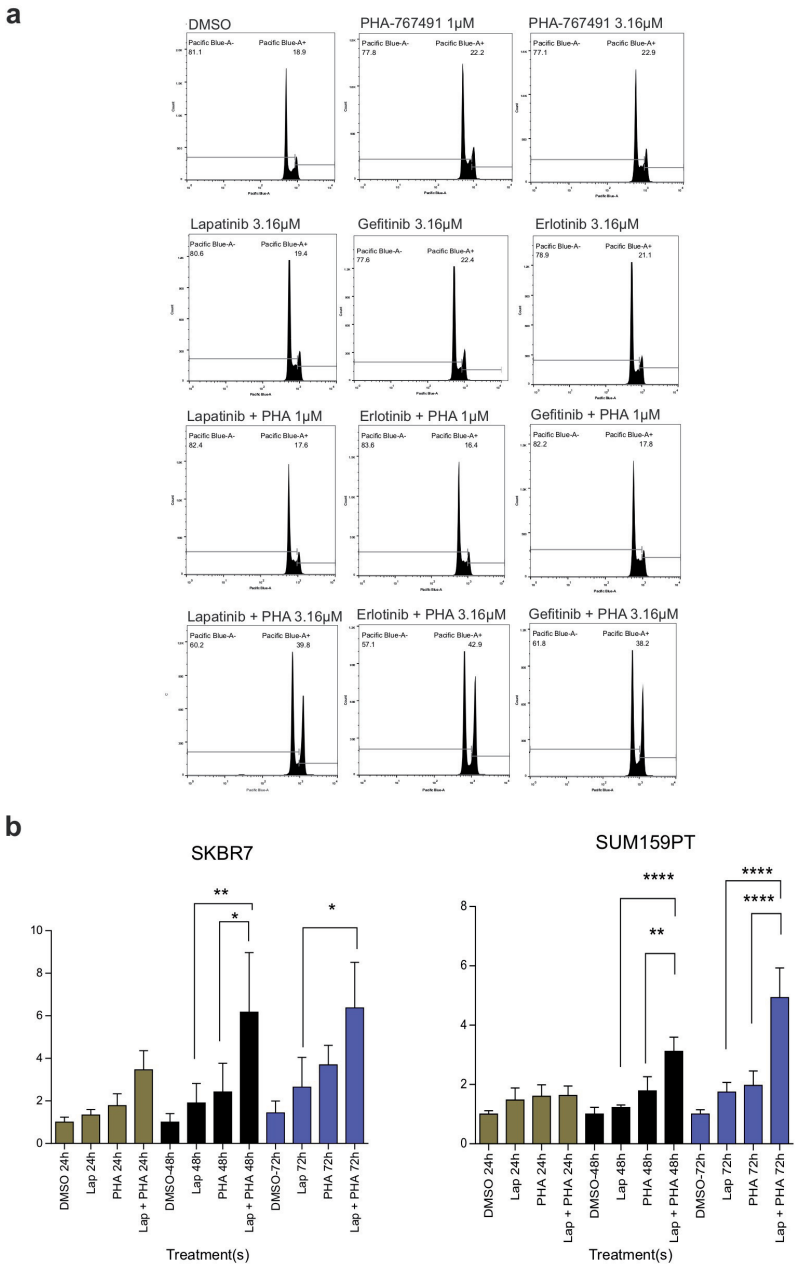

Additional File 3. Figure S3. EGFR-TKIs and PHA-767491 synergise to induce G2/M cell cycle arrest and apoptosis. a. Cell cycle distribution histograms of Hs578T and SKBR7 cells after 48h treatment with EGFR-TKIs (lapatinib, erlotinib or gefitinib at 3.16 μM) alone or combined with PHA-767491 (1μM or 3.16μM), as indicated. **b.** Induction of apoptosis by EGFR-TKI and PHA-767491 co-treatment. SKBR7 and SUM149PT cells were treated with lapatinib (3.16 μM), PHA-767491 (3.16 μM), alone or combined, as indicated, for 24h, 48h or 72h, respectively, and then stained with Annexin-V and Hoechst, followed by imaging and image quantification. Relative cell death was quantified by normalising the intensity of Annexin-V signal to that of DMSO control. One-way ANOVA **** $P \leq 0.0001$, *** $P \leq 0.001$, ** $P \leq 0.01$, * $P \leq 0.05$.

Table S1 (Related to Figure 6)				
Genes	**HR**	**p-value**	**95% CI low**	**95% CI high**
MOCS3	0.11	0.00	0.031	0.415
SNIP1	0.28	0.01	0.099	0.778
CTGF	1.33	0.02	1.047	1.683
ZCCHC24	1.40	0.05	1.001	1.963
TIMP3	1.43	0.03	1.031	1.989
HEG1	1.44	0.03	1.032	2.013
N4BP2L2	1.44	0.05	0.997	2.092
PRKD3	1.53	0.05	1.009	2.328
LBH	1.54	0.05	1.002	2.353
HOXC6	1.54	0.01	1.106	2.157
ANGPTL4	1.55	0.04	1.015	2.378
TNS1	1.56	0.01	1.128	2.163
PMP22	1.58	0.01	1.132	2.211
ROCK2	1.61	0.05	0.998	2.583
SHOX2	1.69	0.03	1.049	2.715
MITF	1.71	0.04	1.031	2.821
ACAP2	1.75	0.03	1.044	2.950
RANBP2	1.76	0.04	1.032	3.000
JRKL	1.76	0.00	1.200	2.583
SLC38A2	1.84	0.04	1.038	3.254
ZFYVE16	1.84	0.03	1.071	3.154
LPCAT1	1.84	0.01	1.154	2.931
MLXIP	1.89	0.01	1.164	3.076
TSC22D1	1.93	0.01	1.158	3.231
RASA1	1.95	0.00	1.236	3.074
DIP2C	2.04	0.05	1.015	4.095
CRYBG3	2.04	0.04	1.046	3.994
SMAD6	2.07	0.04	1.023	4.177
ARID4A	2.23	0.03	1.096	4.530
C17orf85	2.27	0.02	1.152	4.471
GCNT3	2.31	0.00	1.361	3.926
DDX3X	2.32	0.05	0.982	5.492
APAF1	2.94	0.04	1.026	8.414
LMBR1L	3.06	0.03	1.099	8.491

Additional File 5. Supplementary Table 1. 34 clinically relevant genes specifically down-regulated after co-treatment with Lapatinib and PHA-767491 in Hs578T and SKBR7 cells.

Chapter 4

Targeting the P-TEFb complex through CDK9 inhibition to combat triple-negative breast cancer

Ronan P. McLaughlin[1], Jichao He[1], Jessica Karuntu[1], Vera van der Noord[1], Marcel Smid[2], Annemieke M. Timmermans[2], Anita M.A.C. Trapmn-Jansen[2], Renée Foekens[2], Solomon Tadesse[3], Yi Long[3], Sarah Al Haj Diab[3], John W.M. Martens[2], John A. Foekens[2], Shudong Wang[3], Yinghui Zhang[1], Bob van de Water[1]

[1]Division of Drug Discovery and Safety, Leiden Academic Centre for Drug Research, Leiden University, 2300 RA Leiden, The Netherlands.

[2]Department of Medical Oncology and Cancer Genomic Netherlands, Erasmus MC Cancer Institute, Erasmus University Medical Center, 3000 CA Rotterdam, The Netherlands.

[3]Centre for Drug Discovery and Development, School of Pharmacy and Medical Sciences, University of South Australia Cancer Research Institute, Adelaide, South Australia, 5000, Australia.

This chapter is based on a manuscript in preparation

ABSTRACT

Positive transcription elongation factor b (P-TEFb) complex is composed of cyclin-dependent kinase 9 (CDK9), Cyclin T1, Cyclin T2, and Cyclin K. The function of P-TEFb is crucial for the elongation of mRNA transcripts. Increasing evidence indicates the CDK9-dependent transcriptional addiction in cancer. Thus, disruption of P-TEFb has evolved into an attractive therapeutic strategy for cancer treatment. Here, using a selection of CDK inhibitors, we demonstrate that targeting CDK9 dramatically reduces proliferation and concomitantly induces apoptosis in a large panel of triple-negative breast cancer (TNBC) cell lines, suggesting CDK9 is a potent target for TNBC. Blockage of P-TEFb-mediated signal transduction prevents phosphorylation of RNA Polymerase II (RNAPII), thereby reducing levels of short-lived mRNA transcripts of various pro-survival factors such as MCL1, BCL-xL, Survivin and XIAP, involving proteasome-mediated degradation. Transcriptomic profiling of the effect of CDK9 inhibition on regulation of global gene expression in TNBC cells revealed down-regulation of genes enriched for pathways governing transcription, cell cycle progression, TGF-β, Wnt/β-catenin and BMP oncogenic signalling. RNAi-mediated silencing further uncovered a cluster of vital CDK9-dependent transcription factors (EN1, SOX9, and PLAG1) essential for the proliferation of TNBC cells, whose expression is significantly higher in TNBC tumours. Altogether, our data highlight the utility of targeting the P-TEFb-mediated transcriptional machinery as a novel approach for combating TNBC.

Key words: TNBC, P-TEFb, CDK9, RNAPII, MCL1, CDK9 inhibitors, transcriptional addiction

INTRODUCTION

Triple-negative breast cancer (TNBC) is a particularly aggressive subtype of breast cancer which lacks expression of targetable oncogenic receptors such as the oestrogen receptor (ER), the progesterone receptor (PR), and the human epidermal growth factor receptor 2 (HER2)[1]. The apparent lack of targetable disease drivers in TNBC is currently responsible for the far poorer prognosis of patients with this disease, compared to those with ER+ or HER2+ breast cancer[2]. TNBC can be divided into multiple subtypes based on gene expression, each with their own drug response profile. This heterogeneity has further confounded efforts to improve targeted therapy for this devastating disease[1,3]. Despite multiple efforts, the identification of TNBC-specific weaknesses and effective targeted therapies has yet to be translated into clinical benefit.

Genetic changes in cancer cells lead to dysregulated transcriptional programmes which render cancer cells highly dependent upon exceptionally high rates of transcription of certain oncogenes critical to promoting proliferation (e.g. MYC)[4,5]. The expression of short-lived pro-survival genes is therefore exquisitely sensitive to disruption of the complexes which regulate transcription[6,7]. Consequently, targeting transcriptional addiction has thus emerged as an important therapeutic strategy in cancer. Rather than targeting pharmacologically intractable, disease-driving oncogenes such as MYC, attention has turned to the complexes which govern mRNA transcription in cancer cells. To this end, blocking the activity of a subgroup of cyclin-dependent kinases (CDKs), which are critical for productive mRNA transcription, may represent a valuable tool in combating TNBC.

The positive transcription elongation factor b (P-TEFb) complex, in conjunction with CDK7, is indispensable for ensuring transcriptional initiation and overcoming promoter-proximal pausing of RNA Polymerase II (RNAPII, or Pol II)[8,9]. P-TEFb is composed of catalytic CDK9 and its regulatory cyclins; Cyclin T1, Cyclin T2 and Cyclin K[8,9]. Phosphorylation of RNAPII's C-terminal domain (CTD) at Ser5 by CDK7, the catalytic component of master transcription factor TFIIH, initiates transcription but also recruits negative elongation factors (e.g. NELF and DSIF) which pause RNAPII during this process[10,11]. Relief of promoter-proximal pausing is provided by P-TEFb/CDK9-mediated phosphorylation of RNAPII's CTD at Ser2 and of DSIF upon activation by the bromodomain containing protein 4 (BRD4), facilitating the dissociation of NELF and thereby permitting productive mRNA elongation[12,13]. Since P-TEFb is a pre-requisite for efficient transcription, it is unsurprising that high levels of P-TEFb recruitment are found at super-enhancer regions[14]. Super-enhancers are clusters of enhancers with high transcriptional activity and which are characterised by exceptionally high levels of bound transcription factors to drive transcription of one or multiple genes[14]. Evidence suggests that super-enhancers are responsible for maintaining the oncogenic state in multiple malignancies, since they often regulate super-enhancer-associated genes involved in cancer progression, such as the oncogene MYC[14]. Moreover, they are also frequently acquired at key oncogenes where they impart enhanced responsiveness to upstream signalling, thereby acting as conduits for dysregulated signal transduction pathways and their terminal transcription factors[15]. Cancers may therefore be addicted to aberrant transcriptional programmes fuelled by super-enhancer-driven expression of key transcriptional regulators, which renders them susceptible to disruption of P-TEFb function. Previously published data, using CDK7 inhibitor THZ1 in TNBC, non-small cell lung

cancer and T-cell lymphomas, identified CDK7-mediated super-enhancer regulation as a targetable cancer-specific dependency[16–18]. Recent data have also demonstrated that broad spectrum CDK inhibitors with potent activity against CDK9 are effective at inhibiting the growth of various cancer cells including leukaemia, lymphoma, and NUT midline carcinoma cells as well as breast tumour cells[19–22]. Altogether, the current data suggest that targeting master transcriptional regulators, such as CDK7 or P-TEFb/CDK9, may represent a potent new strategy to identify novel therapies for TNBC as well as other cancers.

Thus far, however, the effect of more specific P-TEFb/CDK9 inhibitors on TNBC cells is largely unknown. Here we explored the efficacy of a broad panel of CDK9 inhibitors with potent activity against P-TEFb function in TNBC cells. We demonstrated the exceptional sensitivity of TNBC cell lines to CDK9 inhibition, defining the effect of these inhibitors on global gene expression, the balance of pro- and anti-apoptotic factors, and oncogenic signalling in TNBC cells. These compounds inhibited P-TEFb-mediated signal transduction, shutting down key oncogenic pathways such as TGF-β, Wnt/β-catenin and BMP signalling in TNBC cells as well as drastically reducing overall transcription factor function. Silencing of the most strongly down-regulated transcription factors identified by RNA-Seq revealed that TNBC cells depend on a number of these factors for survival, thus identifying a group of transcription regulators as novel prospective therapeutic targets likely associated with essential dysfunctional transcriptional programmes in TNBC.

MATERIALS & METHODS

Inhibitors and antibodies

CDK4/6 inhibitors T2-58, T2-104, T2-106 and T2-112, as well as CDK9 inhibitors I-73 (also named CDKI-73[23]), D10-81, D11-36, D11-69, Y3-21 and Y3-29 were synthesised as reported[24]. Pan-CDK inhibitors dinaciclib (S2768), flavopiridol (S1230), P276-00 (S8058) and roscovitine (S1153), CDK7 inhibitor THZ1 (S7549), and CDK4/6 inhibitors abemaciclib (S7158) and palbociclib (S1579), were purchased at Selleckchem®. All compounds were prepared in DMSO at 10 mM concentration. All primary antibodies used were commercially available, including phospho-CDK9 (T186; CST #2549), CDK9 (CST #2316), phospho-RNAPII Ser2/Ser5 (CST #4735), RNAPII (CST #2629), BCL-xL (CST #2764), XIAP (CST #2045), MCL1 (CST #5453), survivin (CST #2808), γ-H2AX (S139; CST #2577), c-MYC (Santa Cruz sc-789), BRD4 (Bethyl Laboratories A301-985A-M) and tubulin (Sigma Aldrich T-9026).

Cell culture and compound screening

TNBC cell lines used were representative for different TNBC subtypes[1], including basal-like 1 (BL1) HCC38, HCC1143, HCC1937 and MDA-MB-468, basal-like 2 (BL2) HCC70, HCC1806 and SUM149PT, mesenchymal (M) BT549 and Hs578T, mesenchymal stem-like (MSL) MDA-MB-157, MDA-MB-231, MDA-MB-436 and SUM159PT, luminal androgen receptor (LAR) MDA-MB-453, and unclassified SKBR7, SUM52PE, SUM229PE and SUM1315MO2. All TNBC cell lines were maintained in RPMI-1640 medium (Gibco, ThermoFisher Scientific) supplemented with 10% FBS (Thermo Fisher Scientific; 10270106) and 25IU/ml Penicillin and 25µg/ml Streptomycin (ThermoFisher Scientific; 15070-063). Cells were cultured in a humidified incubator at 37°C, 5% CO_2. For drug screening, cells were seeded at the

appropriate densities (90 µl/well) in 2× 96-w plates (Greiner; 655162) or 2× 96-w µCLEAR plates (Greiner; 655090) and incubated overnight at 37°C, 5% CO_2 for drug treatment. Final treatment concentrations were 0.0316 µM, 0.1 µM, 0.316 µM, 1 µM and 3.16 µM (i.e. -1.5, -1, -0.5, 0, and 0.5 Log µM, respectively) with final 0.01% v/v DMSO in all conditions; doxorubicin (1 µM) was used as positive control where appropriate.

Automated imaging

72 hours post-exposure to inhibitors and prior to sulphorhodamine B proliferation assay, cells were stained with 1:1000 Annexin-V (0.9 mg/ml) and 1:10,000 Hoechst 33258 (2 mg/ml) for 45 minutes at 37°C, 5% CO_2. Cells were subsequently imaged using BD Pathway 855 microscope (BD Biosciences). An image analysis pipeline was created in Cell Profiler involving segmentation based on Hoechst 33258 staining to identify the primary cell objects followed by secondary Annexin V-positive objects. Annexin V-positive cells were defined based on an intensity threshold. This threshold was set based on the negative (DMSO) and positive (doxorubicin) controls. For each image the sum of all nuclei and the sum of the Annexin V-positive cells was determined followed by calculation of the percentage of Annexin V-positive cells.

Cell proliferation assay

96 hours post-exposure to inhibitors cells were fixed by adding 30 µl/well of 50% w/v trichloroacetic acid (Sigma; T9159). Plates were incubated at 4°C for 1 hour before being washed five times in H_2O and dried overnight at room temperature. The following day, cells per well were stained with 60 µl of 0.4% w/v sulphorhodamine B (SRB)/1% v/v acetic acid solution (Sigma; 341738) for 2 hours before being washed

four times with 1% v/v acetic acid and dried overnight at room temperature. SRB was subsequently dissolved by adding 150 µl/well of 10 mM Tris and plates were placed on a shaker for 2 hours at room temperature. Absorbance at 540 nm was then measured using TECAN Infinite ® M1000 (Tecan Trading AG, Switzerland). Data were normalised to DMSO control values and percentage of proliferation relative to DMSO was presented.

Cell cycle analysis

Cells were seeded in 6-well plates at the appropriate density. The following day cells were treated with drugs for 48h. Detached cells and attached cells were collected during trypsinisation and collected through centrifugation (1000 rpm, 5 minutes, 4^{o}C). Pelleted cells were re-suspended in 200 µl ice-cold 1 mM EDTA in PBS and fixed by adding 800 µl ice-cold 100% ethanol (-20^{o}C). Cells were washed by two wash steps in PBS (1000 rpm, 5 minutes, room temperature) and pellet was re-suspended in 250 µl of 3 µM DAPI (Sigma Aldrich, 10236276001) in staining buffer (100 µM Tris pH 7.4, 150 mM NaCl, 1 mM $CaCl_2$ and 0.5 mM $MgCl_2$). After 15 min cells were filtered through 70 µm EASYstrainer filters followed by FACS Conto II analysis (BD Biosciences). Data were analysed using FlowJo V10.

Random cell migration assay

50 µl of collagen solution (Type 1; 20 µg/ml) was added to 96-well Screenstar® plates (*Greiner*) and incubated at 37^{o}C, 5% CO_2 for 1 hour followed by washing thrice with PBS. Cells were seeded at the appropriate density and grown overnight at 37^{o}C, 5% CO_2. The following day, cells were stained with Hoechst 33258 (1:10,000, 2 mg/ml) and treated with drug solutions and DMSO vehicle control

(1:1000) at the appropriate concentrations immediately prior to imaging. Cells were then imaged on a Nikon Eclipse Ti confocal microscope at 37^{o}C, 5% CO_2 for 16 hours. Data were analysed using NIS Elements Analysis software 4.3. Nuclei were first segmented using in-house macros after which cells were tracked based on image overlap. Tracking data were then analysed using Microsoft Excel-based in-house macros to calculate the average speed (μm/h) of all cells per well over the duration of drug treatment.

Western blotting

Cell lysates were harvested in RIPA lysis buffer with 1:100 protease inhibitor cocktail (Sigma; P8340). Cellular proteins were denatured in sample buffer containing 10% β-mercaptoethanol (Acros Organics 125472500). Equal amounts of proteins were subsequently loaded into polyacrylamide gels (7.5-15% depending on desired resolution), resolved using SDS-PAGE and subsequently transferred to PVDF membranes (Merck Chemicals; IPVH00010) overnight. PVDF membranes were then blocked with 5% bovine serum albumin (Sigma Aldrich A9647) in Tris-buffered saline containing 0.05% Tween20 and incubated overnight with the appropriate primary antibodies.

Proteasomal degradation of MCL1

Cells were seeded into 6-well plates at the appropriate density and allowed to attach overnight. MG-132 (Selleckchem S2619) at 10 μM was prepared in RPMI-1640 with all aforementioned supplements. Medium was aspirated from cells and replaced with 10 μM MG-132 for 2 hours. Immediately after removing MG-132, cells were treated

with 0.316 μM of the appropriate CDK9 inhibitor for 6 hours, followed by Western Blot assays.

RNA sequencing

Hs578T cells seeded into 6-well plates were treated with CDK9 inhibitors D10-81 (0.1 μM) and Y3-21 (0.1 μM) or I73 (0.316 μM) for 6 hours followed by extraction of RNA using RNeasy Plus Mini Kit (QIAGEN 74136) and stored at -80^{o}C. Transcriptome RNA-Sequencing (RNA-Seq) was performed using Illumina high-throughput RNA sequencing. DNA libraries were prepared from the samples with the TruSeq Stranded mRNA Library Prep Kit. The DNA libraries were sequenced according to the Illumina TruSeq v3 protocol on an Illumina HiSeq2500 sequencer. Paired-end reads were generated of 100 base-pairs in length. Alignment was performed using the STAR aligner (version 2.4.2a) against the human GRCh38 reference genome. Marking duplicates, sorting and indexing were performed using Sambamba (version 0.6.6). Gene expression was quantified using the FeatureCounts software (version 1.4.6) based on the ENSEMBL gene annotation for GRCH38 (release 84). RNA-Seq data were normalised by TMM using EdgeR's normalisation-factor, followed by quantile normalisation and presented in Log2 fold change (Log2 FC) scales[25]. Genes with significant down- or up-regulation (Log2 FC ≥ |1.0|) under indicated conditions were analysed by web-based functional analysis tools Ingenuity Pathway Analysis (IPA, QIAGEN®).

siRNA transfection

Cells were seeded in 96-well plates at the appropriate density. For each siRNA transfection, 50 nM siGENOME siRNAs (Dharmacon) were transfected into cells per 96-well using INTERFERin transfection reagent (Polyplus; 409-50). The

following day medium was refreshed. 48 hours post-transfection, cells were lysed for western blot to confirm knockdown efficiency. 96 hours post-transfection cells were fixed for SRB proliferation assay.

Clinical evaluation of candidate genes

The clinical relevance of candidate genes was evaluated using in-house and publicly available gene expression data of lymph-node negative (LNN) primary breast cancer patients who did not receive adjuvant or neo-adjuvant systemic therapy, as well as available metastasis-free survival data, leading to a cohort of 867 patients. 625 of these were ER+, whilst 242 were ER-. Of the 242 ER-patients, 142 were classified as TNBC. Data were gathered from Gene Expression Omnibus (http://www.ncbi.nlm.nih.gov/geo/) entries GSE2034, GSE5327, GSE2990, GE7390 and GSE11121, with all data available on Affymetrix U133A chip. Raw.cel files were processed using fRMA parameters (median polish) after which batch effects were corrected using ComBat.

Primary breast cancer tissues and derived tissue micro-arrays for CDK9/ pCDK9 analysis by IHC

The tissue microarray used here has been described previously[26]. Briefly, to construct TMAs a total of 412 primary breast cancer tissues were collected from Erasmus Medical Center pathology archive, and subsequently reviewed by a trained pathologist (CvD; MAdB). The TMAs were prepared using an ATA 27 (Beecher Instruments, Sun Prairie, WI, USA). For every tissue, a specialised breast pathologist (CvD; MAdB) marked the tumour area, from which three different cores (diameter: 0.6 mm) were taken as biological replicates and transferred in a TMA recipient block.

Tissue cores of 0.6 mm were taken from each tissue paraffin block and transferred in triplicate into a TMA recipient block. Stained TMA slides were digitalised and analysed using Slidepath software (Leica Microsystems, Solms, Germany). Expression of ER, PR and Her2 proteins was determined by IHC staining, and fluorescence in situ hybridization was performed when staining of Her2 was scored as 2+ (i.e. uncertain amplification), to assess possible amplification of this gene. Samples were excluded for further analysis when tissues had unclear expression of ER, PR or Her2, no information on lymph-node status and/or adjuvant systemic chemotherapy, and/or poor quality of CDK9/pCDK9 staining (defined as: heterogeneous staining between cores belonging to the same specimen and/or lack of triplicate staining due to lack of at least one core), resulting in a final number of 384 tissues for data analysis, respectively. Clinical and histopathological features of these tissues are summarized in Table 1. This study was approved by the Medical Ethics Committee of the EMC, The Netherlands (MEC 02.953) and was performed in accordance to the Code of Conduct of the Federation of Medical Scientific Societies in The Netherlands, and wherever possible we adhered to the Reporting Recommendations for Tumor Marker Prognostic Studies (REMARK). (Altman D. G., McShane L. M., Sauerbrei W. & Taube S. E. Reporting Recommendations for Tumor Marker Prognostic Studies (REMARK): explanation and elaboration. PLoS Med. 9, e1001216 (2012).

Immunohistochemical staining

Sections of 4 µm of the three above-mentioned TMAs were incubated for 1 hour at room temperature with CDK9/pCDK9 antibody (listed above) at a dilution of 1:300 against the proteins. Antigen retrieval was performed prior to antibody incubation by heating the slides for 40 min at 95 °C and washing with Dako antigen retrieval

solution (pH = 6; DakoCytomation, Carpinteria, CA, USA) when the slides were cooled down to room temperature. Staining was visualized by anti-mouse EnVision+ ® System-HRP (DAB) (DakoCytomation, Carpinteria, CA, USA). CDK9/pCDK9 staining was separately scored in both percentage of positive invasive breast carcinoma cells and staining intensity by two independent observers. Six categories were scored for the percentage of positive invasive tumour cells: 0%, 1–10%, 11–25%, 26–50%, 51–70%, and > 70%. All cores present on the three TMAs were scored by an experienced researcher in a blind manner. Staining scores of triplicate cores were validated by a second experienced researcher, who was extensively trained by a specialised breast pathologist. In order to score CDK9/pCDK9 expression as measured by IHC, intensity and quantity categories were transformed into numerical values (Table S1) and a 'histo-score' (as reported in15) was calculated for both the cytoplasmic and nuclear staining components with the following formula: $Histo-score = (intensity\ value)\ x\ (quantity\ value)$. Nuclear CDK9/pCDK9 histo-score distributions were divided into four categories: 0–5, 6–10, 11–15, and 16–20.

Data analysis and statistics

All data were processed in GraphPad Prism 7.0 and/or Microsoft Excel. IC50 values were derived from GraphPad Prism 7.0 using nonlinear regression fitting. Two-way ANOVA with Tukey's correction for multiple testing was used to assess impact of drug treatment on cell cycle distribution. P-values < 0.05 were considered statistically significant. One-way ANOVA with Tukey's correction for multiple testing was used to assess the effect of RNAi-mediated silencing of transcription factors on TNBC cell proliferation. P-values < 0.05 were considered statistically significant.

RESULTS

CDK9 and downstream target genes MCL1 and MYC are highly expressed in TNBC tumours

There is evidence suggesting that TNBC cells become more vulnerable after disruption of the transcriptional machinery through inhibition of CDK7 or BRD4[18,27]. Our overall aim was to evaluate CDK9 as a potential target in TNBC. We firstly assessed the expression level of P-TEFb complex components in TNBC by assessing expression of P-TEFb complex components in TNBC. RNA-Seq transcriptome analysis of 116 TNBC patients in The Cancer Genome Atlas (TCGA) database revealed that P-TEFb complex members CDK9, BRD4 and POLR2A (Subunit A of RNAPII), and known target genes MYC and MCL1, are highly expressed (mean Log2 Expression >10) in most, if not all, 116 TNBC patient tumours (Figure 1A). Cyclin T1/T2 and Cyclin K were, by and large, expressed at a lower level than the aforementioned genes. Differential expression of the oncogenic transcriptional regulator MYC which relies on P-TEFb for its own transactivation[28], was observed in TNBC, consistent with previous reports[19]. In particular, high levels of pro-survival MCL1, the expression of which is dependent upon P-TEFb function[29], were significantly correlated to poor survival of TNBC patients (Figure 1B). To further assess CDK9 as a potential target in TNBC, we performed CDK9 tissue microarray (TMA) staining (Figure 1C) on 384 TNBC patient tumours. TMA analysis revealed that the TNBC tumours were broadly CDK9-positive, with around 75% of tumours showing 80-100% positivity and moderate-strong intensity (*i.e.* histological score 4-9; Figure 1D). These data support the rationale for targeting CDK9 in TNBC, despite the genetic heterogeneity of the disease.

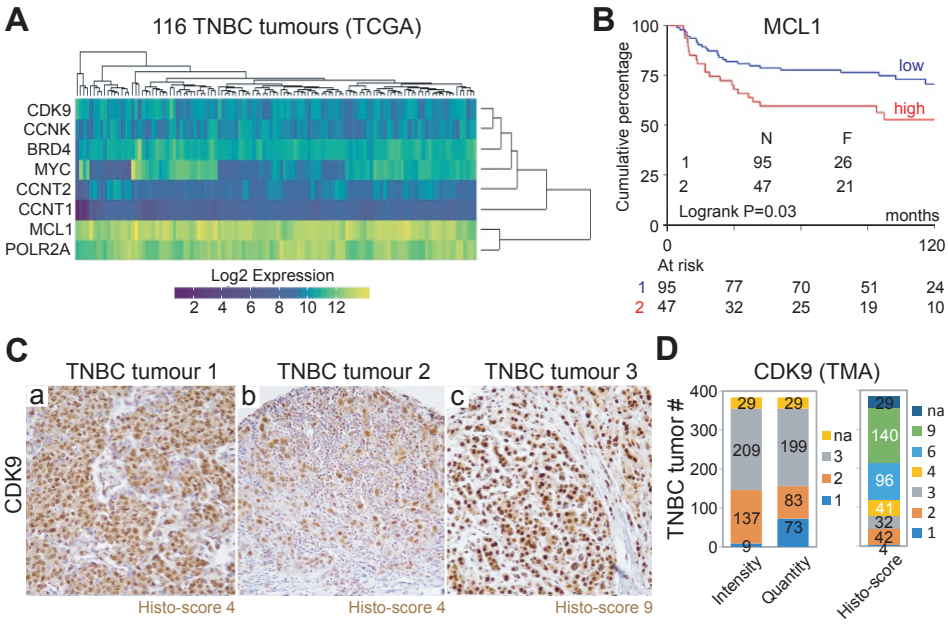

Figure 1. Expression of P-TEFb complex and associated components in TNBC. (**A**) Expression of CDK9, cyclins (CCNT1/2, CCNK), POLR2A (encoding RNAPII subunit A), BRD4, and downstream targets MYC and MCL1 in 116 TNBC patient tumours (RNA-Seq Log2 expression data derived from The Cancer Genome Atlas, TCGA). (**B**) Correlation of MCL1 expression with poor survival of 142 TNBC patients, presented in Kaplan-Meier estimator. (**C**) CDK9 tissue microarray (TMA) staining in TNBC tumours and staining histological scoring. Histological staining was scored (i.e. Histo-score) on intensity of the coloring and by percentage of positivity. In examples of CDK9 staining of 3 tumors, tumour 1 (a) and 2 (b) had moderate intensity and 95% positivity (Histo-score 4), while tumour 3 (c) showed strong intensity and 100% positivity (Histo-score 9). Antibody used: rabbit mAb CDK9 (C12F7) (#2318 CST). (**D**) Positivity, quantity and Histo-scores for CDK9 TMA staining in 384 TNBC cases.

TNBC cells are susceptible to potent CDK9 inhibitors

To address the sensitivity of TNBC cells to CDK inhibitors, particularly to those which potently target CDK9 kinase activity, a total of 18 TNBC cell lines that are representative for different TNBC subtypes were treated with a collection of CDK inhibitors including Y3-21, I-73, D11-69, D11-36, Y3-29 and D10-81, which have the highest potency against CDK9, as well as inhibitors of CDK4/6 (i.e. T2-58, T2-112, T-106, and T2-104) (Figure 2A). The proliferation assays demonstrated that the

TNBC cell lines tested were less responsive to CDK4/6 inhibitors (Figure 2B), but exquisitely sensitive to the CDK9 inhibitors in concentration-dependent manners (Figures 2B and 2C), regardless of TNBC subtypes. For comparative purposes, we also assessed a selection of CDK inhibitors currently in clinical trials or approved for clinical use (Supplementary Figure S1A). The response of different TNBC cell lines to clinically approved CDK4/6-specific inhibitors palbociclib and abemaciclib was largely identical to that seen for our CDK4/6 inhibitors T2-58, T2-112, T2-106 and T2-104 (Supplementary Figure S1A). Consistent with recently published data suggesting that the LAR subtype of TNBC is sensitive to CDK4/6 inhibitors such as palbociclib and ribociclib[30], the LAR subtype cell line MDA-MB-453 was most sensitive to the CDK4/6 inhibitors tested here. Additionally, MDA-MB-231, which belongs to the MSL subtype, was sensitive to CDK4/6-inhibition, in line with published data[31,32]. TNBC cells were largely susceptible to pan-CDK inhibitors dinaciclib and flavopiridol, but not to roscovitine or P276-00 (Supplementary Figure S1A). Of relevance, we demonstrated that all 18 TNBC cell lines tested were vulnerable to CDK7 inhibitor THZ1 (Supplementary Figure S1A), consistent with previous reports[18], with similar sensitivity observed to potent CDK9 inhibitors Y3-21, I-73, D11-69, D11-36, Y3-29 and D10-81 (Figure 2B), further supporting a dependency of TNBC cells on CDK9-mediated transcription.

A

CDK inhibitors (CDKi)

Ki (μM) or % Residual Activity at 10μM

Code	CDK1	CDK2	CDK4	CDK6	CDK7	CDK9
T2-58	3.020	0.355	0.002	0.011	0.780	0.141
T2-112	0.220	0.022	0.008	0.002	0.194	0.258
T2-106	0.297	0.014	0.004	0.006	2.615	>10
T2-104	>10	0.154	0.008	0.011	>10	>10
Y3-21	0.023	0.002	0.017	0.546	0.625	0.001
I-73	0.004	0.003	0.009	0.052	0.091	0.004
D11-69	0.270	0.071	13%	80%	0.079	0.004
D11-36	7%	5%	9%	24%	0%	0.003
Y3-29	0.141	0.059	0.008	0.043	1.090	0.002
D10-81	0.084	0.023	21%	46%	0.019	0.006

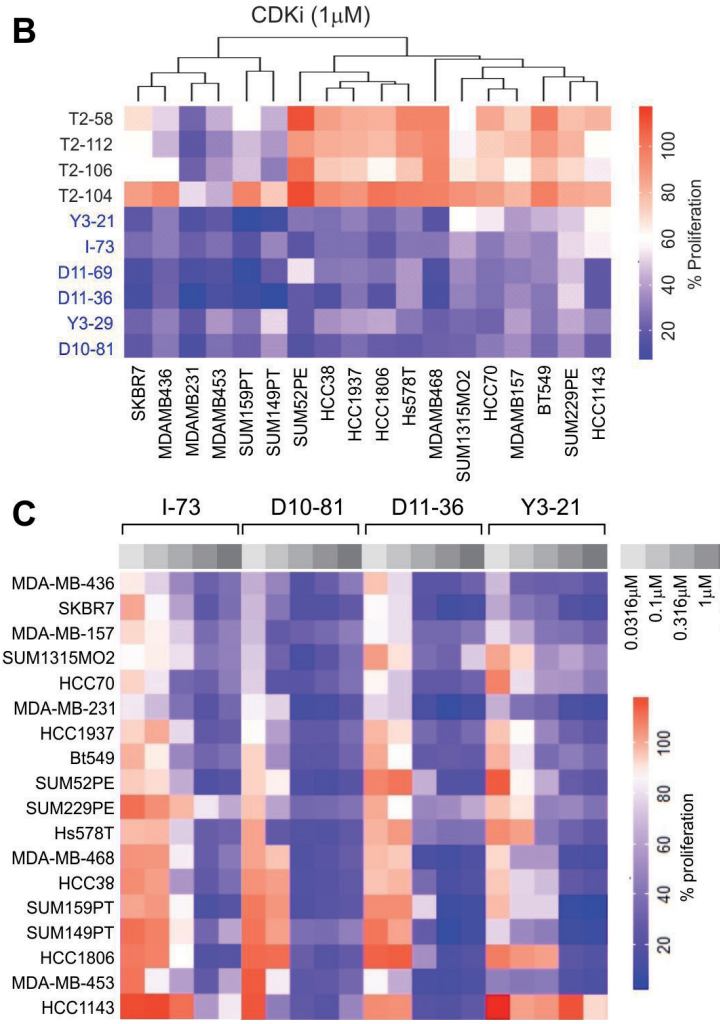

Figure 2. Screen of TNBC cell sensitivity to CDK inhibitors. (A) List of CDK inhibitors (T2-58, T2-112, T2-106 and T2-104, Y2-12, I-73, D11-69, D11-36, and D10-81) showing the CDK kinase inhibitory activity (Ki μM or % residual activity). (**B**) Response of 18 TNBC cell lines to CDK inhibitors, shown at 1μM. (**C**) Inhibitory effect of representative CDK9 inhibitors I-73, D10-81, D11-36 and Y3-21 in dose range on the proliferation of 18 TNBC cell lines. Cells were treated with a dose range of CDK inhibitors ranging from 0.0316-3.16 μM for 4 days, after which proliferation was assessed using SRB assay. Data were shown as % proliferation normalised to DMSO vehicle control (% of control cell growth = (mean sample OD – mean 0-day OD) / (mean DMSO OD – mean 0-day OD) × 100).

Targeting CDK9 blocks P-TEFb signalling transduction in TNBC cells

Next, we investigated the effect of our CDK9 inhibitors on the activity of the P-TEFb complex in TNBC cells. First, we observed that expression of P-TEFb complex components and their targets in TNBC cell lines was consistent with TCGA-derived expression data for patient TNBC tumours (Figure 3A). Particularly high levels of the RNAPII subunit POLR2A and the anti-apoptotic MCL1 were detected in all cell lines (Figure 3A). Western blotting for selected cell lines representative of TNBC subtypes (MSL, M, BL1 and BL2) further confirmed substantial levels of CDK9, RNAPII, BRD4 and MCL1 proteins (Supplementary Figure S2). We then evaluated the effect of four of our representative CDK9 inhibitors on the activity of the P-TEFb complex. Treatment of Hs578T cells with the CDK9 inhibitors D10-81, D11-36, Y3-21 and I-73 at 1 μM for 24h almost completely inhibited phosphorylation of RNAPII's CTD at Ser2 and Ser5, events specifically controlled by CDK9 and CDK7 activity, respectively, and remarkably down-regulated MYC and MCL1, leaving BRD4 unaffected (Figure 3B). To further verify the efficacy of the inhibitors on CDK9/P-TEFb-mediated signalling transduction, Hs578T, BT549 and SKBR7 cells were treated with the inhibitors for 48 hours at lower concentrations (0.01, 0.1 or 0.316 μM). All CDK9 inhibitors (at 0.316 μM) potently inhibited P-TEFb-mediated signalling; D10-81 and Y3-21 were effective at 0.1 μM in abolishing phosphorylation of RNAPII's CTD at Ser2/5 (Figure 3C). Profoundly decreased CDK9 phosphorylation and CDK9 levels were also observed after treatment (Figure 3B and 3C). D10-81 was most effective at suppressing expression of oncogenic MYC, albeit at higher concentrations (Figure 3C). Altogether, these results indicate that our CDK9 inhibitors effectively inhibit P-TEFb-mediated signalling in TNBC cells.

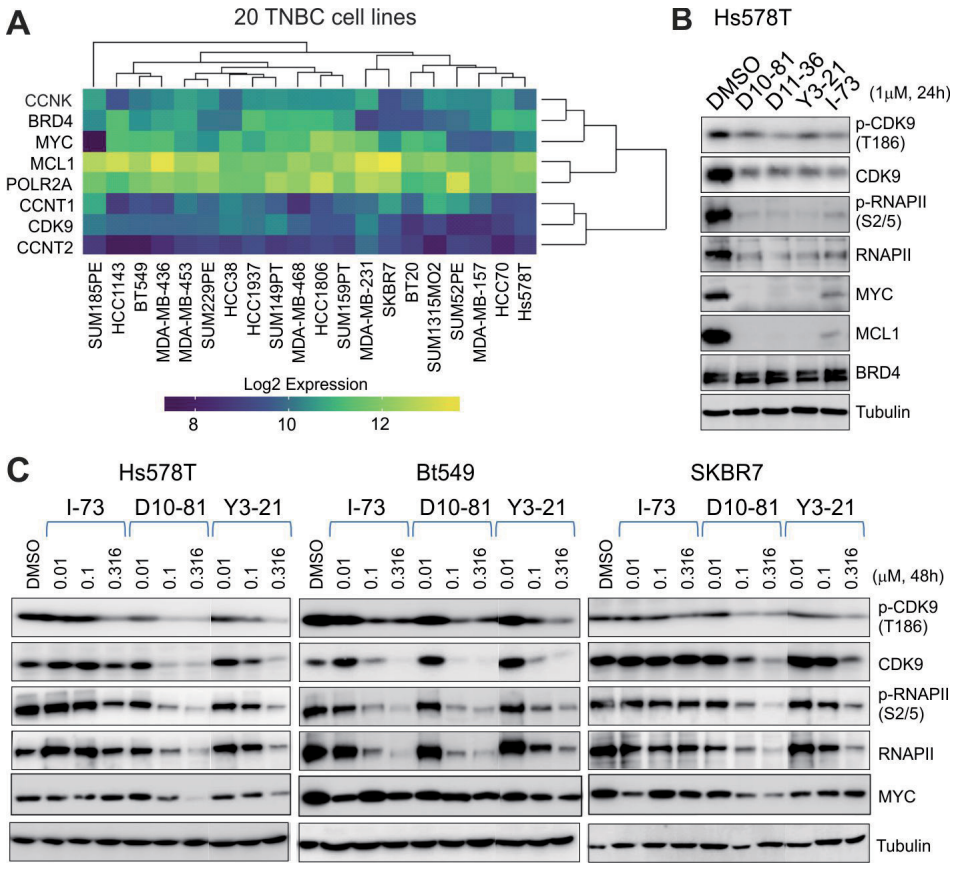

Figure 3. Targeting CDK9 inhibits P-TEFb-mediated transcriptional signaling transduction in TNBC cells. (**A**) Expression of P-TEFb complex members and associated components in various TNBC cell lines, as established by RNA-Seq analysis at Log2 expression levels. (**B**) Effect of CDK9 inhibitors D10-81, D11-36, Y3-21 and I-73 on P-TEFb activity and downstream targets in Hs578T cells. Cells were treated with inhibitors at 1μM for 24h. JQ1, BRD4 inhibitor. (**C**) Impact of I-73, D10-81 and Y3-21 on P-TEFb activity and downstream targets in representative Hs578T, BT549, and SKBR7 TNBC cells 48h post-exposure to each inhibitor in dose range (0.01, 0.1 or 0.316 μM),

Targeting CDK9 suppresses pro-survival proteins in tandem with apoptosis onset in TNBC cells

The anti-proliferative effects of the CDK9 inhibitory compounds, including I-73, Y3-21 and D10-81 (Figure 2C), were subsequently validated in selected TNBC lines Hs578T, BT549 and SKBR7 in separate experiments (Figure 4A). We focused on

I-73 (our previously reported CDKI-73[23,33,34]), Y3-21, and D10-81. Apoptosis assays revealed that these inhibitors induced apoptosis in TNBC cell lines in both a concentration- and time-dependent manner (Figure 4B). The concurrent inverse effects of the three CDK9 inhibitors on cell proliferation and apoptosis were also observed in three additional TNBC cell lines, MDA-MB-231, HCC1806 and HCC38 (Supplementary Figure S3). Given that the CDK9 inhibitors potently induced cell death, we sought to investigate the associated disruption of anti-apoptotic factors in TNBC cells. 48 hours post-treatment, D10-81 (0.1 μM), I-73 (0.316 μM) and Y3-21 (0.1 μM) drastically depleted levels of pro-survival, anti-apoptotic BCL-2 family members MCL1 and BCL-xL in Hs578T, BT549 and SKBR7 cells (Figure 4C). Expression of XIAP (X-linked inhibitor of apoptosis) and survivin, two members of the inhibitors of apoptosis (IAP) family which antagonise apoptosis by binding to and preventing the activation of caspase-3 and caspase-7[35–37], was also down-regulated post-treatment (Figure 4C). Intriguingly, all three inhibitors robustly induced H2AX phosphorylation at S139 (γ-H2AX), a marker indicative of DNA replication stress and DNA double-stranded breaks, implying that targeting P-TEFb/CDK9 also induced indirect DNA damage in TNBC cells (Figure 4C).

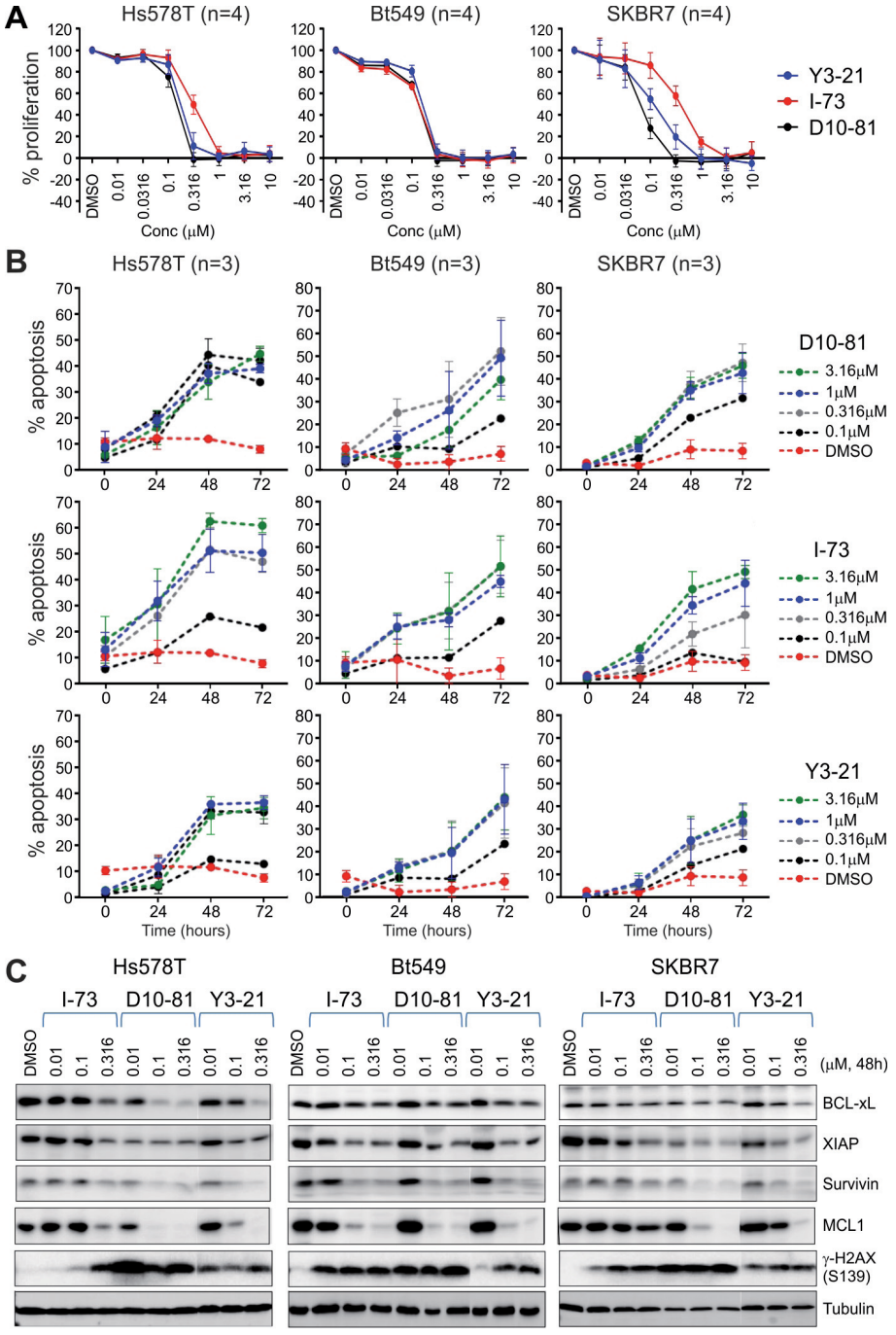

Figure 4. CDK9 inhibitors induce apoptosis in TNBC cells. (**A**) Validation of the anti-proliferative effects of the CDK9 inhibitors D10-81, I-73 and Y3-21 in selected TNBC cell lines Hs578T, BT549 and SKBR7. Data represented as mean +/- standard deviation (n = 4). (**B**) Apoptosis induction by the CDK9 inhibitors in TNBC cell lines Hs578T, BT549 and SKBR7. Cells were exposed to a dose range of each inhibitor (0.1-3.16 μM), and stained with Annexin-V and Hoechst as described for imaging at 24 hours, 48 hours and 72 hours post-exposure to CDK inhibitors or vehicle control (DMSO). Data were shown as % Annexin-V-positive cells, represented as mean +/- standard deviation (n = 3). (**C**) Impact of I-73, D10-81 and Y3-21 in dose range (0.01, 0.1 or 0.316 μM) on the inhibition of anti-apoptotic factors and the induction of DNA damage in representative Hs578T, BT549 and SKBR7 cells, 48 hours post-treatment.

CDK9 inhibitors rapidly down-regulate MCL-1 accompanied by DNA damage induction

Considering MCL1 expression was clearly down-regulated by the CDK9 inhibitors and that the turnover of MCL1 protein occurs very rapidly, we therefore followed the effect of CDK9 inhibitors D10-81, Y3-21 and I-73 on MCL1 expression in TNBC cells over a time period of 48 hours. After 4-8 hours, all three CDK9 inhibitors down-regulated MCL1 protein levels, with Y3-21 and D10-81 being most effective in the three TNBC cell lines evaluated. The CDK9 inhibitors also induced a concomitant increase in γH2AX (S139) levels, coinciding with MCL1 depletion (Figure 5A-C). The effect on MCL1 down-regulation was partly reflected by reduction in RNAPII CTD phosphorylation (Ser2/5), although full depletion of RNAPII levels and phosphorylation were only noted after 24 hours (Figure 5A-C). The rapid degradation of MCL1 was mediated through a ubiquitin-mediated proteasomal manner, since pre-treatment for 2 hours with an inhibitor of the proteosomal machinery, MG-132, rescued the loss of MCL1 protein induced by all three CDK9 inhibitors (Figure 5D). Hence, targeting CDK9 leads to a rapid depletion of anti-apoptotic MCL1 levels in TNBC cells through the proteasomal pathway and is accompanied by activation of the DNA damage response.

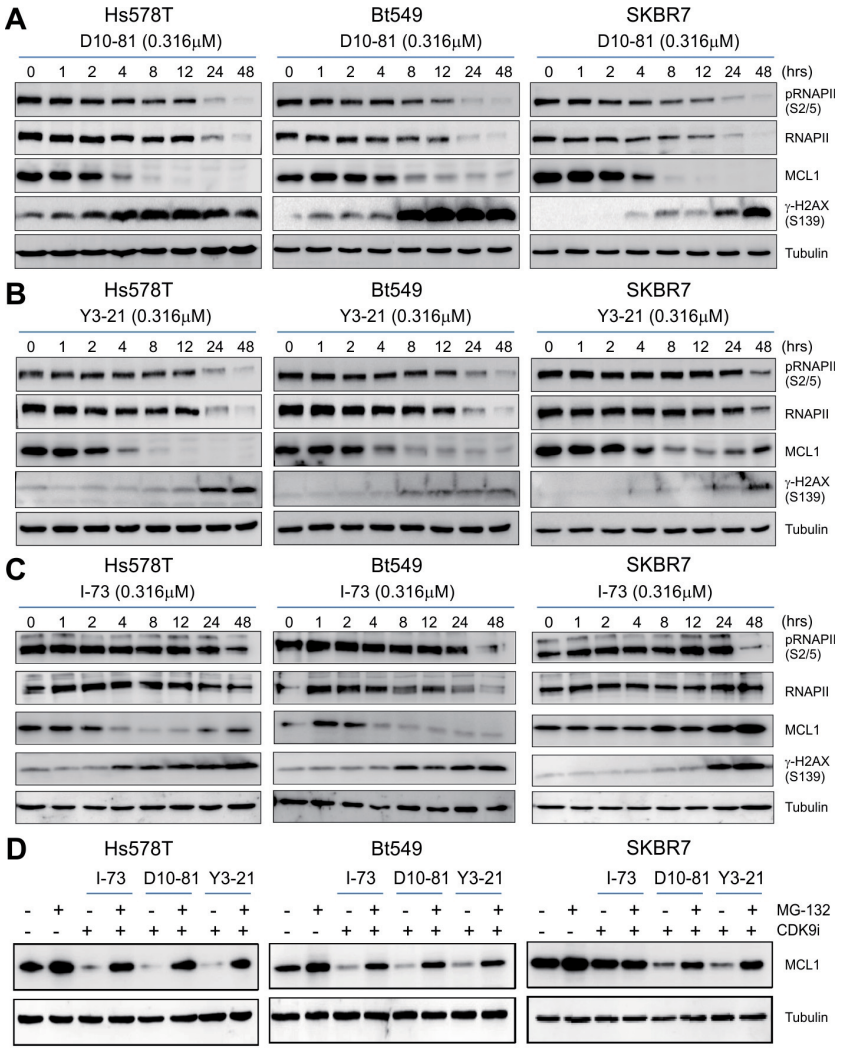

Figure 5. Kinetics of P-TEFb complex inhibition, MCL-1 degradation, and induction of DNA damage in TNBC cells. Effect of D10-81 (**A**), Y3-31 (**B**) and I-73 (**C**) on CDK9-mediated RNAPII phosphorylation, MCL-1 levels and DNA damage marker γ-H2AX (S139) in a time course in representative Hs578T, BT549 and SKBR7 cells. Cells were treated with vehicle control (DMSO) or inhibitor (0.316μM) for the indicated duration. (**D**) Proteasome dependence of CDK inhibitor-mediated MCL1 depletion in TNBC cell lines Hs578T, BT549 and SKBR7. Cells were pre-treated with proteasome inhibitor (MG-132; 10μM) for 2 hours before being treated with vehicle (DMSO) or I-73, D10-81 or Y3-21 (0.316μM) for 6 hours.

CDK9 inhibition leads to transcriptional reprogramming of multiple oncogenic signalling pathways in TNBC cells

Since the P-TEFb complex controls transcription, we anticipated that pharmacological targeting of CDK9 would drastically affect the transcriptional programme in TNBC. We systemically compared the transcriptome by RNA-sequencing of Hs578T cells treated for 6 hours with the CDK9 inhibitors D10-81 (0.1 μM), Y3-21 (0.1 μM) or I-73 (0.316 μM). We identified 3631 genes that were commonly affected by the three CDK9 inhibitors, of which 86% (3137 genes) were down-regulated (Log2 Fold Change (FC) ≤ -1.0) and 14% (494 genes) up-regulated (Log2 FC ≥ 1.0) post-treatment (Figure 6A). These inhibitors altered the transcriptomic profile of Hs578T cells to similar degrees, suggesting a high-degree of target specificity and biological mode-of-action (Figure 6B). Ingenuity Pathway Analysis (IPA) analysis revealed the top 20 canonical pathways (Supplementary S4A) and the top 20 biological function networks (Supplementary Figure S4B) that were most significantly disturbed by these CDK9 inhibitors. Gene Set Enrichment Analysis (GSEA) of the pathways indicated that genes commonly down-regulated by D10-81, I-73 and Y3-21 were enriched for multiple oncogenic machineries (Supplementary Figure S5), including adipogenesis, TGF-β signalling, Wnt/β-catenin signalling, stem cell pluripotency, G1/S checkpoint regulation, EMT, and BMP signalling (Figure 6C), amongst others (Supplementary Figure S4A). Notably, the inhibitors massively suppressed expression of genes involved in gene transcription (Figure 6D, Supplementary Figure S4B), further suggesting that TNBC cells depend on transcriptional CDK9 function. Moreover, activation of the DNA damage response, apoptosis, and necrosis was predicted (Supplementary Figure S4B), consistent with disruption of the pro/anti-apoptotic equilibrium and induction of DNA damage

(γH2AX), as demonstrated (Figure 4C). Of the 3137 commonly down-regulated genes, multiple anti-apoptotic BCL2 family members, such as BCL2, BCL2L11, BCL2L15 and MCL1, as well as the apoptosis inhibitor XIAP, were significantly down-regulated in Hs578T cells after treatment with the inhibitors (Figure 6E). MCL1 transcripts were most profoundly affected, being decreased at least 8-fold, compared to control conditions (Figure 6E). Thus, whilst D10-81, I-73 and Y3-21 enhance the proteasome-mediated degradation of MCL1, they also prevent the transcription of MCL1 and other vital pro-survival genes. Downstream effect analysis also predicted strong suppression of cell cycle progression as a consequence of the sensitivity to D10-81, I-73 and Y3-21 (Figure 6C, Supplementary Figure S4B). A number of key G1/S checkpoint regulators, including cyclin E (CCNE1, CCNE2) and E2F family members (E2F2, E2F3, E2F5, E2F6), and genes in G2/M DNA damage checkpoint regulation, including ABL1, MDM2, WEE1, were suppressed by D10-81, I-73 and Y3-21 (Figure 6F). Given the DNA damage activation and pro-survival downregulation in TNBC cells, we further validated the impact of the inhibitors on cell cycle progression in Hs578T cells, revealing a significant accumulation of cells in G2/M phase, accompanied by significantly reduced numbers of cells in S phase after 48 hour exposure to I-73 and D10-81 at 0.316 μM (Figure 6G).

Since D10-81, I-73 and Y3-21 predominantly affected TGF-β, Wnt/β-catenin, and BMP signalling (Supplementary Figure S5), we scrutinised the down-regulated transcripts involved in these pathways and identified a group of genes whose expression was particularly susceptible to CDK9 inhibition (Figure 6H). SMAD family members (including SMAD1, SMAD4, SMAD5, SMAD6 and SMAD9), which act as signal transducers and transcription factors for the TGF-β pathway[38], were the core

genes most potently down-regulated. Additionally, given that TGF-β, Wnt/β-catenin, and BMP signalling are strongly linked to the migratory and invasive ability of cancer cells, we hypothesised that their downregulation by the CDK9 inhibitors may obstruct TNBC cell migration. Low doses of D10-81, I-73 and Y3-21 (i.e. 0.01 μM), which neither inhibited proliferation nor induced appreciable apoptosis or cell cycle arrest, led to a significant reduction in the migratory ability of Hs578T cells (Figure 6I). The results above demonstrate that targeting CDK9 exerts inhibitory effects on transcription factor function in TNBC cells, leading to reduced levels of pro-survival transcripts (*e.g.* MCL1 and BCL-xL) whilst also downregulating TGF-β, Wnt/β-catenin and BMP signalling, likely resulting in reduced migratory and proliferative capacity.

CDK inhibitors prevent the expression of a selection of transcription factors essential for the proliferation of TNBC cells

It has been shown that inhibition of transcriptional CDKs results in collapse of super-enhancer-driven oncogenic transcriptional programmes and subsequent cancer cell death due to loss of transcription factors (e.g. MYC, SOX9, EGFR, STAT) and other short-lived transcripts (e.g. MCL1) crucial for maintenance of cellular viability[14,16,18,39,40]. Our results showed that D10-81, I-73 and Y3-21 altered the transcriptomic profile of Hs578T cells, affecting the expression of 565 transcription-regulatory genes, of which 543 genes (96%) were markedly down-regulated (Figure 6D). We therefore sought to investigate whether down-regulation of these transcriptional regulators was detrimental to TNBC cell survival and thereby identify genes whose suppression is, at least in part, responsible for the anti-proliferative effects elicited by P-TEFb inhibition. Of the down-regulated 543 transcriptional regulators, the top 80 genes most sensitive to down-regulation by the CDK9

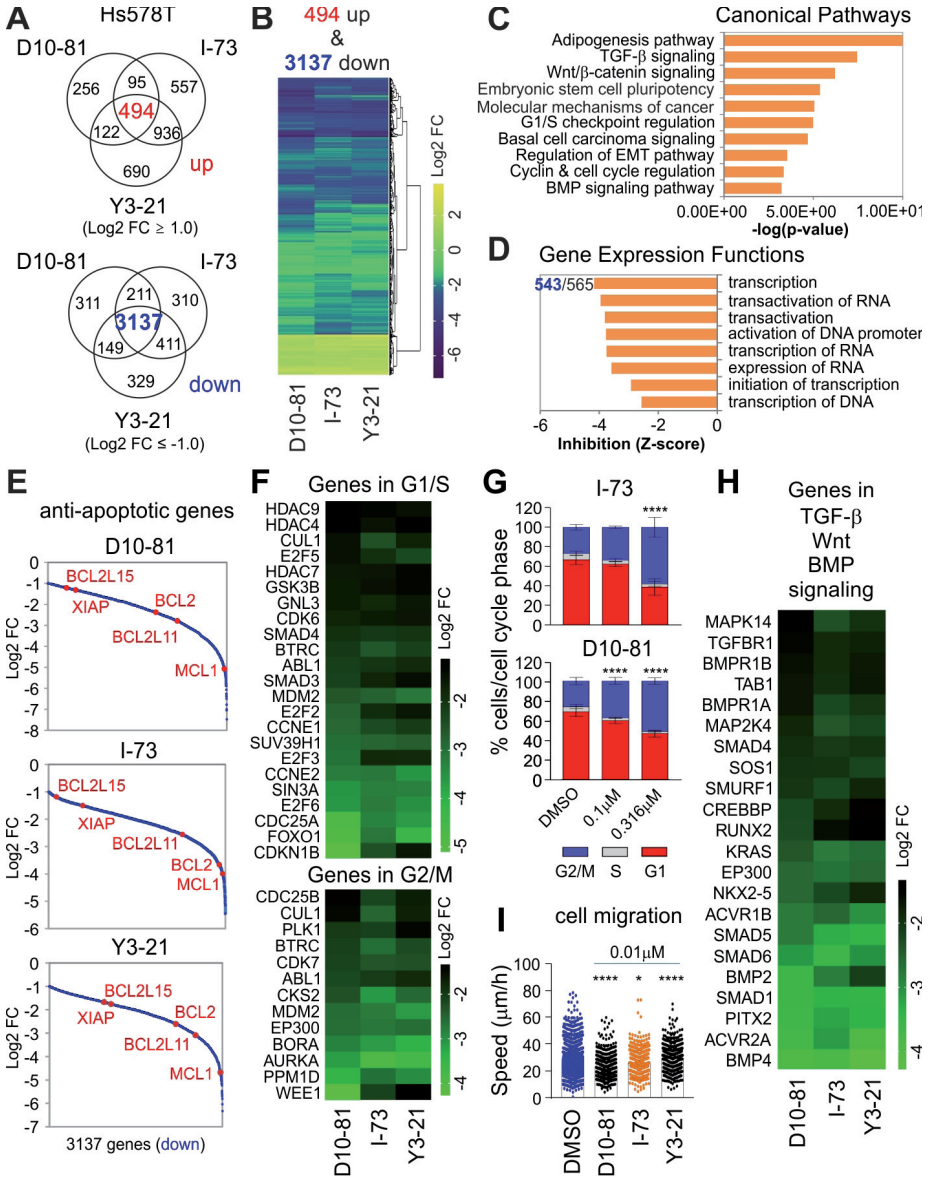

Figure 6. CDK9 inhibitors induce transcriptome reprogramming and disruption of oncogenic canonical pathways in TNBC cells. (**A**) RNA-Seq transcriptome profiling of 494 up- and 3137 down-regulated genes commonly affected by CDK9 inhibitors in TNBC Hs578T cells. Cells were treated with D10-81 (0.1μM), I-73 (0.316μM) or Y3-21 (0.1μM) for 6 hours. Gene expression levels were presented as Log2 Fold Change (Log2 FC), by normalising treatment condition to vehicle control DMSO. A cut-off of Log2 FC ≥ ±1.0 (i.e. FC = 2.0) was used to select significantly up- (Log2 FC ≥ 1.0) and down-regulated (Log2 FC ≤ -1.0) genes. (**B**). Heatmap-based representation of the differentially expressed genes regulated by CDK9 inhibitors. (**C**) Ingenuity Pathway Analysis (IPA) of 494 up- and 3137 down-regulated transcripts revealed significant enrichment of multiple pro-oncogenic signalling pathways (in –log p-value). (**D**). Significant inactivation of gene expression programs by CDK9 inhibition (in Z score). (**E**). Downregulation of BCL2 pro-survival members and IAP factor XIAP by CDK9 inhibitors. (**F**) Genes in G1/S and G2/M cell cycle checkpoints targeted by CDK9 inhibitors. (**G**) Induction of cell cycle G2/M arrest in Hs578T cells by CDK9 inhibitors. Cells were exposed to I-73 or D11-81 (0.1 or 0.316 μM) for 48 hours. Mean ± standard deviation (n = 3). Two-way ANOVA with Tukey's multiple comparison test; **** $p < 0.0001$. (**H**) Genes involved in BMP, TGF-β and Wnt/β-catenin signalling targeted by CDK9 inhibitors. (**I**) Impact of sub-lethal doses of CDK9 inhibitors D10-81, I-73 and Y3-21 on inhibition of cell migration of Hs578T cells. Cells were traced during 16 hours of exposure. Average migration speed was presented as mean ± standard deviation (n = 2). **** $P < 0.0001$. * $P < 0.0191$ (significant if $P < 0.05$)

inhibitors (Log2 FC ≤ -3.0 under D10-81 treatment) compared to DMSO control (Figure 7A) were silenced using siRNA transfection in Hs578T and BT549 cells (Figure 7B). An inhibitory effect of silencing on proliferation was observed for a number of genes, whose knockdown significantly inhibited proliferation (FC ≥ 1.5) in both Hs578T and BT549 cells. Silencing of PLAG1, SERTAD3, RARA, PAX6, NR2C2, SALL1 and EN1 reduced proliferation by at least 50% compared to control conditions (Figure 7B, Supplementary Figure S6A-B). Additionally, differential proliferative responses after gene silencing were observed; Hs578T cells being more sensitive to NRIP1 silencing, whilst BT549 cells being more sensitive to IRF2BP1 silencing (Figure 7B). Subsequent deconvolution screening with either pooled siRNAs or constituent single siRNAs confirmed the silencing effect of a number of transcription factors, including RARA, EN1, GATA2, SOX9, PLAG1, PAX9, and NR2C2, whose knockdown (minimum 2 out of 4 single siRNAs) reduced cell proliferation by >50% in Hs578T (Figure 7C) and BT549 cells (Supplementary Figure S6C).

Having identified a number of transcription regulators critical for the proliferation of two TNBC cell lines, we then investigated the expression of these factors in 1881 breast tumours (stratified according to PAM50 subtypes[41]) by virtue of the gene expression-based outcome for breast cancer online (GOBO) dataset[42] to identify factors specifically enriched in TNBC tumours. The expression of the transcription factors EN1, SOX9 and PLAG1 was significantly higher in basal-like breast tumours, compared to the other intrinsic breast tumour subtypes (Supplementary Figure S6D). Particularly, EN1, SOX9 and PLAG1 were expressed at significantly higher levels in ER- breast tumours compared to ER+ breast tumours, suggesting these transcription

factors represent TNBC-specific dependencies (Figure 7D). Indeed, silencing of these putative TNBC-specific transcription factors SOX9, EN1 and PLAG1 also significantly reduced the proliferation of two other TNBC cell lines, SKBR7 and SUM149PT (Figure 7E; $p < 0.0001$), indicative of the essential roles of these transcription factors in promoting proliferation of TNBC cells.

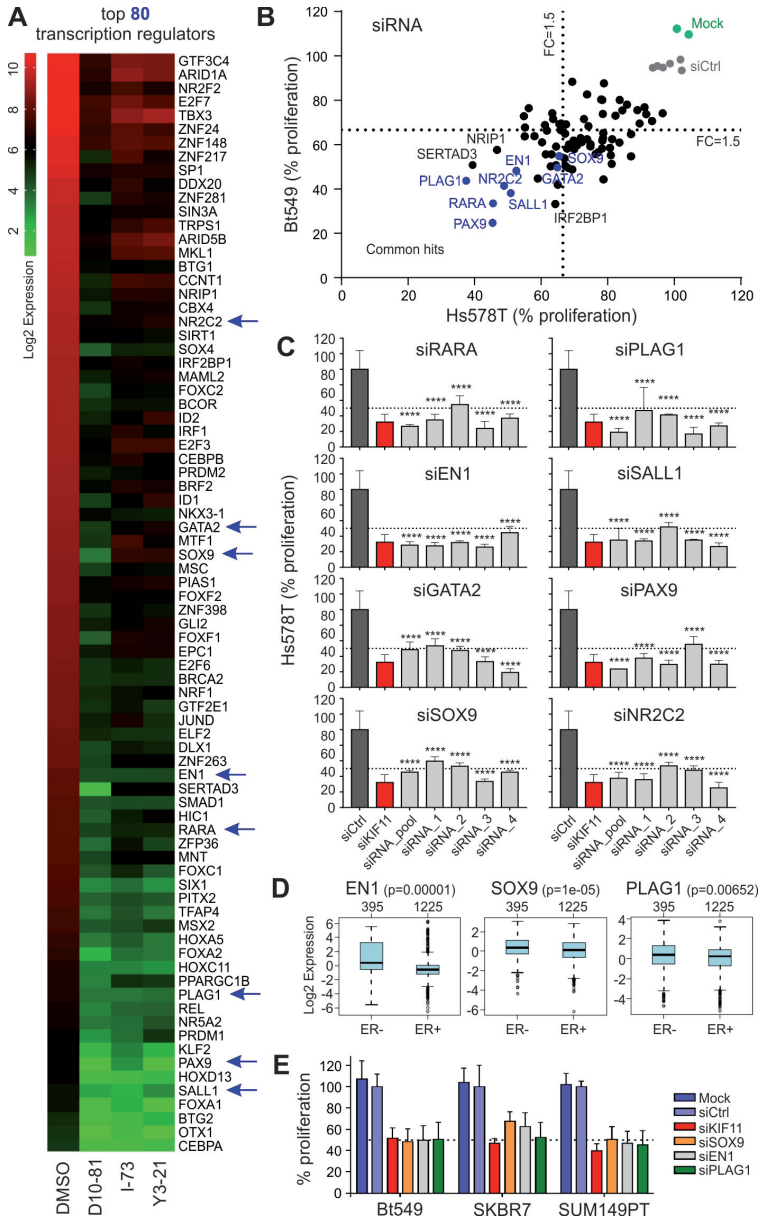

Figure 7. Targeting CDK9 down-regulates a selection of transcription factors essential for the proliferation of TNBC cells. (**A**). Expression of the top 80 transcription regulators (among the 543 genes, Figure 6D) most strongly down-regulated by CDK9 inhibitors D10-81 (0.1 µM), I-73 (0.316 µM) and Y3-21 (0.1 µM), compared to control condition DMSO, shown as Log 2 expression levels. (**B**) siRNA screening of the 80 transcription regulators essential for the proliferation of Hs578T and BT549 TNBC cells. Results shown as % proliferation relative to negative siRNA control (siCtrl, a pool of individual 720 kinase siRNAs from Dharmacon siKinase Library, at stock concentration of 1 µM, with negligible effect on gene expression as determined by RNA seq; data not shown). Mock, no siRNA transfection. Fold change (FC) 1.5, proliferation reduced to 66.6%, compared to siCtrl. (**C**). Validation of transcription factors controlling proliferation in Hs578T cells. Cells were transfected with pooled and 4 individual siRNA sequences for 96 hours. Genes whose silencing reduced proliferation by >50% compared to control, and for which at least 2 out of 4 single siRNAs elicited the same effect, were considered as validated hits. siKIF11, siRNA targeting KIF11, as positive control. Data shown as mean ± standard deviation (n = 2). **** P < 0.0001 One-way ANOVA with Tukey's multiple comparisons test. (**D**). Expression of EN1, SOX9 and PLAG1 in ER- (395) compared with ER+ (1225) breast tumours. Data derived from GOBO dataset[42]. (**E**). Effect of SOX9, EN1 or PLAG1 silencing on the proliferation of BT549, SKBR7 and SUM149PT cells.

DISCUSSION

Inhibition of transcriptional CDKs has become an attractive therapeutic strategy by which the dependence of various cancers on aberrant transcriptional programs can be exploited. The evidence presented here demonstrates that CDK9 and its P-TEFb complex-associated targets RNAPII, MYC and MCL1 are highly expressed in patient TNBC tumours. Importantly, TNBC cells are exceptionally sensitive to disruption of P-TEFb/CDK9-regulated transcriptional machinery by CDK9 inhibitors. Interestingly, TNBC cells showed greater sensitivity to inhibitors of transcriptional regulatory CDKs such as CDK7 or CDK9, compared to those targeting cell cycle regulatory CDKs such as CDK4/6, consistent with recently published results which indicate that androgen receptor-positive TNBC exhibits unique sensitivity to CDK4/6 inhibitors[30]. This is the first demonstration of the efficacy of the CDK9 inhibitor I-73 and the novel analogues D10-81, Y3-21, D11-36, D11-69, and Y3-29 against triple-negative breast cancer cells.

Cancer cells are notoriously dependent on a delicate equilibrium regarding pro- and anti-apoptotic factors; high-levels of pro-survival MCL1, BCL2 and survivin are necessary to maintain enhanced proliferative capacity and to prevent apoptosis induced by external stresses such as anti-cancer drugs[35,43–45]. MCL1 antagonises the action of pro-apoptotic BCL-2 family members by sequestering BIM, thereby preventing BAX/BAK activation and the subsequent collapse of mitochondrial membrane integrity[46]. MCL1 in particular, as both an mRNA transcript and protein, has a remarkably short half-life and rapid turn-over rate[6]. As such, the function of MCL1 is highly sensitive to interference with the transcriptional machinery[7,47]. We demonstrate here that CDK9 inhibitors D10-81, Y3-21 and I-73 potently induced

apoptosis in different TNBC cell lines, accompanied by depletion of anti-apoptotic factors. These inhibitors prevent transcription of MCL1 mRNA, inducing rapid proteasome-dependent degradation of MCL1 protein. However, whilst MCL1 inhibitors have shown effective activity against other cancer cell types[48] we were unable to demonstrate an effect of MCL1 inhibitors in our TNBC cells (data not shown). Likely, MCL1 inhibition is not sufficient in itself to promote TNBC cell death and it is the coordinated loss of a large panel of cyto-protective genes that promotes TNBC cell demise.

The use of transcriptional CDK inhibitors has previously identified groups of transcription factors whose expression is regulated by super-enhancers and which drive oncogenic transcriptional programmes in multiple cancers, including TNBC, to maintain a malignant cell state[14,16,18,39,40]. The expression of these transcription factors is exquisitely sensitive to functional perturbations of transcriptional CDKs, due to the association of P-TEFb with super-enhancers and the dependence of these regions on P-TEFb function to maintain high levels of oncogenic super-enhancer-driven transcription[14,16,18,39,40]. Probing the many transcription factors whose expression was inhibited by D10-81, I-73 and Y3-21, revealed a group of transcription factors, including RARA, EN1, GATA2, SOX9, PLAG1, SALL1, PAX9 and NR2C2, whose silencing was detrimental to TNBC cell proliferation. EN1, SOX9 and PLAG1 were significantly highly expressed in basal-like and ER- breast tumours. Moreover, EN1 and SOX9 have previously been identified as super-enhancer-related transcription factors in BT549 cells and their expression is also highly sensitive to CDK7 inhibitor THZ1[18]. EN1 has also been identified as an essential pro-survival transcription factor in basal-like breast cancer, its overexpression promoting

resistance to taxol and rotenone[49]. Consistently, EN1 also protects murine dopaminergic neurons from apoptotic insults in the form of mitochondrial complex I inhibitor MPTP, by enhancing the translation of respiratory complex I subunit Ndufs1[50]. Thus, given that Ndufs1 is an EN1 target gene and that its caspase 3-mediated cleavage is a pivotal step in the loss of mitochondrial membrane integrity during the apoptotic cascade, elucidating if or how EN1 overexpression protects TNBC cells from apoptosis will shed light on its function in this context[51]. SOX9 is known to regulate activation of Wnt/β-catenin signalling in prostate cancer by up-regulating FZD and LRP family members[52]. SOX9 is highly expressed in TNBC tumours and is an essential regulator of migration, invasion and proliferation in multiple tumours[53]. SOX9 is also a putative cancer stem cell marker and determines the plasticity of cancer cells via an epigenetic switch which allows SOX9 to up-regulate EMT-promoting transcription factors such as SLUG[53–56]. Evaluating the efficacy of the inhibitors tested here against breast cancer stem cell (BCSC)-enriched populations would therefore be prudent. PLAG1 is a proto-oncogene, the overexpression of which is linked to hepatoblastomas, lipoblastomas and adenomas of the salivary glands[57–59]. Ectopic overexpression of PLAG1 leads to uncontrolled proliferation via IGF-2 and it is also known to interact with oncogenic fusion protein CBFB-MYH11 in myeloid leukaemia to promote leukaemogenesis[60]. Other documented downstream targets of PLAG1 include BCL-2, BPGF-1, CRABP-II and PIGF[61]. Although there is a lack of information regarding the role of PLAG1 in TNBC, we show that PLAG1 knockdown reduced the proliferation of multiple TNBC cells, warranting further assessment of its role in their maintenance. It will be essential to further assess whether these transcription factors critical for TNBC cell survival are associated with super-enhancer function and whether targeting CDK9 using inhibitors

I-73, D10-81 and Y3-21 preferentially affects binding of components of the transcriptional apparatus (e.g. BRD4) to the promoters of super-enhancer-associated genes.

Altogether, our results identify targeting the P-TEFb complex via CDK9 inhibition as a potential addition to a rapidly growing arsenal of targeted therapies against TNBC. Whilst the relationship between target specificity and anti-TNBC effects necessitates extensive further investigation, the identification of prospective TNBC-specific transcription factor dependencies which are indirectly targeted by P-TEFb/CDK9 inhibition, exemplifies the potential utility of such an approach in TNBC, but also in other malignancies which may be addicted to aberrant transcriptional programs.

FUNDING

This work was supported by the ERC Advanced grant Triple-BC (grant no. 322737) and the Dutch Cancer Society project (grant nr 2011-5124).

REFERENCES

1. Lehmann, B. D. *et al.* Refinement of Triple-Negative Breast Cancer Molecular Subtypes: Implications for Neoadjuvant Chemotherapy Selection. *PLoS One* **11,** e0157368 (2016).
2. Boyle, P. Triple-negative breast cancer: epidemiological considerations and recommendations. *Ann. Oncol.* **23 Suppl 6,** vi7-12 (2012).
3. Masuda, H. *et al.* Differential response to neoadjuvant chemotherapy among 7 triple-negative breast cancer molecular subtypes. *Clin. Cancer Res.* **19,** 5533–40 (2013).
4. Villicaña, C., Cruz, G. & Zurita, M. The basal transcription machinery as a target for cancer therapy. *Cancer Cell International* **14 (1):**18 (2014).
5. Bywater, M. J., Pearson, R. B., McArthur, G. A. & Hannan, R. D. Dysregulation of the basal RNA polymerase transcription apparatus in cancer. *Nat Rev Cancer* **13 (5):** 299-314 (2013).
6. Iglesias-Serret, D., Piqué, M., Gil, J., Pons, G. & López, J. M. Transcriptional and translational control of Mcl-1 during apoptosis. *Arch. Biochem. Biophys.* **417,** 141–152 (2003).
7. Adams, K. W. & Cooper, G. M. Rapid turnover of Mcl-1 couples translation to cell survival and apoptosis. *J. Biol. Chem.* **282,** 6192–6200 (2007).
8. Peterlin, B. M. & Price, D. H. Controlling the Elongation Phase of Transcription with P-TEFb. *Molecular Cell* **23,** 297–305 (2006).
9. Ni, Z. *et al.* P-TEFb is critical for the maturation of RNA polymerase II into productive elongation in vivo. *Mol. Cell. Biol.* **28,** 1161–1170 (2008).

10. Glover-Cutter, K. *et al.* TFIIH-Associated Cdk7 Kinase Functions in Phosphorylation of C-Terminal Domain Ser7 Residues, Promoter-Proximal Pausing, and Termination by RNA Polymerase II. *Mol. Cell. Biol.* **29,** 5455–5464 (2009).
11. Wu, C. H. *et al.* NELF and DSIF cause promoter proximal pausing on the hsp70 promoter in Drosophila. *Genes Dev.* **17,** 1402–1414 (2003).
12. Itzen, F., Greifenberg, A. K., Christian, A. B. & Geyer, M. Brd4 activates P-TEFb for RNA polymerase II CTD phosphorylation. *Nucleic Acids Res.* **42 (12):** 7577–7590 (2014).
13. Moon, K. J. *et al.* The bromodomain protein Brd4 is a positive regulatory component of P-TEFb and stimulates RNA polymerase II-dependent transcription. *Mol. Cell* **19,** 523–534 (2005).
14. Lovén, J. *et al.* Selective inhibition of tumor oncogenes by disruption of super-enhancers. *Cell* **153,** 320–334 (2013).
15. Hnisz, D. *et al.* Convergence of Developmental and Oncogenic Signaling Pathways at Transcriptional Super-Enhancers. *Mol. Cell* **58,** 362–370 (2015).
16. Cayrol, F. *et al.* THZ1 targeting CDK7 suppresses STAT transcriptional activity and sensitizes T-cell lymphomas to BCL2 inhibitors. *Nat. Commun.* **8,** 14290 (2017).
17. Christensen, C. L. *et al.* Targeting Transcriptional Addictions in Small Cell Lung Cancer with a Covalent CDK7 Inhibitor. *Cancer Cell* **26,** 909–922 (2014).
18. Wang, Y. *et al.* CDK7-Dependent Transcriptional Addiction in Triple-Negative Breast Cancer. *Cell* **163,** 174–186 (2015).
19. Horiuchi, D. *et al.* MYC pathway activation in triple-negative breast cancer is synthetic lethal with CDK inhibition. *J. Exp. Med.* **209,** 679–96 (2012).
20. Boffo, S., Damato, A., Alfano, L. & Giordano, A. CDK9 inhibitors in acute myeloid leukemia. *J. Exp. Clin. Cancer Res.* **37 (1):** 36 (2018).
21. Dey, J. *et al.* Voruciclib, a clinical stage oral CDK9 inhibitor, represses MCL-1 and sensitizes high-risk Diffuse Large B-cell Lymphoma to BCL2 inhibition. *Sci. Rep.* **7 (1):** 18007 (2017).
22. Brägelmann, J. *et al.* Systematic Kinase Inhibitor Profiling Identifies CDK9 as a Synthetic Lethal Target in NUT Midline Carcinoma. *Cell Rep.* **20,** 2833–2845 (2017).
23. Walsby, E. *et al.* A novel Cdk9 inhibitor preferentially targets tumor cells and synergizes with fludarabine. *Oncotarget* **5,** 375–85 (2014).
24. Tadesse, S. *et al.* Highly Potent, Selective, and Orally Bioavailable 4-Thiazol- *N* -(pyridin-2-yl)pyrimidin-2-amine Cyclin-Dependent Kinases 4 and 6 Inhibitors as Anticancer Drug Candidates: Design, Synthesis, and Evaluation. *J. Med. Chem.* **60 (5):** 1892-1915 (2017).
25. Robinson, M. D., McCarthy, D. J. & Smyth, G. K. edgeR: a Bioconductor package for differential expression analysis of digital gene expression data. *Bioinformatics* **26,** 139–40 (2010).
26. Liu, N. Q. *et al.* Prognostic significance of nuclear expression of UMP-CMP kinase in triple negative breast cancer patients. *Sci Rep.* **6:** 32027 (2016).
27. Zawistowski, J. S. *et al.* Enhancer remodeling during adaptive bypass to MEK inhibition is attenuated by pharmacologic targeting of the P-TEFb complex. *Cancer Discov.* **7,** 302–321 (2017).
28. Gargano, B., Amente, S., Majello, B. & Lania, L. P-TEFb is a crucial co-factor for Myc transactivation. *Cell Cycle* **6,** 2031–2037 (2007).
29. Gregory, G. P. *et al.* CDK9 inhibition by dinaciclib potently suppresses Mcl-1 to induce durable apoptotic responses in aggressive MYC-driven B-cell lymphoma in vivo. *Leukemia* **29 (6):** 1437-41 (2015).

30. Asghar, U. S. *et al.* Single-cell dynamics determines response to CDK4/6 inhibition in triple-negative breast cancer. *Clin. Cancer Res.* **23,** 5561–5572 (2017).
31. Dean, J., Thangavel, C., Mcclendon, A., Reed, C. & Knudsen, E. Therapeutic CDK4/6 inhibition in breast cancer: key mechanisms of response and failure. *Oncogene* **29,** 4018–4032 (2010).
32. Qin, G. *et al.* Palbociclib inhibits epithelial-mesenchymal transition and metastasis in breast cancer via c-Jun/COX-2 signaling pathway. *Oncotarget* **6 (39):** 41794-808 (2015).
33. Lam, F. *et al.* Targeting RNA transcription and translation in ovarian cancer cells with pharmacological inhibitor CDKI-73. *Oncotarget* **5,** 7691–704 (2014).
34. Cao, S. *et al.* Inhibition of CDK9 induces apoptosis and potentiates the effect of cisplatin in hypopharyngeal carcinoma cells. *Biochem. Biophys. Res. Commun.* **482,** 536–541 (2017).
35. Dohi, T., Beltrami, E., Wall, N. R., Plescia, J. & Altieri, D. C. Mitochondrial survivin inhibits apoptosis and promotes tumorigenesis. *J. Clin. Invest.* **114,** 1117–1127 (2004).
36. Tamm, I. *et al.* IAP-family protein Survivin inhibits caspase activity and apoptosis induced by Fas (CD95), bax, caspases, and anticancer drugs. *Cancer Res.* **58,** 5315–5320 (1998).
37. Deveraux, Q. L., Takahashi, R., Salvesen, G. S. & Reed, J. C. X-linked IAP is a direct inhibitor of cell-death proteases. *Nature* **388,** 300–304 (1997).
38. Mori, S. *et al.* TGF-β and HGF transmit the signals through JNK-dependent Smad2/3 phosphorylation at the linker regions. *Oncogene* **23,** 7416–7429 (2004).
39. Augert, A. & MacPherson, D. Treating Transcriptional Addiction in Small Cell Lung Cancer. *Cancer Cell* **26,** 783–784 (2014).
40. Chipumuro, E. *et al.* CDK7 inhibition suppresses super-enhancer-linked oncogenic transcription in MYCN-driven cancer. *Cell* **159,** 1126–39 (2014).
41. Bernard, P. S. *et al.* Supervised risk predictor of breast cancer based on intrinsic subtypes. *J. Clin. Oncol.* **27 (8):** 1160-7 (2009).
42. Ringné R, M., Fredlund, E., Hä Kkinen, J., Ke Borg, Å. & Staaf, J. GOBO: Gene Expression-Based Outcome for Breast Cancer Online. *PLoS One* **6 (3): e17911** (2011).
43. Yeh, Y.-Y. *et al.* Up-regulation of CDK9 kinase activity and Mcl-1 stability contributes to the acquired resistance to cyclin-dependent kinase inhibitors in leukemia. *Oncotarget* **6,** 2667–2679 (2015).
44. Akagi, H. *et al.* Suppression of myeloid cell leukemia-1 (Mcl-1) enhances chemotherapy-associated apoptosis in gastric cancer cells. *Gastric Cancer* **16,** 100–110 (2013).
45. Simonian, P. L., Grillot, D. a & Nuñez, G. Bcl-2 and Bcl-XL can differentially block chemotherapy-induced cell death. *Blood* **90,** 1208–16 (1997).
46. Perciavalle, R. M. *et al.* Anti-apoptotic MCL-1 localizes to the mitochondrial matrix and couples mitochondrial fusion to respiration. *Nat. Cell Biol.* **14,** 575–583 (2012).
47. Wei, G. *et al.* Chemical Genomics Identifies Small-Molecule MCL1 Repressors and BCL-xL as a Predictor of MCL1 Dependency. *Cancer Cell* **21,** 547–562 (2012).
48. Kotschy, A. *et al.* The MCL1 inhibitor S63845 is tolerable and effective in diverse cancer models. *Nature* **538**, 477-482 (2016).
49. Beltran, A., Graves, L. & Blancafort, P. Novel role of Engrailed 1 as a prosurvival transcription factor in basal-like breast cancer and engineering of interference peptides block its oncogenic function. *Oncogene* **33,** 4767–4777 (2013).
50. Alvarez-Fischer, D. *et al.* Engrailed protects mouse midbrain dopaminergic neurons

against mitochondrial complex I insults. *Nat. Publ. Gr.* **14 (10):** 1260-6 (2011).
51. Ricci, J.-E. *et al.* Disruption of Mitochondrial Function during Apoptosis Is Mediated by Caspase Cleavage of the p75 Subunit of Complex I of the Electron Transport Chain. *Cell* **117,** 773–786 (2004).
52. Ma, F. *et al.* SOX9 drives WNT pathway activation in prostate cancer. *J. Clin. Invest.* **126,** 1745–1758 (2016).
53. Larsimont, J. C. *et al.* Sox9 Controls Self-Renewal of Oncogene Targeted Cells and Links Tumor Initiation and Invasion. *Cell Stem Cell* **17,** 60–73 (2015).
54. Wu, Z.-Q. *et al.* Canonical Wnt signaling regulates Slug activity and links epithelial–mesenchymal transition with epigenetic Breast Cancer 1, Early Onset (BRCA1) repression. *PNAS* **109 (41):** 16654-16659 (2012).
55. Yang, C., Zhao, X., Cui, N. & Liang, Y. Cadherins Associate with Distinct Stem Cell-Related Transcription Factors to Coordinate the Maintenance of Stemness in Triple-Negative Breast Cancer. *Stem Cells Int.* **2017:** 5091541 (2017).
56. Guo, W. *et al.* Slug and Sox9 cooperatively determine the mammary stem cell state. *Cell* **148,** 1015–1028 (2012).
57. Van Dyck, F., Declercq, J., Braem, C. V. & Van De Ven, W. J. M. PLAG1, the prototype of the PLAG gene family: Versatility in tumour development (Review). *International Journal of Oncology* **30,** 765–774 (2007).
58. Hibbard, M. K. *et al.* PLAG1 fusion oncogenes in lipoblastoma. *Cancer Res.* **60,** 4869–4872 (2000).
59. Matsuyama, A., Hisaoka, M., Nagao, Y. & Hashimoto, H. Aberrant PLAG1 expression in pleomorphic adenomas of the salivary gland: A molecular genetic and immunohistochemical study. *Virchows Arch.* **458,** 583–592 (2011).
60. Landrette, S. F. *et al.* Plag1 and Plagl2 are oncogenes that induce acute myeloid leukemia in cooperation with Cbfb-MYH11. *Blood* **105,** 2900–2907 (2005).
61. Voz, M. L. *et al.* Microarray screening for target genes of the proto-oncogene PLAG1. *Oncogene* **23,** 179–191 (2004).

SUPPLEMENTARY FIGURES

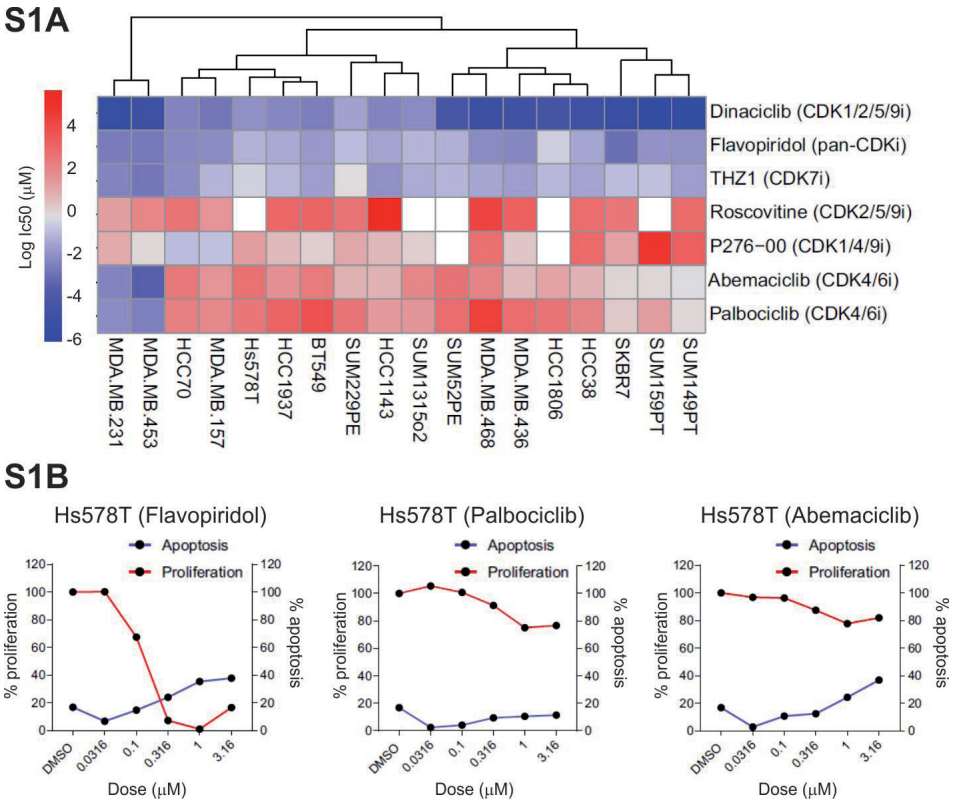

Supplementary Figure S1. Preferential sensitivity of TNBC cell lines to CDK inhibitors targeting CDK9 compared with CDK4/6-specific inhibitors. S1A. Heatmap showing the proliferation inhibitory concentrations (IC50s) of commercially available (THZ1) and clinically-approved or clinically-tested (abemaciclib, palbociclib, dinaciclib, flavopiridol, P276-00, roscovitine) CDK inhibitors in 18 TNBC cell lines. IC50s were calculated by GraphPad Prism, using nonlinear regression fitting. Areas in white: no inhibition of proliferation below 50% of control, meaning that IC50 cannot be calculated. **S1B.** Impact of CDK4/6-specific inhibitors (abemaciclib and palbociclib) and a pan-CDK inhibitor (flavopiridol) on proliferation and apoptosis induction in Hs578T cells. Data shown as % proliferation normalised to DMSO control (calculated as previously described) and % annexin-V-positive cells (for derivation see materials & methods). Data represented as mean +/- standard deviation (n = 2).

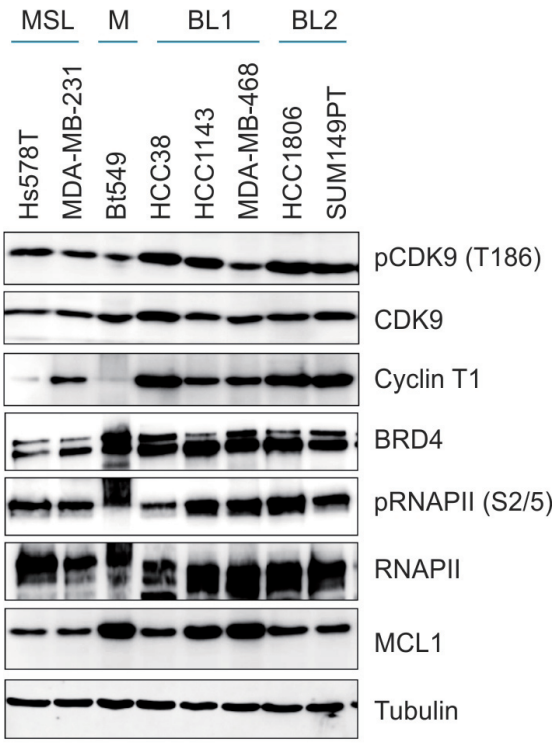

Supplementary Figure S2. Western blot analysis of the protein expression of P-TEFb complex members and downstream target genes (MCL-1 and MYC) in TNBC cell lines representative of four TNBC molecular subtypes. M: Mesenchymal. MSL: Mesenchymal stem-like. BL1: Basal-like 1. BL2: Basal-like 2. Cell lines were grown in 6-well plates for 24 hours before being lysed and subjected to immunoblotting.

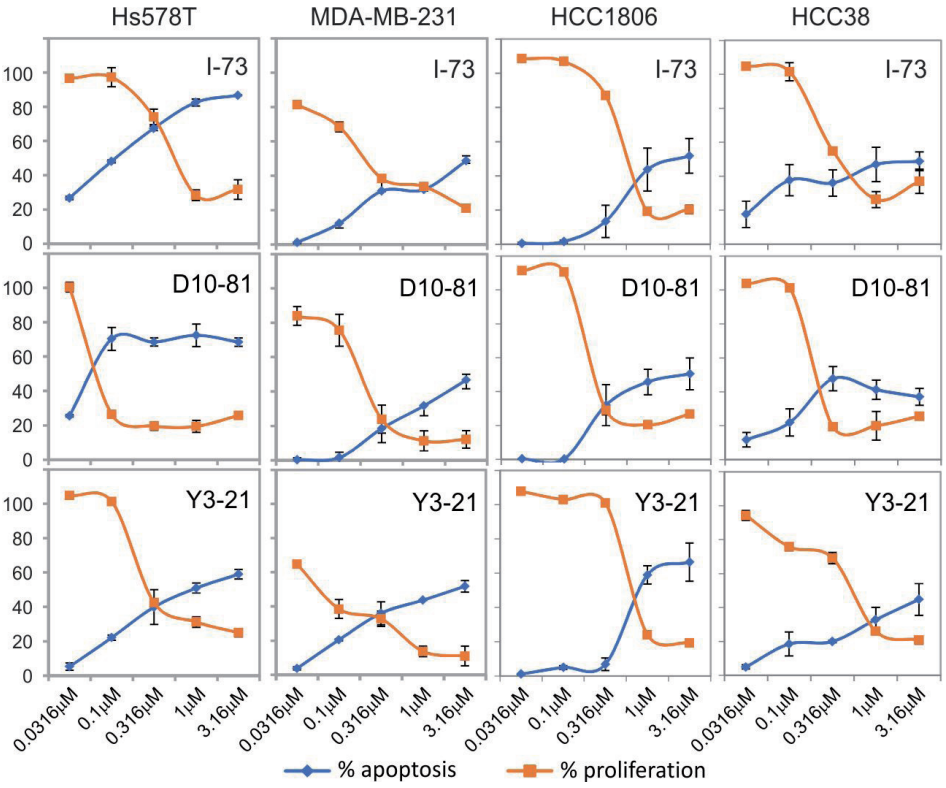

Supplementary Figure S3. Concurrent proliferation inhibition and apoptosis induction by CDK9 inhibitors in TNBC cells. Effect of I-73, D10-81 and Y3-21 on apoptosis induction in the representative Hs578T, MDA-MB-231, HCC1806 and HCC38 TNBC cells 72 hours post-exposure to inhibitor. Percentage of Annexin-V+ apoptotic cells was calculated using Cell Profiler software (see materials and methods). Data represented as mean +/- standard deviation (n = 2). Proliferation 96h post treatment normalised to DMSO control as described previously.

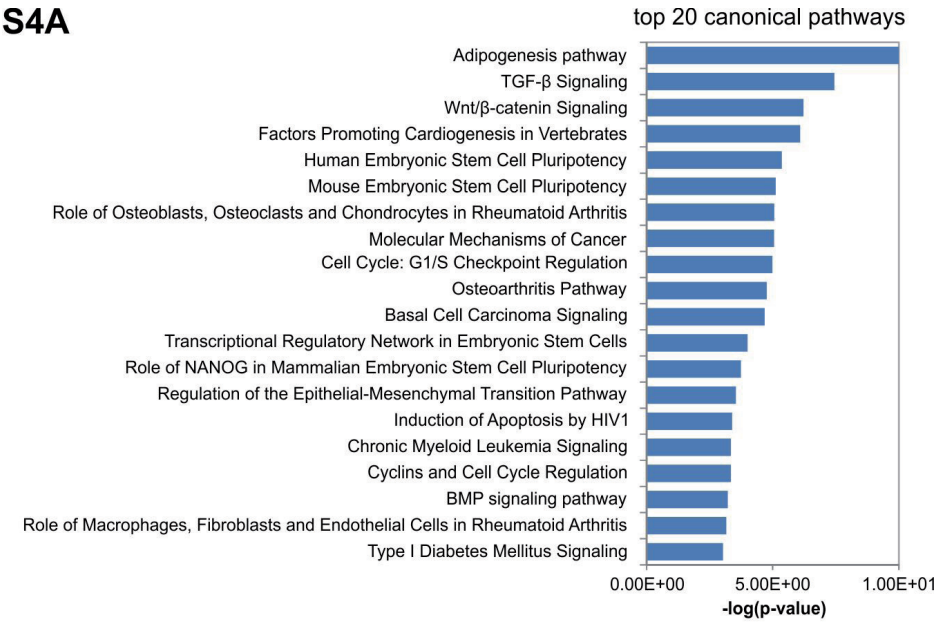

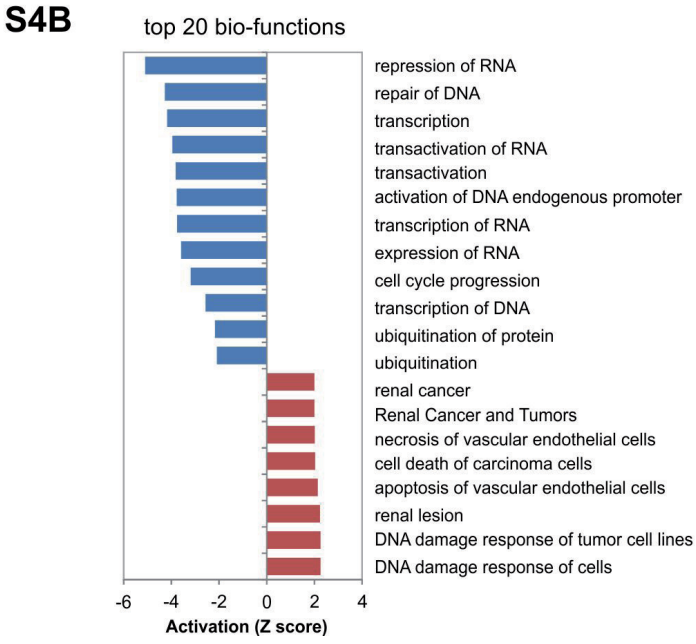

Supplementary Figure S4. CDK9 inhibitors distort the transcriptomic profile of TNBC cells. Top 20 canonical pathways (**S4A**) and top 20 biological function networks (**S4B**) significantly disrupted by CDK9 inhibition in Hs578T cells post-exposure to CDK9 inhibitors D10-81, I-73 and Y3-21.

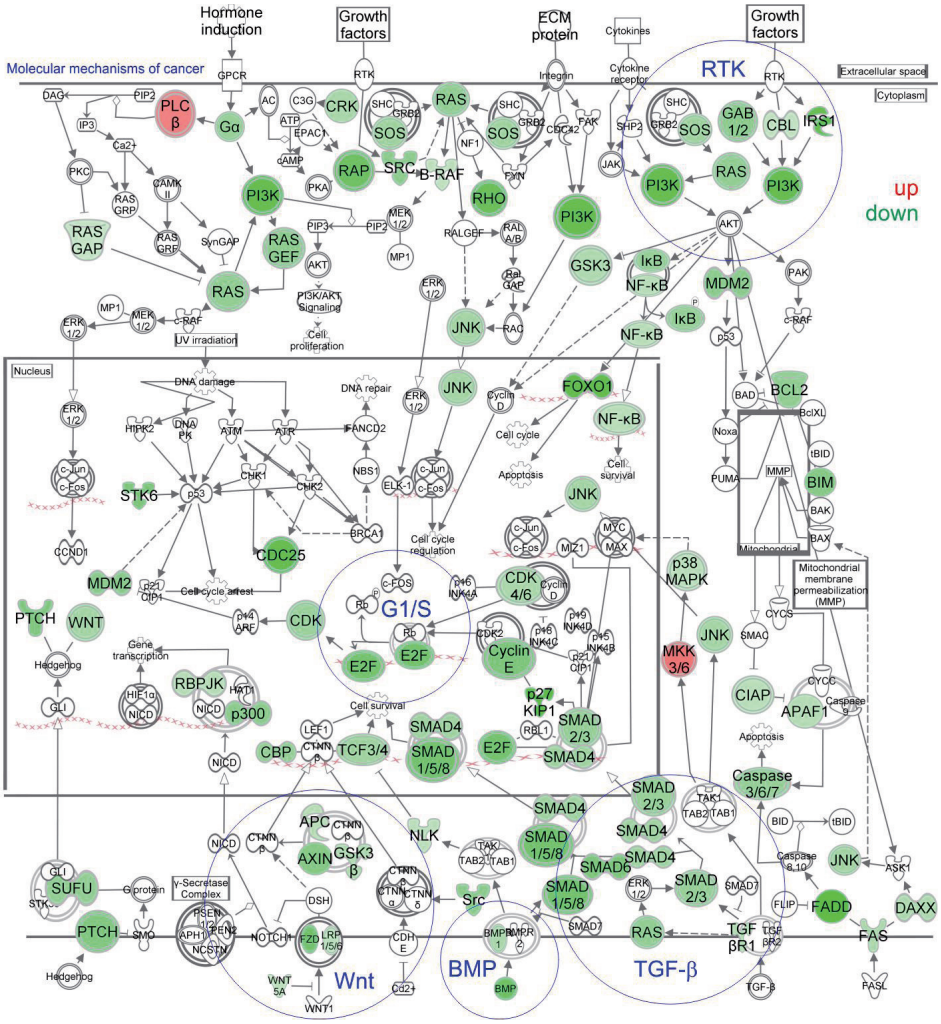

Supplementary Figure S5. Massive disruption of molecular mechanisms of cancer by CDK9 inhibitors. Effect was shown for the CDK9 inhibitor D10-81 representatively.

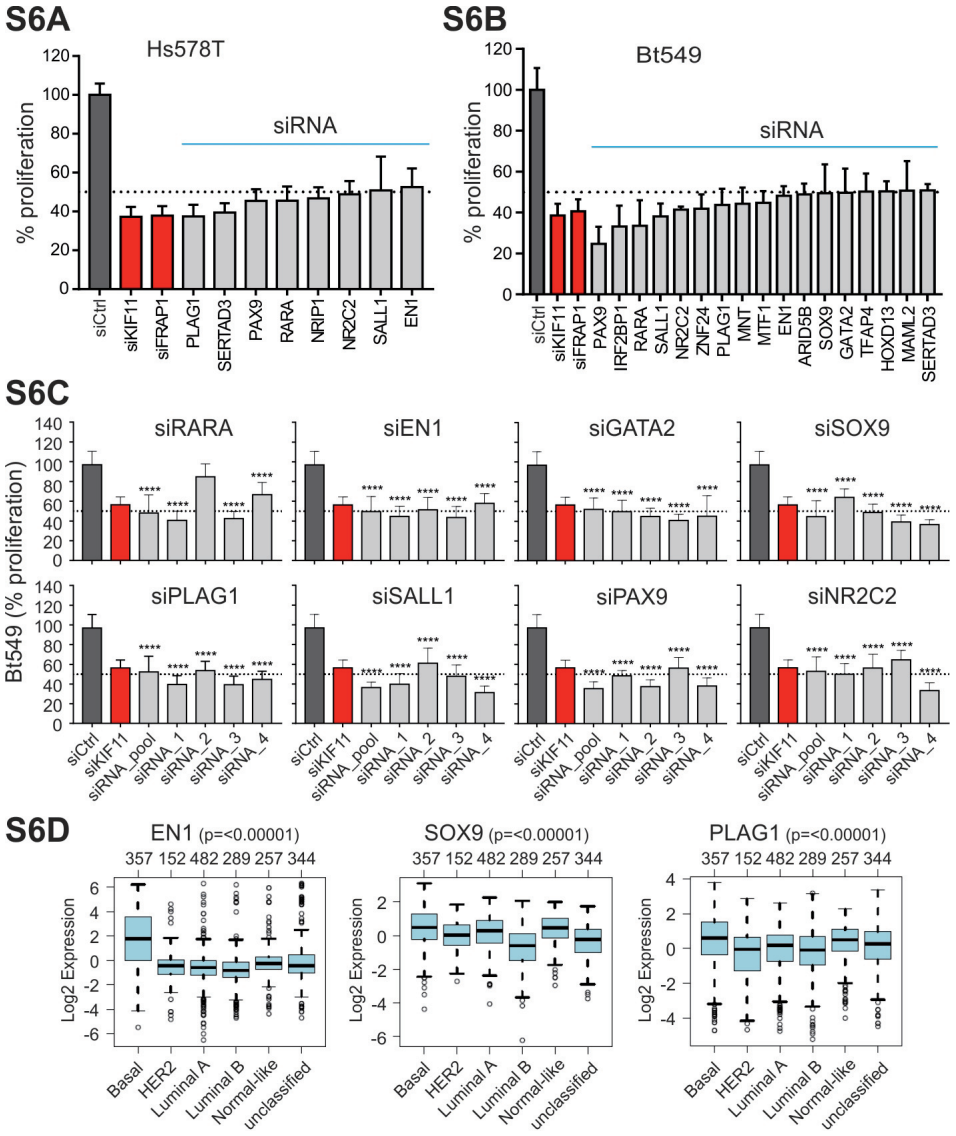

Supplementary Figure S6. CDK9 inhibitors D10-81, Y3-21 and I-73 suppress transcription factors essential for the proliferation of TNBC cells. S6A-B. Results of primary screen of CDK inhibitor-sensitive transcription factor silencing in Hs578T and BT549 cells. Genes whose silencing reduced the proliferation by ≥ 50% compared to negative siRNA control (siCtrl) are shown. Data are shown as % proliferation normalised to control (siKpool). Positive siRNA controls are shown in red (siKIF11 and siFRAP1). **S6C**. Results of deconvolution validation of transcription factors in BT549 cells. Genes for which transfection with 2 or more single siRNA sequences reduced proliferation by ≥ 50% were considered as validated hits. Results shown as % proliferation normalised to siCtrl. **S6D.** Expression of the transcription factors EN1, SOX9 and PLAG1 in the basal-like subtype, across breast cancer intrinsic subtypes (data derived from GOBO).

Chapter 5

The synergistic effect of combined P-TEFb and EGFR inhibition on triple-negative breast cancer

Ronan P. McLaughlin[1], Jichao He[1], Jessica Karuntu[1], Vera van der Noord[1], John W.M. Martens[2], John A. Foekens[2], Marcel Smid[2], Solomon Tadesse[3], Yi Long[3], Sarah Al Haj Diab[3], Shudong Wang[3], Yinghui Zhang[1], Bob van de Water[1]

[1]Division of Drug Discovery and Safety, Leiden Academic Centre for Drug Research, Leiden University, 2300 RA Leiden, The Netherlands.

[2]Department of Medical Oncology and Cancer Genomic Netherlands, Erasmus MC Cancer Institute, Erasmus University Medical Center, 3000 CA Rotterdam, The Netherlands.

[3]Centre for Drug Discovery and Development, School of Pharmacy and Medical Sciences, University of South Australia Cancer Research Institute, Adelaide, South Australia, 5001, Australia.

This chapter is based on a manuscript in preparation

ABSTRACT

There is a lack of effective targeted therapies against triple negative breast cancer (TNBC). Despite expressing EGFR, TNBC is generally resistant to EGFR-tyrosine kinase inhibitors (EGFR-TKIs). Increasing evidence suggests multiple cancers depend upon aberrant transcriptional programs controlled by the positive transcription elongation factor b (P-TEFb) complex. Consequently, we explored the sensitivity of TNBC cells to disruption of P-TEFb-mediated transcriptional regulation and its potential to overcome resistance to EGFR-TKIs. Here we show that combining CDK9 inhibitors I-73 and Y3-21 with EGFR-TKIs lapatinib and gefitinib, abolishes the resistance of TNBC cells to these agents. Co-treatment resulted in strong anti-proliferative synergistic responses associated with cell cycle arrest, depletion of anti-apoptotic protein MCL-1, and induction of apoptosis. Transcriptomic profiling revealed that targeting EGFR and CDK9 simultaneously, potentiated the inhibitory effect of CDK9 inhibition on gene expression, down-regulating genes linked to stem cell pluripotency, TGF-β signalling, and cell cycle progression, whilst blocking growth factor-mediated networks such as downstream MAPK/MEK signalling. Co-inhibition of EGFR and CDK9 signalling preferentially obstructed the function of multiple transcription factors, the expression of a number of which was associated with a significantly shorter metastasis-free survival in TNBC patients. In summary, interruption of P-TEFb/CDK9-mediated transcription abrogates the resistance of TNBC cells to EGFR inhibition, thereby preventing TNBC cell proliferation, emphasising the potential of combining such targeted therapies in treating drug-resistant TNBC.

INTRODUCTION

Triple-negative breast cancer (TNBC) is a virulent form of breast cancer associated with a dismal prognosis and metastatic propensity when compared to hormone receptor- and HER2-positive breast cancer[1–3]. TNBC displays remarkable genetic heterogeneity, precluding the identification of bona fide oncogenic drivers amenable to pharmacological manipulation, thus preventing the development of effective targeted therapies[4–7]. However, emerging evidence suggests that targeting key transcriptional regulators, such as positive transcription elongation factor b (P-TEFb), which act as downstream convergence points for signals transduced via receptor tyrosine kinase (RTK)-mediated signalling, may represent a strategy to identify novel therapies and synergistic combinations with enhanced efficacy for TNBC as well as other cancers[8,9]. P-TEFb is a complex composed of catalytic cyclin-dependent kinase 9 (CDK9) and its partner Cyclin T1 which phosphorylates the C-terminal domain (CTD) of RNA Polymerase II (RNAPII) at Ser2 to allow productive mRNA elongation[10–13]. The activity of P-TEFb is partly controlled by bromodomain-containing protein 4 (BRD4) which, in the presence of Hexim1, is essential for the formation of the complex, its binding to the CTD of RNA II and its activation, by promoting the dissociation of negative transcription elongation factors such as 7SK snRNA[11,13,14].

Multiple research groups have elaborately investigated the potential of disrupting CDK7 or P-TEFb/CDK9 transcriptional function in various malignancies, including ovarian cancer, neuroblastoma, acute myeloid leukaemia (AML) and T-cell leukaemias[15–18]. The identification of super-enhancer associated genes dependent upon CDK7-mediated transcription in EGFR-tyrosine kinase inhibitor (EGFR-TKI)-resistant TNBC cells by means of CRISPR-Cas screening suggested that RTK-

targeted therapies could be augmented by combining them with inhibitors of transcription[19]. Moreover, in response to RTK-targeted therapies, cancers are capable of reprogramming their signalling circuitry to avoid RTK-targeted therapy-induced apoptosis[20,21]. This results in the enhanced expression of alternative RTKs which funnel growth factor-regulated signal transduction, thereby diminishing the efficacy of RTK-targeted therapies which seek to exploit the addiction of cancer cells to oncogenic growth factor-mediated signalling[20,22]. Recent data show that in TNBC tumours treated with MEK1/2 inhibitor trametinib, disruption of P-TEFb function mitigates this adaptive bypass mechanism[9]. By preventing enhancer remodelling-mediated up-regulation of alternative RTKs FGFR2, PDGRB and DDR1, through which MEK1/2 activation can continue unabated, an enhanced response to trametinib was observed[9]. Also, preventing activation of P-TEFb by use of BRD4 inhibitor I-BET151 profoundly suppressed TNBC xenograft growth, whilst silencing of CDK9 attenuated trametinib-mediated enhanced expression of DDR1 and PDGFRB and downstream ERK1/2 activation in TNBC cell lines *in vitro*[9]. At the molecular level, co-treatment with P-TEFb/CDK9 inhibitors or BRD4 inhibitors precluded recruitment of RNAPII to active gene promoters involved in the up-regulation of PDGFR and FGFR[9].

Nonetheless, information on the effectiveness of combining EGFR-TKIs with agents that disrupt P-TEFb/CDK9 function in EGFR-TKI-resistant TNBCs is unavailable. EGFR overexpression and amplification, as well as reliance on EGFR-regulated signal transduction are common in TNBC tumours and higher expression of EGFR confers a poorer prognosis to patients[23–28]. Considering the aforementioned extensive pre-clinical testing of BRD4 inhibitors in combination with RTK- and MEK-

targeted therapies, there is a clear justification for combined targeting of RTK-mediated signaling and P-TEFb-regulated transcription in TNBC[29,30]. Eradicating the proclivity of drug-resistant TNBC cells for transcriptional plasticity in response to targeted therapy, may enhance the response to RTK-targeted agents such as EGFR-TKIs which have yet to demonstrate appreciable clinical benefit in TNBC[23,28,31].

Here we investigated the impact of combining EGFR-TKIs and P-TEFb/CDK9 inhibitors in a panel of TNBC cell lines, the majority of which are insensitive to EGFR-TKIs[19]. Our results demonstrate that combining potent P-TEFb/CDK9 inhibitors with clinically approved EGFR-TKIs synergistically inhibits the proliferation of TNBC cells, induces apoptosis, and down-regulates important components of the transcriptional machinery critical to TNBC cell survival.

MATERIALS & METHODS

Cell Culture

TNBC cell lines used were representative for different TNBC subtypes[32], including basal-like 1 (BL1) HCC38, HCC1143, HCC1937 and MDA-MB-468; basal-like 2 (BL2) HCC70, HCC1806 and SUM149PT,; mesenchymal (M) BT549 and Hs578T; mesenchymal stem-like (MSL) MDA-MB-157, MDA-MB-231, MDA-MB-436 and SUM159PT; luminal androgen receptor (LAR) MDA-MB-453; and unclassified SKBR7, SUM52PE, SUM229PE and SUM1315MO2. All TNBC cell lines were maintained in RPMI-1640 medium (*Gibco, ThermoFisher Scientific*) supplemented with 10% FBS (*Thermo Fisher Scientific; 10270106*) and 25IU/ml Penicillin and 25µg/ml Streptomycin (*ThermoFisher Scientific*; *15070-063*). Cells were cultured in a humidified incubator at 37^{o}C, 5% CO_2.

Kinase inhibitor combination screen

CDK9 inhibitors I-73[33] and the new generation inhibitor Y3-21 were acquired from the Centre for Drug Discovery and Development, University of South Australia. EGFR inhibitors lapatinib (S1028) and gefitinib (S1025), and BRD4 inhibitor JQ1 (S7110) were purchased from Selleckchem®. Cells were seeded at the appropriate densities (90 µl/well) in 2x 96-w plates (for SRB; *Greiner; 655162*) and 2x 96-w µCLEAR plates (for imaging; *Greiner*; *655090*) and incubated overnight at 37^{o}C, 5% CO_2. Cells were subsequently treated with a dose range of inhibitors (0.0316 µM – 3.16 µM), e.g. EGFR inhibitors lapatinib and gefitinib or BRD4 inhibitor JQ1, combined with two single doses of I-73 (0.1 µM or 0.316 µM) or Y3-21 (0.0316 µM or 0.1 µM). Cells were subsequently incubated at 37^{o}C, 5% CO_2 for 96 hours, followed by proliferation assay.

Automated imaging of apoptosis

72 hours post-exposure to inhibitors and prior to sulphorhodamine B proliferation assay, cells were stained with 1:1000 Annexin-V (0.9 mg/ml) and 1:10,000 Hoechst 33258 (2 mg/ml) for 45 minutes at 37^{o}C, 5% CO_2. Cells were subsequently imaged using BD Pathway 855 microscope (BD Biosciences). An image analysis pipeline was created in Cell Profiler involving segmentation based on Hoechst 33258 staining to identify the primary cell objects followed by secondary Annexin V-positive objects. Annexin V-positive cells were defined based on an intensity threshold. This threshold was set based on the negative (DMSO) and positive (doxorubicin) controls. For each image the sum of all nuclei and the sum of the Annexin V-positive cells was determined followed by calculation of the percentage of Annexin V-positive cells.

Sulphorhodamine B (SRB) proliferation assay

SRB Assay was performed as previously described after 96 hours' exposure to indicated inhibitors[34,35].

Western blotting

Cell lysates were harvested in RIPA lysis buffer with 1:100 protease inhibitor cocktail (Sigma; P8340). Cellular proteins were denatured in sample buffer containing 10% β-mercaptoethanol (Acros Organics 125472500). Equal amounts of proteins were subsequently loaded into polyacrylamide gels (7.5-15% depending on desired resolution), resolved using SDS-PAGE and subsequently transferred to PVDF membranes (Merck Chemicals; IPVH00010) overnight. PVDF membranes were then blocked with 5% bovine serum albumin (Sigma Aldrich A9647) in Tris-buffered saline containing 0.05% Tween20 and incubated overnight with the appropriate primary antibodies: phospho-CDK9 (T186; CST 2549), CDK9 (CST 2316), phospho-RNAPII (S2/5; CST 4735), RNAPII (CST 2629), BRD4 (Bethyl Laboratories A301-985A-M), BCL-xL (CST 2764), MCL1 (CST 5453), γ-H2AX (S139; CST 2577) and tubulin (Sigma Aldrich T-9026).

Cell cycle analysis

Cells were seeded in 6-well plates at the appropriate density. The following day cells were treated with drugs for 48 hours. Detached cells and attached cells were collected during trypsinisation and collected through centrifugation (1000 rpm, 5 minutes, 4^{o}C). Pelleted cells were re-suspended in 200 µl ice-cold 1 mM EDTA in PBS and fixed by adding 800 µl ice-cold 100% ethanol (-20^{o}C). Cells were washed by two wash steps in PBS (1000 rpm, 5 minutes, room temperature) and pellet was

re-suspended in 250 µl of 3 µM DAPI (Sigma Aldrich, 10236276001) in staining buffer (100 µM Tris pH 7.4, 150 mM NaCl, 1 mM $CaCl_2$ and 0.5 mM $MgCl_2$). After 15 minutes cells were filtered through 70 µm EASYstrainer filters followed by FACS Conto II analysis (BD Biosciences). Data were analysed using FlowJo V10.

RNA-sequencing

Hs578T cells were seeded into 6-well plates, in triplicate, at the appropriate density and allowed to attach overnight at 37^{o}C, 5% CO_2. Lapatinib and I-73 solutions were prepared at 3.16 µM and 0.1 µM, respectively and cells were treated with each inhibitor separately or in combination, or DMSO as control for 6 hours. RNA was subsequently extracted using RNeasy Plus Mini Kit (QIAGEN *74136*) according to the manufacturer's instructions and stored at -80^{o}C. Transcriptome RNA-Sequencing (RNA-Seq) was performed using Illumina high-throughput RNA sequencing. DNA libraries were prepared from the samples with the TruSeq Stranded mRNA Library Prep Kit. The DNA libraries were sequenced according to the Illumina TruSeq v3 protocol on an Illumina HiSeq2500 sequencer. Paired-end reads were generated of 100 base-pairs in length. Alignment was performed using the STAR aligner (version 2.4.2a) against the human GRCh38 reference genome. Marking duplicates, sorting and indexing were performed using Sambamba (version 0.6.6). Gene expression was quantified using the FeatureCounts software (version 1.4.6) based on the ENSEMBL gene annotation for GRCH38 (release 84). RNA-Seq data were normalised by TMM using EdgeR's normalisation-factor, followed by quantile normalisation and presented in Log2 fold change (Log2 FC) scales[36]. Genes with significant down- or up-regulation (Log2 FC ≥ |0.68|) under indicated conditions were analysed by web-based functional analysis tool Ingenuity Pathway Analysis (IPA).

Clinical evaluation of candidate genes

The clinical relevance of synergy-related genes identified by transcriptomic profiling was evaluated using in-house and publicly available gene expression data of lymph node-negative (LNN) primary breast cancer patients who did not receive adjuvant or neo-adjuvant systemic therapy, as well as available metastasis-free survival (MFS) data, thereby generating a cohort of 867 patients. 625 of these were ER+, whilst 242 were ER-. Of the 242 ER-patients, 142 were classified as TNBC. Data were gathered from Gene Expression Omnibus (http://www.ncbi.nlm.nih,gov/geo/) entries GSE2034, GSE5327, GSE2990, GE7390 and GSE11121, with all data available on Affymetrix U133A chip. Raw.cel files were processed using fRMA parameters (median polish) after which batch effects were corrected using ComBat[37,38].

Data analysis & statistics

50% proliferation inhibition (IC50) values were derived from GraphPad Prism 7.0 using nonlinear regression fitting. The synergistic effect of drug combinations was analysed by combination index calculations (CI)[39–41], using the formula “CI = D1/D1x + D2/D2x, in which D1 and D2 are the respective combination doses of drug 1 and drug 2 that yield an effect of 50% of proliferation inhibition, and D1x and D2x are the corresponding single doses for drug 1 and drug 2 that result in 50% of proliferation inhibition (i.e. IC50). Two-way ANOVA with Tukey’s multiple comparison test was used to assess impact of drug treatment on cell cycle distribution. P-values < 0.05 were considered statistically significant.

RESULTS

Co-targeting CDK9 and BRD4 synergistically inhibits proliferation and blocks P-TEFb-mediated signal transduction in TNBC cells

Since BRD4, is a positive regulator of P-TEFb[11], firstly we examined the expression of BRD family members in 116 TNBC patient tumours using available TCGA datasets (Supplementary Figure S1A). BRD2 and BRD4 were particularly highly expressed across all TNBC tumours analysed. To evaluate the utility and validity of our TNBC cell line panel, we compared the expression of BRD members in 20 in-house TNBC cell lines (Supplementary Figure S1B). The expression of BRD members in the cell line panel was largely comparable with their expression in the tumours, suggesting that the cell lines are useful models for testing sensitivity to BET inhibitors. Again, BRD2 and BRD4 were amongst the most highly expressed BRD members in the TNBC cell lines.

We have previously demonstrated that TNBC cells are vulnerable to disruption of P-TEFb-mediated transcriptional regulation by inhibiting CDK9 kinase activity. We therefore sought to address whether TNBC cells are also sensitive to inhibition of BRD4, the recruiter of the P-TEFb complex. To this end, 18 TNBC cell lines were treated with BRD4 inhibitor JQ1 for 96 hours at concentrations ranging from 0.0316-3.16 μM. An overwhelmingly refractory response to JQ1 was observed in the cell line panel (Figure 1A-B), except cell lines MDA-MB-231, MDA-MB-453 and SUM149PT, which were sensitive to JQ1 at doses lower than 1 μM. Next, to determine whether blocking P-TEFb function via CDK9 inhibition could sensitise TNBC cells to BRD4 inhibition by JQ1, the same panel of TNBC cell lines were treated with the same dose range of JQ1 combined with previously tested potent

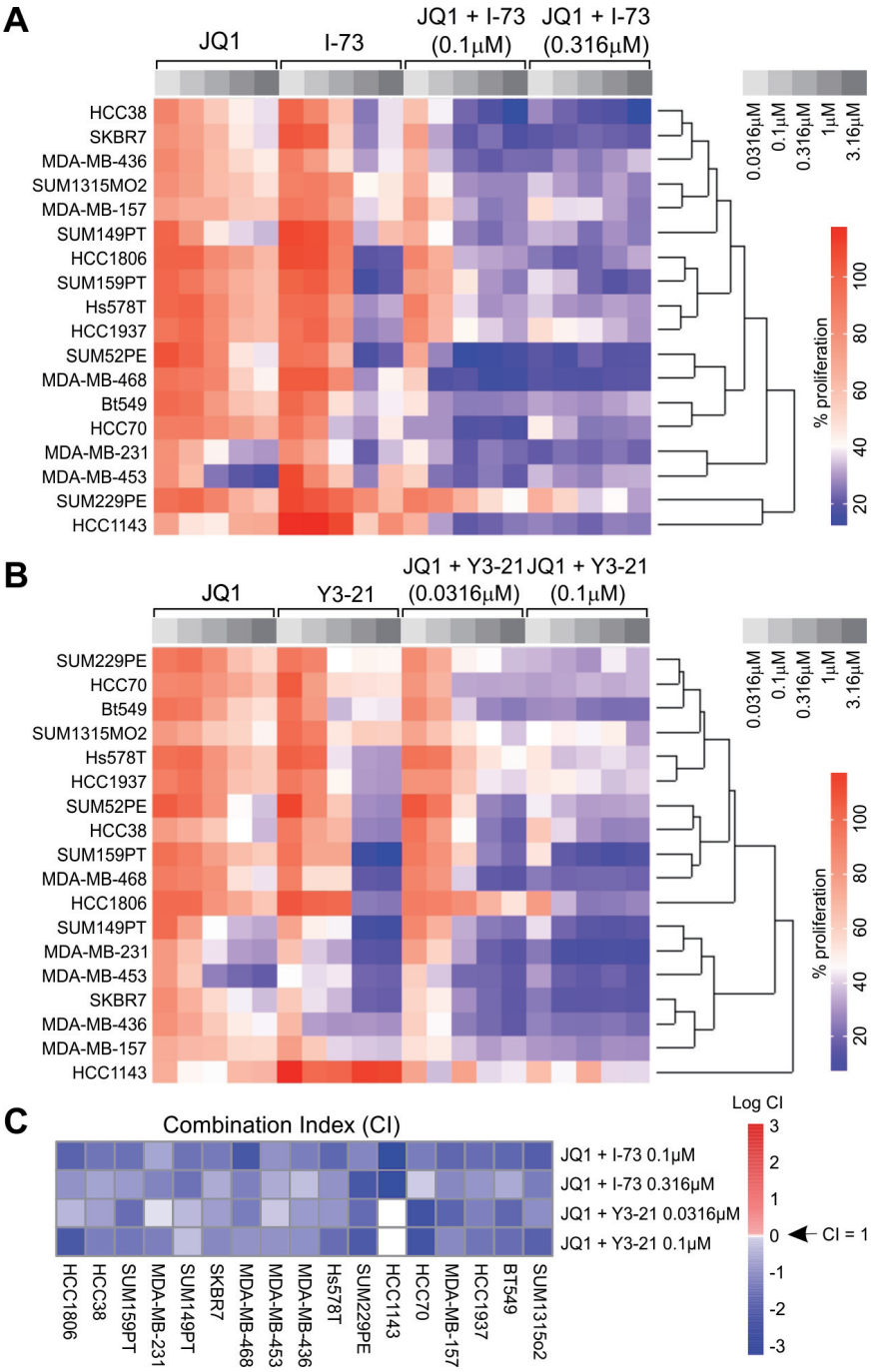

Figure 1. CDK9 inhibitors I-73 and Y3-21 synergise with BRD4 inhibitor JQ1 in TNBC cells. A. Anti-proliferative effect of combining JQ1 in a concentration range with I-73 (0.1 or 0.316μM) in a panel of TNBC cell lines**. B.** Anti-proliferative effect of combining JQ1 in concentration range with Y3-21 (0.0316 or 0.1μM) in a panel of TNBC cell lines. Proliferation was evaluated using SRB assay after 4 days' treatment. Results shown as percentage proliferation normalised to DMSO control. **C.** Combination index (CI) assessment of the synergistic effect of JQ1 + I-73 and JQ1 + Y3-21 on TNBC cell proliferation inhibition. The CI values were presented in natural logarithm (Log CI). CI > 1, antagonism; CI = 1, additivity; CI < 1, synergy.

CDK9 inhibitors I-73 (0.1μM or 0.316 μM) and Y3-21 (0.0316μM or 0.1 μM). These concentrations are ineffective or only slightly effective at inhibiting proliferation and P-TEFb signalling transduction in TNBC cells. Striking synergy was observed between JQ1 and I-73 (Figure 1A), as well as between JQ1 and Y3-21 (Figure 1B), as exemplified by synergistic combination indices (CI < 1.0) (Figure 1C), with superior reductions in cell proliferation compared to either I-73, Y3-21 or JQ1 alone. Furthermore, co-treatment with JQ1 (0.1 or 0.316 μM) and I-73 (0.1 μM) abolished P-TEFb-mediated phosphorylation of RNAPII at Ser2 and Ser5, respectively, in Hs578T, MDA-MB-157, HCC1143 and SUM149T cells (Figure 2A-D). RNAPII and the positive regulator BRD4 were also depleted as a result of the combination. Remarkably, CDK9 and BRD4 co-inhibition severely reduced levels of pro-survival BCL-2 family proteins MCL-1 and BCL-xL, and increased levels of γ-H2AX. These results indicate that simultaneously targeting CDK9 and BRD4 using I-73 and JQ1 is synergistic in TNBC cells, thereby eliminating P-TEFb/CDK9-mediated signal transduction and inducing DNA damage, consequently leading to cell death.

Targeting CDK9 overcomes resistance to EGFR inhibition in TNBC cells

TNBC cell lines highly express the receptor tyrosine kinase EGFR but are generally insensitive to EGFR-TKIs. Previously, we revealed that a dual cdc7/CDK9 inhibitor (PHA-767491) sensitises TNBC cells to EGFR-TKIs. Given the impact of combined P-TEFb and BET inhibition in TNBC, we further investigated whether I-73 would sensitise TNBC cells to EGFR-TKIs lapatinib or gefitinib. Co-treatment of a panel of EGFR-TKI-resistant TNBC cell lines with I-73 (0.1 μM or 0.316 μM) or Y3-21 (0.0316 μM or 0.1 μM) in combination with either lapatinib (0.0316-3.16 μM) or gefitinib (0.0316-3.16 μM) led to a remarkable reduction in cell proliferation 96 hours post-

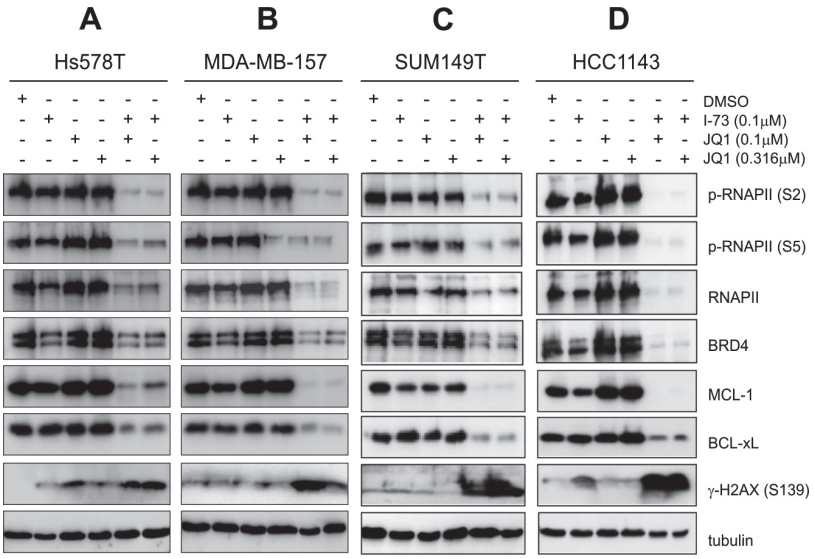

Figure 2. Synergistic effect of I-73 and JQ1 on P-TEFb signalling and downstream targets. Immunoblot-based analysis showing the impact of JQ1 and I-73 co-treatment on inhibition of P-TEFb-mediated RNAPII Ser2/Ser5 phosphorylation, downregulation of the P-TEFb regulator BRD4, suppression of anti-apoptotic BCL-xL and MCL-1, and induction of apoptotic phospho-γ-H2AX in Hs578T (**A**), MDA-MB-157 (**B**), SUM149PT (**C**) and HCC1143 (**D**) TNBC cells. Cells were treated for 48 hours with I-73 (0.1μM), JQ1 (0.1 or 0.316μM) alone or combination as indicated. DMSO was used as control. Tubulin was used as sample loading control.

exposure, superior to either monotherapy (Figures 3A-B, Supplementary Figure S2). CI values well below 1.0 (CI < 1) indicated that the interaction between the EGFR-TKIs and the CDK9 inhibitors was synergistic in nature (Figure 3C). The synergistic effect of lapatinib and I-73 on proliferation inhibition was further validated in representative TNBC cell lines Hs578T, BT549 and SKBR7, further confirming the synergistic concentrations of I-73 (0.1-0.316 μM) (Figure 4A). Remarkably, co-treatment with I-73 (0.1 μM) and lapatinib induced apoptosis to a greater extent than lapatinib or I-73 alone in Hs578T, SUM149T, HCC1143, MDA-MB-436, MDA-MB-468 and MDA-MB-231 cells (Figure 4B). Immunoblot analysis revealed that apoptosis induction by co-treatment with lapatinib and I-73 was preceded by inhibition of RNAPII phosphorylation and subsequent depletion of MCL-1 (Figure 4C); I-73 at 0.1 μM only led to modest reduction in the levels of MCL-1 protein, but when combined

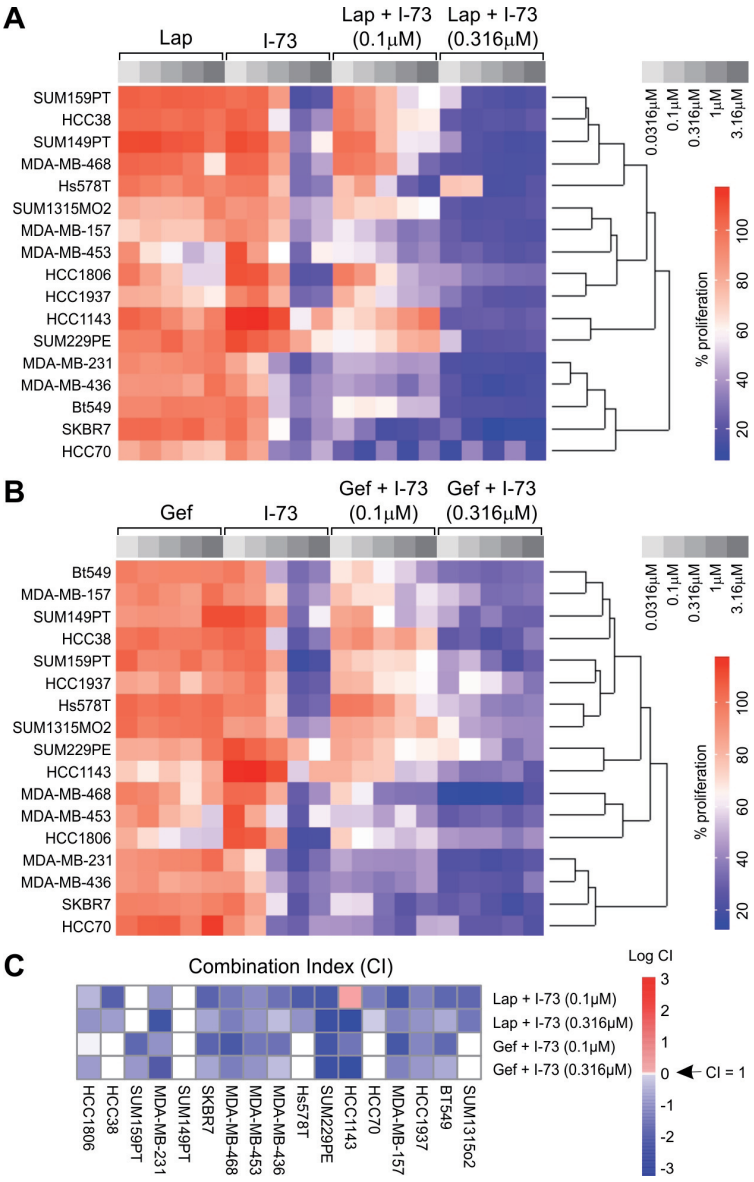

Figure 3. CDK9 inhibitor I-73 reverses the resistance of TNBC cells to EGFR-tyrosine kinase inhibitors. A. Effect of EGFR-TKI lapatinib (Lap) in concentration range combined with I-73 (0.1 μM or 0.316 μM) on the proliferation of TNBC cell lines. **B.** Effect of EGFR-TKI gefitinib (Gef) in concentration range combined with I-73 (0.1 μM or 0.316 μM) on the proliferation of TNBC cell lines. Data shown as percentage proliferation normalised to DMSO control. **C.** Synergistic CI evaluation of Lap + I-73 and Gef + I-73 combinations. Data shown as Log CI values. CI > 1, antagonism; CI = 1, additivity; CI < 1, synergy.

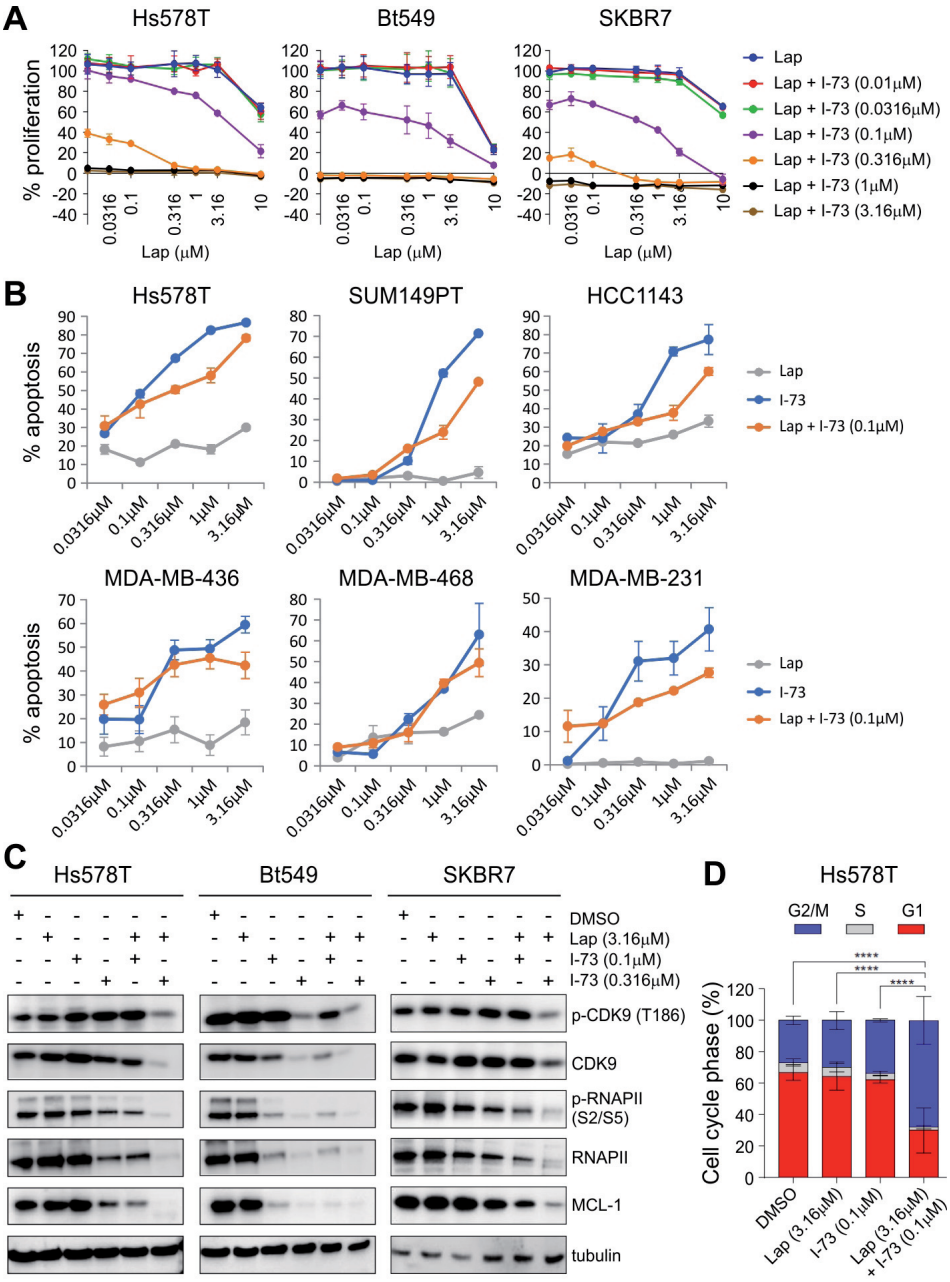

Figure 4. Synergistic effect of I-73 and lapatinib on P-TEFb signalling inhibition, cell cycle G2/M arrest and apoptosis induction. A. Dose response matrix combination of I-73 and lapatinib (Lap) in TNBC cell lines Hs578T, BT549 and SKBR7, Data shown as percentage proliferation normalised to DMSO control. Representative of three independent experiments performed in triplicate. **B.** I-73 and lapatinib combination induced apoptosis in TNBC cell lines Hs578T, SUM149T, HCC1143, MDA-MB-436, MDA-MB-468 and MDA-MB-231. Cells were treated with lapatinib, I-73, or a concentration range of lapatinib combined with I-73 at 0.1 μM for 72 hours. Induction of apoptosis was measured by calculating the percentage Annexin V-positive cells normalised to Hoechst-positive cells. Data shown as mean +/- standard deviation (n = 2). **C.** I-73 and lapatinib synergistic effect on inhibition of P-TEFb-mediated RNAPII phosphorylation and down-regulation of anti-apoptotic protein MCL-1 in Hs578T, BT549 and SKBR7 TNBC cells. Cells were harvested after 48 hours' co-treatment with I-73 and lapatinib, as indicated. **D.** I-73 and lapatinib co-treatment induced superior G2/M cell cycle arrest in Hs578T cells, compared to either monotherapy. Data were shown as percentage cells per cell cycle phase (G2/M, S or G1) normalized to DMSO control, and represented as mean +/- standard deviation (n = 4). Two-way ANOVA with Tukey's multiple comparison test; ****p < 0.0001.

with lapatinib MCL-1 was completely ablated in Hs578T and BT549 cells 48 hours post-treatment. I-73 at 0.316 μM drastically depleted MCL-1 levels in Hs578T, BT549 and SKBR7 cells, this effect also being enhanced upon addition of lapatinib at 3.16 μM. Consistent with the induction of apoptosis, the combination of lapatinib and I-73 induced strong G2/M cell cycle arrest to a significantly greater extent than single treatment with either lapatinib (3.16 μM) or I-73 (0.1 μM) (Figure 4D). In short, the resistance of TNBC cells to EGFR-TKIs can be reversed by combining such agents with CDK9 inhibitors, leading to apoptosis and cell cycle arrest.

Co-inhibition of EGFR and CDK9 profoundly alters gene transcription in TNBC cells

To illuminate the transcriptional changes associated with the CDK9 inhibition-mediated reversal of intrinsic resistance to EGFR-TKIs in TNBC cells, we performed RNA sequencing-based transcriptomic analysis of Hs578T TNBC cells treated for 6 hours with lapatinib (3.16 μM), I-73 (0.1 μM) and their combination, respectively. By normalizing treatment conditions to control conditions, a cut-off of Log2 fold change (Log2 FC) ≥ ±0.68 (FC = 1.5) was used to classify significantly differentially expressed genes after treatment with monotherapies (I-73 at 0.1 μM or lapatinib at 3.16 μM) or combination. Comparing the transcripts which were differentially expressed under co-treatment with those altered under single treatment with either lapatinib (Lap + I-73 vs Lap, Log2 FC ≥ ±0.68) or I-73 (Lap + I-73 vs I-73, Log2 FC ≥ ±0.68), identified a total of 2220 overlapping genes, 529 of which were up-regulated and 1691 of which were down-regulated (Figure 5A). These 2220 genes were selected as lapatinib and I-73 synergy-related genes. Ingenuity Pathway Analysis (IPA)-based assessment of the synergy-related transcripts revealed an enrichment of genes involved in mammalian embryonic stem cell pluripotency, TGF-β

signalling, regulation of cell cycle progression, and JAK-STAT canonical signalling pathways, amongst others, in the down-regulated set (Figure 5B). This set of genes was mainly clustered in regulatory networks of gene transcription and expression as well as protein ubiquitination (Figure 5C). Clearly, I-73 strongly synergised with lapatinib to target genes which were insensitive to EGFR inhibition alone, particularly those involved in stem cell pluripotency (Figure 5D), G1/S checkpoint regulation (Figure 5E), and TGF-β signalling (Figure 5F). For instance, the expression of SMAD1, BMP4, TRAF6, ACVR2A and PITX2, which are crucial for Wnt/β-catenin-, TGF-β- and BMP-mediated signal transduction as well as activation of downstream JNK and p38-MAPK kinases[42,43], was inhibited by I-73 and this effect was augmented after combination with lapatinib (Figure 5F). Additionally, the I-73-mediated inhibition of key regulators of mammalian embryonic stem cell pluripotency associated with EMT (e.g. RARA)[44] and a chemo-resistant cancer stem cell phenotype (KDM5B)[45], was also enhanced by the addition of lapatinib (Figure 5D). Similarly, co-treatment of Hs578T cells with I-73 and lapatinib potentiated the inhibitory effect of I-73 on 293 transcription regulatory genes (Figure 6A). These included ZNF, FOX, E2F and KLF transcription factor family members (Figure 6B). Strikingly, the synergistic interaction of lapatinib and I-73 potently blocked P-TEFb transcriptional function by targeting genes involved in transcription initiation (Figure 6C), including E2F2, E2F3, and CDK9 itself, as well as targets downstream of BRD4 (Figure 6D), such as BCL1L1, MCL1, CDC25[46]. Thus, lapatinib potentiates the inhibitory effects of I-73 on transcriptional regulators, thereby shutting down pathways critical for cancer cell survival and adaptation to targeted agents. Furthermore, while lapatinib synergized with I-73 in gene expression regulation, their

synergistic effect also resulted in suppression of multiple growth factor-mediated networks, such as IGF, HGF, MBP and GDF, which guide alternative RTK-mediated signal transduction (Supplementary Figure S3A), Of relevance, MEK signalling downstream of RTKs was strongly attenuated (Supplementary Figure S3B), a number of genes being vulnerable to the synergistic effect, including SPRY2, RND3, and pro-survival BCL-2 members BCL2L1, BCL1L11 and MCL1. In particular, these results are therefore relevant to circumstances where TNBC cells are addicted to oncogenic growth factor- and RTK-mediated signalling and where TNBC cells are resistant to MEK inhibition.

Transcriptional regulators sensitive to CDK9 and EGFR co-inhibition are associated with poor prognosis in TNBC patients

Considering the profound inhibition of expression of transcriptional regulators after co-treatment with I-73 and lapatinib, we subsequently evaluated the association between expression of these transcripts and metastasis-free survival (MFS) in a cohort of 142 TNBC patients. Amongst 293 synergy-related transcriptional regulators, high expression of 15 transcription factors, which were strongly down-regulated by co-treatment with lapatinib and I-73, was associated with a significantly poorer MFS in this cohort (Figure 7A). These included TRIM13, KLF9, DACT1, KLF2, GTF2E1, KLF6, PITX2, JMID1C, GATA2, RBM5, FOXO1, ZFP36, RRPB, PPM1D and NOS1AP. Multiple Kruppel-like family (KLF) transcription factors were down-regulated by co-treatment (Figure 6B), with high expression levels of KLF2, KLF6 and KLF9 being significantly correlated with a poor MFS in TNBC patients (Figure 7A). Representative Kaplan-Meier (KM) survival curves for TRIM13, DACT1, KLF9, and KLF6 are shown (Figure 7B). These data suggest that CDK9 and EGFR co-targeted

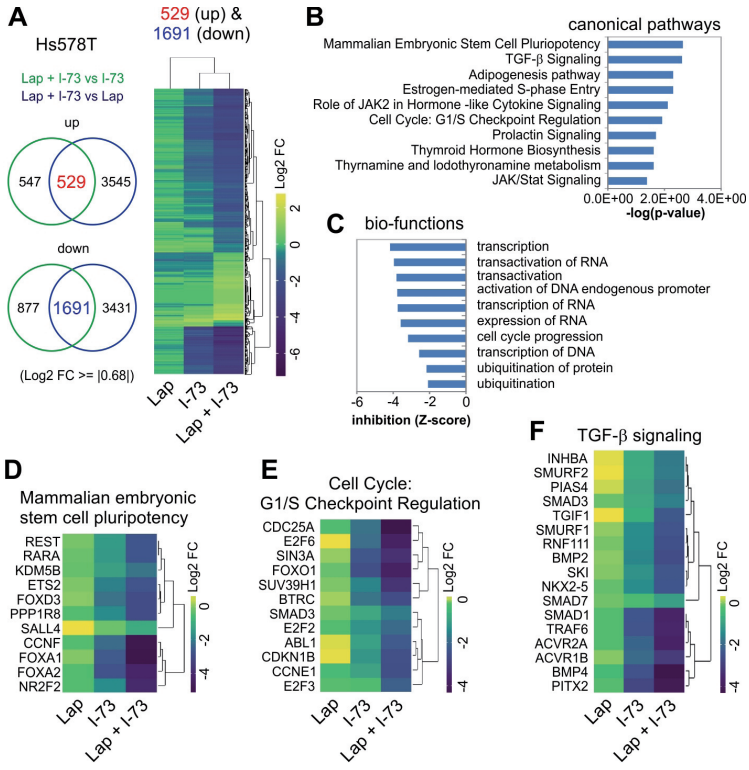

Figure 5. I-73 and lapatinib co-treatment disrupts the transcriptomic profile of TNBC cells. TNBC Hs578T cells were treated for 6 hours with Lap (3.16μM), I-73 (0.1μM), combined Lap + I-73 at the same doses, or DMSO as control, and harvested for RNA purification and RNA-Sequencing, Gene expression levels were presented in Log2 fold change (Log2 FC) normalized to control DMSO. **A.** Venn diagram and clustering of 529 up- and 1691 down-regulated genes in I-73 and lapatinib combination. Expression levels of genes under Lap + I-73 combined treatment were compared to those under single treatment Lap (Lap + I-73 vs Lap) or I-73 (Lap + I-73 vs I-73), Genes that overlapped in both comparisons and which were significantly up- (Log2 FC ≥ +0.68) or down-regulated (Log2 FC ≤ -0.68), were selected as synergy-related genes. The differential expression signature is shown in the heatmap. **B**. Top canonical pathways in which the Lap + I-73 synergy-regulated and differentially expressed genes are enriched, revealed by Ingenuity Pathway Analysis® (IPA). Significance was presented as –log p(value). **C.** Enrichment of Lap + I-73 synergy-related genes in top biological functions. Inhibitory effect was presented as Z-score. **D.** Expression of Lap + I-73 synergy-sensitive factors regulating mammalian embryonic stem cell pluripotency. **E.** Regulators of G1/S cell cycle in response to Lap + I-73 synergy. **F.** Sensitivity of TGF-β pathway members to Lap + I-73 synergy.

therapies are potentially effective in down-regulating transcription factors that are expressed at higher levels in TNBC tumours and which are correlated with poor disease outcomes in TNBC patients.

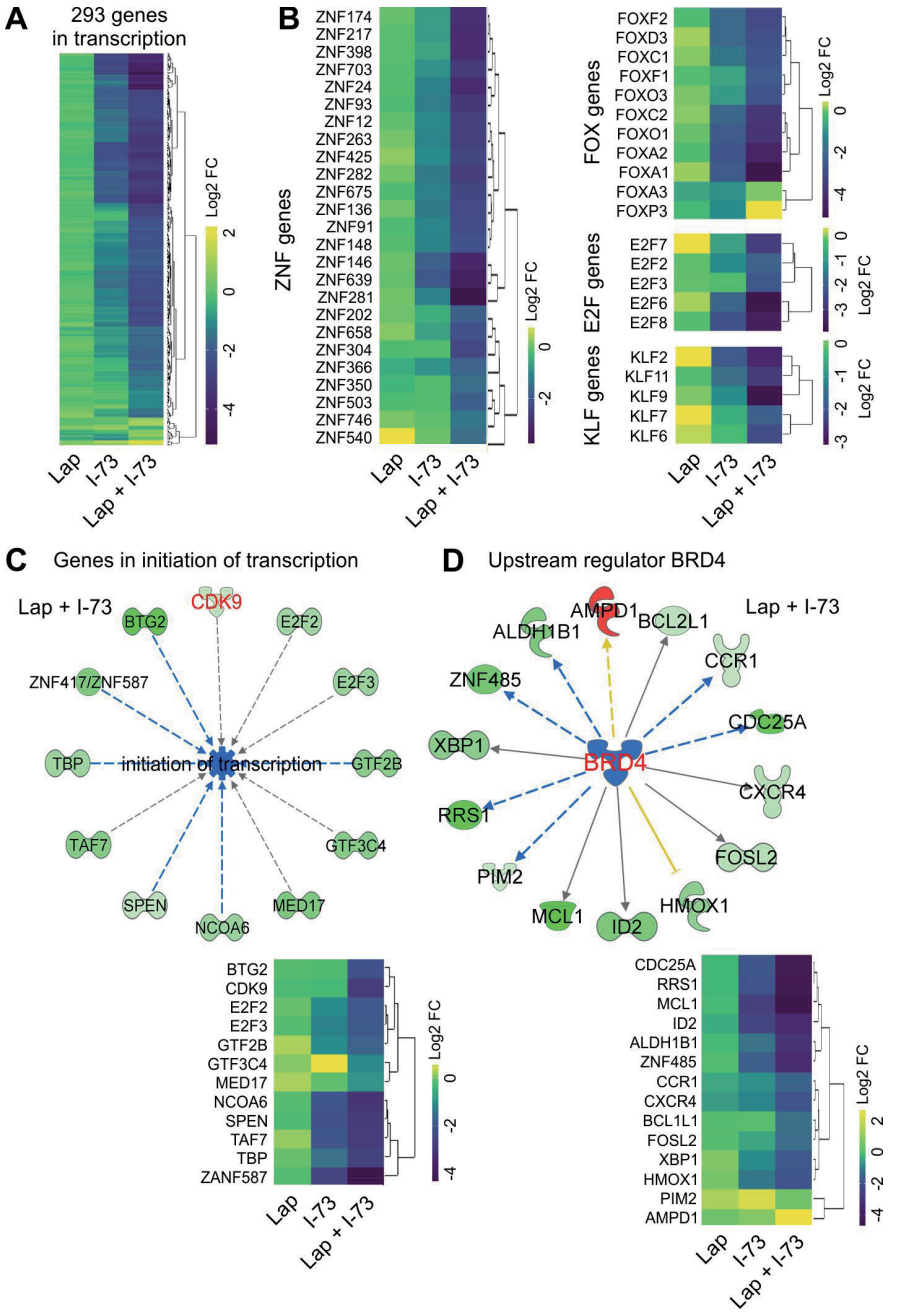

Figure 6. Synergistic effect of I-73 and lapatinib on P-TEFb-mediated transcription regulators. A. 293 Lap + I-73 synergy-related genes functioning as transcription regulators. **B.** Sensitivity of ZNF, FOX, E2F and KLF transcription factor family members to Lap + I-73 synergy. **C.** Disruption of CDK9 involved transcription initiation by Lap + I-73 synergy. **D.** Suppression of BRD4 downstream targets by Lap + I-73 synergy. The colours of the nodes are as follows; red represents up-regulation, green represents down-regulation, and blue indicates inhibition. The colours of the lines indicating effects are as follows: blue represents inhibition, yellow indicates an inconsistent effect, whereas grey represents events lacking prediction.

A

	TNBC patients				RNA-seq TNBC Hs578T cells		
Symbol	HR	pval	95% CI low	95% CI high	Lap Log2 FC	I-73 Log2 FC	Lap + I-73 Log2 FC
TRIM13	3.00	0.001	1.58	5.71	-0.32	-1.55	-3.03
KLF9	2.53	0.002	1.39	4.61	0.02	-1.04	-3.03
DACT1	1.71	0.003	1.20	2.44	0.12	-2.86	-3.89
KLF2	1.79	0.003	1.22	2.65	0.16	-1.94	-2.68
GTF2E1	2.43	0.012	1.22	4.83	-0.01	-1.66	-3.90
PITX2	3.75	0.013	1.32	10.63	-0.17	-2.77	-4.09
KLF6	1.79	0.014	1.13	2.86	0.10	-0.22	-2.20
JMJD1C	1.70	0.024	1.07	2.69	0.10	-1.25	-2.56
GATA2	1.92	0.025	1.09	3.40	-0.21	-1.26	-3.25
RBM5	2.03	0.027	1.08	3.81	-0.01	-1.41	-3.49
FOXO1	1.59	0.033	1.04	2.45	-0.13	-2.54	-3.86
ZFP36	1.74	0.036	1.04	2.91	0.32	-1.36	-2.51
RRP8	2.49	0.038	1.05	5.91	-0.17	-0.30	-2.58
PPM1D	1.95	0.038	1.04	3.68	-0.08	-1.35	-2.77
NOS1AP	3.71	0.040	1.06	12.96	-0.09	-0.47	-1.34

B

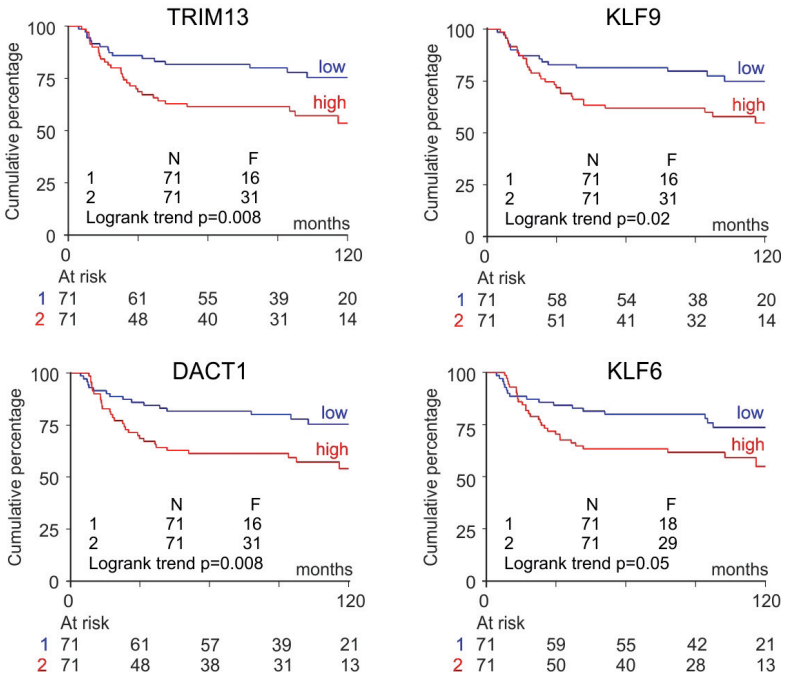

Figure 7. Clinical relevance of transcription factors down-regulated by I-73 and lapatinib co-treatment in TNBC patients. **A.** Fifteen Lap + I-73 synergy-related transcription factors in association with TNBC clinical outcome. Evaluation was based on the cohort of 142 TNBC patients (Erasmus Medical Rotterdam data and public data), Metastasis-free survival (MFS) was taken as end point. Hazard ratio (HR), p-value (pval) and 95% confidence intervals (95% CI) were based on Cox univariate regression analysis. Lap Log2 FC, I-73 Log2 FC and combined Lap + I-73 Log2 FC, show inhibitory effect on gene expression, as revealed by RNA-Seq transcriptomic analysis in TNBC Hs578T cells. **B.** Representative Kaplan-Meier (KM) MFS survival curves for 142 TNBC patients with expression of Lap + I-73 synergy-related genes TRIM13, DACT1, KLF9 or KLF6.

DISCUSSION

TNBC is an aggressive, heterogeneous, difficult-to-treat subtype of breast cancer which at present cannot be successfully treated with effective targeted agents designed to exploit the specific dependencies of these tumours[32,47]. EGFR-targeted therapy in the form of anti-EGFR monoclonal antibodies or EGFR-TKIs has yet to show tangible clinical benefit in TNBC patients, despite high levels of EGFR expression in TNBC tumours, highlighting the need for rational combination therapies[23,48]. One of the major obstacles to the development of such molecular targeted therapies is the presence of *de novo* resistance or the subsequent development of acquired resistance[21,49]. In order to address these issues, we utilised CDK inhibitors I-73 and Y3-21 with potent activity against P-TEFb/CDK9 to sensitise drug-resistant TNBC to EGFR-TKIs, thereby demonstrating that co-inhibition of EGFR and CDK9 represents a valid strategy to sensitise TNBC cells to EGFR-TKIs currently in clinical practice.

Here, we show that I-73 and Y3-21 were capable of abrogating the refractory response of TNBC cells to JQ1, with down-regulation of MCL-1 only observed after co-treatment. Combined inhibition of BRD4 and CDK9 has recently been assessed in an *in vitro* model of rhabdoid tumours, in which co-treatment with JQ1 and LDC000067 down-regulated the expression of anti-apoptotic genes and known oncogene c-MYC leading to apoptosis induction *in vitro* and profound reductions in tumour growth *in vivo*[50]. CDK9 inhibition is also synthetic lethal with presence of the BRD4-NUT fusion oncogene in NUT midline carcinoma (NMT), where CDK9 represents as a non-oncogenic addiction due to its critical role in regulating transcriptional elongation and MYC expression[51]. Similar to the results described

herein, CDK9 inhibition led to depletion of MCL-1, enhanced γ-H2AX and induction of cell death[51]. All these data support the assertion that CDK9 and BRD4, the major controllers of P-TEFb transcriptional function, are potential targets in cancers addicted to aberrant transcription. Further validation of this synergy between CDK9 and BRD4 inhibition requires a more extensive array of BET inhibitors. In this regard, using BET inhibitors currently under investigation in clinical trials for TNBC or other solid malignancies, such as I-BET762, OTX015 or BAY1238097, would be of relevance[52].

To our knowledge, this study is the first to demonstrate that the CDK9 inhibitors I-73 and Y3-21 sensitise TNBC cells to EGFR-TKIs lapatinib and gefitinib, and to investigate the transcriptional disruption associated with co-treatment. Co-treatment of EGFR-TKI-resistant TNBC cells with lapatinib and I-73 potently inhibits TNBC cell proliferation, induces apoptosis associated with profound G2/M cell cycle arrest, in a manner superior to either monotherapy. Transcriptomic profiling revealed that synergistic inhibition of EGFR and CDK9 led to transcriptional reprogramming in EGFR-TKI-resistant TNBC cells. Co-treatment down-regulated CDK9 and components involved in transcription initiation, thereby suppressing expression of transcription factors such as ZNF, FOX, E2F and KLF, as well as those involved in regulating stem cell pluripotency, G1/S checkpoint and TGF-β signalling. Crucially, this transcriptional reprogramming suppresses numerous downstream targets of IGF, HGF, GDF and MBP growth factor-mediated networks, including the MEK signalling pathway. This could highlight a promising strategy for overcoming adaptive resistance to other RTK- and MEK-targeted therapies, in TNBC and also other cancer types.

A selection of the lapatinib and I-73 synergy-related transcription factors found to be highly expressed in a subset of TNBC tumours were linked to a significantly poorer MFS in TNBC and breast cancer patients in general. Most strikingly, a group of KLF transcription factors, including KLF2, KLF6 and KLF9, were associated with poor clinical outcome. Additionally, our previous work confirmed that a number of these factors, including GATA2, are indispensable factors for TNBC cell proliferation *in vitro*. DACT1 prevents the degradation of β-catenin associated with enhanced GSK-3β phosphorylation, thereby promoting its nuclear translocation and the subsequent transcriptional activation of genes downstream of Wnt/β-catenin-mediated signal transduction[53]. Chromatin immunoprecipitation in ovarian carcinoma cell lines demonstrated that PITX2 is frequently associated with gene promoters downstream of Wnt/β-catenin signalling, and that PITX2 itself can directly activate canonical Wnt signalling[54]. Further functional evaluation of the role of these transcription factors in the control of TNBC proliferation and EGFR-related signal transduction is therefore warranted.

In conclusion, we provide evidence that CDK inhibitors potently targeting CDK9 activity sensitise TNBC cells to the BET inhibitor JQ1 and the EGFR-TKIs lapatinib and erlotinib. Co-treatment of TNBC cell lines with lapatinib and I-73 induces apoptosis and cell cycle arrest associated with depletion of pro-survival factors, profound inhibition of transcription, and obstruction of growth factor-mediated downstream MAPK signalling networks, as evidenced by transcriptomic profiling. This co-treatment preferentially inhibits the function of multiple transcription factors, some of which are significantly associated with poor prognosis in TNBC patients.

Further evaluation of the synergistic interactions in an *in vivo* context, as well as functional genomic studies of synergy-sensitive transcription factors, would be beneficial for ascertaining the true clinical relevance of such combination therapies.

FUNDING

This work was supported by the ERC Advanced grant Triple-BC (grant no. 322737) and the Dutch Cancer Society project (grant nr 2011-5124).

REFERENCES

1. Boyle, P. Triple-negative breast cancer: epidemiological considerations and recommendations. *Ann. Oncol.* **23 Suppl 6,** vi7-12 (2012).
2. de Ruijter, T. C., Veeck, J., de Hoon, J. P. J., van Engeland, M. & Tjan-Heijnen, V. C. Characteristics of triple-negative breast cancer. *J. Cancer Res. Clin. Oncol.* **137,** 183–92 (2011).
3. Dent, R. *et al.* Pattern of metastatic spread in triple-negative breast cancer. *Breast Cancer Res. Treat.* **115,** 423–8 (2009).
4. Kalimutho, M. *et al.* Targeted Therapies for Triple-Negative Breast Cancer: Combating a Stubborn Disease. *Trends Pharmacol. Sci.* **36,** 822–46 (2015).
5. Masuda, H. *et al.* Differential response to neoadjuvant chemotherapy among 7 triple-negative breast cancer molecular subtypes. *Clin. Cancer Res.* **19,** 5533–40 (2013).
6. Radovich, M. *et al.* Characterizing the heterogeneity of triple-negative breast cancers using microdissected normal ductal epithelium and RNA-sequencing. *Breast Cancer Res. Treat.* **143,** 57–68 (2014).
7. Irshad, S., Ellis, P. & Tutt, A. Molecular heterogeneity of triple-negative breast cancer and its clinical implications. *Curr. Opin. Oncol.* **23,** 566–577 (2011).
8. Hnisz, D. *et al.* Convergence of Developmental and Oncogenic Signaling Pathways at Transcriptional Super-Enhancers. *Mol. Cell* **58,** 362–370 (2015).
9. Zawistowski, J. S. *et al.* Enhancer remodeling during adaptive bypass to MEK inhibition is attenuated by pharmacologic targeting of the P-TEFb complex. *Cancer Discov.* **7,** 302–321 (2017).
10. Ahn, S. H., Kim, M. & Buratowski, S. Phosphorylation of serine 2 within the RNA polymerase II C-terminal domain couples transcription and 3' end

processing. *Mol Cell* **13,** 67–76 (2004).

11. Moon, K. J. *et al.* The bromodomain protein Brd4 is a positive regulatory component of P-TEFb and stimulates RNA polymerase II-dependent transcription. *Mol. Cell* **19,** 523–534 (2005).

12. Peterlin, B. M. & Price, D. H. Controlling the Elongation Phase of Transcription with P-TEFb. *Molecular Cell* **23,** 297–305 (2006).

13. Itzen, F., Greifenberg, A. K., Christian, A. B. & Geyer, M. Brd4 activates P-TEFb for RNA polymerase II CTD phosphorylation. **42,** 7577–7590 (2014).

14. Yang, Z. *et al.* Recruitment of P-TEFb for stimulation of transcriptional elongation by the bromodomain protein Brd4. *Mol. Cell* **19,** 535–545 (2005).

15. Lam, F. *et al.* Targeting RNA transcription and translation in ovarian cancer cells with pharmacological inhibitor CDKI-73. *Oncotarget* **5,** 7691–704 (2014).

16. Gao, Y., Liang, Y., Zhang, T., Gray, N. S. & George, R. E. Optimizing selective CDK7 inhibition in MYCN-driven neuroblastoma. *Mol. Cancer Ther.* **14,** (2015).

17. Cayrol, F. *et al.* THZ1 targeting CDK7 suppresses STAT transcriptional activity and sensitizes T-cell lymphomas to BCL2 inhibitors. *Nat. Commun.* **8,** 14290 (2017).

18. Xie, S. *et al.* Antitumor action of CDK inhibitor LS-007 as a single agent and in combination with ABT-199 against human acute leukemia cells. *Acta Pharmacol. Sin.* **37,** 1–9 (2016).

19. Wang, Y. *et al.* CDK7-Dependent Transcriptional Addiction in Triple-Negative Breast Cancer. *Cell* **163,** 174–186 (2015).

20. Duncan, J. S. *et al.* Dynamic reprogramming of the kinome in response to targeted MEK inhibition in triple-negative breast cancer. *Cell* **149,** 307–21 (2012).

21. Groenendijk, F. H. & Bernards, R. Drug resistance to targeted therapies: déjà vu all over again. *Mol. Oncol.* **8,** 1067–83 (2014).

22. Stuhlmiller, T. J. *et al.* Inhibition of lapatinib-induced kinome reprogramming in ERBB2-positive breast cancer by targeting BET family bromodomains. *Cell Rep.* **11,** 390–404 (2015).

23. Nakai, K., Hung, M. C. & Yamaguchi, H. A perspective on anti-EGFR therapies targeting triple-negative breast cancer. *American Journal of Cancer Research* **6,** 1609–1623 (2016).

24. Secq, V. *et al.* Triple negative breast carcinoma EGFR amplification is not associated with EGFR, Kras or ALK mutations. *Br. J. Cancer* **110,** 1045–52 (2014).

25. Martin, V. *et al.* Molecular characterization of EGFR and EGFR-downstream pathways in triple negative breast carcinomas with basal like features. *Histol. Histopathol.* **27,** 785–792 (2012).

26. Baselga, J. *et al.* Randomized phase II study of the anti-epidermal growth factor receptor monoclonal antibody cetuximab with cisplatin versus cisplatin alone in patients with metastatic triple-negative breast cancer. *J. Clin. Oncol.* **31,** 2586–92 (2013).

27. Dickler, M. N., Cobleigh, M. a, Miller, K. D., Klein, P. M. & Winer, E. P. Efficacy and safety of erlotinib in patients with locally advanced or metastatic breast cancer. *Breast Cancer Res. Treat.* **115,** 115–21 (2009).

28. Schuler, M. *et al.* A phase II trial to assess efficacy and safety of afatinib in extensively pretreated patients with HER2-negative metastatic breast cancer. *Breast Cancer Res. Treat.* **134,** 1149–1159 (2012).

29. Fujita, T., Ryser, S., Piuz, I. & Schlegel, W. Up-Regulation of P-TEFb by the MEK1-Extracellular Signal-Regulated Kinase Signaling Pathway Contributes to Stimulated Transcription Elongation of Immediate Early Genes in Neuroendocrine Cells. *Mol. Cell. Biol.* **28,** 1630–1643 (2008).

30. Bonnet, F., Vigneron, M., Bensaude, O. & Dubois, M. F. Transcription-independent phosphorylation of the RNA polymerase II C-terminal domain (CTD) involves ERK kinases (MEK1/2). *Nucleic Acids Res.* **27,** 4399–4404 (1999).

31. Baselga, J. *et al.* Phase II and tumor pharmacodynamic study of gefitinib in patients with advanced breast cancer. *J. Clin. Oncol.* **23,** 5323–33 (2005).

32. Lehmann, B. D. *et al.* Refinement of Triple-Negative Breast Cancer Molecular Subtypes: Implications for Neoadjuvant Chemotherapy Selection. *PLoS One* **11,** e0157368 (2016).

33. Walsby, E. *et al.* A novel Cdk9 inhibitor preferentially targets tumor cells and synergizes with fludarabine. *Oncotarget* **5,** 375–85 (2014).

34. Vichai, V. & Kirtikara, K. Sulforhodamine B colorimetric assay for cytotoxicity screening. *Nat. Protoc.* **1,** 1112–1116 (2006).

35. Zhang, Y. *et al.* Elevated insulin-like growth factor 1 receptor signaling induces antiestrogen resistance through the MAPK/ERK and PI3K/Akt signaling routes. *Breast Cancer Res.* **13 (3):** R52 (2011).

36. Robinson, M. D., McCarthy, D. J. & Smyth, G. K. edgeR: a Bioconductor package for differential expression analysis of digital gene expression data. *Bioinformatics* **26,** 139–40 (2010).

37. McCall, M. N., Bolstad, B. M. & Irizarry, R. A. Frozen robust multiarray analysis

(fRMA). *Biostatistics* **11,** 242–253 (2010).

38. Johnson, W. E., Li, C. & Rabinovic, A. Adjusting batch effects in microarray expression data using empirical Bayes methods. *Biostatistics* **8,** 118–127 (2007).

39. Huang, L., Jiang, Y. & Chen, Y. Predicting Drug Combination Index and Simulating the Network-Regulation Dynamics by Mathematical Modeling of Drug-Targeted EGFR-ERK Signaling Pathway. *Sci. Rep.* **7:** 40752 (2017).

40. Chou, T. C. Drug combination studies and their synergy quantification using the chou-talalay method. *Cancer Research* **70,** 440–446 (2010).

41. Foucquier, J. & Guedj, M. Analysis of drug combinations: current methodological landscape. *Pharmacology Research and Perspectives* **3 (3):** e00149 (2015).

42. Yu, L., Hébert, M. C. & Zhang, Y. E. TGF-β receptor-activated p38 MAP kinase mediates Smad-independent TGF-beta responses. *EMBO J.* **21,** 3749–59 (2002).

43. Mori, S. *et al.* TGF-β and HGF transmit the signals through JNK-dependent Smad2/3 phosphorylation at the linker regions. *Oncogene* **23,** 7416–7429 (2004).

44. Doi, A. *et al.* Enhanced expression of retinoic acid receptor alpha (RARA) induces epithelial-to-mesenchymal transition and disruption of mammary acinar structures. *Mol. Oncol.* **9,** 355–364 (2015).

45. Kuo, Y.-T. *et al.* JARID1B Expression Plays a Critical Role in Chemoresistance and Stem Cell-Like Phenotype of Neuroblastoma Cells. *PLoS One* **10 (5):** e0125343 (2015).

46. Hong, S. H. *et al.* Epigenetic reader BRD4 inhibition as a therapeutic strategy to suppress E2F2-cell cycle regulation circuit in liver cancer. *Oncotarget* **7(22):** 32628-40 (2016).

47. Bayraktar, S. & Glück, S. Molecularly targeted therapies for metastatic triple-negative breast cancer. *Breast Cancer Research and Treatment* **138,** 21–35 (2013).

48. Bernsdorf, M. *et al.* Effect of adding gefitinib to neoadjuvant chemotherapy in estrogen receptor negative early breast cancer in a randomized phase II trial. *Breast Cancer Res. Treat.* **126,** 463–470 (2011).

49. Pazarentzos, E. & Bivona, T. G. Adaptive stress signaling in targeted cancer therapy resistance. *Oncogene* **34,** 5599–606 (2015).

50. Moreno, N. *et al.* Combined BRD4 and CDK9 inhibition as a new therapeutic

approach in malignant rhabdoid tumors. *Oncotarget* **8(49):** 84986-84995 (2017).

51. Brägelmann, J. *et al.* Systematic Kinase Inhibitor Profiling Identifies CDK9 as a Synthetic Lethal Target in NUT Midline Carcinoma. *Cell Rep.* **20,** 2833–2845 (2017).

52. Erez-Salvia, M. P. & Esteller, M. Bromodomain inhibitors and cancer therapy: From structures to applications. *Epigenetics* **12 (5):** 323-339 (2017).

53. Yuan, G. *et al.* Oncogenic function of DACT1 in colon cancer through the regulation of β-catenin. *PLoS One* **7 (3):** e34004 (2012).

54. Basu, M. & Roy, S. S. Wnt/jS-catenin pathway is regulated by PITX2 homeodomain protein and thus contributes to the proliferation of human ovarian adenocarcinoma cell, SKOV-3. *J. Biol. Chem.* **288,** 4355–4367 (2013).

SUPPLEMENTARY FIGURES (OVERLEAF)

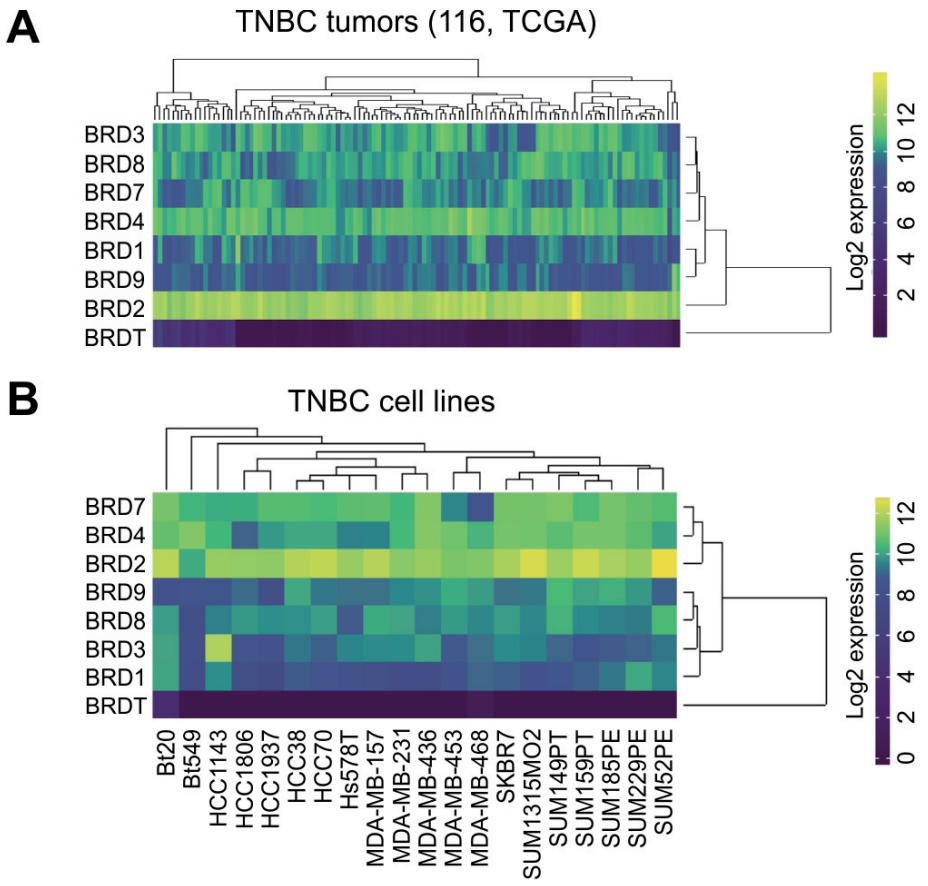

Supplementary Figure S1. A. Expression of BRD family members in 116 patient TNBC tumours. Data derived from TCGA RNA-Seq database. Data shown as RNA-seq-based Log_2 expression level. **B.** Expression of BRD family members in a panel of TNBC cell lines. Data shown as RNA-seq-based Log_2 expression level.

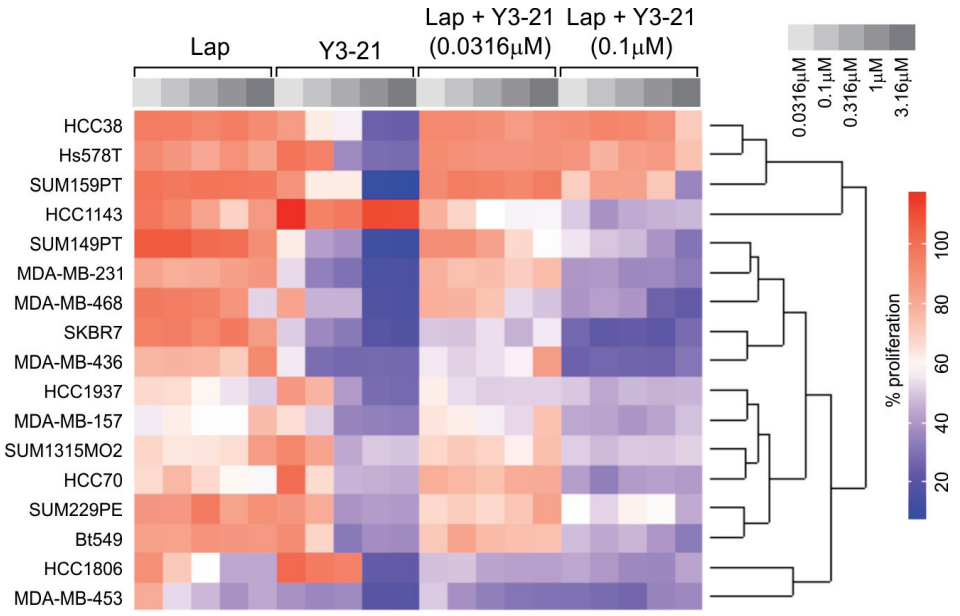

Supplementary Figure S2. A. Combining CDK9 inhibitor Y3-21 (0.0316 or 0.1 μM) with EGFR inhibitor lapatinib in concentration range (0.0316-3.16 μM) enhances proliferative inhibition in TNBC cell lines. Proliferation was evaluated using SRB assay after 4 days' treatment. Results shown as percentage proliferation normalised to DMSO control.

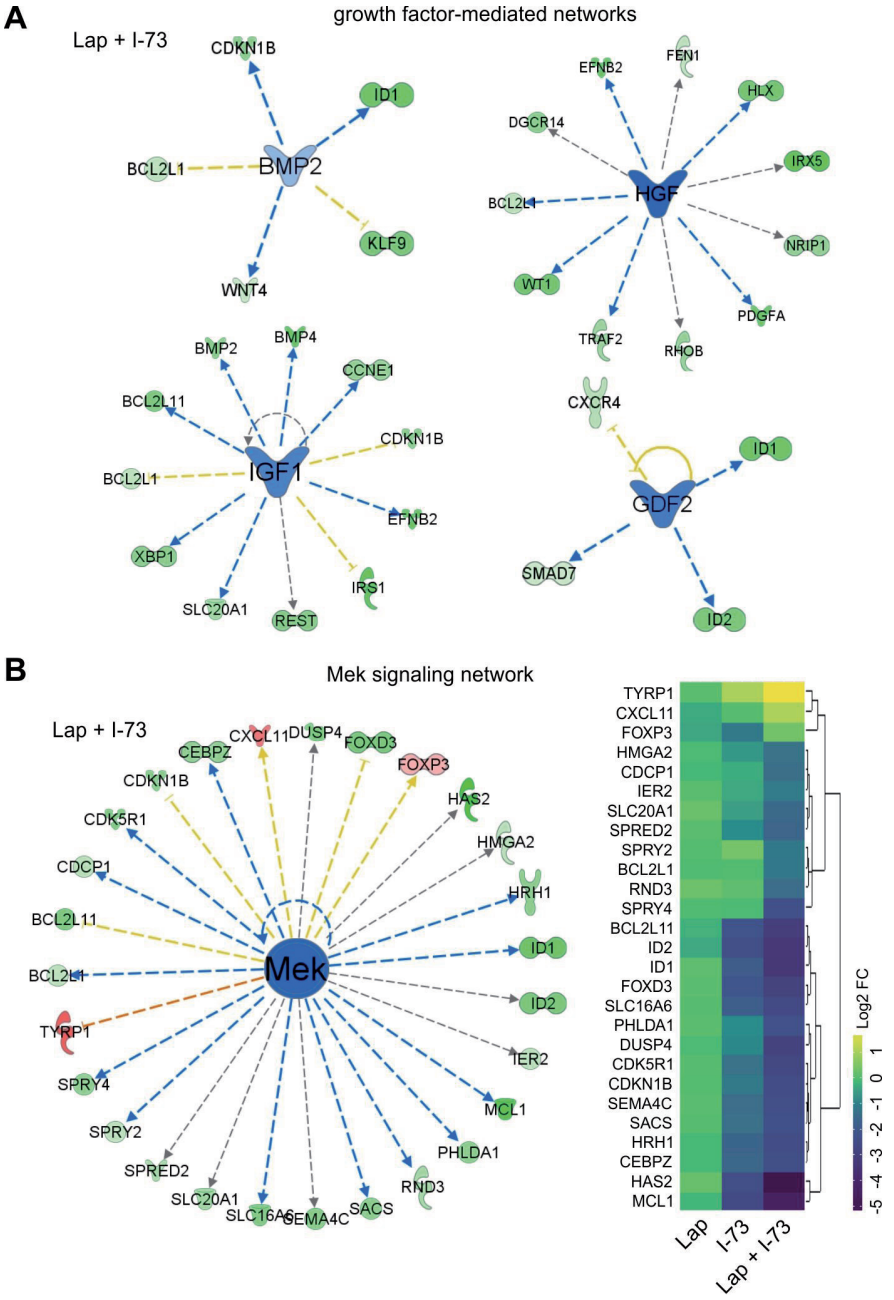

Supplementary Figure S3. CDK9 inhibitor I-73 and EGFR inhibitor lapatinib synergise to block growth factor-mediated networks (**A**) and MAPK/MEK downstream signalling (**B**). The colours of the nodes are as follows; red represents up-regulation, green represents down-regulation, and blue indicates inhibition. The colours of the lines indicating effects are as follows: blue represents inhibition, yellow indicates an inconsistent effect, whereas grey represents events lacking prediction. The heatmap in (**B**) shows the Log_2 fold change (FC) in expression of genes involved in MAPK/MEK-mediated signal transduction after treatment with lapatinib (3.16 μM), I-73 (0.1 μM) or lapatinib (3.16 μM) combined with I-73 (0.1 μM).

Chapter 6

Discussion & Future Perspectives

Breast cancer is the most frequently occurring cancer in women worldwide, and as such represents a substantial clinical burden[1]. It is a profoundly heterogeneous disease which can be sub-classified into multiple histological and molecular subtypes based on anatomical origin and transcriptomic profiling[2–4]. One of the most aggressive forms of breast cancer is the triple-negative subtype (TNBC), which is associated with endemic drug resistance and a significantly poorer survival compared to hormone receptor-positive (HR+) or human epidermal growth factor receptor 2-positive (HER2+) breast cancer[5–9]. Standard clinical management of TNBC is complicated by an acute lack of effective targeted therapies which exploit the unique properties of TNBC cells in order to subvert their aberrant proliferation and subsequent dissemination to distant organs[10]. The principle objective of the studies which constitute this thesis was to identify novel drug targets and/or targeted agents which effectively kill TNBC cells *in vitro*, either as monotherapies or in combination with clinically approved inhibitors. The findings of the chapters presented in this thesis are thus discussed in a broader context whilst relevant points for future investigation are also proposed.

1. The importance of targeting the cell cycle in TNBC

Dysfunctional cell division is one of the key hallmarks of cancer and is linked to abnormalities in the intricate molecular machinery which governs the transition of cells through the strictly controlled transitions that constitute the mammalian cell cycle. Targeting aberrant regulation of this cycle by inhibiting the function of various cyclin-dependent kinases (CDKs) or other kinases involved in cell cycle regulation (e.g. cdc7) is therefore an attractive strategy for targeting TNBC and other cancers. Cancers frequently exhibit altered CDK function resulting in dysregulation of the tightly controlled checkpoints which govern progression into different sections of the

cell cycle[11]. In **Chapter 2** the heterogeneity characteristic of TNBC is evidenced by the differential response of a panel of TNBC cell lines to multiple MEK and AKT inhibitors. Excessive activation of MAPK and/or PI3K pathways is common in TNBC tumours. Deletion of PTEN which negatively regulates Akt activation, or activating mutations in the catalytic subunit of PI3K (PIK3CA) can lead to constitutive Akt activity to which TNBC cells can become addicted[12]. Activating mutations in RAS or RAF, which are located upstream of MEK and ERK, are surprisingly rare in TNBC, however[13,14]. Nonetheless, basal-like tumours are often enriched for an activated RAS transcriptional programme and alterations in negative regulators of RAS/RAF (e.g. DUSP4 and NF1) have been extensively described and linked to metastatic behaviour in TNBC[14–18]. Importantly, in **Chapter 2** we demonstrate that the resistance of cells to dual MEK and Akt inhibition cannot be attributed to crosstalk between MAPK and PI3K pathways since neither MEK nor Akt inhibitors induced up-regulation of the opposing pathway in cell lines resistant to both inhibitors. In order to identify potential vulnerabilities in these double-resistant cell lines, we utilised transcriptomic and proteomic data to identify gene signatures capable of distinguishing double-resistant cell lines from those sensitive to either MEK or Akt inhibition. Cell lines resistant to both inhibitors are enriched for a gene expression signature strongly linked to cell cycle regulation and DNA damage. This enrichment renders double-resistant cell lines relatively more sensitive to CDK inhibitors, which potently induce apoptosis and inhibit proliferation. These results thus highlight the importance of transcriptomic and proteomic profiling in identifying potential novel druggable targets and in the stratification of patients according to drug sensitivity.

In **Chapter 3**, despite high-level EGFR expression in TNBC tumours, we show that TNBC cell lines are overwhelmingly resistant to EGFR-tyrosine kinase inhibitors

(EGFR-TKIs). We confirmed that the resistance of these cells to EGFR-TKIs cannot be attributed to lack of target inhibition since multiple inhibitors effectively reduced EGF-mediated phosphorylation of EGFR in both TKI-resistant and TKI-sensitive TNBC cell lines. By screening a TNBC cell line panel with a kinase inhibitor library in combination with EGFR-TKIs, we demonstrated that simultaneous inhibition of cdc7 and CDK9 function (using kinase inhibitor PHA-767491) sensitised EGFR-TKI-resistant TNBC cells to EGFR inhibition, resulting in cell cycle arrest and eventual apoptosis. Cdc7 is critical for accurate DNA synthesis during S-phase; it phosphorylates mini-chromosome maintenance proteins including MCM2 which subsequently activate DNA helicases which unwind the double-helix and recruit replication factors necessary for DNA synthesis[19,20]. Cdc7 and p53 are both essential for accurate regulation of the G1/S checkpoint; p53 mutations are ubiquitous in TNBC which results in dysfunction or loss of a p53-dependent cdc7-inhibition checkpoint[21]. Since cdc7 inhibition in non-transformed human fibroblasts does not lead to cell cycle arrest due to the presence of intact p53, cdc7 therefore represents a valid, specific anti-cancer target[21]. Moreover, by analysing the association of cdc7 expression with metastasis-free survival (MFS) in a cohort of TNBC patients, we confirmed in **Chapter 3** that cdc7 expression is inversely correlated with MFS in TNBC. Given that PHA-767491 inhibits both cdc7 and CDK9 activity, the evaluation of cdc7-selective inhibitors in TNBC is therefore warranted, particularly in cell lines or tumours lacking functional p53, either as monotherapies or in combination with RTK-targeted agents such as EGFR-TKIs.

2. Exploiting the dysfunctional, CDK-regulated transcriptional machinery in TNBC

During their development, cancers accrue a myriad of damaging genetic and/or epigenetic lesions and aberrations which ultimately disrupt the signal transduction cascades controlling cell proliferation, survival and motility, amongst others[17,22,23]. Despite the fact that the genomic landscape of tumours is littered with innumerable mutations, multiple cancers are addicted to activation of particular signal transduction pathways as a result of activation of certain oncogenes. This renders such cancers sensitive to targeted agents which repress oncogene-driven signal transduction. Whilst targeting RTK-mediated signalling is effective against cancers with clear oncogenic drivers such as oestrogen receptor-positive (ER+) breast cancer, androgen receptor-positive (AR+) prostate cancer or EGFR-mutant non-small cell lung cancer (NSCLC), in TNBC the lack of immediately discernible and pharmacologically amenable driver pathways or mutations severely limits the use of such therapies[24]. Moreover, targeting RTK-mediated signal transduction is often confounded by the functional redundancy that exists within and between multiple families of RTKs, as well as adaptive transcriptional responses in response to oncogenic RTK inhibition which promote up-regulation of alternative RTKs[25,26]. Instead, inhibiting the transcriptional machinery at the root of all RTK-fuelled signal transduction in TNBC represents one method of exploiting so-called “non-oncogene addiction”, a phenomenon whereby despite the absence of mutations in selected genes, malignant cells rely upon their function for their own survival as a result of oncogene-mediated distortion of signal transduction or cellular processes[27]. Amplification of c-MYC in many breast tumours confers a dependency on exceptionally high levels of transcription in order to sustain the MYC-driven

transcriptional programmes which contribute to the maintenance of an oncogenic state[28]. This transcriptional addiction can also be targeted in TNBC and covalent CDK7 inhibitor THZ1 has shown pre-clinical benefit in this context[29].

Consequently, we evaluated the potential of a selection of CDK inhibitors which prevent the function of key transcriptional regulators (e.g. P-TEFb/CDK9 and TFIIH), in addition to CDK1 and CDK2, as possible options for targeted therapy in TNBC in **Chapter 4**. Taking the molecular heterogeneity of TNBC into account, we screened a panel of 20 TNBC cell lines representative of all TNBC molecular subtypes described by Lehmann et al (2016)[4]. Strikingly, inhibitors with potent activity against CDK1, CDK2, CDK9 and CDK7 were extremely effective at preventing the proliferation of TNBC cells at concentrations as low as 100 nM. These anti-proliferative effects were accompanied by induction of apoptosis and G2/M cell cycle arrest. Inhibition of cell migration speed at sub-lethal concentrations also highlighted the potential of these agents to prevent initiation of the metastatic cascade. These effects were comparable to those elicited by clinically-approved pan-CDK inhibitors dinaciclib and flavopiridol, suggesting such compounds could have similar efficacy in a clinical context. Contrastingly, CDK4/6-selective inhibitors such as palbociclib and abemaciclib were generally ineffective, suggesting that targeting CDK4/6-mediated cell cycle progression is futile, except in TNBC cells which express androgen receptor (AR)[30]. This is consistent with other studies which delineate a clear dependency on CDK4/6-mediated regulation of G1/S transition in ER+ or HER2+ breast cancers and in AR+ prostate cancers[31–34]. Androgens and oestrogens promote cell cycle progression by up-regulating Cyclin D1 expression, which can therefore be counteracted by using CDK4/6 inhibitors in combination with anti-hormonal therapy[35]. The tumourigenesis of HER2+ breast cancers is also dependent on concomitant CDK4 activity[36].

Nevertheless, considerable functional redundancy exists between CDKs; CDK12 also phosphorylates the CTD of RNA Polymerase II at Serine 2 to promote transcriptional elongation. The expression of DNA damage response (DDR)-associated genes and NRF2 target genes is particularly sensitive to disruption of CDK12 function, strongly suggesting that CDK12 is involved in the transcriptional regulation of adaptive cellular stress responses[37–39]. Additionally, CDK12 function is required for the termination of transcription; CDK12 depletion prevented the 3' end processing of c-FOS mRNA transcripts induced by EGF stimulation in human embryonic kidney cells, also suggesting that it is required for successful transduction of RTK-mediated signalling via terminal transcription factors[40]. Interestingly, the specificity of CDK12 for particular transcripts has not yet been unequivocally established[38,41]. Considering its aforementioned roles in transcriptional regulation, CDK12 could theoretically compensate for decreased CDK9 activity, and therefore P-TEFb activity, in order to drive productive elongation of mRNA transcripts and overcome growth inhibition by CDK9-specific inhibitors. However, this hypothesis clearly requires experimental validation by assessing and comparing the effects of CDK12 and CDK9 depletion in TNBC cells, either by using RNAi or CRISPR-Cas9 technologies or by developing highly selective and effective inhibitors for these kinases. A CDK12-specific inhibitor THZ531 has been synthesised and exhibited potent activity against T-cell acute lymphoblastic lymphoma (T-ALL) models[42]. Nevertheless, a high degree of structural homology exists between members of the CDK family, particularly in the ATP-binding site, often precluding the development of ATP-competitive inhibitors highly selective for individual CDKs[43,44]. Resistance to single targeted agents invariably develops in the clinic, and for this reason rational combination therapies are increasingly being considered as compulsory in

oncology[25,45]. In several TNBC models and in patient tumours, kinase inhibition induces up-regulation of alternative RTKs which bypass the inhibitory effects of these agents thereby permitting the development of resistance[46,47]. Considering the profound inhibition of proliferation, depletion of BCL-2 family member proteins, and attenuation of transcriptional elongation seen after CDK inhibitor treatment, we therefore combined the CDK inhibitors I-73 and LY3-21 with EGFR-TKIs and bromodomain (BET) inhibitors in **Chapter 5** to determine whether they could sensitise drug-resistant TNBC to such compounds. We confirmed that these agents strongly synergise in *in vitro* models of TNBC, leading to superior inhibition of cell proliferation, cell cycle arrest and induction of apoptosis.

To scrutinise the mechanism of action of these CDK inhibitors and rational combinations further, we performed RNA sequencing to determine the global impact of treatment on gene expression and signal transduction. Transcriptomic profiling identified a select list of CDK inhibitor-sensitive transcription factors significantly enriched in basal-like breast tumours. By virtue of RNA interference-based screening, we confirmed in **Chapter 4** that expression of a number of these transcription factors was essential for the proliferation of multiple TNBC cell lines. SOX9, EN1 and PLAG1 were associated with epithelial-to-mesenchymal transition (EMT), maintenance of basal-like subtype, mitochondria-regulated protection from cell death stimuli, and IGF-mediated signal transduction[48–52]. Moreover, we showed in **Chapter 5** that combined EGFR-TKI and I-73 treatment enhances the impact of I-73 on gene transcription. Additionally, I confirmed that expression of a number of transcription factors differentially and significantly down-regulated after co-treatment with EGFR-TKI and I-73 was strongly linked to poor prognosis in TNBC patients. The use of transcriptional CDK inhibitors in multiple malignancies has permitted the identification

of “super enhancer-associated genes” which are indispensable for cancer cell survival and exquisitely sensitive to CDK7 inhibition[29,53–55]. Considering that SOX9 and EN1 have previously been identified as super enhancer-associated genes in specific TNBC cell lines, expanding the list of such genes should constitute a future priority. Detecting these enhancer regions by virtue of their enrichment for specific epigenetic markers (e.g. acetylation of H3K27 or methylation of H3K4) using Ch-IP sequencing in TNBC cells and xenograft tumours treated with the effective novel CDK inhibitors and rational combinations identified in this thesis could allow identification of novel super enhancer-associated genes in TNBC. This would therefore provide further mechanistic insight whilst illuminating knowledge of the transcriptional programmes which drive heterogeneous tumours like TNBC. Whilst directly targeting transcription factor function remains pharmacologically problematic, an increased understanding of the programmes driving growth and tumour adaptation to therapy could permit the evidence-based identification of synthetic lethal interactions

3. The limitations of *in vitro* compound screening

Notwithstanding the remarkable sensitivity of TNBC cells to these CDK inhibitors *in vitro*, the contribution of the tumour microenvironment to intrinsic or acquired resistance cannot be understated[56–58]. *In vitro* models cannot recapitulate the intricate complexity conferred by the tumour vasculature and surrounding tissues which directly and indirectly control the availability of nutrients and the ability of therapeutics to reach the tumour bulk[59]. Crucially, assessing single CDK inhibitor efficacy, as well as combining EGFR-TKIs (e.g. lapatinib) and I-73, in a PDX-based or xenotransplantation model will be vital in elucidating whether it is possible to replicate the strong synergy observed *in vitro* in **Chapter 5**. Such models would also

provide information on whether this combination is likely to have clinical efficacy in tumours which express high levels of EGFR or which depend on EGFR pathway functionality. More importantly, whether the efficacy or eventual synergy observed is due to inhibition of the aforementioned CDK inhibitor-sensitive or synergy-associated transcription factors indispensable for cell growth *in vitro*, should be investigated. Intriguingly, recent evidence derived from *in vitro* and *in vivo* models of glioblastoma (GBM) revealed a distinct lack of overlap between the transcription elongation factors required for GBM survival in vitro and those necessary for tumour outgrowth in orthotopic patient-derived xenografts (PDX)[60]. Specifically, genes regulating productive transcriptional elongation and pause-release, in particular JMJD6 and BRD4, were essential for enhancer-mediated transcriptional adaptation to the tumour microenvironment[60]. In general, an increased dependency on pause-release and elongation machinery was observed *in vivo.* The tumour microenvironment presents wholly different challenges to tumour proliferation than those encountered by homogenous populations of cancer cell lines cultured on plastic. *In vivo*, tumour cells must adapt to hypoxic conditions and the scarcity of nutrients, whilst also disarming infiltrating immune cells with the power to destroy them, thereby subverting the anti-tumour immune response[61]. Importantly, they must also physically interact, and communicate, with surrounding stromal cells in order to survive and establish a tumour-permissive environment[61–64]. Therefore, an increased dependency on transcriptional programmes which regulate adaptive stress responses is to be expected. In contrast, *in vitro* culture systems are by and large designed to eliminate such stresses. Cultured cell lines receive abundant nutrients and the absence of immunogenic pressure or stromal influence allows these cells to expand rapidly and with ease, facilitating phenotypic drift from the tumour from which they were originally

derived[61,65,66]. It is thus imperative to consider *in vitro* systems such as those utilised throughout this thesis, as mere models and not, therefore, an accurate reflection of the potential of targeted agents in the clinic[65]. Additionally, xenotransplantation of cancer cell lines into mice is associated with its own limitations; unlike PDX-based models, cell line-derived xenografts do not retain the original tumour architecture and do not preserve inter-and intra-tumoural heterogeneity[67,68]. Moving forward, it would therefore be of utmost importance to verify whether any overlap exists between the TNBC-specific transcriptional programmes sensitive to CDK inhibition identified *in vitro* in **Chapters 4 and 5** of this thesis, and those required for TNBC tumour growth *in vivo*. Comparison of RNA seq-derived transcriptomic profiles of PDX-derived tumours treated with single agent I-73 or in combination with EGFR-TKIs, with the profiles of TNBC cell lines cultured *in vitro* or xenotransplanted into mice, may permit further research to focus on the most relevant pathways for *in vivo* tumour growth, instead of those which represent *in vitro* artefacts. However, the fact that the reliance of GBM cells on the function of transcriptional elongation and pause-release factors was enhanced in an *in vivo* context, is reassuring considering how disruption of such molecules so potently eliminates the propensity of TNBC cells to grow *in vitro*.

4. <u>Manipulating the connection between CDK function and the DNA damage response (DDR)</u>

Apart from their impact on CDK9-regulated, P-TEFb-mediated transcriptional elongation, the effective CDK inhibitors tested here also have potent activity against CDK1. The formation of CDK1-Cyclin B1 complexes is an essential component of the mitotic checkpoint during cell division, these complexes being responsible for the reorganisation of nuclear architecture prior to cytokinesis. Although CDK1's primary function is in regulating mitosis, it is also known to influence the stability of proteins

required for precise DNA damage repair, particularly the stability of BRCA1[69]. Depletion of CDK1 can substantially and selectively enhance the efficacy of PARP inhibitors in HR-proficient, BRCA1 wild-type cancer cells, leaving untransformed cells relatively unaffected by combined CDK1 and PARP inhibition[69]. Considering the strong induction of G2/M cell cycle arrest and γ-H2AX induction elicited by I-73 and D11-81 in **Chapter 4**, and the induction of γ-H2AX and PARP1 cleavage by dinaciclib in **Chapter 2**, it is tempting to attribute such effects to inhibition of CDK1 or CDK2. Regardless, dissecting phenotypic responses remains troublesome with pan-CDK inhibitors due to lack of target specificity. However, these DNA damage-related responses could theoretically be exploited by combining the CDK inhibitors described here with currently used chemotherapeutics such as doxorubicin, gemcitabine or cisplatin[70].

Whilst particular attention has been given to inhibitors with potent activity against P-TEFb/CDK9 and other CDKs, namely CDK1, CDK2 and CDK7, the consequences of CDK12 inhibition have not been addressed. CDK12 also phosphorylates the CTD of RNA Polymerase II (POLR2A) and specifically regulates the expression of genes involved in DNA-damage repair[37,71,72]. Recent studies have demonstrated that pan-CDK inhibitor dinaciclib also targets CDK12 function in addition to CDK1, CDK2, CDK5 and CDK9[73]. Treatment of TNBC cells with dinaciclib inhibited the expression of genes linked to homologous recombination (HR) and DDR, effects which were also seen after CDK12 depletion. Dinaciclib-induced CDK12 inhibition or RNAi-mediated CDK12 depletion reduced the capacity of BRCA1/2 wild-type (wt) cells and tumours for HR after exposure to γ-irradiation and were therefore sensitised to PARP inhibitors[73]. Crucially, dinaciclib-mediated CDK12 inhibition abrogated acquired resistance to PARP inhibitors in several PDX models of TNBC[73]. PI3K inhibition in

TNBC cells also induces DNA damage which augments the response of BRCA-wt/HR-proficient cells to PARP1/2 inhibitors, emphasising the links between PI3K signalling and the DNA-damage response (DDR)[74]. Considering that MEK-i/Akt-i double-resistant cells are highly sensitive to pan-CDK inhibitors such as dinaciclib, there is a clear rationale for combining dinaciclib or MEK/AKT inhibition with PARP inhibitors and chemotherapy or radiotherapy in such instances. Investigating whether Akt or MEK inhibitors alter the DNA-damage response themselves, across the differentially sensitive subgroups identified in **Chapter 1**, could therefore also potentially identify DNA-damaging agents as possible combination therapies together with MEK or Akt inhibitors. Additionally, combining the CDK inhibitors evaluated in **Chapter 4** with PARP inhibitors in TNBC cells both proficient and deficient in HR could therefore identify novel rational synergistic combinations for specific groups of TNBC patients. Such combinations may allow the use of lower doses and thereby avoid the off-target toxicity associated with either therapy.

5. Future Perspectives

One of the principle concerns regarding the translation of pre-clinically effective CDK inhibitors to the clinic is the induction of systemic toxicity. First-generation pan-CDK inhibitors flavopiridol and roscovitine showed immense promise in pre-clinical investigations but ultimately failed to deliver in the clinic[75–78]. Similarly, dinaciclib has shown limited potential in patients with solid tumours[75]. A recently completed phase 1 clinical trial of dinaciclib in various multiple solid malignancies revealed that dose-limiting effects included pancytopenia, hyperuricemia and hypotension[79]. Additionally, dinaciclib exhibited potent growth inhibitory effects on normal patient lymphocytes treated *ex vivo*[79]. In breast cancer specifically, dinaciclib has yet to demonstrate superior efficacy over standard-of-care chemotherapy-based treatments such as

capecitabine in patients with advanced disease, with severe neutropenia being reported in around 75% of patients[80]. Pharmacokinetic limitations were also problematic; short half-lives were seen for 2 hour infusions with dinaciclib whilst longer infusions induced hepatotoxicity[79].

In order to maximise the benefit from CDK inhibitors and to combat the high rates of attrition currently associated with the development of such agents, three unsettled issues concerning their use and design must therefore be addressed. Primarily, and as previously mentioned, disentangling the relationships between phenotypic effects and target inhibition is crucial. Without a clear understanding of mechanism of action, clinical translation will be extremely difficult. To this end, functional genomic screening to verify whether phenotypic effects such as apoptosis, cell cycle arrest or autophagy are associated with disruption of particular CDKs in TNBC would be highly appropriate. It is envisaged that pan-CDK inhibitors such as I-73, D11-81 or LY3-21 owe their antineoplastic effects to the combined inhibition of multiple CDKs. Nonetheless, through transcriptomic profiling in **Chapters 4 and 5** we showed that these agents overwhelmingly affect transcription factor function, strongly suggesting that inhibition of transcriptional CDKs is a significant component of their inhibitory effects. Secondly, the identification of patients who will derive maximum benefit from such treatments is absolutely paramount. The clinical trials in which pan-CDK inhibitors have been evaluated, assessed end-point responses such as target inhibition, side-effects, disease progression and long-term survival yet often lacked genomic or transcriptomic profiling of tumours from patients who responded to anti-CDK therapy[79]. Consequently, elucidating whether certain gene signatures or genomic lesions can distinguish CDK inhibitor-sensitive from CDK inhibitor-resistant patients as well as signatures associated with less toxicity, would be invaluable. The

utility of such an approach was emphasised in **Chapter 2**, in which we established a rationale for CDKs as an alternative targeted therapy in TNBC resistant to both MEK and AKT inhibitors, due to the enhanced expression of a cell cycle-related gene signature in these tumours. Considering the mounting pre-clinical evidence that CDK inhibition is synthetic lethal with MYC amplification, stratifying patients based on such a marker would be prudent[81,82]. Disruption of CDK1 function is synthetic lethal with KRAS-mutations in pancreatic ductal adenocarcinoma cell lines and colorectal cancer xenografts and with PARP inhibition in BRCA-mutant and BRCA-wt breast cancers, denoting other possible indications for the use of CDK inhibitors[69,83]. Thirdly, and of particular relevance for their use in combination therapies, absence of a malleable therapeutic window has hampered efforts to successfully combine CDK inhibitors and standard-of-care treatments[75]. The impact of selective CDK9 inhibition on the survival of normal, non-cancerous cells is yet to be determined. The evidence that cancers depend upon transcriptional CDKs such as CDK7 and CDK9 for the execution of oncogenic transcriptional programmes may allow for discrimination between normal and malignant tissue, though disruption of other CDKs such as CDK1 is known to be detrimental for the proliferation and mitosis of normal cells and for maintenance of genomic stability in pluripotent stem cells[84,85]. The clinical balancing act of achieving superior efficacy whilst avoiding the onset of dangerous toxicity is extremely challenging. Thorough toxicological assessment of CDK inhibitors such as I-73 in human tissues which are frequently the sites of adverse reactions is therefore essential. The use of *in vitro* or *ex vivo* screening systems which utilise primary human hepatocytes, renal cells and/or bone marrow-derived haematopoietic stem cells is of particular relevance here. Previously published data showing the substantial selectivity of I-73 for tumour cells over CD34+

haematopoietic cells or human embryonic kidney cells is reassuring in this regard[86,87]. Nonetheless, the dearth of objective responses, as well as the premature termination of clinical trials of pan-CDK inhibitors in a monotherapeutic context, is testament to the necessity for rational combination therapies in solid malignancies.

6. Conclusions

Collectively, the work presented in this thesis stresses the importance of inhibiting CDK function in TNBC as a means to bypass or overcome resistance to already-established molecular-targeted agents and as effective monotherapies. The use of high-throughput screening and compound libraries was essential to the identification of novel molecular targeted therapies effective against *in vitro* models of TNBC, as well as rational synergistic combinations with superior potency. Extensive pre-clinical toxicity testing is, however, required before these results can be translated to a clinical context, as well as further delineation of the relationship between target inhibition and phenotypic response. Additionally, this thesis highlights the importance of omic-based technologies in identifying novel targets and evaluating the transcriptional response of cancer cells to targeted therapies in order to elucidate the signalling networks most sensitive to CDK inhibition.

References

1. Jemal, A., Bray, F. & Ferlay, J. Global Cancer Statistics. *CA Cancer J Clin.* **61,** 69–90 (2011).
2. Makki, J. Diversity of Breast Carcinoma : Histological Subtypes and Clinical Relevance. *Clin Med Insights Pathol.* **8:** 23–31 (2015).
3. Malhotra, G. K., Zhao, X., Band, H. & Band, V. Histological, molecular and functional subtypes of breast cancers. *Cancer Biol. Ther.* **10,** 955–960 (2014).
4. Lehmann, B. D. *et al.* Refinement of Triple-Negative Breast Cancer Molecular Subtypes: Implications for Neoadjuvant Chemotherapy Selection. *PLoS One* **11,** e0157368 (2016).

5. Press, D. Update on triple-negative breast cancer : prognosis and management strategies. *Int J Womens Health* **4:** 511–520 (2012).

6. de Ruijter, T. C., Veeck, J., de Hoon, J. P. J., van Engeland, M. & Tjan-Heijnen, V. C. Characteristics of triple-negative breast cancer. *J. Cancer Res. Clin. Oncol.* **137,** 183–92 (2011).

7. Cheang, M. C. U. *et al.* Basal-like breast cancer defined by five biomarkers has superior prognostic value than triple-negative phenotype. *Clin. Cancer Res.* **14,** 1368–76 (2008).

8. Boyle, P. Triple-negative breast cancer: epidemiological considerations and recommendations. *Ann. Oncol.* **23 Suppl 6,** vi7-12 (2012).

9. Dent, R. *et al.* Pattern of metastatic spread in triple-negative breast cancer. *Breast Cancer Res. Treat.* **115,** 423–8 (2009).

10. Crown, J., O'Shaughnessy, J. & Gullo, G. Emerging targeted therapies in triple-negative breast cancer. *Ann. Oncol.* **23 Suppl 6,** vi56-65 (2012).

11. Malumbres, M. & Barbacid, M. Cell cycle, CDKs and cancer: a changing paradigm. *Nat. Rev. Cancer* **9,** 153–166 (2009).

12. Liu, J. C. *et al.* Combined deletion of Pten and p53 in mammary epithelium accelerates triple-negative breast cancer with dependency on eEF2K. *EMBO Mol. Med.* **6,** 1542–1560 (2014).

13. Shah, S. P. *et al.* The clonal and mutational evolution spectrum of primary triple-negative breast cancers. *Nature* **486,** 395–399 (2012).

14. Network, T. C. G. A. Comprehensive molecular portraits of human breast tumors. *Nature* **490,** 61–70 (2012).

15. Hoeflich, K. P. *et al.* In vivo Antitumor Activity of MEK and Phosphatidylinositol 3-Kinase Inhibitors in Basal-Like Breast Cancer Models. *Clin Cancer Res.* **15 (14):** 4649-64 (2009)

16. Bartholomeusz, C. *et al.* High ERK protein expression levels correlate with shorter survival in triple-negative breast cancer patients. *Oncologist* **17,** 766–74 (2012).

17. Balko, J. M. *et al.* Molecular profiling of the residual disease of triple-negative breast cancers after neoadjuvant chemotherapy identifies actionable therapeutic targets. *Cancer Discov.* **4,** 232–245 (2014).

18. Wallace, M. D. *et al.* Comparative oncogenomics implicates the neurofibromin 1 gene (NF1) as a breast cancer driver. *Genetics* **192,** 385–396 (2012).

19. Yamada, M., Masai, H. & Bartek, J. Regulation and roles of Cdc7 kinase under replication stress. *Cell Cycle* **13,** 1859–66 (2014).

20. Rainey, M. D., Quachthithu, H., Gaboriau, D. & Santocanale, C. DNA Replication Dynamics and Cellular Responses to ATP Competitive CDC7 Kinase Inhibitors. *ACS Chem. Biol.* **12,** 1893–1902 (2017).

21. Rodriguez-Acebes, S. *et al.* Targeting DNA replication before it starts: Cdc7 as a therapeutic target in p53-mutant breast cancers. *Am. J. Pathol.* **177,** 2034–45 (2010).

22. Burrell, R. A., McGranahan, N., Bartek, J. & Swanton, C. The causes and consequences of genetic heterogeneity in cancer evolution. *Nature* **501,** 338–345 (2013).

23. Chatterjee, A., Rodger, E. J. & Eccles, M. R. Epigenetic drivers of tumourigenesis and cancer metastasis. *Seminars in Cancer Biology* **51:** 149-159 (2018).

24. Metzger-Filho, O. *et al.* Dissecting the heterogeneity of triple-negative breast cancer. *Journal of Clinical Oncology* **30,** 1879–1887 (2012).

25. Wilson, T. R. *et al.* Widespread potential for growth-factor-driven resistance to anticancer kinase inhibitors. *Nature* **487,** 505–509 (2012).

26. Stuhlmiller, T. J. *et al.* Inhibition of lapatinib-induced kinome reprogramming in ERBB2-positive breast cancer by targeting BET family bromodomains. *Cell Rep.* **11,** 390–404 (2015).

27. Nagel, R., Semenova, E. A. & Berns, A. Drugging the addict: non-oncogene addiction as a target for cancer therapy. *EMBO Rep.* **17,** 1516–1531 (2016).

28. Chipumuro, E. *et al.* CDK7 inhibition suppresses super-enhancer-linked oncogenic transcription in MYCN-driven cancer. *Cell* **159,** 1126–39 (2014).

29. Wang, Y. *et al.* CDK7-dependent transcriptional addiction in triple-negative breast cancer. *Cell* **163,** 174–86 (2015).

30. Asghar, U. S. *et al.* Single-cell dynamics determines response to CDK4/6 inhibition in triple-negative breast cancer. *Clin. Cancer Res.* **23,** 5561–5572 (2017).

31. Stice, J. P. *et al.* CDK4/6 Therapeutic Intervention and Viable Alternative to Taxanes in CRPC. *Mol. Cancer Res.* **15,** 660–669 (2017).

32. Finn, R. S. *et al.* PD 0332991, a selective cyclin D kinase 4/6 inhibitor, preferentially inhibits proliferation of luminal estrogen receptor-positive human breast cancer cell lines in vitro. *Breast Cancer Res.* **11 (5):** R77 (2009).

33. Witkiewicz, A. K., Cox, D. & Knudsen, E. S. CDK4 / 6 inhibition provides a potent adjunct to Her2-targeted therapies in preclinical breast cancer models *Genes Cancer*: **5 (7-8):** 261-272 (2014).

34. Malumbres, M. CDK4/6 Inhibitors resTORe Therapeutic Sensitivity in HER2+Breast Cancer. *Cancer Cell* **29,** 243–244 (2016).

35. Kilker, R. L., Hartl, M. W., Rutherford, T. M. & Planas-Silva, M. D. Cyclin D1 expression is dependent on estrogen receptor function in tamoxifen-resistant breast cancer cells. *J. Steroid Biochem. Mol. Biol.* **92,** 63–71 (2004).

36. Yu, Q. *et al.* Requirement for CDK4 kinase function in breast cancer. *Cancer Cell* **9,** 23–32 (2006).

37. Blazek, D. *et al.* The Cyclin K/Cdk12 complex maintains genomic stability via regulation of expression of DNA damage response genes. *Genes Dev.* **25,** 2158–72 (2011).

38. Paculová, H. & Kohoutek, J. The emerging roles of CDK12 in tumorigenesis. *Cell Division* **12:7** (2017).

39. Li, X., Chatterjee, N., Spirohn, K., Boutros, M. & Bohmann, D. Cdk12 is a gene-selective RNA polymerase II kinase that regulates a subset of the transcriptome, including Nrf2 target genes. *Sci. Rep.* **6,** 21455 (2016).

40. Eifler, T. T. *et al.* Cyclin-Dependent Kinase 12 Increases 3′ End Processing of Growth Factor-Induced c-FOS Transcripts. *Mol. Cell. Biol.* **35,** 468–478 (2015).

41. Chilà, R., Guffanti, F. & Damia, G. Role and therapeutic potential of CDK12 in human cancers. *Cancer Treatment Reviews* **50,** 83–88 (2016).

42. Zhang, T. *et al.* Covalent targeting of remote cysteine residues to develop CDK12 and CDK13 inhibitors. *Nat. Chem. Biol.* **12,** 876–884 (2016).

43. Echalier, A., Hole, A. J., Lolli, G., Endicott, J. A. & Noble, M. E. M. An inhibitor's-eye view of the atp-binding site of CDKs in different regulatory states. *ACS Chem. Biol.* **9,** 1251–1256 (2014).

44. Kry, V., Baumli, S. & Fürst, R. Perspective of Cyclin-dependent kinase 9 (CDK9) as a Drug Target. **9,** 2883–2890 (2012).

45. Groenendijk, F. H. & Bernards, R. Drug resistance to targeted therapies: déjà vu all over again. *Mol. Oncol.* **8,** 1067–83 (2014).

46. Zawistowski, J. S. *et al.* Enhancer remodeling during adaptive bypass to MEK inhibition is attenuated by pharmacologic targeting of the P-TEFb complex. *Cancer Discov.* **7,** 302–321 (2017).

47. Duncan, J. S. *et al.* Dynamic reprogramming of the kinome in response to targeted MEK inhibition in triple-negative breast cancer. *Cell* **149,** 307–21 (2012).

48. Kawai, T. *et al.* SOX9 is a novel cancer stem cell marker surrogated by osteopontin in human hepatocellular carcinoma. *Sci. Rep.* **6,** 30489 (2016).

49. Su, Y. *et al.* Somatic Cell Fusions Reveal Extensive Heterogeneity in Basal-like Breast Cancer. *CellReports* **11,** 1549–1563 (2015).

50. Voz, M. L., Agten, N. S., Van De Ven, W. J. M. & Kas, K. PLAG1, the main translocation target in pleomorphic adenoma of the salivary glands, is a positive regulator of IGF-II. *Cancer Res.* **60,** 106–113 (2000).

51. Van Dyck, F., Declercq, J., Braem, C. V. & Van De Ven, W. J. M. PLAG1, the prototype of the PLAG gene family: Versatility in tumour development (Review). *International Journal of Oncology* **30,** 765–774 (2007).

52. Alvarez-Fischer, D. *et al.* Engrailed protects mouse midbrain dopaminergic neurons against mitochondrial complex I insults. *Nat. Neurosci.* **14 (10):** 1260-6 (2011).

53. Gao, Y., Liang, Y., Zhang, T., Gray, N. S. & George, R. E. Optimizing selective CDK7 inhibition in MYCN-driven neuroblastoma. [abstract]. In: Proceedings of the AACR-NCI-EORTC International Conference: Molecular Targets and Cancer Therapeutics; 2015 Nov 5-9; Boston, MA. Philadelphia (PA): AACR; *Mol Cancer Ther.* **12**, Suppl 2: Abstract nr B165 (2015).

54. Cayrol, F. *et al.* THZ1 targeting CDK7 suppresses STAT transcriptional activity and sensitizes T-cell lymphomas to BCL2 inhibitors. *Nat. Commun.* **8,** 14290

(2017).

55. Christensen, C. L. *et al.* Targeting transcriptional addictions in small cell lung cancer with a covalent CDK7 inhibitor. *Cancer Cell* **26,** 909–22 (2014).

56. Holohan, C., Van Schaeybroeck, S., Longley, D. B. & Johnston, P. G. Cancer drug resistance: an evolving paradigm. *Nat. Rev. Cancer* **13,** 714–26 (2013).

57. Yu, Y. *et al.* Cancer-associated fibroblasts induce epithelial-mesenchymal transition of breast cancer cells through paracrine TGF-β signalling. *Br. J. Cancer* **110,** 724–732 (2014).

58. Ramos, P. & Bentires-Alj, M. Mechanism-based cancer therapy: resistance to therapy, therapy for resistance. *Oncogene* **34 (28)**: 3617-26 (2014).

59. Byrne, A. T. *et al.* Interrogating open issues in cancer precision medicine with patient-derived xenografts. *Nature Reviews Cancer* **17,** 254–268 (2017).

60. Miller, T. E. *et al.* Transcription elongation factors represent in vivo cancer dependencies in glioblastoma. *Nature* **547,** 355–359 (2017).

61. Choi, S. Y. C. *et al.* Lessons from patient-derived xenografts for better in vitro modeling of human cancer. *Advanced Drug Delivery Reviews* **79,** 222–237 (2014).

62. Raz, Y. & Erez, N. An inflammatory vicious cycle: Fibroblasts and immune cell recruitment in cancer. *Experimental Cell Research* **319,** 1596–1603 (2013).

63. Cirri, P. & Chiarugi, P. Cancer associated fibroblasts: the dark side of the coin. *Am. J. Cancer Res.* **1,** 482–97 (2011).

64. Sun, X. *et al.* IL-6 secreted by cancer-associated fibroblasts induces tamoxifen resistance in luminal breast cancer. *Oncogene* **33,** 4450 (2014).

65. Voskoglou-Nomikos, T., Pater, J. L. & Seymour, L. Clinical predictive value of the in vitro cell line, human xenograft, and mouse allograft preclinical cancer models. in *Clinical Cancer Research* **9,** 4227–4239 (2003).

66. Hughes, P., Marshall, D., Reid, Y., Parkes, H. & Gelber, C. The costs of using unauthenticated, over-passaged cell lines: How much more data do we need? *BioTechniques* **43,** 575–586 (2007).

67. Derose, Y. S. *et al.* Tumor grafts derived from women with breast cancer authentically reflect tumor pathology, growth, metastasis and disease outcomes. *Nat. Med.* **17,** 1514–1520 (2011).

68. Daniel, V. C. *et al.* A primary xenograft model of small-cell lung cancer reveals irreversible changes in gene expression imposed by culture in vitro. *Cancer Res.* **69,** 3364–3373 (2009).

69. Johnson, N. *et al.* Compromised CDK1 activity sensitizes BRCA-proficient cancers to PARP inhibition. *Nat. Med.* **17,** 875–882 (2011).

70. Johnson, N. & Shapiro, G. I. Cyclin-dependent kinases (cdks) and the DNA damage response: rationale for cdk inhibitor-chemotherapy combinations as an anticancer strategy for solid tumors. *Expert Opin. Ther. Targets* **14,** 1199–212 (2010).

71. Ekumi, K. M. *et al.* Ovarian carcinoma CDK12 mutations misregulate expression of DNA repair genes via deficient formation and function of the Cdk12/CycK complex. *Nucleic Acids Res.* **43,** 2575–2589 (2015).

72. Bartkowiak, B., Yan, C. & Greenleaf, A. L. Engineering an analog-sensitive CDK12 cell line using CRISPR/Cas. *Biochim. Biophys. Acta - Gene Regul. Mech.* **1849,** 1179–1187 (2015).

73. Johnson, S. F. *et al.* CDK12 Inhibition Reverses De Novo and Acquired PARP Inhibitor Resistance in BRCA Wild-Type and Mutated Models of Triple-Negative Breast Cancer. *Cell Rep.* **17,** 2367–2381 (2016).

74. Ibrahim, Y. H. *et al.* PI3K inhibition impairs BRCA1/2 expression and sensitizes BRCA-proficient triple-negative breast cancer to PARP inhibition. *Cancer Discov.* **2,** 1036–1047 (2012).

75. Asghar, U., Witkiewicz, A. K., Turner, N. C. & Knudsen, E. S. The history and future of targeting cyclin-dependent kinases in cancer therapy. *Nat Rev Drug Discov.* **14 (2):** 130–146 (2015).

76. MacCallum, D. E. *et al.* Seliciclib (CYC202, R-Roscovitine) induces cell death in multiple myeloma cells by inhibition of RNA polymerase II-dependent transcription and down-regulation of Mcl-1. *Cancer Res.* **65,** 5399–5407 (2005).

77. Le Tourneau, C. *et al.* Phase i evaluation of seliciclib (R-roscovitine), a novel oral cyclin-dependent kinase inhibitor, in patients with advanced malignancies. *Eur. J. Cancer* **46,** 3243–3250 (2010).

78. Carvajal, R. D. *et al.* A phase II study of flavopiridol (alvocidib) in combination with docetaxel in refractory, metastatic pancreatic cancer. *Pancreatology* **9,** 404–409 (2009).

79. Mita, M. M. *et al.* Phase 1 safety, pharmacokinetic and pharmacodynamic study of the cyclin-dependent kinase inhibitor dinaciclib administered every three weeks in patients with advanced malignancies. *Br J Cancer* **117 (9):** 1258-1268 (2017).

80. Mita, M. M. *et al.* Randomized phase II trial of the cyclin-dependent kinase inhibitor Dinaciclib (MK-7965) versus capecitabine in patients with advanced breast cancer. *Clin. Breast Cancer* **14,** 169–176 (2014).

81. Kang, J., Sergio, C. M., Sutherland, R. L. & Musgrove, E. a. Targeting cyclin-dependent kinase 1 (CDK1) but not CDK4/6 or CDK2 is selectively lethal to MYC-dependent human breast cancer cells. *BMC Cancer* **14,** 32 (2014).

82. Horiuchi, D. *et al.* MYC pathway activation in triple-negative breast cancer is synthetic lethal with CDK inhibition. *J. Exp. Med.* **209,** 679–96 (2012).

83. Costa-Cabral, S. *et al.* CDK1 Is a Synthetic Lethal Target for KRAS Mutant Tumours. *PLoS One* **11 (2):** e0149099 (2016).

84. Neganova, I. *et al.* CDK1 plays an important role in the maintenance of pluripotency and genomic stability in human pluripotent stem cells. *Cell Death Dis.* **5,** e1508 (2014).

85. Vassilev, L. T. *et al.* Selective small-molecule inhibitor reveals critical mitotic

functions of human CDK1. *Proc. Natl. Acad. Sci.* **103,** 10660–10665 (2006).

86. Walsby, E. *et al.* A novel Cdk9 inhibitor preferentially targets tumor cells and synergizes with fludarabine. *Oncotarget* **5,** 375–85 (2014).

87. Cao, S. *et al.* Inhibition of CDK9 induces apoptosis and potentiates the effect of cisplatin in hypopharyngeal carcinoma cells. *Biochem. Biophys. Res. Commun.* **482,** 536–541 (2017).

Appendix

Summary (English)

Resumen (Español)

Samenvatting (Nederlands)

List of Publications

Curriculum Vitae

Acknowledgements

Summary (English)

Targeted therapy for triple-negative breast cancer

Triple-negative breast cancer (TNBC) is an aggressive form of breast cancer distinguishable from breast cancers dependent upon hormone-regulated growth pathways by the absence of oestrogen and progesterone receptors, as well as the lack of HER2 (human epidermal growth factor receptor 2) expression or gene amplification. Consequently, anti-hormonal therapies (e.g. tamoxifen), which are highly efficacious in HR+ breast cancer, are redundant in the context of TNBC. At present, clinical management of TNBC consists of chemotherapy, radiotherapy and tumour-reductive surgery. The therapeutic arsenal with which TNBC can be treated has failed to expand appreciably since the introduction of chemotherapy, emphasising the desperate need for the development of novel targeted agents to combat this intractable illness. As such, the principle aim of this thesis was to identify novel TNBC-specific dependencies amenable to pharmacological manipulation, with a key emphasis on the identification of novel synergistic combinations comprised of clinically approved agents in conjunction with novel targeted molecules.

Chapter 2 explored the differential sensitivity of TNBC cells to MEK and Akt inhibitors. Kinase inhibitor-based screening of TNBC cell lines showed that they cluster into three separate groups based on their sensitivity to multiple MEK and Akt inhibitors; Group 1 (Akt inhibitor-resistant), Group 2 (MEK inhibitor-resistant) or Group 3 (resistant to both MEK and Akt inhibitors). An increased level of phospho-Akt and mutations in PIK3CA, PIK3R1 and/or PTEN distinguished MEK inhibitor-resistant, Akt inhibitor-sensitive cell lines from those resistant to Akt inhibitors yet sensitive to MEK inhibitors. Co-treatment of double-resistant cell lines with MEK and

Akt inhibitors was not sufficient to overcome their resistance to either agent, nor did it lead to synergistic responses in the other groups. To identify alternative, more appropriate targets for this difficult-to-treat subgroup, transcriptomics- and proteomics-based gene-set enrichment analyses unveiled a significant enrichment of genes linked to cell cycle regulation in MEK/Akt inhibitor double-resistant cell lines. Importantly, cell lines resistant to both MEK and Akt inhibitors showed greater sensitivity to pan-CDK inhibitors dinaciclib and flavopiridol. These agents potently inhibited CDK-mediated signal transduction and induced DNA damage, suggesting that the MEK/AKt inhibitor double-resistant subgroup may benefit from alternative targeted therapy in the form of CDK inhibitors.

Chapter 3 delineates the resistance of TNBC cells to a panel of epidermal growth factor receptor (EGFR)-tyrosine kinase inhibitors. Here, I demonstrate that EGFR is expressed at higher levels in TNBC tumours compared to ER+ breast tumours and high expression of EGFR is associated with cell lines conforming to a basal-like subtype. The response of a panel of TNBC cells to EGFR-tyrosine kinase inhibitors (EGFR-TKIs) was therefore evaluated; the majority of TNBC lines being resistant to EGFR-targeted therapy, despite the fact that silencing EGFR markedly attenuated their proliferation. This phenomenon was independent of EGFR pathway functionality since EGF-mediated stimulation of both EGFR-TKI-resistant and EGFR-TKI-sensitive TNBC cell lines activated downstream signalling which was inhibited by treatment with lapatinib, erlotinib and gefitinib. To identify novel compounds which could sensitise EGFR-TKI-resistant TNBC cells to these drugs, I performed a kinase inhibitor library screen in combination with a clinically relevant dose of lapatinib. This screen identified a dual cdc7/CDK9 inhibitor (PHA-767491) as the most promising candidate compound. Combining PHA-767491 with multiple EGFR-TKIs

substantially reduced the proliferation of TNBC cells compared to either monotherapy and induced apoptosis in multiple TNBC cell lines. This co-treatment inhibited signal transduction crucial for cdc7-regulated DNA replication and the initiation of productive mRNA transcription controlled by CDK9, with concomitant G2/M cell cycle arrest. Moreover, increased expression of cdc7 and RNA Polymerase II, the downstream target of CDK9, was associated with poorer metastasis-free survival in TNBC patients. Transcriptomic profiling revealed down-regulation of pathways governing proliferation, transcription and cell survival in TNBC cells treated with combination therapy. Additionally, an elevated expression of several genes involved in the aforementioned signaling pathways, and whose expression is sensitive to the combination, was associated with a worse metastasis-free survival in CMTN patients, suggesting targeting CDK9 in conjunction with EGFR may represent a powerful strategy to combat TNBC.

To scrutinise the potential of targeting aberrant CDK9-mediated transcriptional regulation as a novel target for TNBC, the efficacy of a panel of CDK inhibitors with prominent activity against P-TEFb/CDK9 function was assessed in TNBC cell lines in **Chapter 4.** TNBC cells were sensitive to inhibitors with strong activity against CDK1, CDK2, CDK7 and CDK9, highlighting their exquisite dependence on regulation of the cell cycle and transcription. Treatment with these inhibitors abolished P-TEFb/CDK9-controlled phosphorylation of RNA Polymerase II and rapidly attenuated the expression of multiple anti-apoptotic factors including MCL-1 and BCL-xL. Accordingly, these inhibitors induced dose-dependent apoptosis and DNA damage in TNBC cell lines. CDK9 inhibitor-induced depletion of MCL-1 was found to occur in a proteasome-dependent manner, since proteasome inhibitor MG-132 prevented MCL-1 depletion. Transcriptomic profiling was subsequently performed in order to

elucidate which pathways and transcriptional programmes were most sensitive to disruption by these CDK9 inhibitors. TGF-β, BMP and Wnt/β-catenin signalling, as well as genes involved in cell cycle progression, DNA repair and epithelial-to-mesenchymal transition (EMT), featured prominently amongst the down-regulated genes. The most strongly affected transcripts were enriched for transcription factors; a number of these (SOX9, EN1 and PLAG1) were crucial for the proliferation of multiple TNBC cell lines and were highly expressed in basal-like tumours. Altogether, these findings demonstrate that CDK inhibitors with potent anti-P-TEFb/CDK9 activity are highly efficacious against *in vitro* models of TNBC.

Since resistance to single targeted therapies almost invariably develops in the clinic, the effect of combining the CDK9 inhibitors described in **Chapter 4** with clinically-approved agents or agents under pre-clinical investigation was evaluated in **Chapter 5**. Strong synergy was observed when combining pre-clinical BET inhibitor JQ1 with I-73 or LY3-21, resulting in depletion of MCL-1 and BCL-2 with concomitant activation of the DNA damage response. Combining I-73 and LY3-21 with EGFR-TKIs lapatinib and gefitinib synergistically reversed the insensitivity of TNBC cells to EGFR-tyrosine kinase inhibition and induced G2/M cell cycle arrest accompanied by apoptosis. RNA sequencing-based analysis revealed that co-treatment of TNBC cells with I-73 and lapatinib augmented the general inhibition of transcription induced by I-73. TGF-β signalling, cell cycle progression and stem cell pluripotency were amongst the pathways most strongly down-regulated under co-treatment conditions. A number of transcriptional regulators specifically down-regulated by combining I-73 and lapatinib were associated with a significantly poorer metastasis-free survival in a cohort of TNBC patients. In short, inhibiting P-TEFb/CDK9 function can alleviate the resistance of TNBC cells to EGFR-TKIs and BET inhibitors.

In conclusion, the work presented in this thesis illustrates that CDK inhibitors with potent activity against P-TEFb/CDK9 can be used to target common transcriptional nodes in cancers addicted to receptor tyrosine kinase-mediated signal transduction or which depend on delicately controlled cell cycle progression.

Resumen (Español)
Terapias dirigidas contra el cáncer de mama triple negativo

El cáncer de mama triple negativo (CMTN) es un cáncer virulento que se destaca por la falta de expresión de receptores para hormonas (estrógeno y progesterona) y la ausencia de amplificación del gen HER2, por lo que el tratamiento de este cáncer con terapias antihormonas es inútil. Hoy día, el tratamiento de CMTN consiste en quimioterapia, radioterapia y cirugía para remover tumores. Sin embargo, el abanico de tratamientos con el que se puede tratar estos tumores no se ha ampliado lo suficientemente en los años posteriores a la introducción de la quimioterapia, creando, de esta manera, la urgente necesidad de desarrollar nuevas terapias dirigidas que funcionen de una manera eficaz. Por lo tanto, el objetivo principal de esta tesis es la identificación de nuevas dependencias moleculares en las células CMTN susceptibles a manipulación farmacológica, con un énfasis particular en el descubrimiento de nuevas combinaciones sinérgicas compuestas por agentes clínicamente ya aprobados y nuevas terapias dirigidas molecularmente.

El **Capítulo 2** investiga la respuesta proliferativa de células de CMTN a inhibidores de las quinasas MEK y AKT. Las células se clasificaron en tres grupos de acuerdo a su respuesta proliferativa después de ser tratadas con dichos inhibidores: Grupo 1 (resistente a MEK pero sensible a AKT), Grupo 2 (sensible a MEK pero resistente a AKT) y Grupo 3 (resistente tanto a inhibidores de MEK como a los de AKT). Es importante remarcar que la resistencia palpable de las células del Grupo 3 no se debió a la intercomunicación entre las dos vías de señalización, puesto que tratamiento no indujo un aumento en la activación de la vía de señalización opuesta. De la misma manera, al tratar las células del Grupo 3

con combinaciones de inhibidores contra MEK o AKT, no se observó sinergia alguna. Para identificar dianas alternativas y más apropiadas para este subgrupo se llevaron a cabo tanto análisis transcriptómicos como proteómicos de las células pertenecientes a este grupo. Los análisis mostraron un enriquecimiento de genes vinculados con la regulación del ciclo celular en las células resistentes tanto a inhibidores de MEK como a los de AKT. Como resultado, las células del Grupo 3 mostraron una sensibilidad más alta a inhibidores de quinasas dependientes de ciclinas (CDKs), específicamente a dinaciclib y a flavopiridol. Estos inhibidores previnieron potentemente la señalización mediada por CDKs e indujeron daño al ADN, lo que sugiere que CMTNs similares a los de Grupo 3 podrían aprovechar de terapia alternativa en forma de inhibidores de CDKs.

El **Capítulo 3** detalla la resistencia de las células de CMTN a varios inhibidores del receptor del factor de crecimiento epidérmico (EGFR -por sus siglas en inglés-). Esto demuestra que los tumores CMTN expresan niveles de EGFR más altos de los que se observan en tumores dependientes de receptores de hormonas. Considerando esto, se investigó de manera profunda la proliferación de células de CMTN en respuesta a múltiples inhibidores de EGFR. La mayoría de las células mostró resistencia a los inhibidores de EGFR a pesar de que la expresión de este receptor fuera imprescindible para su supervivencia. También se comprobó que esta resistencia no está relacionada con una falta de integridad o funcionalidad de la vía de transducción de señal mediada por EGFR. Para poder identificar compuestos que pudieran sensibilizar células de CMTN resistentes a inhibidores de EGFR, se realizó un tratamiento a las mismas esas células utilizando 273 inhibidores de quinasas en combinación con una concentración clínicamente relevante de lapatinib (un inhibidor de EGFR). A

través de esta biblioteca, se identificó un inhibidor de cdc7 y CDK9, su nombre siendo PHA-767491, como el candidato compuesto más prometedor. Al combinar PHA-767491 con múltiples inhibidores de EGFR, se observó una inducción de apoptosis además de una reducción sustancial en la proliferación de las células de CMTN. Esta combinación inhibió la transducción de señales requeridas para la replicación de ADN mediada por cdc7 y también la de las que se requieren para la iniciación de transcripción de ARN mensajero (ARNm) mediada por CDK9, con una detención del ciclo celular concomitante. Además, la expresión elevada de cdc7 o ARN Polimerasa II (ARN Pol II; la enzima requerida para la transcripción de ARNm y cuya función depende de la acción de CDK9) se vinculó con una baja supervivencia libre de metástasis en los pacientes CMTN. Al perfilar transcriptómicamente las vías de señalización afectadas por la combinación, se observó una inhibición de las vías que son necesarias para la proliferación, transcripción y supervivencia celular, entre otras. Cabe destacar que una expresión elevada de varios genes involucrados en las vías de señalización anteriormente mencionadas, y cuya expresión es sensible a la combinación, se vinculó con una baja supervivencia libre de metastasis en pacientes de CMTN. Considerándolo todo, la inhibición de EGFR en conjunción con inhibidores de cdc7 y/o CDK9, representa una estrategia potente para combatir CMTN.

Para escudriñar la potencial de inhibir la regulación de transcripción aberrante mediada por CDK9, la eficacia de inhibidores de CDKs, sobre todo los con actividad potente contra P-TEFb/CDK9, se evaluó en líneas celulares de CMTN en **Capítulo 4**. Células de CMTN son exquisitamente sensibles a inhibidores contra CDK1, CDK2, CDK7 y CDK9, así enfatizando su dependencia de la regulación del ciclo celular y transcripción. Estos inhibidores abolieron la

fosforilación de ARN Pol II mediada por P-TEFb/CDK9, llevando a la atenuación de factores pro-supervivencia como MCL-1 y BCL-xL. En consecuencia, los inhibidores indujeron la muerte de las células de CMTN e invocaron daño al ADN. La depleción de MCL-1 procede de manera dependiente del proteasoma, puesto que un inhibidor del proteasoma previno la depleción de MCL-1 inducida por los inhibidores. Con posterioridad, los perfiles transcriptómicos de células tratadas con los CDK9 inhibidores se analizaron con la intención de identificar cuáles vías de señalización se afectaban más por la inhibición de P-TEFb/CDK9 y así poder profundizar conocimiento sobre su eficacia. Tanto señalamiento a través de TGF-β, BMP y Wnt/β-catenin, como genes involucrados en la progresión del ciclo celular, reparación de daño a ADN y la transición epitelial a mesénquima (EMT), contaban entre las vías de señalización y genes más afectados por el tratamiento. Las transcripciones de ARNm más afectadas por los inhibidores se destacaron por su enriquecimiento en factores de transcripción, de los cuales SOX9, EN1 y PLAG1 eran imprescindible para la proliferación de varias células de CMTN. Por añadidura, se notó una expresión bastante alta de esos genes en tumores basales tales como CMTN. En conjunto, en este capítulo se indica que inhibidores de P-TEFb/CDK9 son altamente eficaces en modelos de CMTN.

Dado que la resistencia a terapias dirigidas invariablemente se desarrolla en pacientes, en **Capítulo 5** se evaluó la potencial de combinar inhibidores de otras quinasas con los inhibidores de CDK9 descritos en **Capítulo 4**. Se observó sinergia al combinar JQ1 (inhibidor de BRD4) con I-73 o LY3-21, llevando a la depleción de MCL-1 y BCL-2 y la activación de señalamiento vinculado al daño de ADN. La adición de I-73 o LY3-21 superó la resistencia de células de CMTN a inhibidores de EGFR como lapatinib y gefitinib, induciendo detención del ciclo

celular acompañada por apoptosis. Un análisis transcriptómico reveló que el tratamiento de las células de CMTN con una combinación de I-73 y lapatinib aumentó la inhibición general de transcripción otorgada por I-73 a las células de CMTN. Señalización a través de TGF-β, progresión por el ciclo celular y la pluripotencia de células madre se contaban entre las vías de señalización más fuertemente inhibidas por la combinación. La expresión de algunos reguladores de transcripción afectados por la combinación se asoció también con una baja supervivencia libre de metástasis en los pacientes de CMTN. En síntesis, se demuestra en este capítulo que la inhibición de P-TEFb/CDK9 es suficiente para superar la resistencia de las células CMTN a inhibidores de EGFR y BET.

Para concluir, las investigaciones delineadas en esta tesis demuestran que inhibidores con actividad potente contra P-TEFb/CDK9 no sólo podrían ser utilizados contra nodos de transcripción aberrantes en aquellos cánceres adictos a la transducción de señales mediada por receptores tirosina quinasas, sino también contra aquellos cánceres que no pueden prescindir de una regulación estricta de la progresión del ciclo celular.

Nederlandse samenvatting
Doelgerichte therapie voor triple negatieve borstkanker

Triple negatieve borstkanker (TNBK) is een agressieve vorm van borstkanker die, anders dan de hormoongevoelige vormen, gekenmerkt wordt door het ontbreken van de volgende hormoonreceptoren: de estrogeen receptor (ER), de progesteron receptor (PR) en de HER2 receptor. Dit heeft tot gevolg dat anti-hormonale therapieën zoals tamoxifen niet werken in TNBK en de huidige therapie nog steeds bestaat uit een combinatie van het chirurgisch verwijderen van de tumor, chemotherapie en/of bestraling. Na de ontdekking van chemotherapie, zijn geen nieuwe behandelingen voor TNBK op de markt gekomen, wat eens te meer duidelijk maakt dat ontwikkeling van nieuwe specifieke geneesmiddelen essentieel is voor de genezing van deze ziekte. Daarom was het voornaamste doel van dit proefschrift het ontdekken van nieuwe TNBK-specifieke afhankelijkheden, met een belangrijke nadruk op nieuwe synergetische combinaties bestaande uit klinisch goedgekeurde middelen in combinatie met nieuwe doelgerichte moleculen.

In **hoofdstuk 2** werden de verschillen in gevoeligheid van TNBK cellen voor MEK- en Akt-remmers onderzocht. Screening van kinase remmers in TNBK cellijnen liet zien dat deze cellijnen in drie afzonderlijke groepen te verdelen zijn op basis van gevoeligheid voor meerdere MEK- en Akt-remmers; Akt-remmer resistente cellijnen (Groep 1), MEK-remmer resistente cellijnen (Groep 2) of MEK- en Akt-remmer resistente cellijnen (Groep 3). Een verhoogd niveau van gefosforyleerd Akt en mutaties in PIK3CA, PIK3R1 en/of PTEN onderscheiden MEK-remmer-resistente/Akt-remmer-gevoelige cellijnen van Akt-remmer-resistente/MEK-remmer-gevoelige cellijnen. Behandeling van dubbelresistente cellijnen met een

combinatie MEK- en Akt-remmers veranderde niets aan de ongevoeligheid van deze cellijnen, noch resulteerde het in synergistische responsen in de andere groepen. Analyse van transcriptomics en proteomics data liet significant hogere niveaus zien van genen betrokken bij regulatie van de celcyclus in MEK/Akt-remmer dubbelresistente cellijnen. Daarnaast waren cellijnen die resistent zijn tegen zowel MEK- als Akt-remmers gevoeliger voor pan-CDK-remmers dinaciclib en flavopiridol. Behandeling met deze remmers verminderde CDK-gemedieerde signaaltransductie en induceerde DNA-beschadiging, hetgeen suggereert dat de MEK/Akt-remmer dubbelresistente subgroep kan profiteren van een alternatieve therapie in de vorm van CDK-remmers.

In **hoofdstuk 3** wordt de resistentie van TNBK cellijnen voor epidermale groeifactor receptor (EGFR) – tyrosine kinaseremmers (TKIs) beschreven. EGFR niveaus zijn hoger in TNBK in vergelijking met ER positieve tumoren en daarnaast geassocieerd met het basale cellijn subtype. Uit onderzoek naar de respons van verscheidene TNBK cellijnen op EGFR-TKIs bleek dat de meerderheid van de TNBK cellijnen resistent was tegen EGFR-remmers, ondanks dat het verminderen van de EGFR expressie zelf de groei van de cellijnen duidelijk remde. Deze verschillen in gevoeligheid waren onafhankelijk van de functionaliteit van EGFR signalering: in alle cellijnen werd deze signalering geactiveerd na behandeling met EGF en geremd na behandeling met de EGFR-TKIs lapatinib, erlotinib en gefitinib. Om nieuwe remmers te identificeren die EGFR-TKI-resistente TNBK cellen gevoelig zouden kunnen maken, werden TNBK cellijnen behandeld met verscheidene kinaseremmers in combinatie met een klinisch relevante dosis van lapatinib. Het combineren van de dubbele cdc7/CDK9-remmer PHA-767491 (PHA) met EGFR-TKIs verminderde de groei en induceerde apoptose in TNBK cellen in

vergelijking met monotherapie, wat PHA een veelbelovende kandidaat remmer maakt. De dubbele behandeling van PHA met EGFR-TKIs verminderde signalering die essentieel is voor cdc7 gereguleerde DNA replicatie en CDK9 gecontroleerde initiatie van transcriptie en leidde gelijktijdig tot een stop in de G2-M fase in de celcyclus. Bovendien waren verhoogde niveaus van cdc7 en RNA polymerase II, het eiwit waar CDK9 direct op aangrijpt, geassocieerd met een grotere kans op het ontwikkelen van uitzaaiingen in TNBK patiënten. Combinatie therapie in TNBK cellen resulteerde in remming van signaalroutes betrokken bij celgroei, transcriptie en overleving, wat suggereert dat gerichte remming van CDK9 in combinatie met EGFR remming een krachtige strategie kan zijn om TNBK te bestrijden.

In **hoofdstuk 4** is de effectiviteit van een verscheidene CDK-remmers met sterke anti-P-TEFb/CDK9 activiteit vastgesteld, om zo de potentie van het aangrijpen van de afwijkende transcriptie regulatie via CDK9 te onderzoeken. TNBK cellijnen waren gevoelig voor remmers van CDK1, CDK2, CDK7 en CDK9, wat benadrukt dat deze cellen erg afhankelijk zijn van regulatie van de celcyclus en transcriptie. Behandeling met deze remmers voorkwam de P-TEFb/CDK9-gemedieerde fosforylering van RNA polymerase II en de expressie van verschillende anti-apoptotische factoren, zoals MCL-1 en BCL-xL. Daarnaast induceerden deze remmers apoptose en DNA schade in de TNBK cellijnen. De depletie van MCL-1 door CDK9-remmers vond plaats via een proteasoom-afhankelijke manier, aangezien de proteasoom remmer MG-132 de MCL-1 depletie voorkwam. Om te achterhalen welke moleculaire routes en transcriptionele programma's het meest worden beïnvloed door deze remmers, werd het transcriptoom na behandeling met deze CDK9-remmers in kaart gebracht. Genen betrokken bij TGF-β, BMP en

Wnt/β-catenin signaleringsroutes, progressie van de celcyclus, het herstellen van DNA schade, en epitheliaal-naar-mesenchymaal transitie (EMT) waren de meest verminderd tot expressie gekomen genen. De transcripten die het meest aangetast werden waren voornamelijk transcriptiefactoren. Een aantal van deze (SOX9, EN1 en PLAG1) waren cruciaal voor de proliferatie van verschillende TNBK cellijnen en kwamen hoog tot expressie in basale-achtige tumoren. Samenvattend laten deze resultaten dus zien dat CDK-remmers met anti-p-TEFb/CDK9 activiteit erg efficiënt zijn in in vitro modellen van TNBK.

Aangezien resistentie tegen therapieën met één aangrijpingspunt zich bijna altijd ontwikkeld in de kliniek, is in **hoofdstuk 5** het effect van het combineren van de CDK9-remmers beschreven in **hoofdstuk 4** met geneesmiddelen die ofwel geaccepteerd zijn voor klinisch gebruik, ofwel zich momenteel in pre-klinische onderzoeksfasen bevinden, getest. Sterke synergie werd gezien bij combinatie van de pre-klinische BET-remmer JQ1 met CDK9-remmers I-73 of LY3-21. Deze synergie leidde tot vermindering van MCL-1 en BCL-2 expressie, en activering van de respons die DNA schade herstelt. Combinatie van I-73 en LY3-21 met EGFR-TKIs lapatinib en gefitinib herstelde de gevoeligheid van TNBK cellen voor EGFR tyrosine kinase inhibitie en induceerde een halt in de G2/M fase van de celcyclus, wat gepaard ging met apoptose. Via het kwantitatief in kaart brengen van de algehele RNA expressie, ofwel 'RNA sequencing', werd achterhaald dat de combinatiebehandeling van I-73 en lapatinib de inhibitie van transcriptie door I-73 versterkte. De signaleringsroutes die hierbij het meest verstoord werden waren TGF-β signalering, progressie van de celcyclus en stamcel pluripotentie. Een aantal transcriptionele regulators die specifiek verlaagd tot expressie kwamen door de combinatie van I-73 en lapatinib waren geassocieerd het vormen van

uitzaaiingen in een cohort van TNBK patiënten. Kortom, het remmen van P-TEFb/CDK9 activiteit kan de resistentie van TNBK cellen tegen EGFR-TKIs en BET-remmers teniet doen.

Concluderend, het werk in dit proefschrift laat zien dat EGFR-resistente TNBK tumoren gevoelig gemaakt kunnen worden met behandeling met CDK-remmers, welke transcriptie remmen via P-TEFb/CDK9 in tumoren die afhankelijk zijn van EGFR-gemedieerde signaaltransductie en/of een nauwkeurig gecontroleerde celcyclus hebben.

List of Publications

Molecular targeted therapy for triple-negative breast cancer. ***Ronan P. McLaughlin****, John A. Foekens, John W.M. Martens, Yinghui Zhang, Bob van de Water* (Manuscript in preparation).

A cell cycle-related gene signature is associated with resistance to MEK and Akt inhibitors in triple- negative breast cancer. *Vera E. van der Noord[1],* ***Ronan P. McLaughlin[1]****, Marcel Smid, John A. Foekens, John W.M. Martens, Yinghui Zhang, Bob van de Water* (Manuscript submitted). [1]Both authors contributed equally.

Blockage of cdc7/CDK9 signalling sensitises triple-negative breast cancer to EGFR-targeted therapy. ***Ronan P. McLaughlin****, Jichao He, Vera van der Noord, Jevin Redel, Marcel Smid, John A. Foekens, John W.M. Martens, Yinghui Zhang, Bob van de Water* (Manuscript submitted).

Targeting the P-TEFb complex through CDK9 inhibition to combat triple-negative breast cancer. *Ronan P. McLaughlin[1], Jichao He[1], Jessica Karuntu[1], Vera van der Noord[1], Marcel Smid[2], Annemieke M. Timmermans, Anita M.A.C. Trapman-Jansen, Renée Foekens, Yi Long, Sarah Al Haj Diab, John W.M. Martens, John A. Foekens, Shudong Wang, Yinghui Zhang, Bob van de Water* (Manuscript in preparation).

The synergistic effect of combined P-TEFb and EGFR inhibition on triple-negative breast cancer. ***Ronan P. McLaughlin****, Jichao He, Jessica Karuntu, Vera van der Noord, John W.M. Martens, Marcel Smid, John A. Foekens, Yi Long, Sarah Al Haj Diab, Yinghui Zhang, Bob van de Water, Shudong Wang* (Manuscript in preparation).

Curriculum Vitae

Ronan Patrick McLaughlin was born on the 11th July 1990 in Edinburgh, Scotland. He attended Holy Rood RC High School from 2002-2008. He subsequently studied Biological Sciences at the University of Edinburgh, ultimately specialising in Reproductive Biology and graduating with a 1st class BSc degree.

Ronan then moved westwards to Glasgow where he began his MRes studies in Molecular Medicine at the University of Glasgow, undertaking a research placement at the Paul O'Gorman Leukaemia Research Centre where he investigated the role of polo-like kinases in acute myeloid leukaemia under the supervision of Prof. Mhairi Copland and Dr. Ross Kinstrie. Ronan subsequently explored the epigenetic signature of glioblastoma stem cells in a collaborative project between the Beatson Institute for Cancer Research and the University of Glasgow, under the supervision of Prof. Anthony Chalmers, Dr. Nati Gomez and Dr. Katherine West.

After receiving an MRes degree in Molecular Medicine with merit, Ronan's desire to forge a career within cancer research prompted him to seek a PhD position within Professor Bob van de Water's lab at the Leiden Academic Centre for Drug Research in Leiden, The Netherlands. This project revolved around the identification of novel drug targets and combination therapies for triple-negative breast cancer, funded by the European Research Council (ERC).

Acknowledgements

I would like to thank Prof. Bob van de Water for granting me the opportunity to contribute to this exciting research project. It's been an honour to have worked in your laboratory. My sincere gratitude goes to Dr. Yinghui Zhang for her unwavering support, expertise, and dedication, without which life would have been infinitely more difficult. A special thanks to Prof. John Foekens, Prof. John Martens and Dr. Marcel Smid at Erasmus MC for their constructive criticism as well as the clinical data used in this thesis. Additionally, I wish to thank Prof. Shudong Wang at the University of South Australia for such a fruitful collaboration and for provision of the CDK inhibitors which became the most exciting aspect of my research.

I would like to thank the Drug Discovery and Safety division for their advice and company during my PhD. Zuzanna, gracias por haberme soportado en los momentos difíciles y por haberme escuchado cuando necesitaba desahogarme. Sin nuestras pláticas hubiera enloquecido. Ha sido un deleite compartir la oficina (y muchos dulces) contigo. Natalia, nuestras pláticas me hicieron reír. ¡Suerte y gracias! To Vera, Jevin, Jessica, and Susan, thank you for letting me guide you in your studies and for all the hard work you put into our research. I'm especially indebted to you, Vera, for the immense amount of hard work and dedication you poured into the projects we worked on together. Sali, thank you for ensuring I had sufficient supplies of carbohydrates and coffee over the last couple of years. Teşekkür ederim!

To my family, thank you for your seemingly endless disposition to listen to my rants (Mum and Dad), your far superior experience with word processing (Hannah), and for your continual love and support (Granny and Aodhán). I thank my friends for always lending an ear (or a glass…) whenever I needed to let off steam. David, no habría llegado a este momento si no te hubiera conocido. Siempre estuviste apoyándome a pesar de lo que fuera, incluso en momentos en los que toda esperanza parecía haberse desvanecido. Gracias desde lo más profundo de mi corazón por tu apoyo y amor, porque estos han sido imprescindibles en

convencerme de esforzarme aún más para alcanzar lo inalcanzable y para enfrentarme a los retos de la vida con una sonrisa. Te amo y tengo tantas ganas de pasar el resto de mi vida junto a ti.